

**Synthesis of nitrogen-, oxygen- and phosphine- donor palladium(II)  
complexes for the catalytic hydrogenation and methoxycarbonylation  
of alkenes and alkynes**

By

**THANDEKA ADELINAH TSHABALALA**

Submitted in fulfilment of the academic requirements for the degree of

**DOCTOR OF PHILOSOPHY**

In

**CHEMISTRY**

in the College of

Agriculture, Engineering and Science

**at the**

University of KwaZulu-Natal

Pietermaritzburg

Supervisor: Prof Stephen Ojwach

June 2019

## DECLARATION

I, Thandeka Adelinah Tshabalala declare that the thesis, synthesis of Nitrogen-, Oxygen- and Phosphine- donor palladium(II) complexes for the catalytic hydrogenation and methoxycarbonylation of alkenes and alkynes reports on research results of my own work, carried out in the School of Chemistry and Physics, University of KwaZulu-Natal, Pietermaritzburg campus. Where use of work of others has been made, it is duly accredited through reference citation. This thesis has not been submitted for the award of any qualification at any University.

Signed:  .....

Date: ....15/08/2019.....

**T.A Tshabalala**

As the supervisor of the candidate, I have approved the submission of this thesis for examination.

Signed:  .....

Date: ....15/08/2019.....

**Prof Stephen Ojwach**

## DEDICATION

*This thesis is dedicated to my Son, Asavela B.U. Khusi, with lots of LOVE*

*You never know how strong you are, until being strong is the only  
choice you have.*

*-Cayla Mills-*

## ACKNOWLEDGEMENTS

*But Jesus beheld them, and said unto them, "With man this is impossible; but with God all things are possible." ~ Matthew 19:26 KJV*

I would like to express my deepest gratitude to the following people who have helped expand my reach and in their unique way, were able to challenge my way of thinking, open my eyes to great wealth that knowledge bring and continuously encouraged me to dream big dreams and to strive to reach them....

- ❖ First and foremost, I would like to thank God Almighty. Thank you Lord for the gift of life, the opportunity to explore the marvellous works of your hand through-out my studies and for the special people you have strategically placed in my life to direct, assist and support me through the beautiful journey you have set before me.
- ❖ I am especially grateful to my parents (Mandlakayise and Thembeni Tshabalala), who supported me emotionally, spiritually and financially, without whom I would never have enjoyed so many opportunities. Thank you for your love and teaching me that my job in life was to learn, to be happy, and to know and understand myself; only then could I know and understand others.
- ❖ I would like to convey my warmest gratitude to my supervisor Prof Stephen Ojwach, who gave me the opportunity to conduct my study in his research group. I would like to also thank him for his guidance, generous contribution of knowledge and experience, valuable comments, attending conferences, his patience with me and encouragement from the start until the end of my study.
- ❖ Special thanks to C\* change program and NRF for financial support and bursaries, without which my study at UKZN would have not been possible.
- ❖ I wish to thank my colleagues and friends at the department of chemistry for sharing with me numerous coffees, lunches and laughter at all time.

*Ke Ya leboha!*

## PREFACE

The role of transition metal complexes in catalytic synthesis of alkynes and alkenes has extremely advanced over the past century. The search for effective catalytic systems is ongoing and researchers are continuously exploring different chemical properties of different complexes in order to obtain effective catalysts for these reactions. The main areas of interest are catalyst activity, selectivity and stability in hydrogenation and methoxycarbonylation reactions. In attempts to achieve a balance between catalyst activity, stability and selectivity we investigated some mixed nitrogen-, oxygen-, and phosphine- donor palladium complexes in catalytic hydrogenation reactions. Therefore, this thesis is made-up of seven-chapters.

**Chapter 1**, covers an introduction to homogeneous and heterogeneous catalytic hydrogenation reactions of alkenes and alkynes. The chapter highlights the significance of homogeneous hydrogenation reactions over heterogeneous reactions. This chapter also reviews the relevant literature on catalytic homogeneous hydrogenation of alkenes and alkynes. It presents a review on homogeneous rhodium (II), ruthenium(II) and palladium(II) complexes as molecular hydrogenation catalysts. The importance of finding a balance between homogeneous and heterogeneous catalysis by heterogenization of homogeneous systems using biphasic catalysis is highlighted towards the end of the chapter. The chapter concludes by presenting the rationale and highlights the main objectives of the whole study.

**Chapter 2**, describes the synthesis, characterization and catalytic application in the methoxycarbonylation of hexenes and octenes using (benzimidazolylmethyl)amine palladium(II) complexes. The study focussed on the role of the complex structure, nature of the phosphine derivatives, acid-promoter and olefin substrates in the methoxycarbonylation reactions of alkenes. The findings of this study have been published in *Transit. Met. Chem.* **43** (2018) 339–346.

In **Chapter 3**, the catalytic hydrogenation of alkenes and alkynes using (benzimidazolylmethyl)amine palladium(II) complexes are discussed. This work demonstrated the influence of the coordinating and non-coordinating solvents in the catalytic hydrogenation of alkenes. The effects of cationic versus neutral complexes are also discussed. Mass spectrometry was used to investigate the mechanistic pathways for the hydrogenation reactions. Furthermore, density functional theory (DFT) studies were used to account for the reactivity trends of the two sets of palladium complexes. The findings of this work have been submitted and accepted at *Inorg. Chim. Acta* **483** (2018) 148-155.

**Chapter 4**, reports the synthesis and characterization of new N<sup>^</sup>O (imino)phenol palladium(II) complexes. This aimed to improve the stability of the first part and involves the use of new hemilabile complexes in hydrogenation reactions of alkenes and alkynes. Indeed, higher catalytic activities and selectivities were observed with this catalytic systems. Density functional theory studies supported the hemi-labile

nature of the ligands, and offered insights into the catalytic activity trends observed. The findings of this work have been submitted and accepted at *J. Organomet. Chem.* **873** (2018) 35-42.

In **Chapter 5**, the synthesis of new N<sup>^</sup>P (diphenylphosphino)benzalidene ethanamine palladium(II) complexes is presented. In this Chapter, we changed from employing a hard-hard donor ligand (N<sup>^</sup>O) to a hard-soft donor ligand (N<sup>^</sup>P), to try and investigate the impact of incorporating a softer-donor P atom in the ligand motif on catalytic behaviour. Indeed, the (diphenylphosphino)benzalidene ethanamine palladium(II) complexes were the most active and selective in the hydrogenation of alkenes and alkynes compared to (benzimidazolylmethyl)amine palladium(II) complexes and (imino)phenol palladium(II) complexes.

**Chapter 6** is an improvement of **Chapter 5** which is aimed at bridging the gap between the homogeneous and heterogeneous catalysis. It describes the synthesis and characterization of water-soluble cationic N<sup>^</sup>P (diphenylphosphino)benzalidene ethanamine palladium(II) complexes. It further discusses the results of their application as catalysts in high pressure homogeneous and biphasic hydrogenation reactions of alkenes and alkynes. It focuses on facilitating the ease of separation of the catalytic products from the reaction mixture and recycling the catalysts. Finally, general conclusions on the key findings of this study and the future prospects are presented in **Chapter 7**.



## RESEARCH OUTPUTS

This thesis is based on the following original publications and conference presentations.

### Publications:

1. Thandeka A. Tshabalala and Stephen O. Ojwach. Tuning the regioselectivity of (benzimidazolylmethyl)amine palladium(II) complexes in the methoxycarbonylation of hexenes and octenes. *Transit. Met. Chem.* **43** (2018) 339-346.
2. Thandeka A. Tshabalala and Stephen O. Ojwach. Kinetics and chemoselectivity studies of hydrogenation reactions of alkenes and alkynes catalyzed by (benzoimidazol-2-ylmethyl)amine palladium(II) complexes. *Inorg. Chim. Acta* **483** (2018) 148-155.
3. Thandeka A. Tshabalala and Stephen O. Ojwach. Hydrogenation of alkenes and alkynes catalysed by N<sup>∞</sup>O (imino)phenol palladium(II) complexes: Structural, kinetics and chemoselectivity studies. *J. Organomet. Chem.* **873** (2018) 35-42.

### Conference presentations

*Tuning the regioselectivity of (benzimidazolylmethyl)amine palladium(II) complexes in the methoxycarbonylation of hexenes and octenes.* Thandeka A. Tshabalala and Stephen O. Ojwach. 28th annual conference of the Catalysis Society of South Africa held at Kwa Maritane Bush Lodge, Pilanesberg in the North-West Province of South Africa. 17 - 18 November 2018

## ABSTRACT

Reactions of *N*-(1H-benzoimidazol-2-ylmethyl-2-methoxy)aniline (**L1**) and *N*-(1H-benzoimidazol-2-ylmethyl-2-bromo)aniline (**L2**) with *p*-TsOH, Pd(AOc)<sub>2</sub> and two equivalents of PPh<sub>3</sub> or PCy<sub>3</sub> produced the corresponding palladium complexes, [Pd(**L1**)(OTs)(PPh<sub>3</sub>)] (**1**), [Pd(**L2**)(OTs)(PPh<sub>3</sub>)] (**2**) and [Pd(**L1**)(OTs)(PCy<sub>3</sub>)] (**3**) respectively in good yields. The new palladium complexes **1-3**, and the previously reported complexes [Pd(**L1**)ClMe] (**4**) and [Pd(**L2**)ClMe] (**5**) gave active catalysts in the methoxycarbonylation of terminal and internal olefins to produce branched and linear esters. The effects of complex structure, nature of phosphine derivative, acid promoter and alkene substrate on the catalytic activities and selectivity have been studied and are herein reported.

The ligands *N*-(1H-benzoimidazol-2-ylmethyl-2-methoxy)aniline (**L1**), *N*-(1H-benzoimidazol-2-ylmethyl-2-bromo)aniline (**L2**), *N*-(1H-benzoimidazol-2-ylmethyl)benzenamine (**L3**) and *N*-(1H-benzoimidazol-2-ylmethylamino)benzenethiol (**L4**), were synthesized following our published literature method. The palladium complexes [Pd(**L1**)Cl<sub>2</sub>] (**6**), [Pd(**L2**)Cl<sub>2</sub>] (**7**) [Pd(**L3**)Cl<sub>2</sub>] (**8**), [Pd(**L4**)Cl<sub>2</sub>] (**9**), [Pd(**L2**)ClMe] (**10**) and [Pd(**L2**)ClPPh<sub>3</sub>]BAr<sub>4</sub> (**11**), were prepared following our recently published procedure. The (benzoimidazol-2-ylmethyl)amine palladium(II) complexes **6-11**, have been employed as catalysts in the homogeneous hydrogenation of alkenes and alkynes under mild conditions. A correlation between the catalytic activity and the nature of the ligand was reaffirmed. Kinetic studies of the hydrogenation reactions of styrene established *pseudo*-first-order

dependence on the styrene substrate. On the other hand, partial orders with respect to H<sub>2</sub> and catalyst concentrations were obtained. The nature of the solvent used, influenced the hydrogenation reactions, in that coordinating solvents resulted in lower catalytic activities. Kinetics and mechanistic studies performed are consistent with the formation of a palladium monohydride active species.

Reactions of 2-(2-methoxyethylimino)ethylphenol (**L5**), 2-(2-hydroxyethylimino)ethylphenol (**L6**), 2-(2-aminoethylimino)ethylphenol (**L7**) and 2-(2-hydroxyethylimino)methylphenol (**L8**) with [PdCl<sub>2</sub>(COD)] afforded the neutral palladium complexes [PdCl<sub>2</sub>(**L5**)] (**12**), [PdCl<sub>2</sub>(**L6**)] (**13**), [PdCl<sub>2</sub>(**L7**)] (**14**), [PdCl<sub>2</sub>(**L8**)] (**15**) respectively. Treatment of complex **12** with PPh<sub>3</sub> gave the cationic complex [Pd(**L5**)ClPPh<sub>3</sub>]<sup>+</sup> (**16**), while reactions of **15** with Pd(OAc)<sub>2</sub>, in the presence of PPh<sub>3</sub> and *p*-TsOH produced the corresponding palladium complex, [Pd(**L5**)(OTs)(PPh<sub>3</sub>)] (**17**). The molecular structure of **15a** (derivative of **15**) contained two bidentate anionic ligand (**L8**). Complexes **12-17** formed active catalysts in hydrogenation of alkenes and alkynes, in which the catalytic activities were largely dependent on the pendant donor atom of the ligand motif. Isomerization reactions were dominant in terminal alkenes hydrogenation reactions, while hydrogenation of alkynes to alkanes occurred in two steps *via* alkene intermediates. Kinetics data were consistent with homogeneous active species. Density functional theory studies supported the hemi-labile nature of the ligands, and offered insights into the catalytic activity trends observed.

Compounds [2-(2-(diphenylphosphino)benzylidene)methoxyethanamine] (**L9**), [2-(2-(diphenylphosphino)benzylideneamino)ethanol] (**L10**), (2-(diphenylphosphino)benzylidene)ethane-1,2-diamine (**L11**) and (2-(diphenylphosphino)benzylidene)diethylethane-1,2-diamine (**L12**) were prepared by a condensation reaction between 2-(diphenylphosphino)benzaldehyde and the corresponding amines. The imino-diphenylphosphino palladium(II) complexes, [PdCl<sub>2</sub>(**L9**)] (**18**), [PdCl<sub>2</sub>(**L10**)] (**19**), [PdCl<sub>2</sub>(**L11**)] (**20**), [PdCl<sub>2</sub>(**L12**)] (**21**) were prepared from the reactions of **L9-L12** with Pd(COD)Cl<sub>2</sub>. On the other hand, reactions of **L9** with Pd(AOc)<sub>2</sub> in the presence of equivalent amounts of *p*-TsOH and PPh<sub>3</sub> afforded [Pd(**L9**)(OTs)(PPh<sub>3</sub>)]<sup>+</sup>TsO<sup>-</sup> (**22**) while subsequent treatment of complex **18** with one equivalent of NaBAR<sub>4</sub> (Ar<sub>4</sub> = 3,5-(CF<sub>3</sub>)<sub>2</sub>C<sub>6</sub>H<sub>3</sub>) in the presence of PPh<sub>3</sub> afforded the cationic complex, [Pd(**L5**)(Cl)(PPh<sub>3</sub>)] BAR<sub>4</sub><sup>-</sup> (**23**). Complexes **18-23** were characterized by mass spectrometry, elemental analysis, <sup>1</sup>H, <sup>13</sup>C and <sup>31</sup>P NMR spectroscopy. Complexes **18-23** were found to be active catalysts in the hydrogenation of alkenes and alkynes in which isomerization of terminal alkenes also occurred. Kinetic experiments, stoichiometry poisoning, mercury poisoning and kinetic reproducible data indicated the homogeneous nature of the active species.

The water-soluble palladium(II) complexes, [Pd(**L9**)(TPPMS)(PPh<sub>3</sub>)]<sup>+</sup>TsO<sup>-</sup> (**24**), [Pd(**L10**)(TPPMS)(OTs)]<sup>+</sup>TsO<sup>-</sup> (**25**), [Pd(**L11**)(TPPMS)(PPh<sub>3</sub>)]<sup>+</sup>TsO<sup>-</sup> (**26**) and [Pd(**L12**)(TPPMS)(PPh<sub>3</sub>)]<sup>+</sup>TsO<sup>-</sup> (**27**) were synthesized from the reactions of **L9-L12** with Pd(AOc)<sub>2</sub> and *p*-TsOH in the presence of PPh<sub>3</sub> followed by adding TPPMS in butanone. The complexes, **24-27**, were highly soluble in methanol, ethanol and water

but were insoluble in chlorinated solvents. Complexes **24-27** were found to form active catalysts for the high pressure hydrogenation of alkenes and alkynes in biphasic media. The complexes were recyclable and retained significant catalytic activities after six cycles. Reaction parameters such as temperature, and aqueous/organic ratio affected the catalyst recycling efficiencies.

## TABLE OF CONTENTS

DECLARATION.....	ii
DEDICATION.....	iii
ACKNOWLEDGEMENTS.....	v
PREFACE.....	vi
RESEARCH OUTPUTS.....	ix
ABSTRACT.....	x
TABLE OF CONTENTS.....	xiv
LIST OF FIGURES.....	xxv
LIST OF SCHEMES.....	xxxii
LIST OF TABLES.....	xxxiv
ABBREVIATIONS.....	xxxvi
<b>CHAPTER 1.....</b>	<b>1</b>
Introduction and literature review of transition metal complexes as catalysts in hydrogenation and methoxycarbonylation reactions.....	1
1.1. Introduction.....	1
1.2. Catalytic methoxycarbonylation of alkenes and alkynes.....	2
1.2.1. Mechanism of palladium (II) catalysed methoxycarbonylation reactions.....	3
1.3. Hydrogenation reactions of alkynes and alkenes.....	6

1.3.1. Heterogeneous catalytic hydrogenation of alkenes and alkynes.....	6
1.3.2. Homogeneous catalytic hydrogenation of alkenes and alkynes.....	9
1.4. Application of transition metal catalysts in catalytic homogeneous hydrogenation reactions.....	10
1.4.1. Rhodium and ruthenium-based catalysts in hydrogenation reactions of alkenes and alkynes.....	11
1.4.1.1. Rhodium-based catalysts in the hydrogenation of alkenes.....	11
1.4.1.2. Ruthenium-based catalyst in the hydrogenation reactions.....	13
1.4.2. Palladium-based catalysts in catalytic hydrogenation reactions.....	15
1.4.2.1. Phosphine-donor palladium complexes.....	15
1.4.2.2. Nitrogen-donor palladium complexes.....	16
1.4.2.3. Hemilabile palladium(II) complexes as hydrogenation catalysts.....	19
1.4.3. Mechanism of the hydrogenation of alkynes with palladium(II) complexes....	22
1.5. Biphasic catalytic hydrogenation reactions of unsaturated hydrocarbons.....	24
1.6. Rationale of study.....	27
1.7. Objectives.....	28
1.7.1. General objectives.....	28
1.7.2. Specific objectives.....	28
1.8. References.....	29

<b>CHAPTER 2.....</b>	<b>35</b>
Tuning the regioselectivity of (benzimidazolymethyl)amine palladium(II) complexes in the methoxycarbonylation of hexenes and octenes.....	35
2.1. Introduction.....	35
2.2. Experimental section.....	37
2.2.1. Materials and methods.....	37
2.2.2. Synthesis of palladium(II) complexes.....	38
2.2.2.1. [Pd(L1)(OTs)(PPh <sub>3</sub> )] (1).....	38
2.2.2.2. [Pd(L2)(OTs)(PPh <sub>3</sub> )] (2).....	38
2.2.2.3. [Pd(L1)(OTs)(PCy <sub>3</sub> )] (3).....	39
2.2.3. General procedure for the methoxycarbonylation reactions.....	39
2.3. Results and discussion.....	40
2.3.1. Synthesis and characterization of the palladium complexes 1-5.....	40
2.3.2. Methoxycarbonylation reactions using palladium complexes 1-5 as catalysts.....	44
2.3.2.1. Effect of catalyst structure and phosphine derivatives.....	44
2.3.2.2. Investigation of the effects of solvent and acid promoter on methoxycarbonylation reactions.....	49
2.3.2.3. Methoxycarbonylation of internal olefins using catalysts 1 and 4.....	52



2.3.2.4. Role of ligand and nature of the active species in methoxycarbonylation reactions.....	56
2.4. Conclusions.....	60
2.5. References.....	61
<b>CHAPTER 3.....</b>	<b>64</b>
Kinetics and chemoselectivity studies of hydrogenation reactions of alkenes and alkynes catalyzed by (benzoimidazol-2-ylmethyl)amine palladium(II) complexes.....	64
3.1. Introduction.....	64
3.2. Experimental section.....	66
3.2.1. Materials and methods.....	66
3.2.2. Density Functional Theory (DFT) studies.....	66
3.2.3. General procedure for the hydrogenation reactions of alkenes and alkynes....	67
3.2.4. General procedure for the Hg-poisoning test.....	68
3.3. Results and discussion.....	68
3.3.1. Hydrogenation reactions of alkenes and alkynes using palladium(II) complexes <b>6-11</b> as catalysts.....	68
3.3.2. Kinetic studies of styrene hydrogenation reactions.....	71
3.3.2.1. Effect of complex structure on catalytic hydrogenation of styrene by <b>6-11</b> .....	71

3.3.2.2.	Effect of catalyst concentration and hydrogen pressure on the kinetics of hydrogenation reactions of styrene using complexes <b>7</b> and <b>11</b> .....	73
3.3.2.3.	Effect of temperature and solvents on styrene hydrogenation kinetics.....	78
3.3.2.4.	Effect of the nature of the alkene and alkyne substrates on styrene hydrogenation kinetics and selectivity.....	80
3.3.3.	Theoretical insights of the hydrogenation reactions of alkenes.....	84
3.4.	Proposed mechanism of the hydrogenation of styrene.....	87
3.5.	Conclusions.....	90
3.6.	References.....	91
<b>CHAPTER 4.</b>	.....	<b>94</b>
	Hydrogenation of alkenes and alkynes catalysed by N <sup>^</sup> O (imino)phenol palladium(II) complexes: structural, kinetics and chemoselectivity studies.....	94
4.1.	Introduction.....	94
4.2.	Experimental section.....	96
4.2.1.	Material, instrumentation and methods.....	96
4.2.2.	Synthesis of (ethylimino)ethylphenol amine ligands and palladium(II) complexes.....	97
4.2.2.1.	2-(2-methoxyethylimino)ethylphenol ( <b>L5</b> ).....	97
4.2.2.2.	2-(2-hydroxyethylimino)ethylphenol ( <b>L6</b> ).....	98
4.2.2.3.	2-(2-aminoethylimino)ethylphenol ( <b>L7</b> ).....	98
4.2.2.4.	2-(2-hydroxyethylimino)methylphenol ( <b>L8</b> ).....	99

4.2.2.5. [2-(2-methoxyethylimino)ethyl)phenol PdCl <sub>2</sub> ] ( <b>12</b> ).....	99
4.2.2.6. [2-(2-hydroxyethylimino)ethyl)phenol)PdCl <sub>2</sub> ] ( <b>13</b> ).....	100
4.2.2.7. [2-(2-aminoethylimino)ethyl)phenol )PdCl <sub>2</sub> ] ( <b>14</b> ).....	100
4.2.2.8. [2-(2-hydroxyethylimino)methyl)phenol)PdCl <sub>2</sub> ] ( <b>15</b> ).....	101
4.2.2.9. [2-(2-methoxyethylimino)ethyl)phenol PdClPPh <sub>3</sub> ] ( <b>16</b> ).....	101
4.2.2.10. [{2-(2-methoxyethylimino)ethyl)phenol}Pd(OTs)(PPh <sub>3</sub> )] ( <b>17</b> ).....	102
4.2.3. General procedure for the hydrogenation reactions of alkenes and alkynes.....	102
4.2.4. General procedure for kinetics experiments.....	103
4.2.5. Density Functional Theoretical (DFT) studies.....	103
4.3. Results and discussion.....	104
4.3.1. Synthesis and characterization of (ethylimino)ethyl)phenol amine ligands and their palladium(II) complexes <b>12-17</b> .....	104
4.3.2. Hydrogenation reactions of alkenes and alkynes catalysed by complexes <b>12-17</b> .....	111
4.3.2.1. Preliminary screening of palladium complexes <b>12-17</b> in molecular hydrogenation of styrene.....	111
4.3.2.2. Influence of complex structure on the kinetics of hydrogenation reactions of styrene.....	112

4.3.2.3. Influence of catalyst concentration on the kinetics of hydrogenation reactions of styrene.....	116
4.3.3. Substrate scope and chemo-selectivity studies using complex.....	123
4.3.4. Evidence of hemi-lability from DFT studies.....	127
4.4. Conclusions.....	130
4.5. References.....	131
<b>CHAPTER 5.....</b>	<b>135</b>
Synthesis, kinetic and mechanistic studies of hydrogenation reactions of alkenes and alkynes catalysed by P <sup>^</sup> N (imino-diphenylphosphino) palladium(II) complexes.....	135
5.1 Introduction.....	135
5.2 Experimental section.....	136
5.2.1. Material, instrumentation and methods.....	136
5.2.2. Synthesis of P <sup>^</sup> N (diphenylphosphino)benzalidene ethanamine ligands and their palladium(II) complexes.....	137
5.2.2.1. [2-(2-(diphenylphosphino)benzylidene)methoxyethanamine] (L9).....	137
5.2.2.2. [2-(2-(diphenylphosphino)benzylideneamino)ethanol] (L10).....	138

5.2.2.3.	(2-(diphenylphosphino)benzylidene)ethane-1,2-diamine ( <b>L11</b> ).....	138
5.2.2.4.	(2-(diphenylphosphino)benzylidene)diethylethane-1,2-diamine ( <b>L12</b> ).....	139
5.2.2.5.	[2-(2-(diphenylphosphino)benzylidene)methoxyethanamine) PdCl <sub>2</sub> ] ( <b>18</b> ).....	140
5.2.2.6.	[2-(2-(diphenylphosphino)benzylideneamino)ethanol PdCl <sub>2</sub> ] ( <b>19</b> ).....	140
5.2.2.7.	[(2-(diphenylphosphino)benzylidene)ethane-1,2-diamine PdCl <sub>2</sub> ] ( <b>20</b> ).....	141
5.2.2.8.	[(2-(diphenylphosphino)benzylidene)diethylethane-1,2-diamine PdCl <sub>2</sub> ] ( <b>21</b> ).....	141
5.2.2.9.	[[2-(2-(diphenylphosphino)benzylidene)methoxyethanamine }Pd(OTs)(PPh <sub>3</sub> )] <sup>+</sup> TsO <sup>-</sup> ( <b>22</b> ).....	142
5.2.2.10.	[[2(diphenylphosphino)benzylidene)methoxyethanamine}PdCl (PPh <sub>3</sub> )]BAr <sub>4</sub> ( <b>23</b> ).....	142
5.2.3.	General procedure for the hydrogenation reactions of alkenes and alkynes.....	143
5.3.	Results and discussion.....	144
5.3.1.	Synthesis and characterization of ligands <b>L9-L12</b> and their palladium complexes <b>18-23</b> .....	144

5.3.2. Hydrogenation reactions using complexes <b>18-23</b> .....	150
5.3.2.1. Effect of complex structure on the hydrogenation reactions of styrene.....	151
5.3.2.2. The dependency of the reaction rate on catalyst concentration.....	153
5.3.2.3. The dependency of the reaction rate on hydrogen pressure with respect to <b>18</b> .....	156
5.3.2.4. The dependency of the reaction rate on the temperature and nature of solvents using complex <b>18</b> .....	158
5.3.2.5. Effect of alkene and alkyne substrates on styrene hydrogenation kinetics and selectivity.....	161
5.3.3. Determination of the true active species: Homogeneous <i>vs</i> heterogeneous.....	163
5.3.3.1. Sub-stoichiometric poisoning tests.....	163
5.3.3.2. Mercury poisoning test.....	164
5.3.3.3. Kinetic reproducibility.....	165
5.4. Proposed mechanism of the hydrogenation of styrene using catalyst <b>18</b> .....	167
5.5. Conclusions.....	170
5.6. References.....	171

<b>CHAPTER 6</b> .....	175
Syntheses of P <sup>N</sup> -donor palladium(II) complexes and their applications as recyclable catalysts in biphasic hydrogenation of alkenes.....	175
6.1. Introduction.....	175
6.2. Experimental section.....	176
6.2.1. Material, instrumentation and methods.....	176
6.2.2. Synthesis of biphasic P <sup>N</sup> (diphenylphosphino)benzalidene ethanamine palladium(II) complexes.....	177
6.2.2.1. [{2-(2-(diphenylphosphino)benzylidene)methoxyethanamine} Pd(OTs)(TPPMS)] <sup>+</sup> TsO <sup>-</sup> ( <b>24</b> ).....	177
6.2.2.2. [{2-(2-(diphenylphosphino)benzylideneamino)ethanol} Pd(OTs)(TPPMS)] <sup>+</sup> TsO <sup>-</sup> ( <b>25</b> ).....	178
6.2.2.3.        [{2-(diphenylphosphino)benzylidene)ethane-1,2-diamine} Pd(OTs)(TPPMS)] <sup>+</sup> TsO <sup>-</sup> ( <b>26</b> ).....	179
6.2.2.4.        [{2-(diphenylphosphino)benzylidene)diethylethane-1,2-diamine}Pd(OTs)(TPPMS)] <sup>+</sup> TsO <sup>-</sup> ( <b>27</b> ).....	179
6.2.3. Hydrogenation reactions.....	180
6.2.3.1. Homogeneous experiments.....	180
6.2.3.2. Biphasic hydrogenation experiments.....	181

6.3. Results and discussion.....	181
6.3.1. Synthesis and characterization of palladium(II) complexes <b>24-27</b> .....	181
6.3.2. High pressure catalytic hydrogenation of olefins.....	185
6.3.3. Biphasic catalysis and catalyst recycling in the hydrogenation of styrene using <b>24-27</b> .....	187
6.3.3.1. Effect of aqueous/organic volume ratios and thermal stability on the biphasic hydrogenation of styrene using complex <b>27</b> .....	191
6.4. Conclusions.....	192
6.5. References.....	193
<b>CHAPTER 7</b> .....	195
General concluding remarks and future prospects.....	195
7.1. General conclusions.....	195
7.2. Future prospects.....	197



## LIST OF FIGURES

<b>Figure 1.1:</b> (S)-Naproxen (1) and (S)-Ibuprofen (2).....	3
<b>Figure 1.2:</b> Rhodium complexes for the homogeneous hydrogenation of alkenes and alkynes.....	13
<b>Figure 1.3:</b> Ruthenium-Carbene complexes in the hydrogenation of 1-hexene.....	14
<b>Figure 1.4:</b> Cationic chelating and monohydride ruthenium(II) complexes for homogenous hydrogenation of alkenes.....	15
<b>Figure 1.5:</b> Phosphine-donor palladium(II) complexes for homogeneous hydrogenation reactions.....	16
<b>Figure 1.6:</b> Bidentate nitrogen-donor palladium(0) complexes for homogeneous hydrogenation of alkynes.....	17
<b>Figure 1.7:</b> Tetradentate pyrrole palladium(II) complexes for homogeneous hydrogenation of phenylacetylene.....	18
<b>Figure 1.8:</b> (Pyrazolylmethyl)pyridine and (pyridyl)benzoazole palladium(II) complexes as homogenous catalysts in the hydrogenation of alkenes and alkynes.....	19
<b>Figure 1.9:</b> Hemi-labile palladium(II) complexes containing tridentate P <sup>N</sup> O, P <sup>N</sup> S and N <sup>N</sup> S ligands.....	21
<b>Figure 1.10:</b> Hemi-labile palladium(II) complexes enched on S <sup>O</sup> O and S <sup>O</sup> O ligands.....	22
<b>Figure 1.11:</b> Cationic water-soluble ruthenium complexes for hydrogenation reactions.....	25
<b>Figure 1.12:</b> Water-soluble transition metal complexes for hydrogenation reactions.....	26
<b>Figure 1.13:</b> Ligands studied in this thesis.....	26

<b>Figure 2.1:</b> <sup>1</sup> H NMR spectrum of complex <b>1</b> .....	42
<b>Figure 2.2:</b> <sup>13</sup> C NMR spectrum of complex <b>2</b> .....	42
<b>Figure 2.3:</b> <sup>31</sup> P NMR spectrum of complex <b>1</b> (a), <b>2</b> (b) and <b>3</b> (c) showing two signals due to possible <i>cis-trans</i> -labilization.....	43
<b>Figure 2.4:</b> Mass spectra of complex [Pd(OTs)( PPh <sub>3</sub> )(L <b>2</b> )] ( <b>2</b> ) showing the <i>m/z</i> ratio at 841 amu corresponding to the molecular ion.....	44
<b>Figure 2.5:</b> GC spectra (A) and MS spectra for the branched ester (B) at a retention time of 4.70 min and linear ester at a retention time of 5.19 min for 1-hexene using complex <b>1</b> as a catalyst.....	45
<b>Figure 2.6:</b> The effect of acid-promoters on percentage conversion and regioselectivity towards branched products using complex <b>1</b> .....	52
<b>Figure 2.7:</b> GC chromatogram of the product obtained from the methoxycarbonylation of <i>trans</i> -2-hexene (a) and <i>trans</i> -octene (b) using catalyst <b>4</b> showing the formation of only branched esters.....	54
<b>Figure 2.8:</b> GC spectra (A) and MS spectra (B) of the branched product obtained from the methoxycarbonylation of <i>trans</i> -2-octene using catalyst <b>1</b> .....	56
<b>Figure 2.9:</b> Nature of the active species in the methoxycarbonylation reactions.....	57
<b>Figure 2.10:</b> (a) <sup>1</sup> H NMR spectrum of complex <b>4</b> . (b) <sup>1</sup> H NMR spectrum obtained from the reactions of complex <b>4</b> with PPh <sub>3</sub> under CO (60 bar) atmosphere in the presence of HCl at 90 °C (catalytic conditions).....	58
<b>Figure 2.11:</b> (a) <sup>13</sup> C NMR (DMSO-d <sub>6</sub> ) spectrum of complex <b>4</b> . (b) <sup>13</sup> C NMR spectrum obtained from the reactions of complex <b>4</b> with PPh <sub>3</sub> under CO (60 bar) atmosphere in the presence of HCl at 90 °C (catalytic conditions).....	59
<b>Figure 2.12:</b> <sup>31</sup> P NMR (DMSO-d <sub>6</sub> ) spectrum of the product obtained in the reaction of complex <b>4</b> under.....	60
<b>Figure 3.1:</b> Neutral and cationic (benzoimidazol-2-ylmethyl)amine palladium (II)	

complexes <b>6-11</b> used as catalysts in the hydrogenation reactions.....	69
<b>Figure 3.2:</b> Plot of % conversion <i>vs</i> time for styrene hydrogenation using <b>6-11</b> .....	69
<b>Figure 3.3:</b> Plot of $\ln[\text{Sty}]_0/[\text{Sty}]_t$ <i>vs</i> time for styrene hydrogenation using <b>6-11</b> .....	72
<b>Figure 3.4:</b> Plot of $\ln[\text{styrene}]_0/[\text{styrene}]_t$ <i>vs</i> time for effect of catalyst concentration using complex <b>7</b> (a) and <b>11</b> (b).....	74
<b>Figure 3.5:</b> Plot of $\ln(k_{obs})$ <i>vs</i> $\ln[7]$ (a) and $\ln[11]$ (b) for the determination of the order of reaction with respect to catalyst <b>7</b> and <b>11</b> in the hydrogenation of styrene.....	75
<b>Figure 3.6:</b> Plot of $\ln[\text{styrene}]_0/[\text{styrene}]_t$ <i>vs</i> time for styrene hydrogenation pressures.....	76
<b>Figure 3.7:</b> Plot of $k_{obs}$ <i>vs</i> $P_{H_2}$ (bar) for the determination of the order of reaction with respect to $H_2$ pressure in the hydrogenation of styrene using catalyst <b>7</b> .....	77
<b>Figure 3.8:</b> Plot of $\ln[\text{styrene}]_0/[\text{styrene}]_t$ <i>vs</i> time for the effect of temperature using <b>7</b> .....	78
<b>Figure 3.9:</b> Arrhenius plot (a) and Eyring plot (b) for the determination of the $E_a = 35.61 \pm 1.6 \text{ kJ mol}^{-1}$ , $\Delta H^\ddagger = 32.98 \pm 1.9 \text{ kJ mol}^{-1}$ , and $\Delta S^\ddagger = -127.9 \pm 1.9 \text{ J mol}^{-1} \text{ K}^{-1}$ for the hydrogenation of styrene using catalyst <b>7</b> .....	79
<b>Figure 3.10:</b> Plot of $\ln[\text{substrate}]_0/[\text{substrate}]_t$ <i>vs</i> time for the effect of substrate using <b>7</b> (a) and <b>11</b> (b).....	81
<b>Figure 3.11.</b> Product distribution over time in the hydrogenation of (a) 1-hexene and catalyst <b>7</b> (b) 1-hexene and catalyst <b>11</b> and (c) phenyl-acetylene using catalyst <b>7</b> .....	84
<b>Figure 3.12:</b> Plot of TOF <i>vs</i> NBO charges for palladium(II) metal atom depicting a linear correlation between catalytic activities of complexes <b>6-10</b> and palladium(II) atom NBO charges.....	87
<b>Figure 3.13:</b> ESI-MS spectra for intermediates <b>7a</b> and <b>7b</b> .....	89

<b>Figure 3.14:</b> $^1\text{H}$ NMR spectra for complex <b>7</b> in the presence of hydrogen at room temperature (a), 20 °C (b) and 60 °C (c).....	90
<b>Figure 4.1:</b> $^1\text{H}$ NMR spectrum in DMSO of <b>L5</b> (a) and complex <b>12</b> (b) showing a shift in the ethylene protons.....	105
<b>Figure 4.2:</b> $^{13}\text{C}$ NMR spectrum in DMSO of <b>L8</b> (a) and its corresponding complex <b>15</b> (b).....	106
<b>Figure 4.3:</b> $^{31}\text{P}$ NMR spectrum in $\text{CDCl}_3$ of complex <b>17</b> displaying two signals consistent with the <i>cis</i> and <i>trans</i> arrangements.....	107
<b>Figure 4.4:</b> ESI-MS for complex <b>14</b> showing m/z signal at 318.9 (80%) corresponding to the fragmentation pattern, $\text{M}^+ - \text{Cl}$ (insert showing mass spectrum of the calculated and found isotopic distribution).....	108
<b>Figure 4.5:</b> Thermal ellipsoid plot (50% probability) of <b>15a</b> illustrating the square planar coordination geometry of the Pd(II) ion.....	110
<b>Figure 4.6:</b> GC chromatogram of the product obtained from the hydrogenation of styrene using catalyst <b>12</b> .....	112
<b>Figure 4.7:</b> Plot of $\ln[\text{Sty}]_0/[\text{Sty}]_t$ vs time for styrene hydrogenation using complexes <b>12-17</b> .....	113
<b>Figure 4.8:</b> Plot of $\ln[\text{Sty}]_0/[\text{Sty}]_t$ vs time to establish the dependency of the rates of the reactions on the catalyst concentrations using catalyst <b>12</b> .....	117
<b>Figure 4.9:</b> Plot of $\ln(k_{\text{obs}})$ vs $\ln[\mathbf{12}]$ for the determination of the order of reaction with respect to catalyst <b>12</b> .....	118
<b>Figure 4.10:</b> Plot of $\ln[\text{Sty}]_0/[\text{Sty}]_t$ vs time to establish the dependency of the rates of the reactions on the dihydrogen pressure using catalyst <b>12</b> .....	121
<b>Figure 4.11:</b> Plot of observed rate constant ( $k_{\text{obs}}$ ) vs hydrogen pressure to determine the order of reaction with respect to $\text{H}_2$ concentration for catalyst <b>12</b> .....	122

<b>Figure 4.12:</b> Arrhenius plot (a) and Eyring plot (b) for the determination of the $E_a = 40.17 \pm 1.6$ kJ/mol, $\Delta H^\ddagger = 37.60 \pm 1.6$ kJ/mol, $\Delta S^\ddagger = -118.91 \pm 1.6$ J/mol K and $\Delta G^\ddagger = 420.8 \pm 1.6$ kJ/mol.....	123
<b>Figure 4.13:</b> Effect of substrate on the kinetics of hydrogenation of alkenes and alkynes using catalyst <b>12</b> .....	124
<b>Figure 4.14:</b> Product distribution over time in the hydrogenation of (a) 1-octene; (b) <i>trans</i> -2-octene and (c) phenyl-acetylene using complex <b>12</b> as a catalyst.....	126
<b>Figure 4.15:</b> Plot of TOF in $\text{mol}_{\text{substrate}} \text{mol}_{\text{catalyst}}^{-1} \text{h}^{-1}$ against Pd-Y( $\text{\AA}$ ) showing a correlation between catalytic activities and Pd-Y( $\text{\AA}$ ) bond lengths.....	130
<b>Figure 5.1:</b> $^1\text{H}$ NMR spectrum in DMSO of <b>L9</b> (a) and complex <b>18</b> (b) showing a shift of the ethylene protons from 3.61 to 4.47.....	145
<b>Figure 5.2:</b> $^{31}\text{P}$ NMR (DMSO- $d_6$ ) spectra of ligand <b>L11</b> (a) and complex <b>20</b> (b) to confirm coordination of the PPh $_2$ to the palladium centre.....	147
<b>Figure 5.3:</b> $^{31}\text{P}$ NMR ( $\text{CDCl}_3$ ) spectrum of complex <b>23</b> .....	148
<b>Figure 5.4:</b> FT-IR spectrum of ligand <b>L10</b> and complex <b>19</b> showing a bathochromic shift in <b>L10</b> to form complex <b>19</b> .....	149
<b>Figure 5.5:</b> ESI-MS showing $m/z$ signal at 490.0 (100%) corresponding to the $[\text{Pd}(\text{L9})\text{Cl}]^+$ fragment of <b>18</b> (insert showing mass spectrum of the calculated and found isotopic distribution) of <b>18</b> .....	150
<b>Figure 5.6:</b> Plot of $\ln[\text{Sty}]_0/[\text{Sty}]_t$ vs time for styrene hydrogenation using <b>18-23</b> .....	152
<b>Figure 5.7:</b> Plot of $\ln[\text{Sty}]_0/[\text{Sty}]_t$ vs time for the effect of catalyst concentration using complex <b>18</b> .....	154
<b>Figure 5.8:</b> Plot of $\ln(k_{\text{obs}})$ vs $\ln[\text{18}]$ for the determination of the order of reaction with respect to catalyst <b>18</b> in the hydrogenation of styrene.....	155
<b>Figure 5.9:</b> Plot of $\ln[\text{Sty}]_0/[\text{Sty}]_t$ vs time for the effect of hydrogen pressure using <b>18</b> .....	157

<b>Figure 5.10:</b> Plot of $k_{obs}$ vs $P_{H_2}$ (bar) for the determination of the order of reaction with respect to $H_2$ pressure in the hydrogenation of styrene using catalyst <b>18</b> .....	158
<b>Figure 5.11:</b> Plot of $\ln[Sty]_0/[Sty]_t$ vs time for the effect of temperature using <b>18</b> .....	159
<b>Figure 5.12:</b> Arrhenius plot (a) and Eyring plot (b) for the determination of the $E_a = 20.50 \pm 0.70$ kJ mol <sup>-1</sup> , $\Delta H^\ddagger = 17.91 \pm 0.98$ kJ mol <sup>-1</sup> , and $\Delta S^\ddagger = -224 \pm 0.98$ J mol <sup>-1</sup> K <sup>-1</sup> for the hydrogenation of styrene using catalyst <b>18</b> .....	160
<b>Figure 5.13:</b> Plot of $\ln[Sty]_0/[Sty]_t$ vs time for the effect of substrate using catalyst <b>18</b> .....	162
<b>Figure 5.14:</b> Plot of $\ln[Sty]_0/[Sty]_t$ vs time for the effect of ligand poisoning using catalyst <b>18</b> and 20% PPh <sub>3</sub> , PCy <sub>3</sub> or CS <sub>2</sub> . ....	164
<b>Figure 5.15:</b> Plot of $\ln[Sty]_0/[Sty]_t$ vs time for the effect of mercury (Hg) using catalyst <b>18</b> and 5 drops of Hg.....	165
<b>Figure 5.16:</b> Plot of $\ln[Sty]_0/[Sty]_t$ vs time for runs 1-4 at [styrene]/[ <b>18</b> ] of 5000 with fixed concentration of styrene of 0.5 mL (4.44 mmol).....	166
<b>Figure 5.17:</b> Kinetic results for catalyst <b>18</b> in the hydrogenation of styrene.....	167
<b>Figure 5.18:</b> ESI-MS spectra for intermediate <b>18a</b> .....	167
<b>Figure 6.1:</b> <sup>1</sup> H NMR spectrum in DMSO of <b>L9</b> (a) and complex <b>24</b> (b) showing a shift of the ethylene protons and the appearance of CH <sub>3</sub> protons of OTs in <b>24</b> .....	183
<b>Figure 6.2:</b> <sup>31</sup> P NMR spectrum of complex <b>25</b> .....	184
<b>Figure 6.3:</b> ESI-MS of complex <b>26</b> showing $m/z$ signal at 973.0 (100%) corresponding to the molecular ion, M <sup>+</sup> (insert showing mass spectrum of the calculated and found isotopic distribution).....	185
<b>Figure 6.4:</b> Plot of $\ln[Sty]_0/[Sty]_t$ vs time for styrene hydrogenation using <b>24-27</b> .....	187

<b>Figure 6.5:</b> Conversion of styrene as a function of cycles by complexes <b>24-27</b> .....	188
<b>Figure 6.6:</b> Plot of TOF <i>vs</i> catalysts <b>24-27</b> for runs 1-6.....	190
<b>Figure 6.7:</b> Effect of aqueous / organic solvent volume ratio and temperature on catalyst recycling using complex <b>27</b> .....	191
<b>Figure 7.1:</b> Heterogeneous palladium(II) complexes based on P <sup>N</sup> chelating agent.....	198
<b>Figure 7.2:</b> proposed structure of asymmetric palladium(II) complexes based on P <sup>N</sup> chelating agent.....	198
<b>Figure 7.3:</b> Prochiral alkenes, 1, 1-di-, tri-, and tetra substituted alkenes.....	199
<b>Figure 7.4:</b> Potential substrate for catalytic hydrogenation reactions.....	199

## LIST OF SCHEMES

<b>Scheme 1.1:</b> Catalytic methoxycarbonylation of alkenes and alkynes.....	2
<b>Scheme 1.2:</b> Proposed mechanisms for the methoxycarbonylation of alkenes.....	4
<b>Scheme 1.3:</b> Catalytic hydrogenation of benzene to cyclohexane using Raney Ni or Co.....	7
<b>Scheme 1.4:</b> Catalytic hydrogenation of cyclohex-3-enecarbaldehyde to cyclohexanecarbaldehyde using supported palladium catalysts.....	8
<b>Scheme 1.5:</b> Catalytic hydrogenation of 2-butyne to butane using platinum catalysts.....	8
<b>Scheme 1.6:</b> Catalytic hydrogenation of 2-butyne to cis-butene using Lindlar catalyst.....	9
<b>Scheme 1.7:</b> Catalytic cycle for the hydrogenation of alkenes by $[\text{Rh}(\text{PPh}_3)_3\text{Cl}]$ complex.....	12
<b>Scheme 1.8:</b> Catalytic cycle for the homogenous hydrogenation of 4-octyne.....	24
<b>Scheme 2.1:</b> Synthetic protocol of (benzimidazolylmethyl)amine palladium complexes.....	40
<b>Scheme 2.2:</b> Possible mechanistic pathway for the formation of methyl and ethyl.....	55
<b>Scheme 3.1:</b> Mechanism for the hydrogenation of styrene catalyzed by <b>7</b> as established from ESI-MS, $m/z$ corresponds to the cationic palladium fragments branched esters from <i>trans</i> -2-hexene and <i>trans</i> -2-octene using catalyst <b>4</b> .....	89
<b>Scheme 4.1:</b> Synthesis of (imino)phenol ligands <b>L5</b> - <b>L8</b> bearing pendant arms.....	104



<b>Scheme 4.2:</b> Synthesis of neutral and cationic palladium (II) complexes <b>12 - 17</b> .....	104
<b>Scheme 4.3:</b> Hemi-labile nature of the ligands (Y = OH, NH <sub>2</sub> , OCH <sub>3</sub> ); a strongly coordinating Y group is likely to reduce the catalytic activity by limiting substrate.....	115
<b>Scheme 5.1:</b> Synthesis of imino-diphenylphosphino ligands <b>L9-L12</b> coordination to the metal centre.....	144
<b>Scheme 5.2:</b> Synthesis of neutral and cationic imino-diphenylphosphino palladium(II) complexes <b>18-23</b> .....	145
<b>Scheme 5.3: Proposed</b> mechanism for the hydrogenation of styrene catalysed by <b>18</b> as deduced from mass spectral data of the reaction samples.....	170
<b>Scheme 6.1:</b> Synthesis of water-soluble imino-diphenylphosphino palladium(II) complexes <b>24-27</b> .....	182

## LIST OF TABLES

<b>Table 2.1:</b> Effect of the complex structure and phosphine derivatives on the methoxycarbonylation of 1-hexene.....	47
<b>Table 2.2:</b> Effect of solvent system on methoxycarbonylation of 1-hexene using complex <b>1</b> .....	50
<b>Table 2.3:</b> Methoxycarbonylation of <i>trans</i> -2-hexene and <i>trans</i> -2-octene catalyzed by complexes <b>1</b> and <b>4</b> .....	53
<b>Table 3.1:</b> Effect of catalyst structure on the hydrogenation of styrene by complexes <b>6-11</b> .....	70
<b>Table 3.2:</b> Effect of catalyst concentration and pressure on the hydrogenation of styrene using catalysts <b>7</b> and <b>11</b> .....	77
<b>Table 3.3:</b> Effect of temperature and solvent on the hydrogenation of styrene using catalyst <b>7</b> .....	80
<b>Table 3.4:</b> Effect of substrate on the catalytic performance of complexes <b>7</b> and <b>11</b> .....	83
<b>Table 3.5:</b> DFT calculated data for palladium(II) complexes using B3LYP/LANL2DZ level of theory.....	85
<b>Table 3.6:</b> DFT-calculated HOMO and LUMO frontier molecular orbitals of palladium(II) complexes <b>7-10</b> using LANL2DZ for palladium and 6-311G for all other atoms.....	86
<b>Table 4.1:</b> Crystal data and structure refinement details for complex <b>15a</b> .....	109
<b>Table 4.2:</b> Effect of catalyst structure on the hydrogenation of styrene by complexes <b>1-6</b> .....	114
<b>Table 4.3:</b> Effect of reaction conditions on the hydrogenation of styrene using catalyst <b>12</b> .....	120
<b>Table 4.4:</b> Effect of substrates on the catalytic activity of catalyst <b>12</b> .....	125

<b>Table 4.5:</b> DFT-calculated HOMO and LUMO frontier molecular orbitals of palladium(II) complexes <b>12b-15b</b> .....	128
<b>Table 4.6:</b> DFT-calculated data for the bifunctional palladium(II) complexes.....	129
<b>Table 5.1:</b> Effect of catalyst structure on the hydrogenation of styrene by complexes <b>18-23</b> .....	151
<b>Table 5.2:</b> Kinetic data for the hydrogenation of styrene catalysed by <b>18</b> .....	156
<b>Table 5.3:</b> Effect of temperature and solvent on the hydrogenation of styrene using <b>18</b> .....	161
<b>Table 5.4:</b> Effect of substrates on the catalytic activity of catalyst <b>18</b> .....	162
<b>Table 5.5:</b> Reproducible kinetic data from the effects of catalyst loading.....	167
<b>Table 6.1:</b> Effect of catalyst structure on the hydrogenation of styrene by complexes <b>24-27</b> .....	186
<b>Table 6.2:</b> Comparison of catalytic activities of complexes <b>24-27</b> in the 1 <sup>st</sup> and 6 <sup>th</sup> recycling experiments.....	190

## ABBREVIATIONS

COD	1,5-cyclooctadiene
d	Doublet
<i>J</i>	coupling constant
m	Multiplet
s	Single
t	Triplet
$\delta$	Chemical shift
DCM	Dichloromethane
ESI	Electron spray ionization
GC	Gas chromatography
GC-MS	Gas chromatography-mass spectrometry
MS	Mass spectrometry
IR	Infrared spectroscopy
MHz	Megahertz
NMR	Nuclear Magnetic Resonance
ppm	Parts per million
TOF	Turn over frequency
<i>p</i> -TsOH	para-toluene sulfonic acid
g	gram(s)
mL	millilitres
mmol	millimoles

## CHAPTER 1

### Introduction and literature review of transition metal complexes as catalysts in hydrogenation and methoxycarbonylation reactions

#### 1.1. Introduction

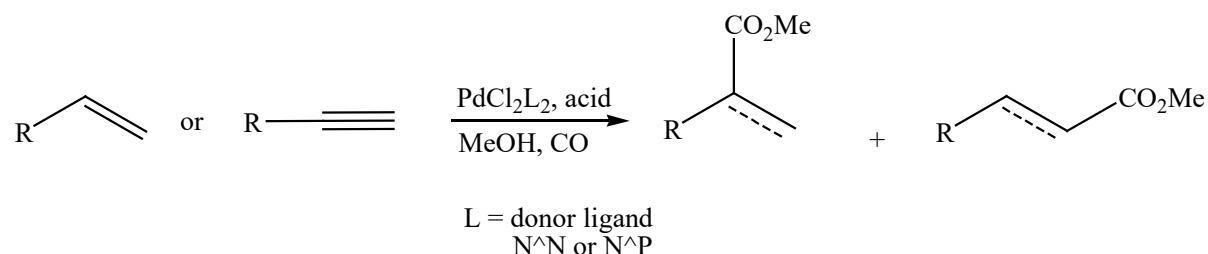
Society faces a growing need to perform chemical reactions by means of less energy, to do them with higher selectivity and less waste. Catalysis plays a very important role in this respect, whereby chemists look for new, more selective catalysts and feasible “atom economic” reactions. The success of basic research in the field of catalysis has a direct effect on solving many fundamental technology, environmental and social problems that solve humanity i.e. the efficient utilization of raw materials (oil, natural gas etc), development of new materials and chemicals, development of systems for environments protection, development of new sources of energy, development of new processes and technologies.<sup>1</sup>

Catalysis have been around for many centuries, even though mankind knew nothing about the chemical process that was involved. This includes, the production of soap, cheese, the fermentation of wine to vinegar, and the leavening of bread are all processes involving catalysis. One of the first formal experiments on catalysis occurred in 1812 by Russian chemist ‘Gottlieb’ Sigismund Constantin Kirchof (1764-1833). He studied the behaviour of starch in boiling water.<sup>2</sup>

Transition metal complexes have been used as catalysts in various industrial processes, in chemical reactions, as well as biological systems.<sup>3</sup> There are many significant chemical processes where transition metal complexes are successfully being employed. These include catalytic hydrogenation and methoxycarbonylation reactions. These chemical reactions are processes used for the addition of hydrogen and carbon monoxide across unsaturated bonds in organic compounds using catalysts. The catalytic hydrogenation and methoxycarbonylation of unsaturated hydrocarbons such as alkenes and alkynes are some of the significant reactions where various transition metal complexes have been applied. It is reported that about 75% of industrially manufactured molecular organic compounds pass through either catalytic hydrogenation or oxidation process.<sup>4</sup>

## 1.2. Catalytic methoxycarbonylation of alkenes and alkynes

Catalytic methoxycarbonylation is a class of carbonylation reactions whereby carbon monoxide is added to a substrate (alkenes, alkynes), with reductive elimination of the products through methanolysis resulting in valuable carboxylic esters (Scheme 1.1).<sup>5</sup>



**Scheme 1.1:** Catalytic methoxycarbonylation of alkenes and alkynes.<sup>5</sup>

The linear and branched carboxylic esters produced are important chemicals used in the manufacturing of solvents, perfumes, drugs and flavouring. The branched esters are of interest in the pharmaceutical industry because they are precursors for an important class of non-steroidal anti-inflammatory drugs such as naproxen<sup>6</sup> and ibuprofen<sup>7</sup> (Fig. 1.1).

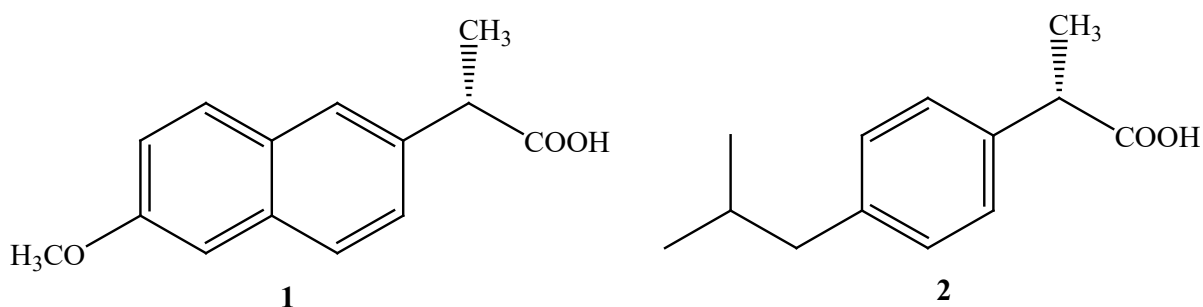
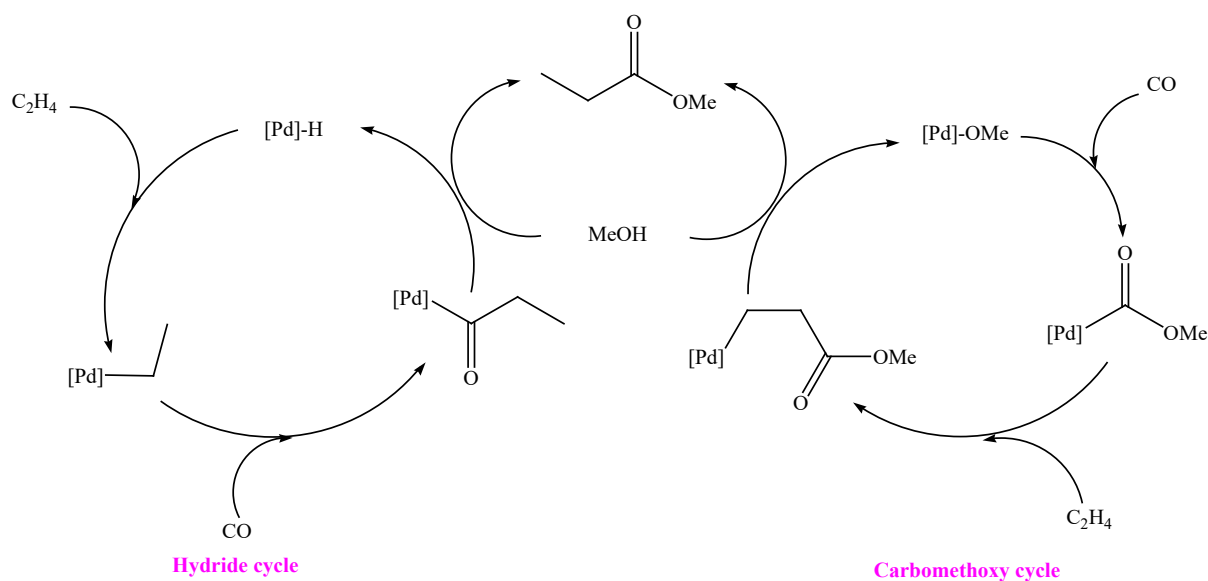


**Figure 1.1:** (S)-Naproxen (**1**) and (S)-Ibuprofen (**2**).<sup>6,7</sup>

### 1.2.1. Mechanism of palladium(II) catalysed methoxycarbonylation reactions

Some years ago, Kiss<sup>8</sup> reported on the Reppe carbonylation of several substrates by palladium–phosphine complexes. It is commonly accepted that in this type of reaction the catalytic cycle starts from the insertion of an olefin into the Pd-hydride bond or into a Pd-carboalkoxy species.<sup>9</sup> Therefore, this clearly indicates that there are two proposed mechanisms (hydride and carbomethoxy) for the methoxycarbonylation reaction. The action of an alkanol on Pd-carbonyl species results in the formation of Pd-carboalkoxy species<sup>10</sup>, while the Pd-hydride species is formed from a hydrogen source (acid, water or hydrogen) and the precursor.<sup>11</sup> A representation of the two mechanisms is shown in Scheme 1.2 and each mechanism has supporting evidence.



**Scheme 1.2:** Proposed mechanisms for the methoxycarbonylation of alkenes.

In the hydride mechanism, the starting point is the Pd-H species and the olefin is inserted into the Pd-H bond, leading to the formation of a Pd-alkyl.<sup>11</sup> Migratory insertion of carbon monoxide results in the formation of a Pd-acyl intermediate. This is followed by nucleophilic attack of the methanol to give either the branched or linear esters depending on the regioselectivity. The carbomethoxy mechanism on the other hand starts by the insertion of carbon monoxide onto the Pd-OMe bond.<sup>12</sup> This is followed by the coordination and insertion of the substrate, which upon methanolysis produces the final products (linear or branched esters).<sup>12</sup>

It has been evident from all the experiments conducted that both the nature of the substrate and the reaction conditions determine which of the two mechanisms occurs. For example, Knifton<sup>13</sup> was able to isolate a hydrido palladium complex,  $\text{HPd}(\text{PPh}_3)_2(\text{SnCl}_3)$  from the carbonylation of olefins using  $\text{PdCl}_2(\text{PPh}_3)_2/\text{SnCl}_2$



catalyst. This gave a strong indication of the hydride mechanism being the route, followed by carbonylation. Noskov *et al.*<sup>14</sup> used IR studies to determine that their system follows a hydride mechanism. This was achieved by performing extensive studies on the kinetics and mechanism of hydrocarboxylation of olefins using a PdCl<sub>2</sub>(PPh<sub>3</sub>)<sub>2</sub> catalyst precursor. They were able to detect a Pd-acyl complex (key intermediate of the hydride mechanism) through *in situ* IR studies.

Verspui *et al.*<sup>15</sup> were able to observe a water soluble Pd-H species, [HPd(TPPTS)<sub>3</sub>]<sup>+</sup> from a mixture of Pd(OAc)<sub>2</sub> and TPPTS using <sup>1</sup>H and <sup>31</sup>P NMR spectroscopy. The Pd-H complex formed Pd-alkyl and Pd-acyl intermediates in the presence of ethane and carbon monoxide. The presence of these intermediates indicated that the system proceeds *via* hydride mechanism because the intermediates are known to be present in the hydride route. Seayad *et al.*<sup>16</sup> performed kinetics and mechanistic studies on the methoxycarbonylation of styrene using cationic palladium complex, Pd(OTs)<sub>2</sub>(PPh<sub>3</sub>)<sub>2</sub>. A cationic hydrido palladium complex, [HPd(CO)PPh<sub>3</sub>]<sub>2</sub><sup>+</sup>(TsO<sup>-</sup>) was isolated and identified using <sup>1</sup>H and <sup>31</sup>P NMR.

A different approach was employed by Cavinato *et al.*<sup>9</sup> whereby they synthesised *trans*-[Pd(COOCH<sub>3</sub>)(PPh<sub>3</sub>)<sub>2</sub>(TsO)], an intermediate formed in the carbomethoxy mechanism. This intermediate was used as a catalyst in the methoxycarbonylation of ethene. The catalyst was unable to catalyse the reaction. Which led to a conclusion that the carbomethoxy mechanism was not the mechanism of choice.

All of these results from the experiments conducted, indicate a greater preference for the hydride mechanism during methoxycarbonylation.

### **1.3. Hydrogenation reactions of alkynes and alkenes**

Hydrogenation reaction is a chemical reaction carried out in special reactors using molecular hydrogen ( $H_2$ ) and a substrate (an alkene or alkyne) in the presence of a transition metal catalyst. The catalytic hydrogenation reactions were contributed to science, by Paul Sabatier (1854-1941).<sup>17</sup> Sabatier together with Victor Grignard were later awarded the 1912 Nobel Price of Chemistry for their achievements in the development of catalytic hydrogenation processes.<sup>17</sup> To date, new discoveries and approaches in high pressure hydrogenation continue to encourage research interest to develop.<sup>18,19</sup>

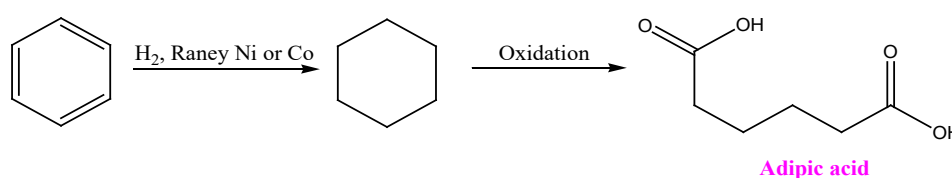
In the absence of transition metal complexes  $H_2$  is unreactive towards alkenes or alkynes. The hydrogenation reactions are carried out using either homogeneous or heterogeneous systems.

#### **1.3.1. Heterogeneous catalytic hydrogenation of alkene and alkynes**

Heterogeneous catalytic hydrogenations are significant reactions that find extensive industrial application in the manufacturing of pharmaceuticals, agrochemicals, fine chemicals, flavours, fragrances and dietary supplements.<sup>20</sup> The reactions are easy to work-up and highly selective, the processes are atom efficient and the catalyst can be

recycled and recovered. It is therefore not surprising that somewhere between 10–20% of the reactions used to produce chemicals today are catalytic hydrogenations.<sup>21</sup>

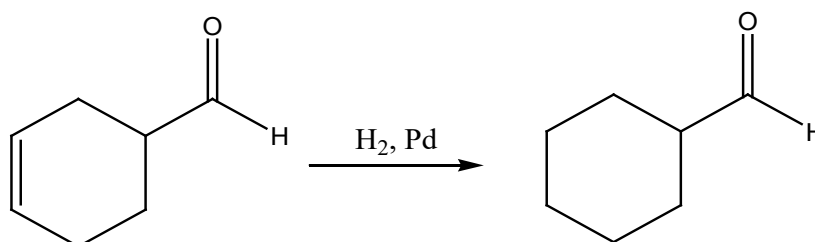
Heterogeneous catalysts may be supported or unsupported. Examples of well-known heterogeneous unsupported catalysts include Raney nickel or cobalt. Raney nickel or cobalt is a fine-grained solid made by chemically extracting the aluminium out of nickel-aluminium or cobalt-aluminium alloys.<sup>22</sup> The Raney nickel or cobalt was discovered in 1926 by American engineer Murray Raney<sup>22</sup> for the hydrogenation of vegetable oils. Later on the Raney nickel or cobalt catalysts were used industrially in the hydrogenation of many organic compounds such as the hydrogenation of benzene to cyclohexane<sup>23</sup> (Scheme 1.3). The cyclohexane thus produced may be used in the synthesis of adipic-acid, a raw material used in the industrial production of polyamides such as nylon.<sup>24</sup>



**Scheme 1.3:** Catalytic hydrogenation of benzene to cyclohexane using Raney Ni or Co.

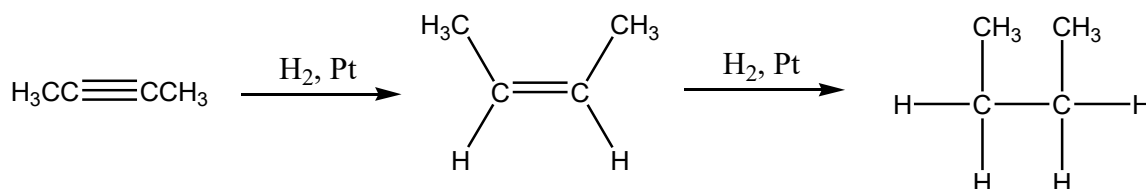
In supported heterogeneous catalysts, the metal is deposited on carbon, graphite, alumina or inorganic salts (e.g. lead salt). Their application depends on the metal used, for example supported palladium can be used in aldehydes for the hydrogenation of

a carbon-carbon double bond without simultaneously reducing a carbonyl bond in the same compound<sup>25</sup> (Scheme 1.4).



**Scheme 1.4:** Catalytic hydrogenation of cyclohex-3-enecarbaldehyde to cyclohexanecarbaldehyde using supported palladium catalysts.

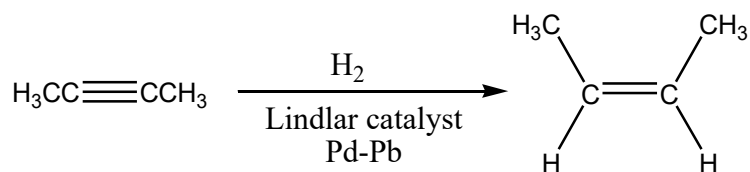
Heterogeneous catalytic hydrogenation of alkynes can be achieved using supported platinum catalysts. For instance, 2-butyne can be converted to *cis*-butene and then butane<sup>26</sup> (Scheme 1.5).



**Scheme 1.5:** Catalytic hydrogenation of 2-butyne to butane using platinum catalysts.

It is very difficult to stop the hydrogenation of an alkyne at the alkene stage, but if the catalyst is suitably deactivated, addition to the triple bond can be achieved without further addition occurring to the resulting double bond. The preferred catalyst for selective hydrogenation of alkynes is palladium partially "poisoned" with a lead salt (Lindlar catalyst).<sup>27,28</sup> This catalyst shows little affinity for adsorbing alkenes and

hence is ineffective in bringing about hydrogenation to the alkane stage<sup>27,28</sup> (Scheme 1.6).



**Scheme 1.6:** Catalytic hydrogenation of 2-butyne to cis-butene using Lindlar catalyst.

Regardless of a wide range of applications of heterogeneous catalysts in hydrogenation, they still suffer from lack of selectivity, relatively high temperatures, difficult mechanistic understanding and to some extent leaching of the active catalysts from the support rendering them less effective with time.<sup>29</sup> For these reasons, homogeneous catalytic systems are being considered as suitable alternatives.<sup>30</sup>

### 1.3.2. Homogeneous catalytic hydrogenation of alkene and alkynes

Homogeneous hydrogenation is one of the most studied fields in organic transformations. The results of these studies have confirmed to be most significant for an understanding of the underlying principles of the activation of substrates (alkenes and alkynes) by transition metal complexes. Over the past 3 decades, homogeneous hydrogenation has been applied in the manufacturing of important pharmaceuticals, where a sophisticated degree of selectivity is mandatory.<sup>31</sup>

Homogeneous catalytic systems are preferred over heterogeneous because they are highly selective, reaction conditions are usually mild (low pressure and temperature), there is ease of tuning reaction sites, they can be studied and the reaction mechanism can be investigated by spectroscopic techniques.<sup>32</sup>

#### **1.4. Application of transition metal catalysts in catalytic homogeneous hydrogenation reactions**

Transition metal catalysed homogeneous hydrogenation reactions are among the most important organic transformations, widely used in the conversion of unsaturated systems to a range of useful domestic and industrial feedstocks.<sup>33,34</sup> Catalysts for these reactions have been derived mainly from platinum<sup>35</sup>, ruthenium<sup>36</sup>, chromium<sup>37</sup>, rhodium<sup>38</sup>, iron<sup>39</sup> and palladium<sup>40</sup> complexes. One of the important properties of these metals that make them suitable for catalytic hydrogenation reactions is the availability of empty *d*-orbitals which can accept electrons from substrates leading to change of oxidation states.<sup>41,42</sup> The ability to change oxidation states make them show high catalytic activities under mild reaction conditions.<sup>43</sup>

In the homogeneous hydrogenation reactions, four steps must be satisfied by the transition metal catalyst: (1) ease of coordination of the alkene or alkyne; (2) ease of coordination of the hydrogen; (3) it must allow the hydrogen to add to the alkene or alkyne; and (4) it must eliminate the hydrogenated product.<sup>44</sup> Furthermore, the major focus in transition metal catalysed homogeneous molecular hydrogenation reactions

has been on ligand design; and the insights gained so far show that the ability to control the catalytic behaviour of these catalyst lies in the coordination environment around the metal atom.

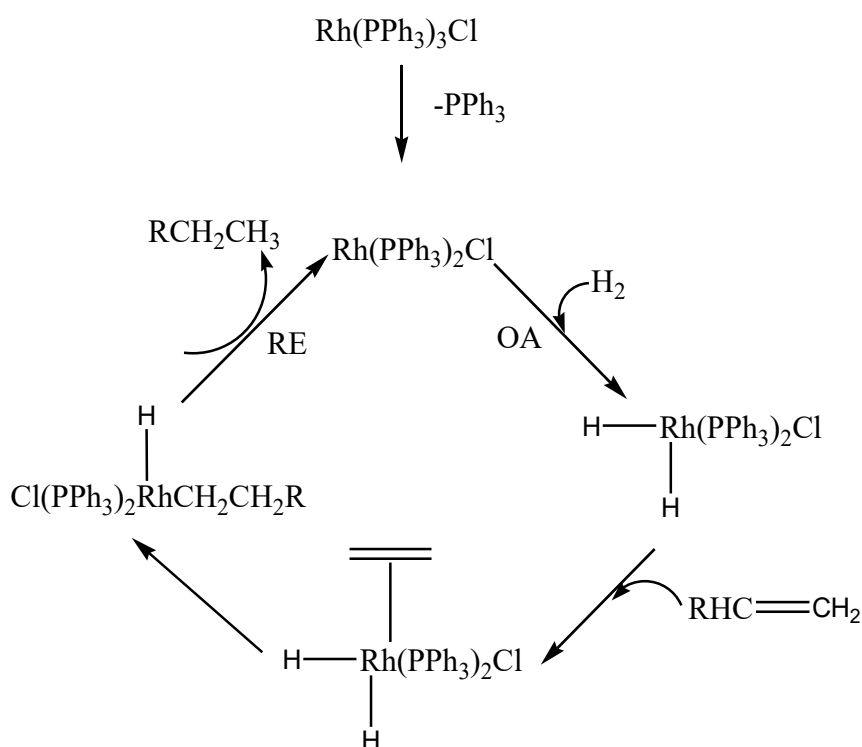
In the next sections, we review the relevant literature on the transition metal catalysts, in particular, ruthenium, rhodium and palladium complexes that have been designed for homogenous hydrogenation reactions. The review will highlight the complex and diverse roles played by a wide range of ligand systems on the performance of transition metal complexes in the catalytic homogeneous hydrogenation reactions.

#### **1.4.1. Rhodium and ruthenium-based catalysts in hydrogenation reactions of alkenes and alkynes**

##### **1.4.1.1. Rhodium-based catalysts in the hydrogenation of alkenes**

Over the past decades homogeneous catalysts have been developed that are clean, often selective, and by maintaining their molecular integrity allow the probing mechanism in detail.<sup>45</sup> A distinctive catalyst, commercially available for many years now is the rhodium(I) complex  $[\text{Rh}(\text{PPh}_3)_3\text{Cl}]$  (Fig. 1.2a) also known as the Wilkinson catalyst.<sup>46</sup> The  $[\text{Rh}(\text{PPh}_3)_3\text{Cl}]$  catalyst is one of the most active homogeneous hydrogenation catalysts known and has been often studied.<sup>47-49</sup> The catalyst is a square-planar, 16-electron complex that readily undergoes oxidative-addition reactions and functions as a hydrogenation catalyst at ambient conditions.

The rates of hydrogenation of several alkenes such as 1-hexene ( $2910 \text{ M}^{-1} \text{ s}^{-1}$ ), 2-methylpent-1-ene ( $2660 \text{ M}^{-1} \text{ s}^{-1}$ ), *cis*-4-methylpent-2-ene ( $990 \text{ M}^{-1} \text{ s}^{-1}$ ), *trans*-4-methylpent-2-ene ( $180 \text{ M}^{-1} \text{ s}^{-1}$ ), cyclohexene ( $3160 \text{ M}^{-1} \text{ s}^{-1}$ ), 1-methylcyclohexene ( $60 \text{ M}^{-1} \text{ s}^{-1}$ ) and styrene ( $9300 \text{ M}^{-1} \text{ s}^{-1}$ ) have previously been determined.<sup>47</sup> The data shows that less hindered olefins are hydrogenated more rapidly,<sup>47</sup> in good agreement with what is expected for olefin coordination.<sup>50</sup> At least 3 mechanistic pathways have been demonstrated for Wilkinson's catalyst. Extensive studies of the influence of various reaction parameters on the reduction rate as well as kinetic studies have led to the following proposed mechanism shown in Scheme 1.7.<sup>44,51</sup>



**Scheme 1.7:** Catalytic cycle for the hydrogenation of alkenes by  $[\text{Rh}(\text{PPh}_3)_3\text{Cl}]$  complex.<sup>12,19</sup>



Just as  $[\text{Rh}(\text{PPh}_3)_3\text{Cl}]$  serves as a model for catalytic hydrogenations by 16-electron square-planar complexes,  $\text{HRh}(\text{PPh}_3)_3\text{CO}$  (Fig. 1.2b) serves as a model for hydrogenations by 18-electron hydride complexes.<sup>31</sup> The carbonyl complex,  $\text{HRh}(\text{PPh}_3)_3\text{CO}$ , has shown considerable selectivity towards terminal alkenes, but is only about half as active as  $[\text{Rh}(\text{PPh}_3)_3\text{Cl}]$ .<sup>52</sup>

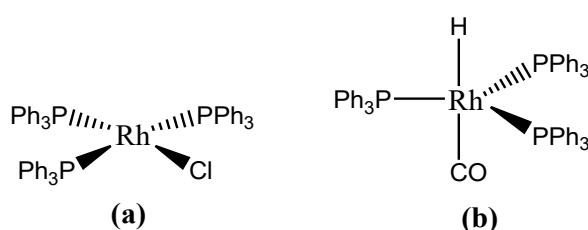


**Figure 1.2:** Rhodium complexes for the homogeneous hydrogenation of alkenes and alkynes.<sup>14,20</sup>

#### 1.4.1.2. Ruthenium-based catalyst in the hydrogenation reactions

Ruthenium(II) complexes have been successfully used as catalysts in the hydrogenation a series of alkenes and alkynes. Examples include,  $[\text{Ru}(\text{PPh}_3)_3\text{Cl}_2]$ ,  $[\text{RuH}(\text{PPh}_3)_3\text{Cl}]$  and  $[\text{RuH}_2(\text{PPh}_3)_4]$ .<sup>53</sup> The ruthenium(II) complexes are almost 15-20 times more active than  $[\text{RhCl}(\text{PPh}_3)_3]$ . However, these compounds are very sensitive to air and are easily poisoned.<sup>53</sup> Other ruthenium complexes of the type  $[\text{HRu}(\text{CO})\text{Cl}(\text{L})_2]$  ( $\text{L} = \text{PPr}^i_3, \text{P}^i\text{Bu}_2\text{Me}$ ) have been reported in the hydrogenation of alkenes and alkynes and are very efficient catalysts.<sup>54,55</sup> For these complexes it has been observed that ( $\text{L} = \text{PPr}^i_3, \text{P}^i\text{Bu}_2\text{Me}$ ) has an effect on the catalytic activity. For example, Yi *et al.* found that the replacement of  $\text{PPr}^i_3$  in  $[\text{HRu}(\text{CO})\text{Cl}(\text{PPr}^i_3)_2]$  with

sterically demanding  $\text{PCy}_3$  ( $[\text{HRu}(\text{CO})\text{Cl}(\text{PCy}_3)_2]$ ), results in high activity ( $\text{TON} = 12\,000\ \text{h}^{-1}$ ) in the hydrogenation of 1-hexene at 4 atm  $\text{H}_2$  and  $50\ ^\circ\text{C}$ .<sup>56</sup>

In a follow-up study, Lee *et al.* observed that the replacement of  $\text{PCy}_3$  in  $[\text{HRu}(\text{CO})\text{Cl}(\text{PCy}_3)_2]$  with IMes in  $[\text{HRu}(\text{CO})\text{Cl}(\text{IMes})_2]$  (Fig. 1.3) leads to a higher catalytic activity from  $\text{TON} = 21\,500\ \text{h}^{-1}$  to  $\text{TON} = 24\,000\ \text{h}^{-1}$  in the hydrogenation of 1-hexene to hexane at  $100\ ^\circ\text{C}$  and 1.0 atm  $\text{H}_2$ .<sup>57</sup>

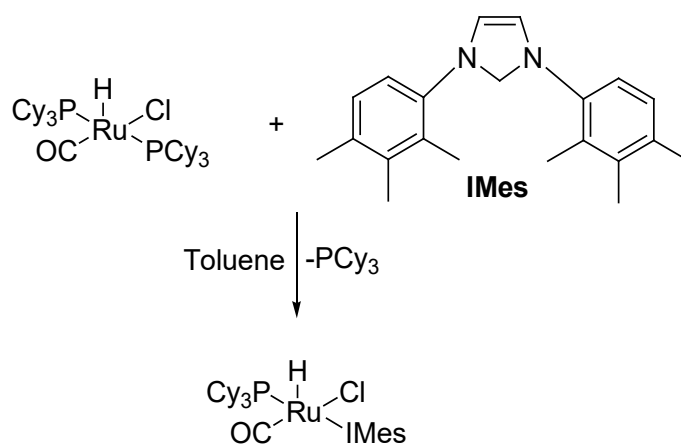


**Figure 1.3:** Ruthenium-Carbene complexes in the hydrogenation of 1-hexene.<sup>26</sup>

Cationic ruthenium complexes have also been reported in the homogeneous hydrogenation of unsaturated hydrocarbons. These include, the cationic NHC ruthenium(II) complexes<sup>58</sup> as well as the monohydride ruthenium(II) complexes<sup>59</sup> (Fig. 1.4). Higher catalytic activities in the catalytic activity of styrene at  $60\ ^\circ\text{C}$  and 60 bar  $\text{H}_2$  were observed with cationic complexes<sup>58</sup> ( $\text{TON} = 35\,000\ \text{h}^{-1}$ ) compared to  $\text{TON} = 27\,000\ \text{h}^{-1}$  for the neutral complexes<sup>56</sup>. This was due to the higher positive charge on

the ruthenium metal in cationic complexes compared to the neutral analogues, therefore, better substrate coordination.<sup>40</sup>

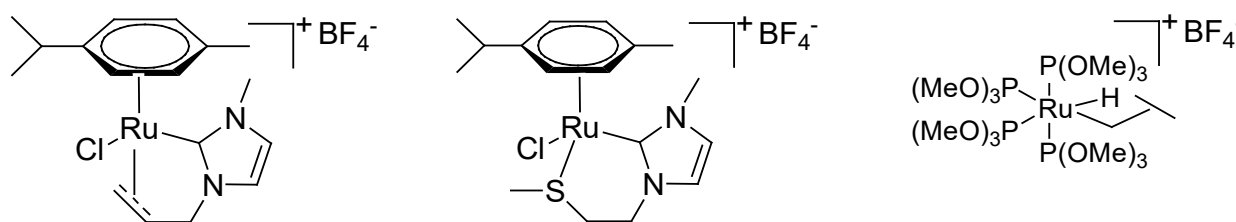


**Figure 1.4:** Cationic chelating and monohydride ruthenium(II) complexes for homogeneous hydrogenation of alkenes.<sup>27,28</sup>

#### 1.4.2. Palladium-based catalysts in catalytic hydrogenation reactions

The interest in current homogeneous catalysis is motivated by the search for efficiency and selectivity in carrying out catalytic transformations. Thus palladium complexes are considered the most effective amongst the reported catalysts in the hydrogenation reactions. They also have the unique ability to selectively hydrogenate alkene and alkynes (to give a mixture of alkenes and alkanes).<sup>40</sup> A variety of ligand designs have been reported such as N<sup>^</sup>N, N<sup>^</sup>O and P<sup>^</sup>O donors that ultimately influence the catalytic activities of the resultant palladium catalysts.

##### 1.4.2.1. Phosphine-donor palladium complexes

Phosphine-donor palladium(II) complexes have been the most widely used as homogeneous catalysts in alkene and alkyne hydrogenation reactions. For example, Drago and Pregosin reported bidentate (2,5-dimethylphospholono)benzene palladium(II) complexes (Fig. 1.5) a homogeneous hydrogenation catalysts for 2-

methyl-2-cyclohexenone to give low conversions of 40% after 24 h.<sup>60</sup> Even though the phosphine-donor palladium(II) catalysts have been successfully used in the homogeneous hydrogenation reactions of alkenes and alkynes, these systems suffer from lack of stability and sensitivity to moisture and air.<sup>61</sup> Therefore suitable alternatives are under probe, which will give better stability in comparison to the phosphine-donor palladium(II) complexes.

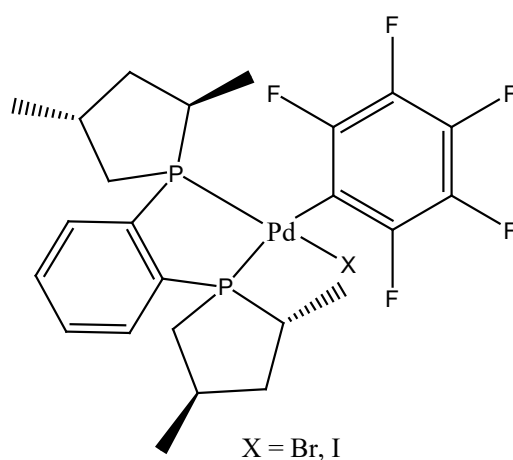


**Figure 1.5:** Phosphine-donor palladium(II) complexes for homogeneous hydrogenation reactions.<sup>29</sup>

#### 1.4.2.2. Nitrogen-donor palladium complexes

Nitrogen-donor palladium catalysts have been investigated for the homogeneous hydrogenation of unsaturated organic compounds with molecular hydrogen. These systems are gaining much prominence due to their better stability and ease of synthesis. The first example of homogeneous palladium(0) catalysts bearing a bidentate nitrogen ligand was the bis(arylimino)acenaphene(bian) (Fig. 1.6a) reported by Van Laren and co-workers.<sup>62</sup> These complexes were able to homogeneously

hydrogenate a wide variety of alkynes to the corresponding (*Z*)-alkenes with good to excellent selectivities (64% - 91%). In addition, the catalysts exhibited stability under hydrogen until the substrate has been semi-hydrogenated to the alkene.<sup>31</sup> For example, hydrogenation of 3-hexyne and 4-octyne at 20 °C and 1 bar of H<sub>2</sub> resulted in high regioselectivity (>99.5 %) for the formation of (*Z*)-3-hexene and (*Z*)-4-octene with excellent yield.<sup>31</sup>

In 2002, van Laren *et al.*<sup>63</sup> further studied the homogeneous hydrogenation of 1-phenyl-1-propyne using pyridine-2-carbaldimine palladium(0) complex (Fig. 1.6b) to afford selectivity for 1-phenyl-1-propyne to (*Z*)-1-phenylpropene of 87%.<sup>32</sup> The nature of the substituent on the imine nitrogen plays a significant role regarding stability of the pre-catalysts under hydrogenation conditions i.e. the better the  $\sigma$ -donating capacity of the substituent, the higher the stability of the catalyst.<sup>32</sup>

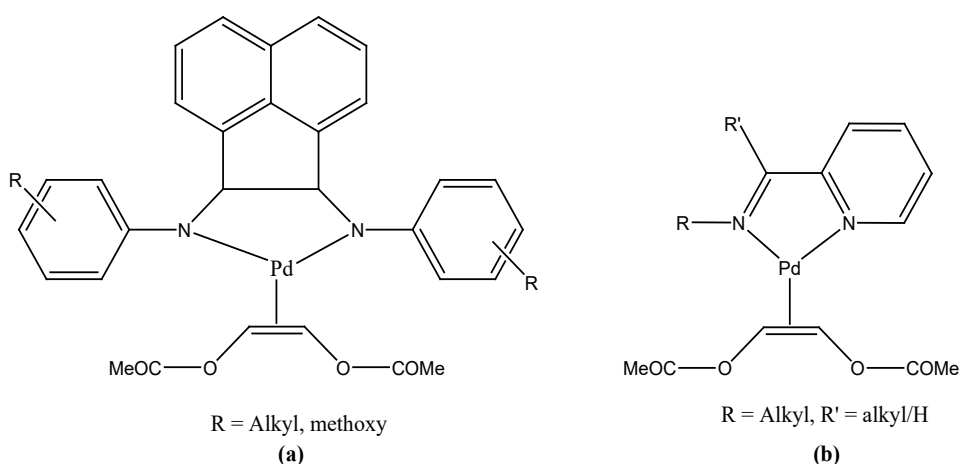


**Figure 1.6:** Bidentate nitrogen-donor palladium(0) complexes for homogeneous hydrogenation of alkynes.<sup>31,32</sup>

The stability of the nitrogen-donor palladium complexes was also observed by Bacchi and co-workers using palladium(II) complexes anchored on Salen (salen, N,N'-bis(salicyldene)ethylenediamine (Fig. 1.7) as catalysts in the homogeneous hydrogenation of phenylacetylene under mild conditions.<sup>64</sup> The Pd(salen) was able to activate molecular hydrogen by heterolytic cleavage, resulting in the protonation of the ligand and formation of a palladium hydride. Finally, transfer of the hydrogen to the substrate gives the hydrogenated product.<sup>33</sup> Moreover, the palladium(II) complexes were able to activate molecular hydrogen to give chemoselectivity of phenylacetylene (15%) to styrene (64%).<sup>33</sup>

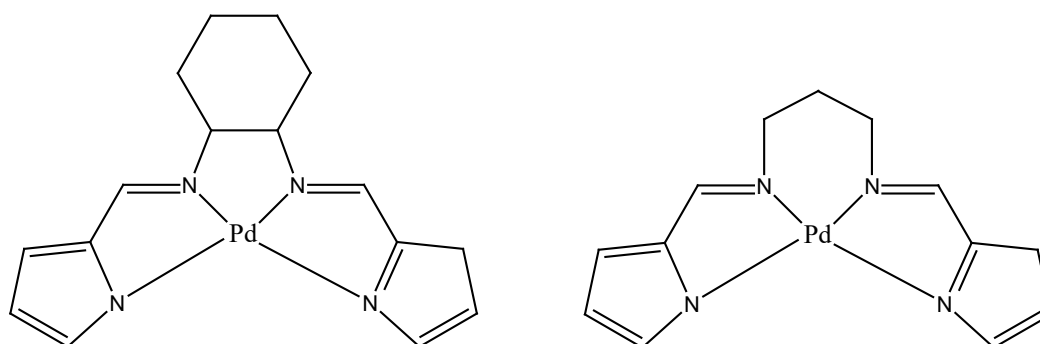


**Figure 1.7:** Tetradentate pyrrole palladium(II) complexes for homogeneous hydrogenation of phenylacetylene.<sup>33</sup>

Recently Ojwach and co-workers employed (pyrazolylmethyl)pyridine<sup>65</sup> (Fig. 1.8a) and (pyridyl)benzoazole<sup>66</sup> (Fig. 1.8b) palladium(II) complexes as homogeneous catalysts in the hydrogenation of alkenes and alkynes. The hydrogenation of styrene to ethylbenzene reached 100% selectivity with these catalysts.<sup>65,66</sup> On the other hand,

the hydrogenation of terminal alkenes are accompanied by isomerization reactions to form internal alkenes. For alkyne reactions, two-step process occur, the first being the production of alkenes followed by alkanes.<sup>34,35</sup>

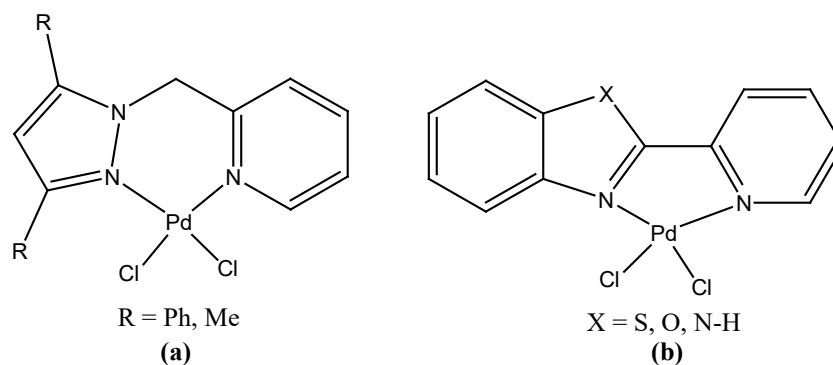


**Figure 1.8:** (Pyrazolylmethyl)pyridine and (pyridyl)benzoazole palladium(II) complexes as homogenous catalysts in the hydrogenation of alkenes and alkynes.<sup>34,35</sup>

#### 1.4.2.3. Hemilabile palladium(II) complexes as hydrogenation catalysts

The term “hemilabile” was first introduced in 1979 by Rauchfuss<sup>67</sup>, however, the phenomenon itself had been observed earlier by Braustein.<sup>68</sup> Hemilabile ligands are polydentate ligands that contain at least two different types of donor groups, one group binds strongly to the metal center, while the other group is weakly coordinating and therefore is easily displaced by the incoming substrate.<sup>69</sup> The incoming substrate should be more strongly coordinating than the hemilabile moiety. The hemilabile ligands systems offer new catalytic properties for the complexes such as higher catalytic activities and stability.<sup>38</sup>

Literature reports on the behavior of hemi-labile ligands have proven to be fruitful in the homogeneous hydrogenation of alkenes and alkynes, as these systems behaved like tridentate as well as bidentate ligands. For example, Bacchi *et al.*<sup>70</sup> applied palladium complexes of the type Pd(PNO)Y (PNO = 2-(diphenylphosphino)benzaldehyde picolinhydrazone, isonicotinhydrazone; Y = CH<sub>3</sub>CO<sub>2</sub>, Cl, I) and Pd(PNS)Y (PNS = 2-(diphenylphosphino)benzaldehyde thiosemicarbazone; Y = CH<sub>3</sub>CO<sub>2</sub>, Cl, I) (Figure 1.9a) in the homogeneous hydrogenation of styrene and phenylacetylene.<sup>39</sup> A correlation between the catalytic activity and the nature of the ligand (Y) group was established.<sup>39</sup> For instance, the hydrazine complexes of the type Pd(PNS)Y are inactive in styrene and phenylacetylene hydrogenation reaction due to the strong chelating effect exerted by the ligand on the metal center. Selectively, Pd(PNO)Y complexes promoted the catalytic hydrogenation of styrene and phenylacetylene.<sup>39</sup> This has been attributed to the presence of the soft donor(phosphorus) which stabilized the complexes during the reaction and a hard donor (nitrogen) allowed the coordination of an unsaturated substrate *via* dissociation of the Pd-O coordination bond.<sup>39</sup> For example, for styrene to ethylbenzene, conversions of 23% - 100% were obtained, whereas, the chemoselectivity of phenylacetylene to styrene gave activities from 31% to 92%.<sup>39</sup> Chemoselectivity is attributed to the inability of the intermediate styrene formed in the hydrogenation of phenylacetylene to coordinate to palladium due to the nature of the hemilabile arm.<sup>39</sup> Therefore, further studies were required to design more effective ligands that can promote higher chemoselectivity with acetylene substrates.<sup>39</sup>



In a follow up study, Bacchi and co-workers<sup>71</sup> designed new palladium(II) complexes of the type Pd(N<sup>^</sup>N<sup>^</sup>S)X (Fig. 1.9b) containing a donor atom with a high affinity (S-donor) for palladium(II) and another one forming a more labile co-ordination bond (pyridine-donor) for the hydrogenation of styrene and phenylacetylene.<sup>40</sup> These new complexes showed improved catalytic activity of 92% from styrene to ethylbenzene.<sup>40</sup> Furthermore, high chemoselectivity 98% from phenylacetylene to styrene were recorded. Kinetic studies of the hydrogenation of phenylacetylene provided clues to help with the elucidation of the catalytic cycle of the reaction.<sup>40</sup>

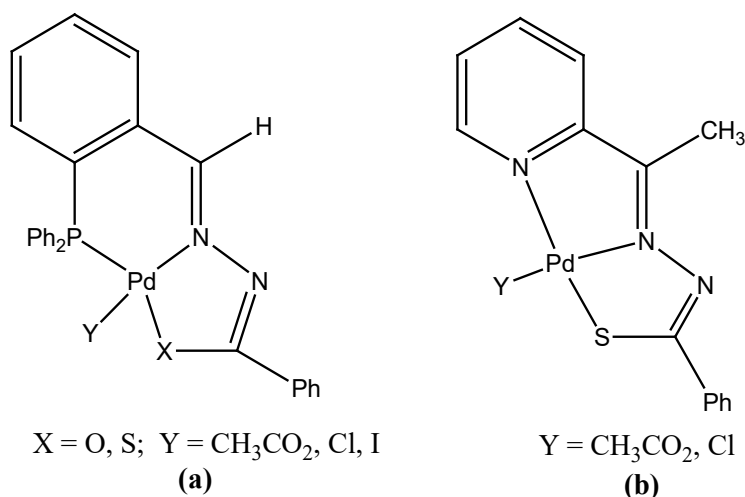


**Figure 1.9:** Hemilabile palladium(II) complexes containing tridentate P<sup>^</sup>N<sup>^</sup>O, P<sup>^</sup>N<sup>^</sup>S and N<sup>^</sup>N<sup>^</sup>S ligands.<sup>40</sup>

Recently Yilmaz *et al.*<sup>72</sup> reported the first examples of olefin hydrogenation catalyzed by palladium(II) complexes containing perfluoroalkylated-thiophene ligands of the type S<sup>^</sup>O<sup>^</sup>S and S<sup>^</sup>O<sup>^</sup>O (Fig. 1.10).<sup>41</sup> These complexes were tested in the homogeneous hydrogenation of styrene and 1-octene.<sup>41</sup> The catalysis results show that the activity is influenced by the nature of the donor atoms. For example, for styrene

as substrate using Pd(S<sup>^</sup>O<sup>^</sup>S)OAc, almost complete hydrogenation was obtained with a TOF of 51 h<sup>-1</sup>, whereas using Pd(S<sup>^</sup>O<sup>^</sup>O)OAc, gives 90% conversion, TOF=372 h<sup>-1</sup>.<sup>41</sup> This data clearly demonstrates the hemilability phenomenon with S<sup>^</sup>O<sup>^</sup>O having two hard and one soft donor atom and S<sup>^</sup>O<sup>^</sup>S contains two soft and one hard donor atoms.<sup>41</sup>

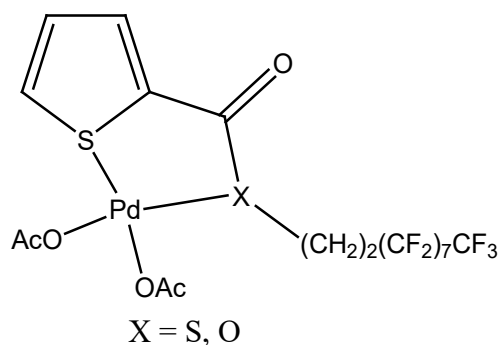


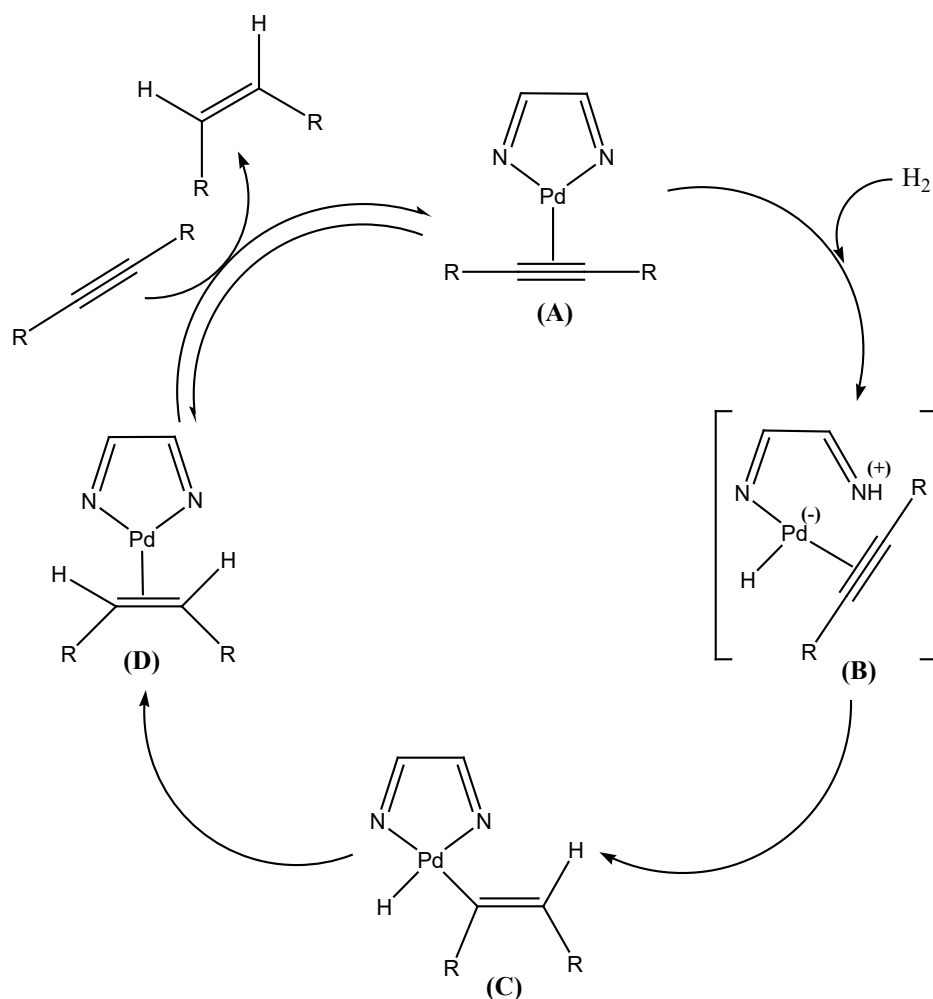
**Figure 1.10:** Hemilabile palladium(II) complexes anchored on S<sup>^</sup>O<sup>^</sup>O and S<sup>^</sup>O<sup>^</sup>S ligands.<sup>41</sup>

### 1.4.3. Mechanism of the hydrogenation of alkynes with palladium(II) complexes

In the absence of a catalyst, the rate of thermodynamically favoured hydrogenation reactions of olefins is insignificant at room temperature. This may be due to symmetry forbidden interaction between hydrogen and olefin molecule.<sup>73</sup> Therefore, activation of both hydrogen and olefin can only take place in the presence of transition metal ion, in this case palladium. Once the molecular hydrogen is activated, the metal-hydride species will be formed.<sup>42</sup> The formation of the metal species have been proposed to occur via three possible mechanisms: oxidative addition, homolytic addition and heterolytic fission of molecular hydrogen to yield a labile hydride.<sup>42</sup> In the oxidative addition, the square-planar d<sup>8</sup> palladium(II) is changed to d<sup>6</sup> octahedral

configuration.<sup>42</sup> In the homolytic addition, the formation of metal-hydride occurs by net homolytic cleavage and this is only promoted by the pentacyanocobaltate anion  $[\text{Co}(\text{CN})_5]^{3-}$ .<sup>74</sup> In the heterolytic fission, the metal-hydrides are formed by a net heterolytic cleavage of a hydrogen molecule and the formal oxidation state of the metal remains unchanged and the anionic ligands are replaced by  $\text{H}^-$  ion.<sup>75</sup>

In 2005, Kluwer *et al.*<sup>76</sup> used kinetic and spectroscopic analysis to propose a plausible mechanism for palladium-catalyzed semi-hydrogenation of 4-octyne (Scheme 1.8).<sup>76</sup> The first step was to form an active intermediate to enter the catalytic cycle. This was achieved by substituting (*vide infra*) coordinated maleic anhydride of the precursor catalyst to form a zerovalent  $\text{Pd}(\text{NN})(\text{alkyne})$  species (**A**). The heterolytic  $\text{H}_2$  activation on species **A** resulted in the formation of intermediate **B**. But this species (**B**) easily collapsed to **C** *via* low-barrier processes according to level DFT calculations, using extended basis set.<sup>77</sup> Attempts were made to detect the palladium-hydride species (**B** or **C**) but they were not successfully detected using PHIP NMR in the hydrogenation of 1-hexyne. Reductive elimination of species **C** led to intermediate **D**. The last step involved catalyst regeneration to initiate a new cycle. The pre-equilibrium between **D** and **A** (*vide infra*) was explained by broken order in 4-octyne (0.65).<sup>77</sup>



**Scheme 1.8:** Catalytic cycle for the homogeneous hydrogenation of 4-octyne.<sup>76</sup>

### 1.5. Biphasic catalytic hydrogenation reactions of unsaturated hydrocarbons

Despite the benefits of homogeneous reactions such as selectivity, there are many challenges that need to be addressed in homogeneous reactions. These include, use of toxic organic solvents, catalyst recovery and contamination of the products.<sup>78</sup> To overcome these challenges, several approaches of heterogenization of homogeneous systems have been discovered.<sup>79</sup> These include, biphasic catalysis, which involves anchoring of single site catalyst on organic and inorganic supports.<sup>80</sup>

In biphasic media, the metal catalyst is heterogeneous with respect to the reactants, but the reaction happens in a homogeneous environment. As such, at the end of a reaction, the catalyst remains in one phase and the product is in the other phase.<sup>81</sup> These biphasic systems allows the catalyst to be recycled without losing its superior homogeneous catalytic activity and selectivity as well as allowing for facile catalyst separation.<sup>81</sup> To date, numerous water-soluble transition metal based catalysts have been employed in biphasic hydrogenation reactions.<sup>80</sup> Examples of water-soluble complexes used in biphasic hydrogenation reactions include cationic 1'-bisquinoine ruthenium complexes (Fig. 1.11)<sup>82</sup>, iridium, rhodium and ruthenium complexes (Fig. 1.12)<sup>80</sup>.

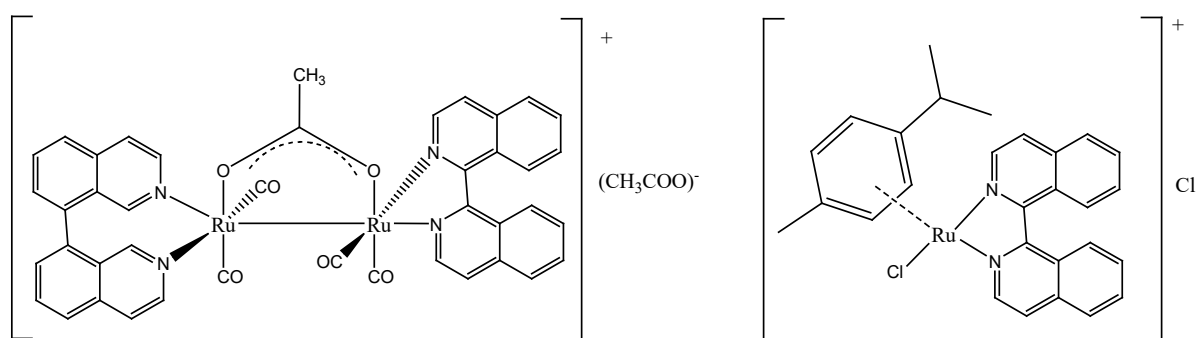


**Figure 1.11:** Cationic water-soluble ruthenium complexes for hydrogenation reactions.<sup>82</sup>

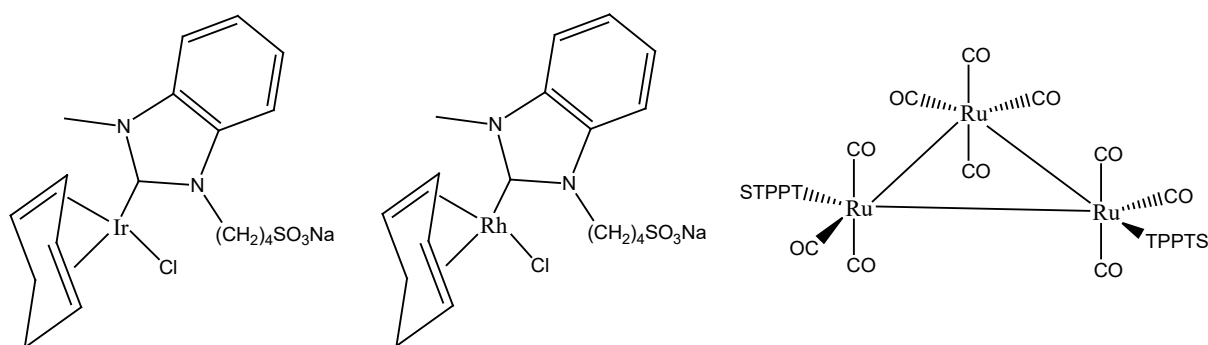


**Figure 1.12:** Water-soluble transition metal complexes for hydrogenation reactions.<sup>80</sup>

Based on the literature review, the current work is aimed at producing a balance between catalyst stability, activity and selectivity. We have thus designed nitrogen-donor ligands (Fig. 1.13a) which are very active, easily prepared under mild reaction conditions and have better stability compared to other donor ligands (phosphine-donor), Chapter 3-4. The nitrogen-donor ligands also allowed regulation of their steric and electronic properties which improves their selectivity and solubility. We have also designed hemilabile ligands (Fig. 1.13b and c) to strike a balance between catalyst activity and stability, Chapter 4-6. The rationale and objectives of this thesis are described in the next sections.

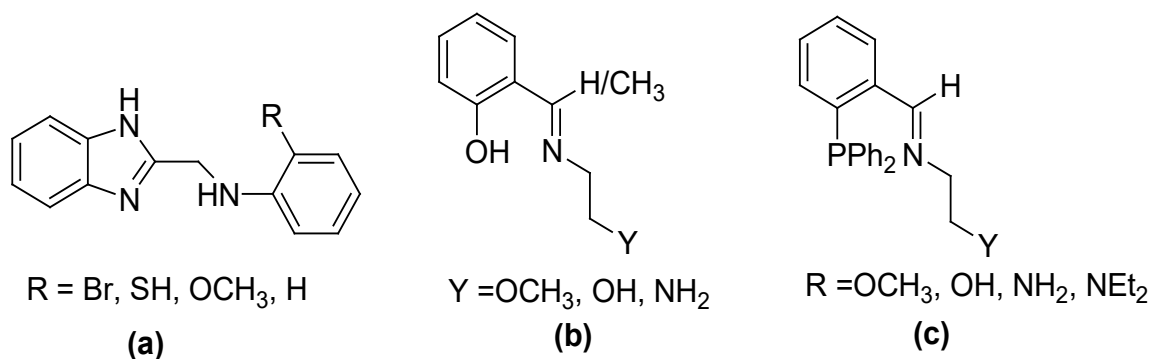


**Figure 1.13:** Ligands studied in this thesis.

## 1.6. Rationale of study

Transition metal alkene and alkyne transformation have played a significant role in petrochemical, fine chemical and pharmaceutical industries. As a result the development of homogeneous catalysts that would transform alkenes and alkynes in catalytic reactions such as the hydrogenation of alkenes and alkynes to saturated hydrocarbons is of great importance. Homogeneous transition metal catalysts offer numerous advantages over well-established heterogeneous catalysts, such as the ease of control of product properties in addition to understanding the mechanisms involved. However, some of the reported homogeneous catalysts often suffer from lack of selectivity and stability due to isomerization in the case of hydrogenation of higher alkenes and alkynes. Due to these reasons, development of new homogeneous catalysts that will eliminate these challenges is a worthy endeavour. Therefore, there is a need for the design of inexpensive, active, stable, selective and recyclable catalytic systems for hydrogenation and methoxycarbonylation of alkenes and alkynes.

This project therefore aimed to design stable and active catalysts of nitrogen and hemilabile palladium complexes for effective homogeneous hydrogenation of alkenes and alkynes. The bridge between homogeneous and heterogeneous catalysis has been attempted by designing single-site catalysts that are water-soluble for biphasic catalysts.

## 1.7. Objectives

From the rationale above, the objectives of this thesis are as follows:

### 1.7.1. General objectives

i) To develop efficient palladium(II) catalysts for the hydrogenation of alkenes and alkynes and to fully understand the catalytic mechanisms and kinetics.

### 1.7.2. Specific objectives

i) To apply the neutral and cationic (benzoimidazol-2-ylmethyl) amine palladium(II) complexes as catalysts in:

- Homogeneous methoxycarbonylation of internal and terminal alkenes
- Homogeneous hydrogenation of alkenes and alkynes.

ii) To synthesise and characterize new palladium(II) complexes bearing (imino)phenol, (diphenylphosphino)benzalidene ethanamine ligands containing potential hemilabile ether or amino pendant donor groups and study their ability to catalyse homogeneous hydrogenation of alkenes and alkynes.

iii) To synthesize and characterize water soluble cationic (diphenylphosphino)benzalidene ethanamine palladium(II) complexes and to apply them in biphasic high-pressure hydrogenation reaction of alkenes.

iv) To carry-out kinetic measurements of the overall catalytic reactions and of as many of the individual mechanistic steps using analytic tools such as NMR spectroscopy and mass spectrometry.



v) To carry-out theoretical calculations (DFT) which will provide important additional information and explain the experimental results.

The results on the work carried-out in attempts to realize the above objectives are described in Chapters 2-6, while Chapter 7 summarizes the major findings and conclusions derived from the entire experiments.

## 1.8. References

- 1 N. Y. Chen, W. E. Garwood and F. G. Dwyer, *Shape selective catalysis in industrial applications*, M. Dekker, 1996.
- 2 Science Classified "Catalysts and Catalysis", 2010, [www.scienceclasified.com](http://www.scienceclasified.com).
- 3 R. A. W. Johnstone, A. H. Wilby and I. D. Entwistle, *Chem. Rev.*, 1985, **85**, 129–170.
- 4 R. Raja, T. Khimyak, J. M. Thomas, S. Hermans and B. F. G. Johnson, *Angew. Chem. Int. Ed.*, 2001, **113**, 4774–4778.
- 5 X. F. Wu, X. Fang, L. Wu, R. Jackstell, H. Neumann and M. Beller, *Acc. Chem. Res.*, 2014, **47**, 1041–1053.
- 6 H. Zhou, J. Cheng, S. Lu, H. Fu and H. Wang, *J. Organomet. Chem.*, 1998, **556**, 239–242.
- 7 E. J. Jang, K. H. Lee, J. S. Lee and Y. G. Kim, *J. Mol. Catal. A Chem.*, 1999, **138**, 25–36.
- 8 G. Kiss, *Chem. Rev.*, 2001, **101**, 3435–3456.
- 9 G. Cavinato, L. Toniolo and A. Vavasori, *J. Mol. Catal. A Chem.*, 2004, **219**, 233–240.
- 10 S. E. E. Profile, palladium complexes containing diphosphine and sulfonated

- ligands for C-C- bond forming reaction. *Memoria presentada por Eduardo J. García Suárez*, 2007.
- 11 I. del Río, C. Claver and P. W. N. M. van Leeuwen, *Eur. J. Inorg. Chem.*, 2001, **2001**, 2719.
  - 12 R. F. Heck, *J. Am. Chem. Soc.*, 1972, **94**, 2712–2716.
  - 13 J. F. Knifton, *J. Org. Chem.*, 1976, **41**, 2885–2890.
  - 14 Y. G. Noskov, A. I. Simonov and E. S. Petrov, *Kinet. Catal.*, 2000, **41**, 511–516.
  - 15 G. Verspui, I. I. Moiseev and R. A. Sheldon, *J. Organomet. Chem.*, 1999, **586**, 196–199.
  - 16 A. Seayad, S. Jayasree, K. Damodaran, L. Toniolo and R. V. Chaudhari, *J. Organomet. Chem.*, 2000, **601**, 100–107.
  - 17 P. Sabatier, *Ind. Eng. Chem.*, 1926, **18**, 1005–1008.
  - 18 H. Ling Poh, F. San ek, Z. ek Sofer and M. Pumera, *Nanoscale*, 2012, **4**, 7006–7011.
  - 19 A. J. McCue, C. J. McRitchie, A. M. Shepherd and J. A. Anderson, *J. Catal.*, 2014, **319**, 127–135.
  - 20 F. Nerozzi, *Platin. Met. Rev.*, 2012, **56**, 236–241.
  - 21 S. A. Jacinto and A. Srebowanta, *Hydrogenation with Low-Cost Transition Metals*, Taylor and Fransis Group, 2015, 77–98.
  - 22 S. Nishimura, *Bull. Chem. Soc. Jpn.*, 1959, **32**, 61–64.
  - 23 A. N. Parvulescu, P. A. Jacobs and D. E. De Vos, *Adv. Synth. Catal.*, 2008, **350**, 113–121.
  - 24 C. Jimenez-Rodriguez, G. R. Eastham and D. J. Cole-Hamilton, *Dalton Trans*, 2005, **2**, 1826–1830.
  - 25 A. J. Bellamy, *The cyclohexane Group*, Supplements to the 2<sup>nd</sup> edistion of Rodd's Chemistry of Carbon Compounds, Modern Comprehensive Treatise, 1975, **11**, 143–173.

- 26 S. D. Jackson, G. D. McLellan, G. Webb, L. Conyers, M. B. T. Keegan, S. Mather, S. Simpson, P. B. Wells, D. A. Whan and R. Whyman, *J. Catal.*, 1996, **162**, 10–19.
- 27 J. Rajaram, A. P. S. Narula, H. P. S. Chawla and S. Dev, *Tetrahedron*, 1983, **39**, 2315–2322.
- 28 J. G. Ulan, E. Kuo, W. F. Maier, R. S. Rai and G. Thomas, *J. Org. Chem.*, 1987, **52**, 3126–3132.
- 29 C. Copÿret, M. Chabanas, R. P. Saint-Arroman and J. Basset, *Angew. Chem. Int. Ed.*, 2003, 156–181.
- 30 E. Peris and R. H. Crabtree, *Coord. Chem. Rev.*, 2004, **248**, 2239–2246.
- 31 P.A. Chaloner, M.A. Esteruelas, Ferenc Joó and L.A. Oro, *React. Kinet. Catal. Lett.*, 1996, **57**, 199–200.
- 32 P. G. Jessop, T. Ikariya and R. Noyori, *Chem. Rev.*, 1999, **99**, 475–493.
- 33 H. E. Hoelscher, W. G. Poynter and E. Weger, *Chem. Rev.*, 1954, **54**, 575–592.
- 34 A. M. Kluwer and C. J. Elsevier, *Homogeneous Hydrogenation of Alkynes and Dienes*, 2008.
- 35 S. Kamiguchi, S. Takaku, M. Kodomari and T. Chihara, *J. Mol. Catal. A Chem.*, 2006, **260**, 43–48.
- 36 T. Suarez and B. Fontal, *J. Mol. Catal. A. Chem.*, 1988, **45**, 335–344.
- 37 M. Chen, Z. Yang, H. Wu, X. Pan, X. Xie and C. Wu, *Int. J. Nanomedicine.*, 2011, **6**, 2873–2877.
- 38 E. Drinkel, A. Briceño, R. Dorta and R. Dorta, *Organometallics*, 2010, **29**, 2503–2514.
- 39 C. Bianchini, A. Meli, M. Peruzzini, P. Frediani, C. Bohanna, M. A. Esteruelas and L. A. Oro, *Organometallics*, 1992, **11**, 138–145.
- 40 E. Negishi, *Handbook of Organopalladium Chemistry for Organic Synthesis*, Wiley & Sons, New York., 2002, **1**, 229–247.

- 41 Q.-A. Chen, Z.-S. Ye, Y. Duan and Y.-G. Zhou, *Chem. Soc. Rev.*, 2013, **42**, 497–511.
- 42 J. J. Verendel, O. Pàmies, M. Diéguez and P. G. Andersson, *Chem. Rev.*, 2014, **114**, 2130–2169.
- 43 W. M. Mo, B. S. Wan and S. J. Liao, *Chine. Chem. Lett.*, 2001, **12**, 817–820.
- 44 J. Halpern, T. Okamoto and A. Zakhariiev, *J. Mol. Catal. A Chem.*, 1977, **2**, 65–68.
- 45 T. A. Tshabalala, S. O. Ojwach and M. A. Akerman, *J. Mol. Catal. A Chem.*, 2015, **406**, 178–184.
- 46 J. A. Osborn, F. H. Jardine, J. F. Young and G. Wilkinson, *J. Chem. Soc. A*
- 47 J. A. Osborn, F. H. Jardine, J. F. Young and G. Wilkinson, *J. Chem. Soc.*, 1966, 1711–1732.
- 48 P. Meakin, J. P. Jesson and C. A. Tolman, *J. Am. Chem. Soc.*, 1972, **94**, 3240–3242.
- 49 J. Halpern, T. Okamoto and A. Zakhariiev, *J. Mol. Catal. A Chem.*, 1978, **2**, 65–68.
- 50 S. Ikeda, *J. Organomet. Chem.*, 1973, **60**, 165–177.
- 51 C. A. Tolman, P. Z. Meakin, D. L. Lindner and J. P. Jesson, *J. Am. Chem. Soc.*, 1974, **96**, 2762–2774.
- 52 P. Pelagatti, A. Bacchi, M. Carcelli, M. Costa, A. Fochi, P. Ghidini, E. Leporati, M. Masi, C. Pelizzi and G. Pelizzi, *J. Organomet. Chem.*, 1999, **583**, 94–105.
- 53 G. Henrici-Olivé and S. Olivé, *Angew. Chem. Int. Ed. English.*, 1976, **15**, 136–141.
- 54 C. Za, B. M. A. Esteruelas, E. Sola, L. A. Oro, U. Meyer and H. Werner, *Angew. Chem.*, 1988, **100**, 1563–1564.
- 55 M. A. Esteruelas, J. Herrero and L. A. Oro, *Organometallics*, 1993, **12**, 2377–2379.
- 56 Q. Liu, H. Zhang and A. Lei, *Angew. Chem. Int. Ed.*, 2011, **50**, 10788–10799.
- 57 H. M. Lee, D. C. Smith, Z. He, E. D. Stevens, C. S. Yi and S. P. Nolan, *Notes*, 2001, 794–797.
- 58 C. Gandolfi, M. Heckenroth, A. Neels, G. Laurency and M. Albrecht,

- Organometallics*, 2009, **28**, 5112–5121.
- 59 P. Ruh, A. Preparation, G. Albetin, A. Stefan, S. Ianelli, G. Peuzzi and E. Bordignon, *Organometallics*, 1991, **10**, 2876–2883.
- 60 D. Drago and P. S. Pregosin, *Organometallics*, 2002, **21**, 1208–1215.
- 61 P. W. N. M. van Leeuwen and J. C. Chadwick, *Homogeneous Catalysts*, Wiley-VCH Verlag GmbH & Co. KGaA, Weinheim, Germany, 2011.
- 62 M. W. Van Laren and C. J. Elsevier, *Angew. Chem. Int. Ed.*, 1999, **38**, 3715–3717.
- 63 M. W. van Laren, M. A. Duin, C. Klerk, M. Naglia, D. Rogolino, P. Pelagatti, A. Bacchi, C. Pelizzi and C. J. Elsevier, *Organometallics*, 2002, **21**, 1546–1553.
- 64 A. Bacchi, M. Carcelli, L. Gabba, S. Ianelli, P. Pelagatti, G. Pelizzi, D. Rogolino, *Inorg. Chim. Acta.*, 2003, **342**, 229–235.
- 65 S. O. Ojwach and A. O. Ogwen, *Transit. Met. Chem.*, 2016, **41**, 539–546.
- 66 S. O. Ojwach, A. O. Ogwen and M. P. Akerman, *Catal. Sci. Technol.*, 2016, **6**, 5069–5078.
- 67 J. C. Jeffrey and T. B. Rauchfuss, *Inorg. Chem.*, 1979, **18**, 2658–2666.
- 68 P. Braunstein, D. Matt, Y. Dusausoy, J. Fischer, A. Mitschler and L. Ricard, *J. Am. Chem. Soc.*, 1981, **103**, 5115–5125.
- 69 L. Canovese and F. Visentin, *Inorg. Chim. Acta.*, 2010, **363**, 2375–2386.
- 70 A. Bacchi, M. Carcelli, M. Costa, A. Leporati, E. Leporati, P. Pelagatti, C. Pelizzi and G. Pelizzi, *J. Organomet. Chem.*, 1997, **535**, 107–120.
- 71 P. Pelagatti, A. Bacchi, M. Carcelli, M. Costa, A. Fochi, P. Ghidini, E. Leporati, M. Masi, C. Pelizzi and G. Pelizzi, *J. Organomet. Chem.*, 1999, **583**, 94–105.
- 72 F. Yilmaz, A. Mutlu, H. Ünver, M. Kurta and I. Kani, *J. Supercrit. Fluids.*, 2010, **54**, 202–209.
- 73 R. H. Crabtree, *The organometallic chemistry of the transition metals*, Wiley, 2009.

- 74 C. Aubert, R. Durand, P. Geneste, C. M.-J. of Catalysis and undefined 1988, Elsevier.
- 75 M. M. T. Khan, *Activation Of Small Inorganic Molecules*, Elsevier Science, 1974.
- 76 A. M. Kluwer, T. S. Koblenz, T. T. Jonischkeit, K. Woelk and C. J. Elsevier, *J. Am. Chem. Soc.*, 2005, **127**, 15470–15480.
- 77 A. Dedieu, S. Humbel, C. J. Elsevier and C. Grauffel, *Theor. Chem. Acc.*, 2004, **112**, 305–312.
- 78 I. W. Davies, L. Matty, D. L. Hughes and P. J. Reider, *J. Am. Chem. Soc.*, 2001, 10139–10140.
- 79 S. Alexander, V. Udayakumar and V. Gayathri, *J. Mol. Catal. A Chem.*, 2009, **314**, 21–27.
- 80 C. Daguenet, R. Scopelliti and P. J. Dyson, *Organometallics*, 2004, **23**, 4849–4857.
- 81 A. Andriollo, *Inorg. Chim. Acta.*, 2381995, **238**, 187–192.
- 82 H. Syska, W. A. Herrmann and F. E. Kühn, *J. Organomet. Chem.*, 2012, **703**, 56–62.

## CHAPTER 2

### **Tuning the regioselectivity of (benzimidazolymethyl)amine palladium(II) complexes in the methoxycarbonylation of hexenes and octenes**

This chapter is adapted from the paper published in *Trans. Met. Chem.* 43 (2018) 339–346 and is based on the experimental work of the first author, Thandeka A Tshabalala. Copyright © 2018 springer. The contributions of the first author include: syntheses and characterization of the compounds, methoxycarbonylation reactions and drafting of the manuscript.

#### **2.1. Introduction**

Transition-metal catalysed carbonylation reactions have become an important tool in both laboratory and industrial organic synthesis for the formation of carbonyl compounds such as esters, amides, ketones and aldehydes<sup>1-4</sup>. To date, palladium complexes are the most widely used catalysts in methoxycarbonylation of olefins due to their high catalytic activities, thermal stability and superior selectivities<sup>5</sup>. For instance, under low pressures of carbon monoxide and moderate temperatures, some of these catalyst systems show high regioselectivity of up to 90% towards either linear or branched ester<sup>6-11</sup>.

Traditionally, phosphine-donor ligands have been used in the preparation of palladium catalysts in the methoxycarbonylation reactions<sup>12</sup>. Another ligand design that is gaining momentum as suitable alternatives to the phosphine systems, are the mixed nitrogen-phosphine donors due to their relative tolerance to impurities, ease of

syntheses and affordability. Such examples include palladium complexes of the type  $[\text{PdCl}_2(\text{Ph}_2\text{PNHpy-}k_2\text{-}P,N)]$  and  $[\text{PdCl}(\text{Ph}_2\text{PNHpy-}k_2\text{-}P,N)(\text{PPh}_3)]\text{Cl}$  which give active and stable catalysts in the methoxycarbonylation of styrene.<sup>5</sup>

From literature reports, it has been established that regioselectivity towards either the branched or linear esters can also be fine-tuned by variation of the steric properties of the auxiliary phosphine ligands.<sup>13-14</sup> In addition, the use of chelating or monodentate phosphine derivatives is known to significantly influence the activity and regioselectivity of the resultant catalysts.<sup>10-11</sup> In our recent contribution, we reported the use of palladium complexes of *N*-(benzoimidazol-2-ylmethyl)amine ligands as catalysts in the methoxycarbonylation of terminal olefins<sup>16</sup>. These complexes show moderate catalytic activities but with rather low regioselectivity giving almost equal proportions of branched and linear esters. In attempts to improve the regioselectivity of these catalysts, we have now modified the complex structure by fine-tuning the basicity of the phosphine ligands in the metal coordination sphere. In addition, internal olefin substrates have been employed to probe the effect of the position of the double bond on regioselectivity of the ester products. Thus, in this contribution, the effect of complex structure, different phosphine derivatives, acid promoter, solvent system and olefin substrates on the methoxycarbonylation reactions have been investigated. In addition, studies of the nature of active species have been performed and will be discussed.



## 2.2. Experimental section

### 2.2.1. Materials and methods

All moisture and air sensitive reactions were performed using standard Schlenk line techniques. All solvents were purchased from Merck and distilled under nitrogen in the presence of suitable drying agents: diethyl ether, hexane and toluene were dried over sodium wire and benzophenone, methanol and absolute ethanol over calcium oxide, while dichloromethane was dried and distilled over phosphorus pentoxide. The chemicals; potassium iodide, sodium hydroxide and potassium hydroxide were purchased from Merck, while deuterated chloroform, styrene, 1-hexene, *trans*-2-hexene, *trans*-2-octene, *p*-TsOH, hydrochloric acid, Pd(OAc)<sub>2</sub> (98%), PPh<sub>3</sub>, 2-methoxyaniline (≥99.5%) and 2-bromoaniline (98%) were purchased from Sigma-Aldrich and used without further purification. The ligands *N*-(1H-benzoimidazol-2-ylmethyl-2-methoxy)aniline (**L1**) and *N*-(1H-benzoimidazol-2-ylmethyl-2-bromo)aniline (**L2**) were synthesized following the published literature method<sup>17</sup>. The palladium complexes [Pd(**L1**)ClMe] (**4**) and [Pd(**L2**)ClMe] (**5**) were prepared following our recently published procedure<sup>16</sup>. Nuclear magnetic resonance spectra were acquired at 400 MHz for <sup>1</sup>H, 100 MHz for <sup>13</sup>C and 162 MHz for <sup>31</sup>P on a Bruker Avance spectrometer equipped with Bruker magnet (9.395 T). All coupling constants are reported in Hertz, Hz. The mass spectra (ESI-MS) were recorded on a Waters API Quattro Micro spectrometer, using 50% MeOH/DMSO, 16-36 V cone voltage, source (720 V) and desolvation temperature of 450 °C. Elemental analyses were carried out using CHNS-O Flash 2000 thermoscientific analyzer. GC-MS analyses were conducted on a micromass LCT premier mass spectrometer.

## 2.2.2. Synthesis of palladium(II) complexes

### 2.2.2.1. $[Pd(L1)(OTs)(PPh_3)]$ (**1**)

To a solution of **L1** (0.11 g, 0.44 mmol) in chloroform (5 mL) was added dropwise a solution of Pd(AcO)<sub>2</sub> (0.10 g, 0.44 mmol) in chloroform (10 mL) followed by a solution of PPh<sub>3</sub> (0.23 g, 0.89 mmol) and p-TsOH (0.07 g, 0.44 mmol) in chloroform (10 mL) and stirred at room temperature for 24 h. The organic volatiles were removed *in vacuo* followed by recrystallization of the crude product from CH<sub>2</sub>Cl<sub>2</sub>-hexane solvent system to give a light yellow solid. Yield = 0.28 g (79%). <sup>1</sup>H NMR (CDCl<sub>3</sub>): δ<sub>H</sub> (ppm): 2.10 (s, 3H, OCH<sub>3</sub>); 2.32 (s, 3H, CH<sub>3</sub>-OTs); 5.33 (s, 2H, CH<sub>2</sub>); 7.02-7.16 (m, 4H, Ph-Aniline; 4H, Ph-Benz); 7.30-7.42 (m, 2H, Ph-OTs); 7.44-7.52 (m, 8H, Ph-PPh<sub>3</sub>); 7.60-7.69 (m, 7H, Ph-PPh<sub>3</sub>); 7.74-7.82 (m, 2H, Ph-OTs). <sup>13</sup>C NMR (CDCl<sub>3</sub>): δ (ppm): 24.30; 39.00; 55.92; 114.56; 115.10; 118.23; 121.95; 123.00; 128.03; 128.88; 128.91; 129.11; 130.46; 137.37; 137.45; 137.92; 138.95; 141.52; 142.22; 144.70; 146.81. <sup>31</sup>P NMR (CDCl<sub>3</sub>): δ (ppm): 29.42; 23.27. MS (ESI) m/z (%) 791 (M<sup>+</sup>, 93%). Anal. Calc. for C<sub>39</sub>H<sub>34</sub>N<sub>3</sub>O<sub>4</sub>PPdS.CHCl<sub>3</sub>: C, 53.53; H, 3.93; N, 4.68. Found: C, 53.75; H, 3.92; N, 4.91.

### 2.2.2.2. $[Pd(L2)(OTs)(PPh_3)]$ (**2**)

Complex **2** was synthesized following the procedure described for **1** using Pd(AcO)<sub>2</sub> (0.1 g, 0.44 mmol), **L2** (0.13 g, 0.44 mmol), p-TsOH (0.07 g, 0.44 mmol), PPh<sub>3</sub> (0.23 g, 0.89 mmol). Yield = 0.35 (93%). <sup>1</sup>H NMR (CDCl<sub>3</sub>): δ<sub>H</sub> (ppm): 2.29 (s, 3H, CH<sub>3</sub>-OTs); 5.42 (s, 2H, CH<sub>2</sub>); 6.92-7.09 (m, 4H, Ph-Aniline); 7.34-7.41 (m, 4H, Ph-Benz); 7.46-7.50 (m, 2H, Ph-OTs); 7.54-7.62 (m, 6H, PPh<sub>3</sub>); 7.64-7.70 (m, 9H, PPh<sub>3</sub>); 7.72-7.84 (m, 2H, Ph-OTs). <sup>13</sup>C NMR (CDCl<sub>3</sub>): 24.3; 52.61; 114.30; 114.55; 115.72; 118.10; 119.44; 127.38; 128.00; 128.63; 128.80; 128.91; 130.43; 132.55; 137.30; 137.46; 146.81. <sup>31</sup>P NMR (CDCl<sub>3</sub>):

$\delta$  (ppm): 29.55; 23.23. MS (ESI)  $m/z$  (%) 841 ( $M^+$ , 69%). Anal. Calc. for  $C_{38}H_{31}BrN_3O_4PPdS \cdot 0.5CHCl_3$ : C, 52.15; H, 3.58; N, 4.74. Found: C, 52.59; H, 3.30; N, 4.80.

### 2.2.2.3. $[Pd(L1)(OTs)(PCy_3)]$ (**3**)

Complex **3** was synthesized following the procedure described for **1** using  $Pd(AcO)_2$  (0.1 g, 0.44 mmol), **L1** (0.11 g, 0.44 mmol), *p*-TsOH (0.15 g, 0.44 mmol),  $PCy_3$  (0.24 g, 0.89 mmol). Yield = 0.38 (91%).  $^1H$  NMR ( $CDCl_3$ ):  $\delta_H$  (ppm): 1.24-1.28 (m, 13H,  $PCy_3$ ); 1.64-1.70 (m, 17H,  $PCy_3$ ); 1.76-1.86 (s, 3H,  $OCH_3$ ); 1.93 (s, 3H,  $CH_3-OTs$ ); 4.84 (s, 2H,  $CH_2$ ); 6.88-7.02 (m, 4H, Ph-Aniline); 7.10-7.22 (m, 4H, Ph-Benz); 7.48-7.56 (m, 4H, Ph- $OTs$ ).  $^{13}C$  NMR ( $CDCl_3$ ): 4.00; 27.20; 28.30; 30.90; 39.10; 55.90; 114.50; 115.30; 118.30; 121.90; 123.00; 128.10; 129.10; 130.10; 132.60; 137.90; 138.90; 141.50; 144.70; 149.80.  $^{31}P$  NMR ( $CDCl_3$ ):  $\delta$  (ppm): 48.53; 53.83. MS (ESI)  $m/z$  (%) 810 ( $M^+$ , 51%). Anal. Calc. for  $C_{39}H_{52}N_3O_4PPdS \cdot CHCl_3$ : C, 52.97; H, 5.96; N, 4.52. Found: C, 53.12; H, 5.57; N, 4.37.

### 2.2.3. General procedure for the methoxycarbonylation reactions

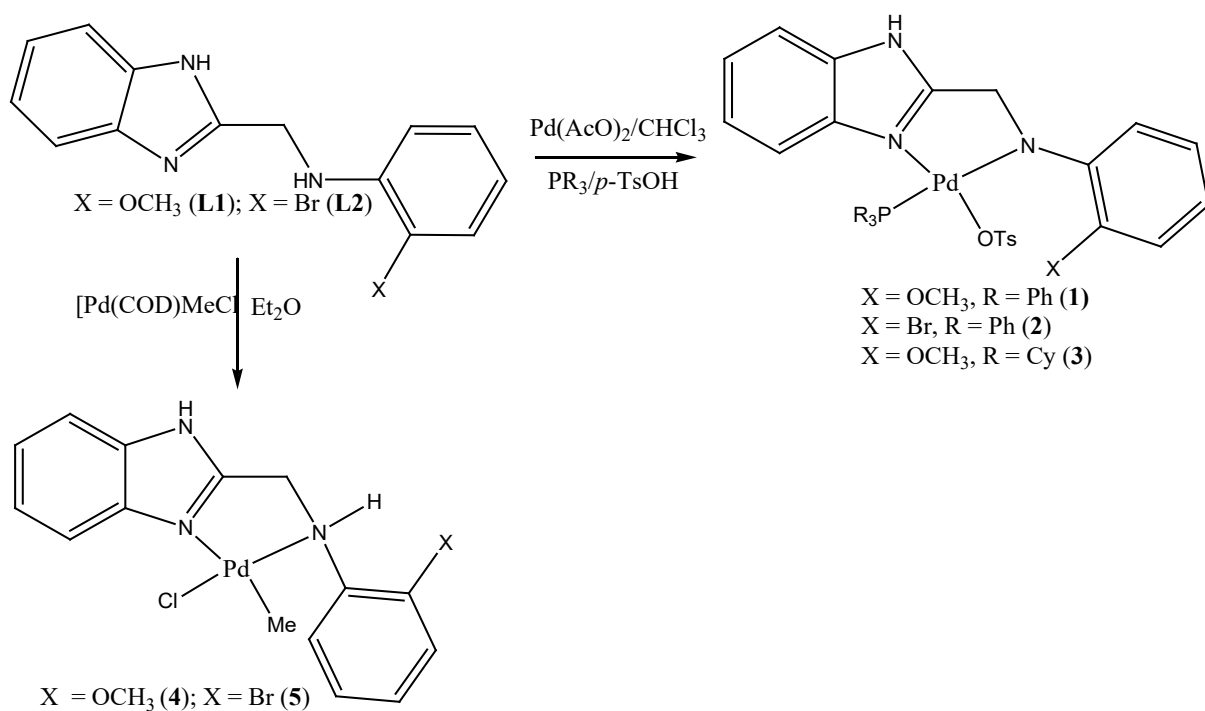
The catalytic methoxycarbonylation reactions were performed in a stainless steel autoclave equipped with temperature control unit and a sample valve. In a typical experiment, complex **1** (22.49 mg, 0.08 mmol),  $PPh_3$  (0.04 g, 0.16 mmol), HCl (0.02 mL, 0.80 mmol) and 1-hexene (2 mL, 15.90 mmol) were dissolved in a mixture of methanol (20 mL) and toluene (40 mL). The reactor was evacuated and the catalytic solution was introduced to the reactor *via* a cannula. The reactor was purged three times with CO, and then set at the required pressure, heated to the desired temperature and the

reaction stirred at 500 rpm. At the end of the reaction time, the reaction was cooled, excess CO was vented off and the samples drawn for GC analysis to determine the percentage conversion of the alkene substrate to esters. GC-MS analyses were run under the following standard chromatography conditions: -25 m CPSil 19 capillary column, 1.2 mm film thickness, Helium carrier column gas 5 psi, injector temperature 250 °C, oven program 50 °C for 4 minutes rising to 200 °C at 20 °C/ min and holding at 200 °C. The identities of the ester products were assigned using standard authentic samples and mass spectral data.

## **2.3. Results and discussion**

### **2.3.1. Synthesis and characterization of the palladium complexes 1-5**

Ligands **L1** and **L2** were prepared by reactions of 2-(chloromethyl)benzoimidazole with the appropriate aniline derivatives following previously reported literature method <sup>17</sup>. Subsequent treatments of **L1** and **L2** with *p*-TsOH, Pd(AcO)<sub>2</sub> and two equivalent of PPh<sub>3</sub> or PCy<sub>3</sub> according to the procedure described by Jaysree *et. al.* <sup>18</sup> afforded the palladium(II) compounds **1-3** respectively in good yields (Scheme 2.1). Complexes **4** and **5** were prepared following our recently published procedure <sup>16</sup>.



**Scheme 2.1:** Synthetic protocol of (benzimidazolymethyl)amine palladium complexes.

The new palladium complexes **1-3** were characterized by  $^1\text{H}$ ,  $^{13}\text{C}$ ,  $^{31}\text{P}$  NMR spectroscopies, mass spectrometry and elemental analyses. For example, the  $^1\text{H}$  NMR spectra of **L1** and its corresponding complex **1** showed  $\text{CH}_2$  proton signals at 4.65 ppm and 5.33 ppm respectively. In addition, the  $\text{CH}_3$  proton signal at 2.32 ppm for **1** confirmed the coordination of  $p\text{-TsO}^-$  anion to the palladium atom (Figure 2.1). Similar  $^1\text{H}$  NMR spectra were observed for complexes **2** and **3**. The presence of carbon in  $\text{CH}_3$  of  $p\text{-TsO}^-$  was also confirmed from the  $^{13}\text{C}$  NMR spectra of **2** (Figure 2.2).

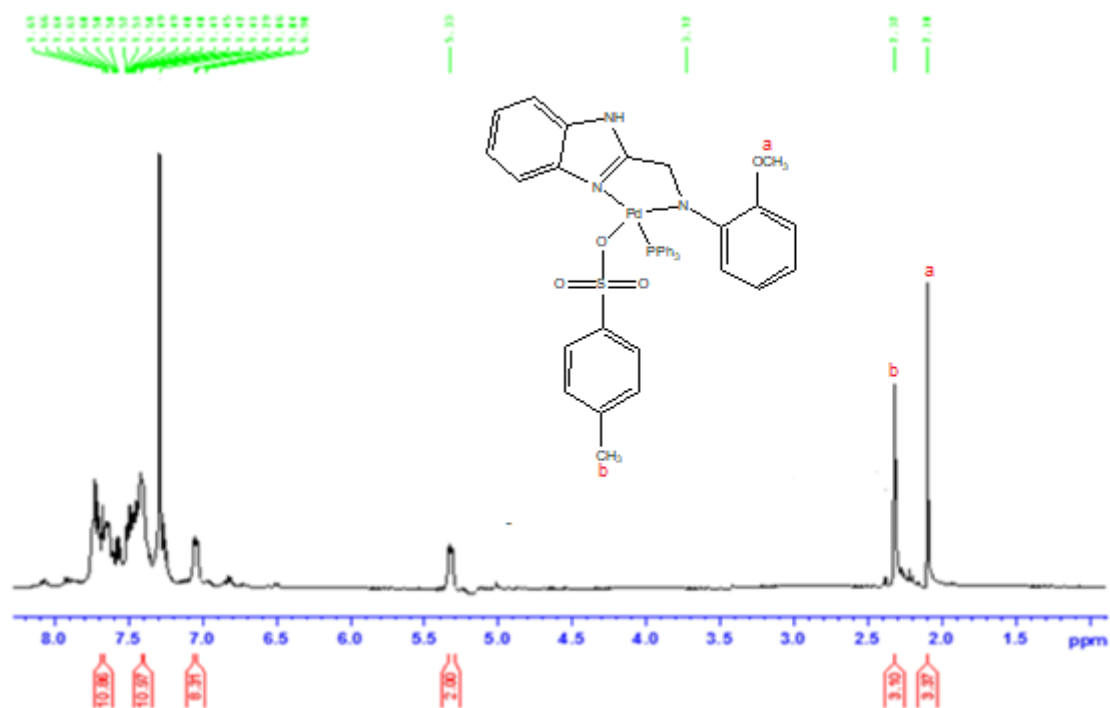


Figure 2.1:  $^1\text{H}$  NMR ( $\text{CDCl}_3$ ) spectrum of complex 1.

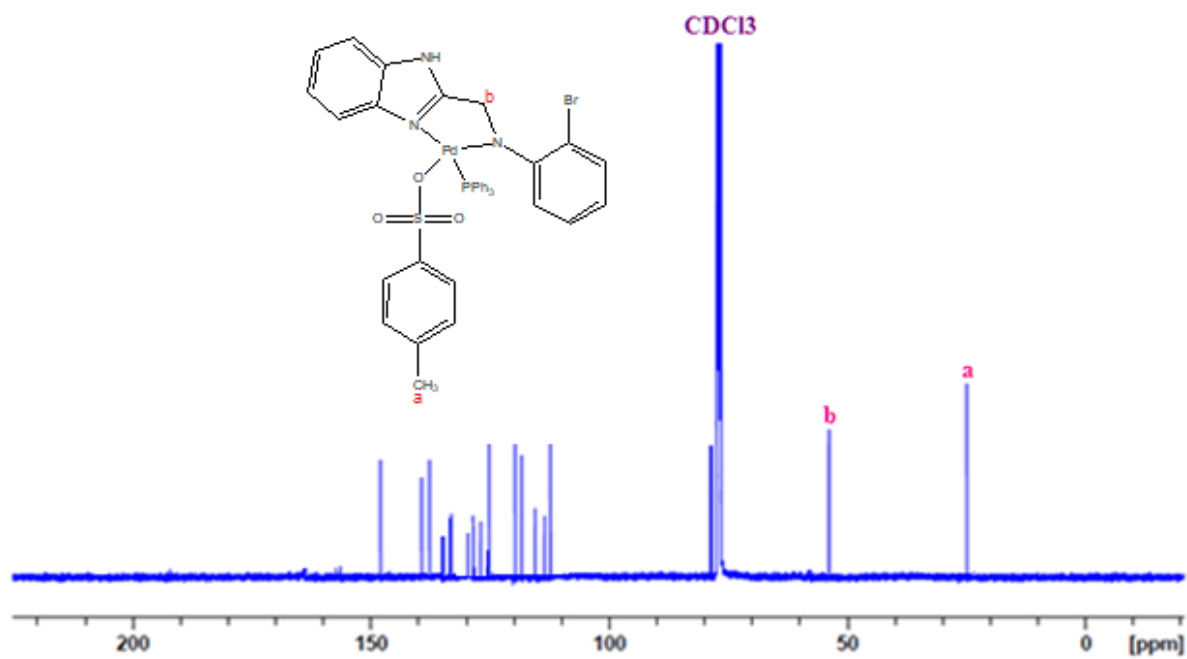
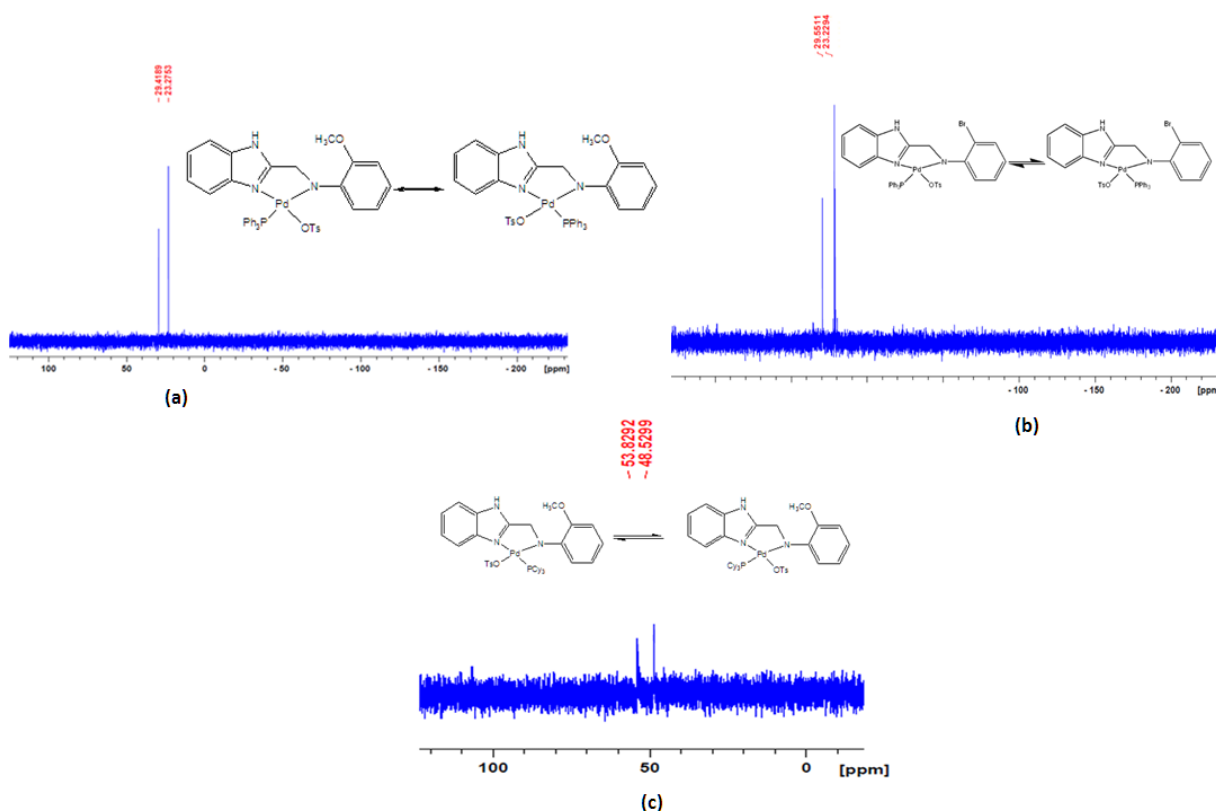


Figure 2.2:  $^{13}\text{C}$  NMR ( $\text{CDCl}_3$ ) spectrum of complex 2.

The  $^{31}\text{P}$  NMR spectra of complexes **1-3** displayed two singlets in the region 23.23 – 48.53 ppm, possibly due to the existence of the *cis* and *trans* isomers (Figures 2.3 a-c). These values fall within the typical  $^{31}\text{P}$  NMR signals in the range 23.20 - 35.70 ppm and 48.53-53.83 ppm reported for related mono-coordinated  $\text{PPh}_3$ <sup>15-20</sup> and  $\text{PCy}_3$  compounds respectively <sup>25</sup>.



**Figure 2.3:**  $^{31}\text{P}$  NMR spectrum ( $\text{CDCl}_3$ ) of complex **1** (a), **2** (b) and **3** (c) showing two signals due to possible *cis-trans*-labilization.

Mass spectrometry was also used to establish the formation and identity of these complexes. For instance, complex **2** showed an  $m/z$  peak at 841 amu, corresponding to its molecular ion (Figure 2.4).

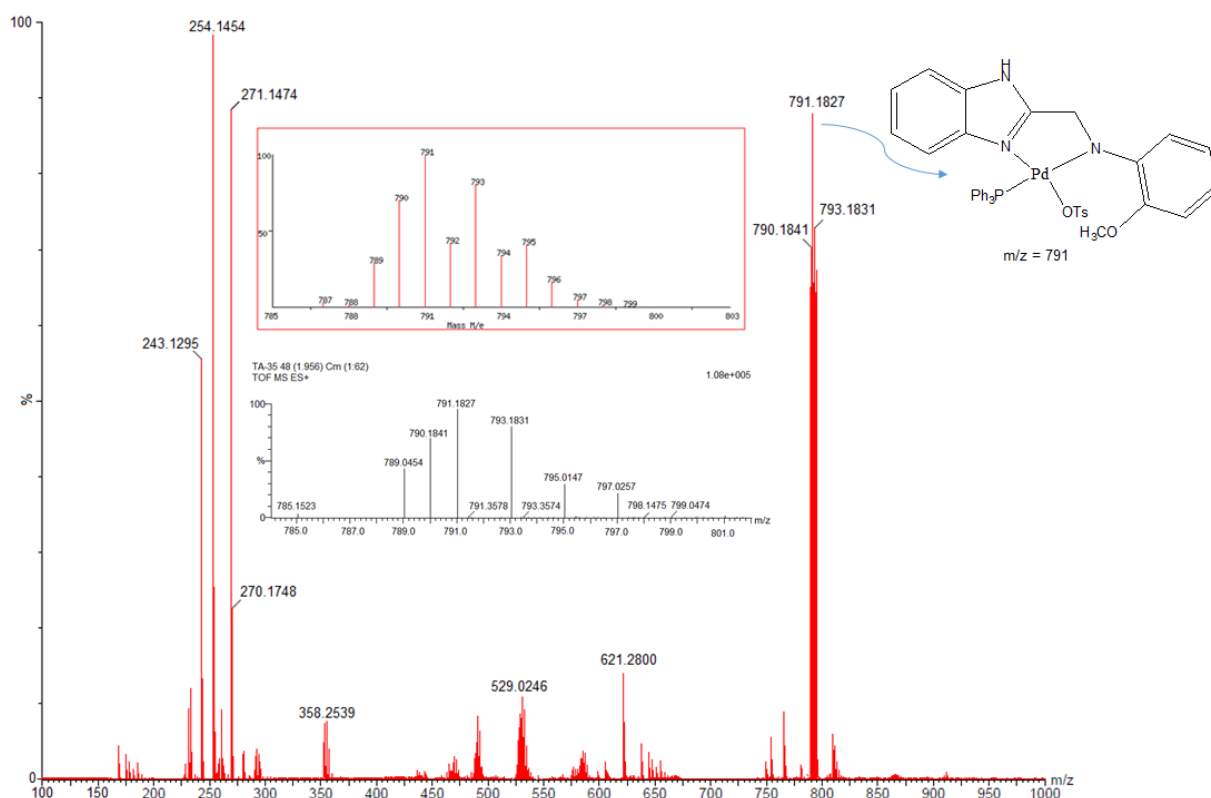


**Figure 2.4:** ESI-MS of the complex  $[\text{Pd}(\text{OTs})(\text{PPh}_3)(\text{L1})]$  (**1**) with the insert showing mass spectrum of the calculated and found isotopic distribution.

### 2.3.2. Methoxycarbonylation reactions using palladium complexes 1-5 as catalysts.

#### 2.3.2.1. Effect of catalyst structure and phosphine derivatives

In our recent report, we showed that the *N*-(benzimidazolylmethyl)amine palladium complexes **4** and **5** catalyze the methoxycarbonylation of terminal olefins to afford almost equal proportions of linear and branched esters<sup>16</sup>. In this current work, we aimed to improve the catalytic activity and regioselectivity of these palladium systems *via* modification of the complex design, use of different phosphine derivatives and internal olefin substrates (Table 2.1). The identities and compositions of the ester products were determined by GC and GC-MS. Figure 3.5 represent a typical GC-MS



trace for 1-hexene respectively. The  $m/z$  peak at 145.12 was observed at 4.70 and 5.19 minutes corresponding to both methyl heptanoate (linear product) and methyl 2-methylhexanoate (branched product) (Figure 2.5). Similar GC-MS spectra were observed for all catalytic reactions.

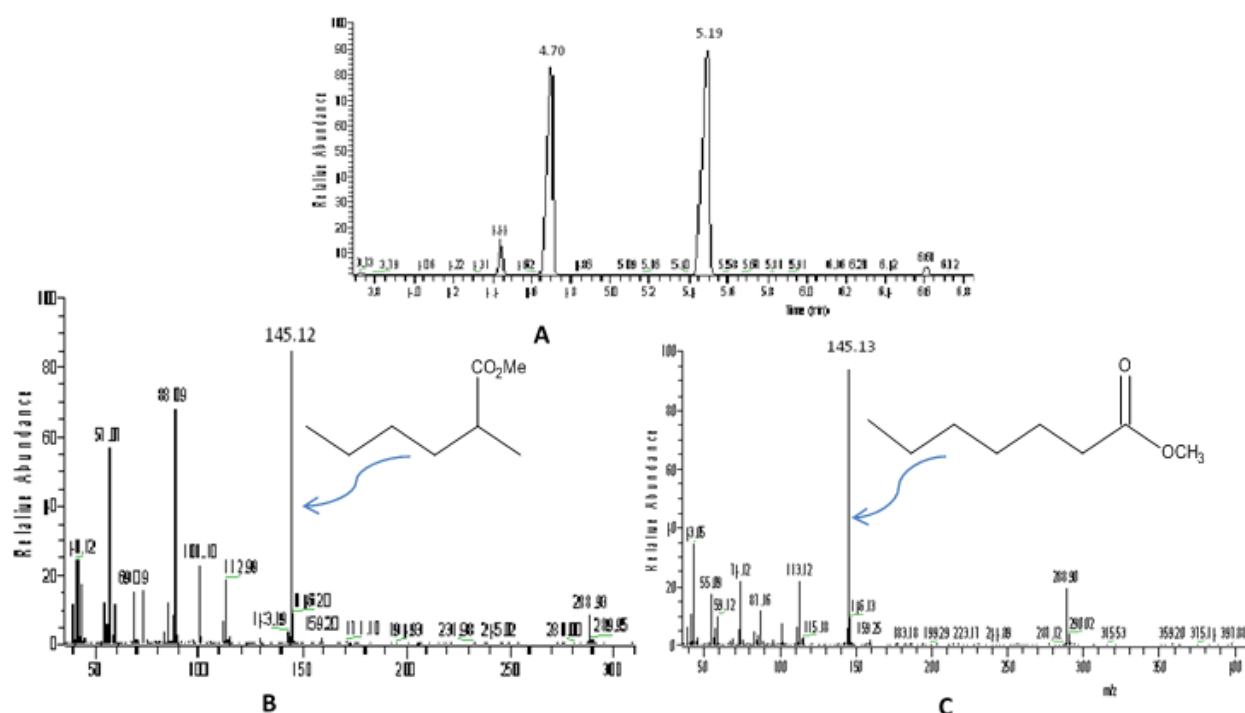


**Figure 2.5:** GC spectra (A) and MS spectra for the branched ester (B) at a retention time of 4.70 min and linear ester at a retention time of 5.19 min for 1-hexene using complex **1** as a catalyst.

Therefore, modification of complex **5** by introducing a tolyl sulfonic group as in complex **2** resulted in a drastic increase in catalytic activity from 39% to 84% respectively (Table 2.1, entries 2 and 5). This trend could be attributed to the presence

of the PPh<sub>3</sub> and tolyl groups in **2**, which are known to enhance the stability of the resultant palladium catalysts.<sup>7,12</sup> We also observed a notable shift of regioselectivity towards linear esters for complexes **1** and **2**, in comparisons to complexes **4** and **5**. For example, percentage compositions of linear esters of 70% and 74% were reported for complexes **1** and **2**, while 60% was reported for both complexes **4** and **5** (Table 2.1, entries 1-2 *vs* 4-5). This is likely to originate from a hindered isomerization of the coordinated 1-hexene substrate due to the bulkier PPh<sub>3</sub> and OTs groups in complexes **1** and **2**.<sup>12</sup>

**Table 2.1:** Effect of the complex structure and phosphine derivatives on the methoxycarbonylation of 1-hexene<sup>a</sup>

$$\text{CH}_2=\text{CH}(\text{CH}_2)_4\text{R} \xrightarrow[\text{CO/MeOH}]{\text{Pd/HCl/PR}_3} \text{R}(\text{CH}_2)_5\text{CO}_2\text{Me} \quad \mathbf{1} + \text{R}(\text{CH}_2)_3\text{CH}(\text{CO}_2\text{Me})\text{CH}_3 \quad \mathbf{b}$$

Entry	Catalyst	Phosphine	Conv. (%) <sup>b</sup>	b/l (%) <sup>c</sup>
1	<b>1</b>	<sup>d</sup> PPh <sub>3</sub>	92	30/70
2	<b>2</b>	PPh <sub>3</sub>	84	26/74
3	<b>3</b>	PPh <sub>3</sub>	76	74/26
4	<b>4</b>	PPh <sub>3</sub>	80	40/60
5	<b>5</b>	PPh <sub>3</sub>	39	40/60
6	<b>4</b>	<sup>e</sup> PCy <sub>3</sub>	32	76/24
7	<b>4</b>	<sup>f</sup> DPPe	19	88/12
8	<b>4</b>	<sup>g</sup> DPEphos	93	31/69
9	<b>4</b>	<sup>h</sup> P(o-tol) <sub>3</sub>	83	28/72
10	<b>4</b>	<sup>i</sup> P(OMe) <sub>3</sub>	48	84/16

<sup>a</sup>Reaction conditions: Pre-catalysts (0.07 mmol), solvent: toluene 40 mL and methanol 30 mL; Pd:1-hexene ratio 200:1, Pd:HCl ratio; 1:10; Pd:PR<sub>3</sub> ratio; 1:2; *p*(CO) = 60 bar; temperature: 90 °C; time 24 h; <sup>b</sup>% of 1-hexene converted after 24 h reaction, <sup>c</sup>branched/linear ester ratio. <sup>d</sup>triphenylphosphine, <sup>e</sup>tricyclohexylphosphine, <sup>f</sup>1,2-bis(diphenylphosphino)ethane, <sup>g</sup>(oxydi-2-1-phenylene)bis-(diphenylphosphine), <sup>h</sup>tri(o-tolyl)phosphine, <sup>i</sup>trimethyl phosphite.

Encouraged by the results obtained upon modification of the auxiliary phosphine ligands in complexes **1** and **2** in the methoxycarbonylation of 1-hexene, we opted to further investigate the effect of various phosphine derivatives; PPh<sub>3</sub>, PCy<sub>3</sub>, Dppe,

DPEphos, P(o-tol)<sub>3</sub> and P(OMe)<sub>3</sub> on the catalytic performance of complex **4** (Table 2.1, entries 6-10). The results obtained clearly illustrate the influence of the phosphine derivatives; affording conversions ranging from 19% to 93% (Table 2.1, entries 4, 6-10). For example, the use of PCy<sub>3</sub> afforded conversions of 32% compared to 80% reported for the PPh<sub>3</sub> analogue (Table 2.1, entries 4 *vs* 6). This could be attributed to the inability of the PCy<sub>3</sub> ligand to stabilize the palladium catalyst leading to decomposition to Pd(0), consistent with the observed Pd(0) deposits in the reaction mixture. The PPh<sub>3</sub> ligand is more basic than PCy<sub>3</sub> and therefore will form stable palladium intermediates which results in higher catalytic reaction.<sup>12</sup> More discerning was the observed decrease in catalytic activity from 80% to 19% on changing from a non-chelating PPh<sub>3</sub> to the chelating Dppe groups (Table 2.1, entries 4 and 7). A possible explanation for this behaviour could be the competition between the olefin substrate and the chelating Dppe ligand for the vacant coordination site of the palladium catalyst.

Regioselectivity of the ester products was also influenced by the nature of the auxiliary phosphine ligands (Table 2.1, entries 4- 10). For instance, the DPEphos, and P(OMe)<sub>3</sub> gave 31% and 84% of the branched esters respectively (Table 2.1, entries 8 *vs* 10). This high regioselectivity towards the branched esters reported for P(OMe)<sub>3</sub> could be largely attributed to reduced steric hindrance, thus favouring formation of bulkier branched esters *via* a 2,1-insertion pathway.<sup>26</sup> This was further supported by the lower regioselectivity towards branched esters of 31% reported for DPEphos compared to 88%, obtained when using the chelating Dppe group (Table 2.1, entries 7-8).

### 2.3.2.2. *Investigation of the effects of solvent and acid promoter on methoxycarbonylation reactions*

We then studied the effect of the solvent system and nature of acid promoter on the catalytic performance of complex **1** using 1-hexene substrate (Table 2.2, entries 1-5). From the results, it was observed that the use of pure methanol resulted in decreased catalytic activities, achieving conversions of 28%, compared 92% obtained in toluene/methanol system (Table 2.2, entries 1 *vs* 2). On the other hand, the use of higher amounts of toluene solvent did not affect the catalytic activities (Table 2.2, entry 1 *vs* 3). The lower catalytic activities afforded with increase in methanol concentration has been reported by Zollezzi *et al* and could be associated with lower reaction temperatures of 65 °C<sup>27</sup>. We also hypothesize that, lower solubility of complex **1** in methanol solvent, may also play a role in the diminished catalytic activities. Indeed, reactions performed in methanol/chlorobenzene solvent system gave higher conversions of 90% (Table 2.2, entry 4).

Interestingly, regioselectivity of the ester products was also influenced by the solvent system employed. For example, the use of pure methanol gave 38% of the branched esters, compared to 51% obtained in a 3:4 mixture of methanol/toluene solvent system (Table 2.2, entries 2 and 3). Poor selectivity with increase in methanol concentration has been reported by other researchers and has been attributed to the formation of Pd(0) species and increased polarity of the solvent system.<sup>11,27-29</sup>

**Table 2.2:** Effect of solvent system on methoxycarbonylation of 1-hexene using complex **1**<sup>a</sup>

Entry	Solvent system	T (°C)	Conv(%) <sup>b</sup>	b/l(%) <sup>c</sup>
1	MeOH/toluene	90	92	30/70
2	MeOH	65	28	38/62
3	MeOH/toluene (1:4)	90	94	51/49
4	MeOH/chlorobenzene(3:4)	90	90	31/69
5	MeOH/toluene <sup>d</sup>	90	76	41/59

<sup>a</sup>Reaction conditions: Complex (0.07 mmol), solvent system: toluene 40 mL and methanol 30 mL; Pd/1-hexene ratio 200:1, Pd:HCl ratio; 1:10; Pd:PR<sub>3</sub> ratio; 1:2; *p*(CO) = 60 bar; temperature: 90 °C; time 24 h; <sup>b</sup>% of 1-hexene converted after 24 h reaction, <sup>c</sup>branched/linear ester ratio. <sup>d</sup>5 drops of mercury using catalyst **4**.

The type of acid promoter in palladium catalyzed methoxycarbonylation is known to significantly influence the catalytic performance of the resultant catalysts and possible industrial applications. We thus studied a wide range of Brønsted and Lewis acids using complex **1** and 1-hexene substrate (Figure 2.6). Consistent with our previous reports<sup>16</sup>, we did not observe any catalytic activities using *p*-TsOH, but conversions of 92% and 81% were achieved using HCl and  $\alpha$ -bromo-*p*-toluic acid. This lack of catalytic activity reported for *p*-TsOH acid has been associated with weaker coordination ability of the *p*-TsO<sup>-</sup> anion, which may not be sufficient to stabilize the active Pd(II) species.<sup>23-24</sup> Indeed, extensive decomposition of complex **1** to Pd(0) black was observed in the reactions performed using *p*-TsOH acid promoter. The improved performance of  $\alpha$ -bromo-*p*-toluic acid is rather intriguing since it offers more industrial relevance than HCl. The efficacy of Lewis acids; EtAlCl<sub>2</sub>, AlCl<sub>3</sub>, AlMe<sub>3</sub> was also probed (Figure 2.6). The catalytic activities of complex **1** significantly increased

with increase in Lewis acidity of the acid-promoter. For example, the most acidic  $\text{AlCl}_3$  recorded the highest conversion of 88%, while the least acidic  $\text{AlMe}_3$ , gave the least catalytic activity of 9% conversions.

Regioselectivity in the presence of Lewis acids significantly differed from those obtained using Brønsted-acids. While comparable regioselectivity was observed using protonic acids, HCl and  $\alpha$ -Bromo-p-toluic acid (54% of the branched esters), Lewis Acids showed marked differences (Figure 2.6). For example,  $\text{EtAlCl}_2$  and  $\text{AlMe}_3$  gave 24% and 100% of the branched esters respectively. This trend point to the generation of different active species and that chain isomerization/migration is predominant when  $\text{AlMe}_3$  was used as the acid promoter.<sup>11,13</sup>

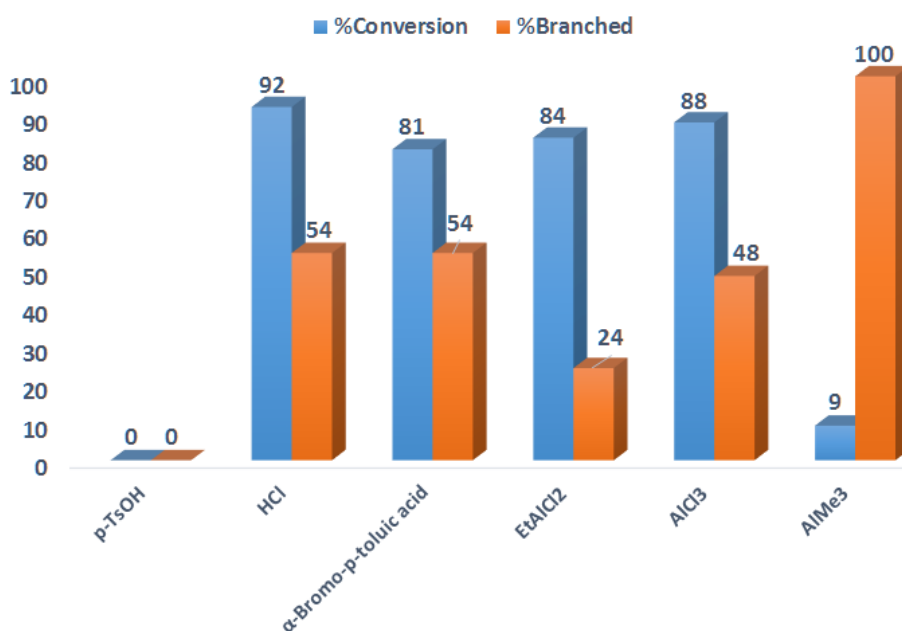


**Figure 2.6:** The effect of acid-promoters on conversion and regioselectivity towards branched products using complex **1**. Complex (0.07 mmol), solvent: toluene 40 mL and methanol 30 mL; Pd:1-hexene ratio 200:1, Pd:acid promoter ratio; 1:10; Pd:Phosphine ratio; 1: 2;  $p(\text{CO}) = 60$  bar; temperature: 90 °C; time 24 h.

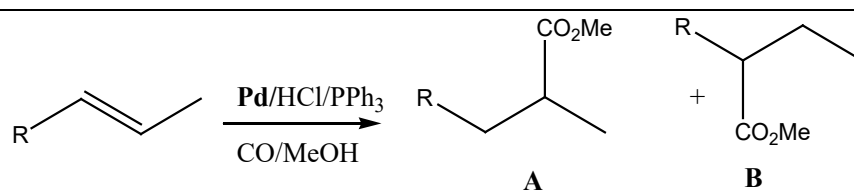
### 2.3.2.3. Methoxycarbonylation of internal olefins using catalysts **1** and **4**

In order to investigate the effect of internal olefins on the catalytic activities and regioselectivity, we used complexes **1** and **4** in the methoxycarbonylation of *trans*-2-hexene and *trans*-2-octene (Table 2.3). From the results, we observed reduced catalytic activities for the internal olefins compared to the terminal olefins. For example, conversions of 80% and 30% were reported for 1-hexene and *trans*-2-hexene respectively using catalyst **4** (Table 2.1, entry 3, and Table 2.3, entry 1). In line with our



previous reports<sup>16</sup>, higher catalytic activity was observed for *trans*-2-hexene (56%) compared to conversions of 12% recorded for *trans*-2-octene (Table 2.3).

**Table 2.3:** Methoxycarbonylation of *trans*-2-hexene and *trans*-2-octene catalyzed by complexes **1** and **4**<sup>a</sup>



Entry	Substrate	Catalyst	Time	Conv. (%) <sup>b</sup>	A (%) <sup>c</sup>	B (%) <sup>c</sup>
1	<i>trans</i> -2-hexene	<b>4</b>	24	30	68	32
2	<i>trans</i> -2-hexene	<b>4</b>	48	56	66	34
3	<i>trans</i> -2-octene	<b>4</b>	24	6	10	90
4	<i>trans</i> -2-octene	<b>4</b>	48	12	24	76
5	<i>trans</i> -2-hexene	<b>1</b>	24	54	100	-
6	<i>trans</i> -2-hexene	<b>1</b>	48	73	100	-
7	<i>trans</i> -2-octene	<b>1</b>	24	21	100	-
8	<i>trans</i> -2-octene	<b>1</b>	48	61	100	-

<sup>a</sup>Reaction conditions: Complexes (0.07 mmol), solvent: toluene 40 mL and methanol 30 mL; [Pd]:[PPh<sub>3</sub>]:[HCl]:[substrate] ratio of 1:2:10:200; p(CO) = 60 bar; temperature: 90°C; <sup>b</sup>% of substrate converted after a given time as determined by GC; <sup>c</sup>determined by GC.

With respect to regioselectivity, only two branched esters, methyl branched isomer **A** and ethyl branched isomer **B**, were obtained (Table 2.3, Figure 2.7 (a)-(b)); indicating

the absence of any isomerization, but rather chain migration/walking as proposed in Scheme 2.2. Another important observation witnessed was the higher composition of ethyl branched isomer **B** using *trans*-2-octene (90%) compared to *trans*-2-hexene (32%), Table 2.3, entries 1 and 3. This is the expected trend, since the ethyl branched isomer **B** is more sterically demanding and is likely to be favoured by the longer chain *trans*-2-octene olefin.

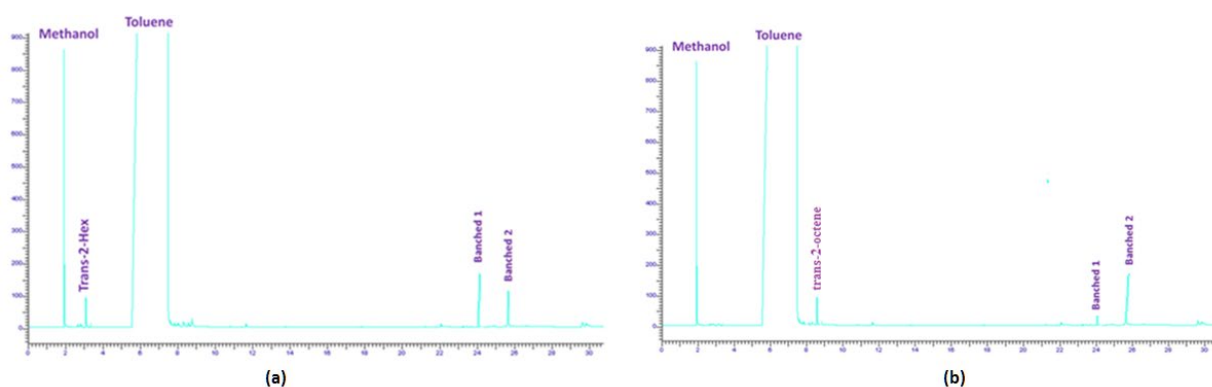
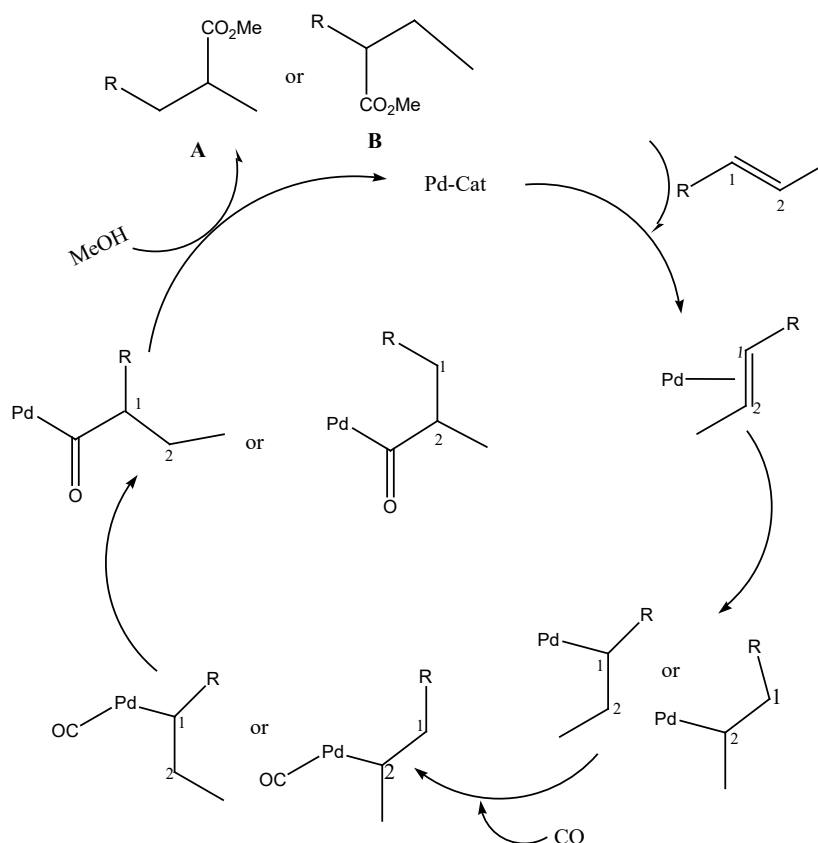


**Figure 2.7:** GC chromatogram of the product obtained from the methoylesterification of *trans*-2-hexene (a) and *trans*-octene (b) using catalyst **4** showing the formation of only branched esters.



**Scheme 2.2:** Possible mechanistic pathway for the formation of methyl and ethyl branched esters from *trans*-2-hexene and *trans*-2-octene using catalyst **4**.

The use of complex **1** in the methoxycarbonylation of the *trans*-2-hexene and *trans*-2-octene showed more interesting results, producing only the methyl branched isomer **A** (Table 2.3, entries 5-8, Figure 2.8). This could be largely attributed to greater steric restrictions imposed by the more bulky tosylate group, thus hindering the formation of the more bulky ethyl branched isomer **B**.<sup>31</sup>

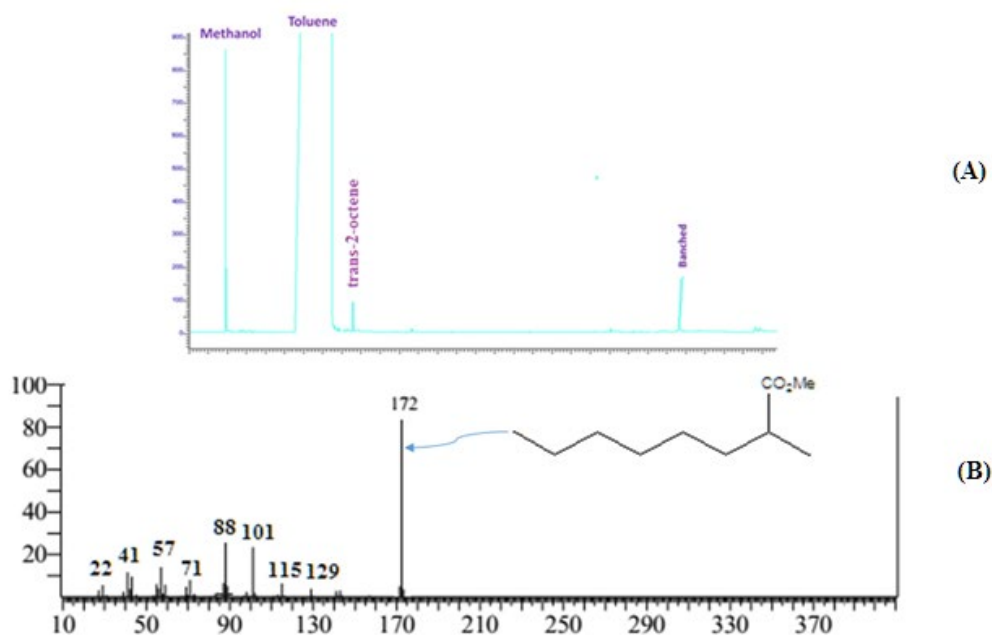


**Figure 2.8:** GC spectra (A) and MS spectra (B) of the branched product obtained from the methoxycarbonylation of *trans*-2-octene using catalyst **1**.

#### 2.3.2.4. Role of ligand and nature of the active species in methoxycarbonylation reactions

In order to understand the role of the ligand motif in controlling the catalytic activities of complexes **1-5** and nature of the active species such as  $[\text{Pd}(\text{L})(\text{PPh}_3)(\text{HOMe})]$ ,  $[\text{Pd}(\text{L})(\text{PPh}_3)\text{H}]$ ,  $[\text{Pd}(\text{L})(\text{PPh}_3)(\text{COOMe})]$ ,  $[\text{Pd}(\text{L})(\text{PPh}_3)(\text{OMe})]$  (Figure 2.9), NMR spectroscopy was used to study the identity of the active species and possible decomposition of the complex under the catalytic conditions. Quantitative amounts of complex **4** (0.050 g, 0.18 mmol) was subjected to 60 bar of CO at 90 °C in the presence of HCl. The product obtained (40% yield) was characterized using  $^1\text{H}$ ,  $^{13}\text{C}$  and  $^{31}\text{P}$  NMR spectroscopy (Figures 2.10-2.12). From the  $^1\text{H}$  NMR (Figure 2.10) and  $^{13}\text{C}$  NMR (Figure 2.11) spectra of the product, it was clear that the ligand was not displaced,

consistent with the observed influence of ligand motif on catalytic activities of complexes **1-5**. Rather, a displacement of the chloride ligand was observed, followed by the migratory insertion of the CO molecule into the Pd-Me bond and coordination of one PPh<sub>3</sub> group (Figures 2.10 - 2.11). This is likely to be the active species ([Pd(L)(PPh<sub>3</sub>)(COOMe)]) where a possible displacement of the PPh<sub>3</sub> group occurs prior to coordination of the alkene substrate as in the carbomethoxy mechanism.<sup>32</sup> In the <sup>31</sup>P NMR (Figure 2.12), a peak at -6.1 ppm is due to the free PPh<sub>3</sub> molecule, while the two signals (32.3 and 26.1 ppm) could be assigned to the *cis* and *trans* isomers of the PPh<sub>3</sub> groups coordinated to the palladium atom.

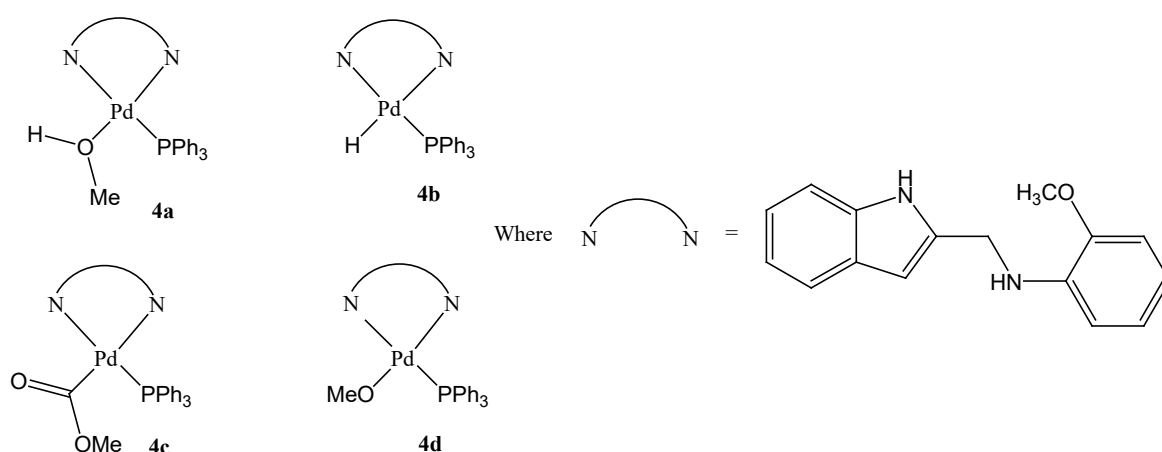


**Figure 2.9:** Nature of the active species in the methoxycarbonylation reactions

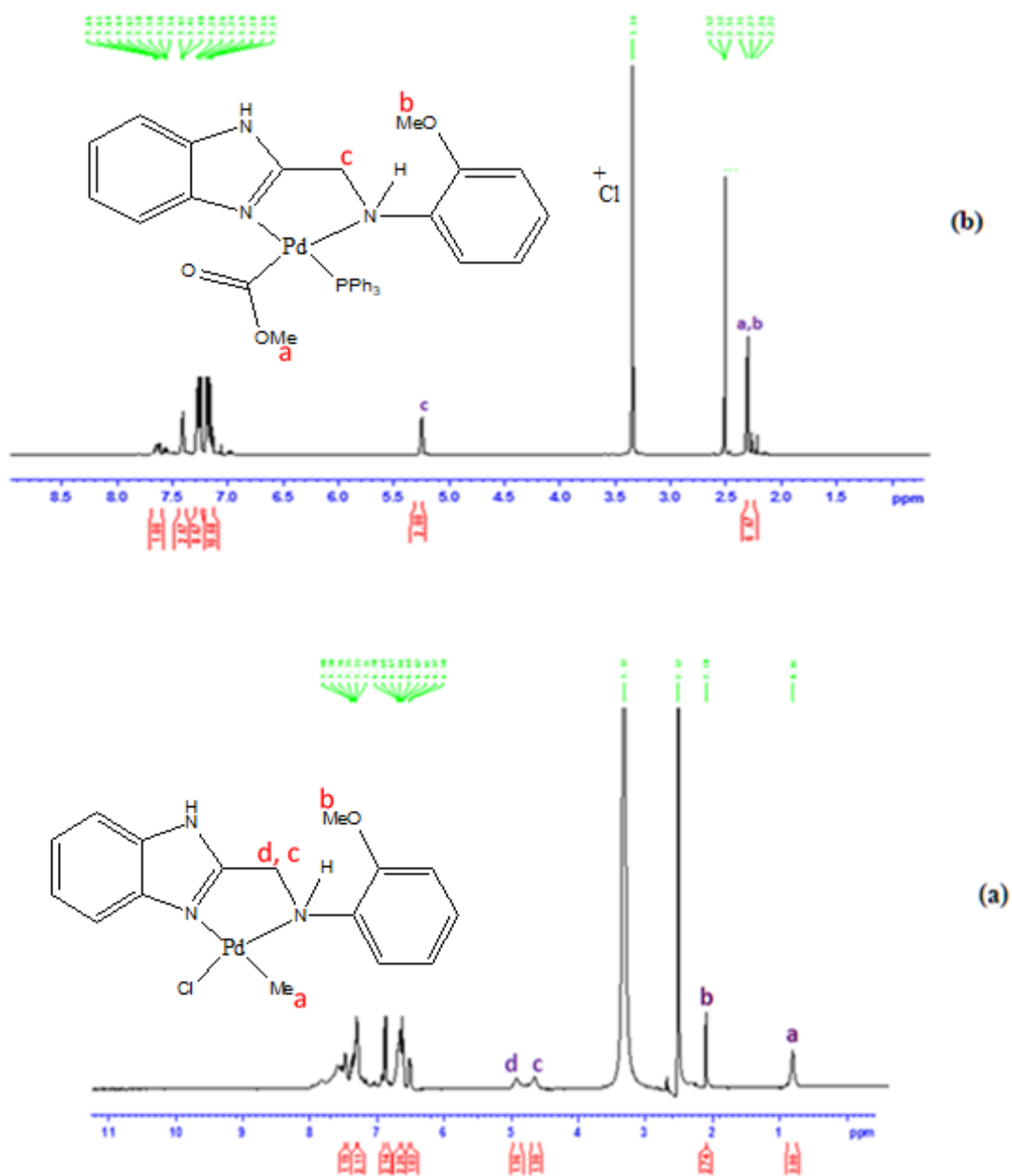


**Figure 2.10:** (a)  $^1\text{H}$  NMR (DMSO- $d_6$ ) spectrum of complex **4**. (b)  $^1\text{H}$  NMR spectrum of the product (**4c**) obtained from the reactions of complex **4** with  $\text{PPh}_3$  under  $\text{CO}$  (60 bar) atmosphere in the presence of  $\text{HCl}$  at  $90^\circ\text{C}$ .

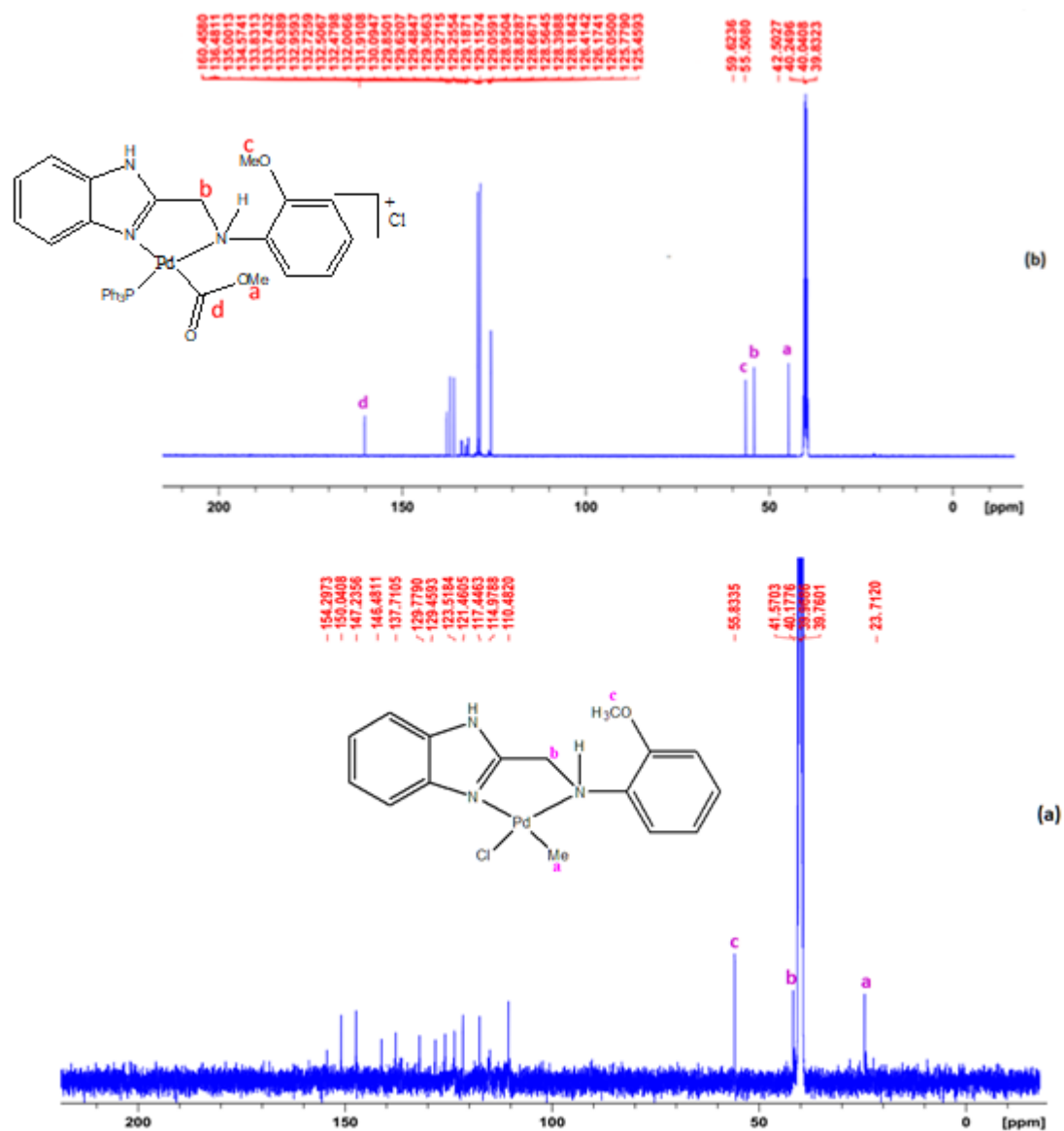


**Figure 2.11:** (a) <sup>13</sup>C NMR (DMSO-d<sub>6</sub>) spectrum of complex **4**. (b) <sup>13</sup>C NMR spectrum of the product (**4c**) obtained from the reactions of complex **4** with PPh<sub>3</sub> under CO (60 bar) atmosphere in the presence of HCl at 90 °C (catalytic conditions).

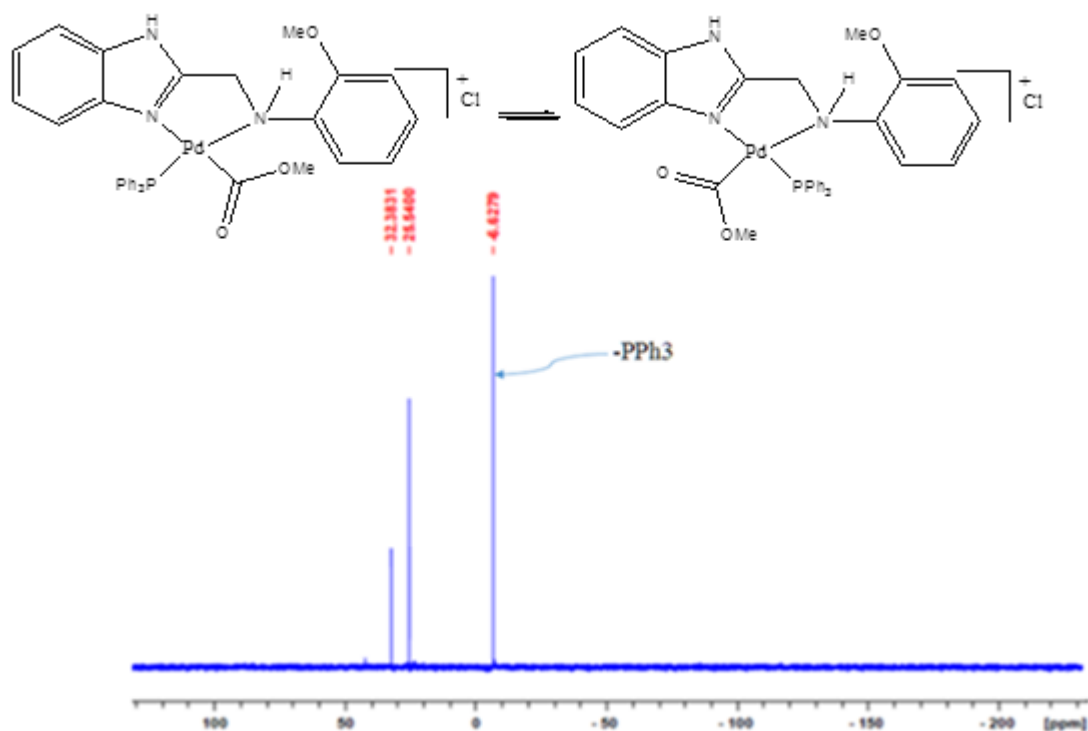


**Figure 2.12:**  $^{31}\text{P}$  NMR ( $\text{DMSO-d}_6$ ) spectrum of the product (**4c**) obtained in the reaction of complex **4** under CO (60 bar) atmosphere in the presence of HCl at 90 °C (catalytic conditions).

To further gain more insight into the nature of the active species, a mercury drop test was performed using complex **4** (Table 2.2, entry 5). No significant reduction on the catalytic activity upon addition of mercury was reported, indicating that the active species was largely homogeneous in nature, which was in good agreement with the NMR studies.



## 2.4. Conclusions

In summary, this work has demonstrated the potential of (benzoimidazol-2-ylmethyl)amine palladium complexes to catalyze the methoxycarbonylation of alkenes to afford 100% chemoselectivity and regioselectivity. The work also showed that by careful design of the complex structure, selection of the phosphine derivative, acidic-promoter and olefin substrate, high catalytic activities and regioselectivity could be achieved. The active palladium species were homogeneous in nature in which the palladium centre is stabilized by the ligands. This work therefore provides a platform to rationally design selective homogeneous palladium catalyst systems for the methoxycarbonylation of both terminal and internal alkenes.

## 2.5. References

- 1 A. Brennführer, H. Neumann and M. Beller, *Angew. Chem. Int. Ed.*, 2009, **48**, 4114–4133.
- 2 Q. Liu, H. Zhang and A. Lei, *Angew. Chem. Int. Ed.*, 2011, **50**, 10788–10799.
- 3 X. F. Wu, X. Fang, L. Wu, R. Jackstell, H. Neumann and M. Beller, *Acc. Chem. Res.*, 2014, **47**, 1041–1053.
- 4 X. F. Wu, H. Neumann and M. Beller, *Chem. Rev.*, 2013, **113**, 1–35.
- 5 P. A. Aguirre, C. A. Lagos, S. A. Moya, C. Zúñiga, C. Vera-Oyarce, E. Sola, G. Peris and J. C. Bayón, *Dalton Trans*, 2007, 5419.
- 6 V. De La Fuente, M. Waugh, G. R. Eastham, J. A. Iggo, S. Castilln, and C. Claver, *Chem. Eur J.*, 2010, **16**, 6919–6921.
- 7 I. Del Río, N. Ruiz, C. Claver, L. A. Van Der Veen and P. W. N. M. Van Leeuwen, *J. Mol. Catal. A Chem.*, 2000, **161**, 39–48.
- 8 S. Jayasree, A. Seayad, B. R. Sarkar and R. V. Chaudhari, *J. Mol. Catal. A Chem.*, 2002, **181**, 221–235.

- 9 Y. Y. Li and C. G. Xia, *Appl. Catal. A Gen.*, 2001, **210**, 257–262.
- 10 C. Jimenez Rodriguez, D. F. Foster, G. R. Eastham and D. J. Cole-Hamilton, *Chem. Commun.*, 2004, 1720–1721.
- 11 R. I. Pugh, P. G. Pringle and E. Drent, *Chem. Commun.*, 2001, **1**, 1476–1477.
- 12 G. Cavinato and L. Toniolo, *Molecules*, 2014, **19**, 15116–15161.
- 13 F. Amoroso, E. Zangrando, C. Carfagna, C. Müller, D. Vogt, M. Hagar, F. Ragaini and B. Milani, *Dalton Trans.*, 2013, **42**, 14583.
- 14 Z. Freixa and P. W. N. M. van Leeuwen, *Dalton Trans.*, 2003, 1890–1901.
- 15 G. Kiss, *Chem. Rev.*, 2001, **101**, 3435–3456.
- 16 T. A. Tshabalala, S. O. Ojwach and M. A. Akerman, *J. Mol. Catal. A Chem.*, 2015, **406**, 178–184.
- 17 N. W. Attandoh, S. O. Ojwach and O. Q. Munro, *Eur. J. Inorg. Chem.*, 2014, **2014**, 3053–3064.
- 18 S. Jayasree, A. Seayad, and R. V Chaudhari, *Org. Lett.*, 2000, **203**, 1-4.
- 19 A. O. Ogwenio, S. O. Ojwach and M. P. Akerman, *Dalton Trans*, 2014, **43**, 1228–1237.
- 20 S. O. Ojwach, I. A. Guzei, J. Darkwa and S. F. Mapolie, *Polyhedron*, 2007, **26**, 851–861.
- 21 G. Iii, M.-B. Derivatives, M. Serratrice, M. A. Cinellu, L. Maiore, M. Pilo, A. Zucca, C. Gabbiani, A. Guerri, I. Landini, S. Nobili, E. Mini, and L. Messori, *Inorg. Chem.*, **2012**, **51**, 3161-3168.
- 22 E. Sindhuja, R. Ramesh and Y. Liu, , *Dalton Trans*, 2012, **41**, 5351.
- 23 V. S. Tkach, D. S. Suslov, N. V. Kurat'eva, M. V. Bykov, M. V. Belova and N. V Kurat'Eva, *Russ. J. Coord. Chem.*, 2011, **37**, 752–756.
- 24 A. Valore, M. Balordi, A. Colombo, C. Dragonetti, S. Righetto, D. Roberto, R. Ugo, T. Benincori, G. Rampinini, F. Sannicolò and F. Demartin, , *Dalton Trans*, 2010, **39**, 10314.
- 25 M. Nandi, J. Jin, and T. V Rajanbabu, *Organometallics*, 2009, **28**, 1855-1861.
- 26 A. Seayad, S. Jayasree, K. Damodaran, L. Toniolo and R. V. Chaudhari, *J. Organomet. Chem.*, 2000, **601**, 100–107.
- 27 S. Zolezzi, S. A. Moya, G. Valdebenito, G. Abarca, J. Parada and P. Aguirre,

- Appl. Organomet. Chem.*, 2014, **28**, 364–371.
- 28 C. Arderne, L. A. Guzei, C. W. Holzapfel and T. Bredenkamp, *ChemCatChem*, 2016, **8**, 1084–1093.
- 29 R. Izquierdo, J. Ferna, L. G. Melean, and P. J. Baricelli, *Catal. Lett.* 2014, **144**, 1717–1727.
- 30 B. K. Munoz, C. Godard, A. Marinetti, A. Ruiz, J. Benet-Buchholz, C. Claver, J. Fraanje, M. Lutz and A. L. Spek, *Dalton Trans*, 2007, **12**, 5524.
- 31 C. Zuniga, D. Sierra, J. Oyarzo, and A. H. Klahn, *J. Chil. Chem. Soc.*, 2012, **57**, 1101–1103.
- 32 G. A. Molander and B. Canturk, *Angew. Chem. Int. Ed.*, 2009, **48**, 9240–9261.
- 33 L. Crawford, D. J. Cole-Hamilton, and M. Buhl, *Organometallics*, 2015, **34**, 438–444.

## CHAPTER 3

### **Kinetics and chemoselectivity studies of hydrogenation reactions of alkenes and alkynes catalyzed by (benzoimidazol-2-ylmethyl)amine palladium(II) complexes**

This chapter is adapted from the paper published in *Inorganica. Chimica. Acta* 483 (2018) 148-155 and is based on the experimental work of the first author, Thandeka A Tshabalala. Copyright © 2018 Elsevier B.V. The contributions of the first author include: carrying out the catalytic reactions and drafting of the manuscript.

#### **3.1. Introduction**

Hydrogenation reactions of alkenes and alkynes are currently one of the dominant industrial processes used for the reduction of unsaturated organic compounds to produce a wide range of relevant products.<sup>1-3</sup> Several metal-based catalysts derived from nickel, palladium, ruthenium, rhodium, iridium and platinum have been employed in the catalytic hydrogenation of alkenes and alkynes under both homogeneous<sup>4,5</sup> and heterogeneous<sup>6,7</sup> conditions. Currently, the major focus in transition metal catalyzed homogeneous molecular hydrogenation reactions has been on ligand design; and the insights gained so far show that the ability to control the catalytic behaviour of these catalyst lies in the coordination environment around the metal atom.

In particular, palladium(II) catalysts are currently receiving much attention in the hydrogenation of alkenes and alkynes due to their superior catalytic activities and

selectivity.<sup>8</sup> Numerous reports have appeared on the homogeneous hydrogenation of alkenes and alkynes using palladium(II) catalysts supported on phosphine-donor ligands. For example, Bacchi *et al*<sup>9</sup> and Drago *et al*<sup>10</sup> employed hydrazonic phosphine palladium(II) and bidentate (2,5-dimethylphospholano) palladium(II) complexes as effective catalysts in the hydrogenation of alkenes. Even though the phosphine-donor palladium(II) catalysts have been successfully used in the homogeneous hydrogenation reactions of alkenes and alkynes, these systems suffer from lack of stability and sensitivity to moisture and air.<sup>11</sup> As a result, nitrogen-donor palladium(II) catalysts are emerging as suitable alternatives due to their better stability and ease of synthesis in comparison to the phosphine-donor palladium(II) complexes. For example, the pyridine-2-carbaldine palladium(0)<sup>12</sup> and bis(arylimino)acenaphthene palladium(0)<sup>13</sup> complexes have been shown to exhibit good selectivity and stability in the homogeneous hydrogenation of alkynes.

In **Chapter 2**, we reported the use of (benzoimidazol-2-ylmethyl)amine palladium(II) complexes<sup>14</sup> as active catalysts in the methoxycarbonylation of higher olefins. Due to the promising results obtained in the methoxycarbonylation reactions by these systems, we chose to explore their propensity to catalyze the molecular hydrogenation of selected alkenes and alkynes. In addition, kinetics and theoretical studies have been performed and are herein discussed.

## 3.2. Experimental section

### 3.2.1. Materials and methods

All moisture and air sensitive reactions were performed using standard Schlenk line techniques. Methanol (ACS reagent,  $\geq 99.8\%$ ), toluene (ACS reagent,  $\geq 99.5\%$ ), dichloromethane (ACS reagent,  $\geq 99.8\%$ ), absolute ethanol (ACS reagent,  $\geq 98\%$ ) and tetrahydrofuran (anhydrous,  $\geq 99.9\%$ ) were purchased from Merck. Solvents were dried and distilled under nitrogen in the presence of suitable drying agents: Toluene and acetone were dried over anhydrous calcium chloride, methanol and absolute ethanol over calcium oxide, dichloromethane over phosphorus pentoxide and stored over 4 Å molecular sieves. The ligands *N*-(1H-benzoimidazol-2-ylmethyl-2-methoxy)aniline (**L1**), *N*-(1H-benzoimidazol-2-ylmethyl-2-bromo)aniline (**L2**), *N*-(1H-benzoimidazol-2-ylmethyl)benzenamine (**L3**) and *N*-(1H-benzoimidazol-2-ylmethylamino)benzenethiol (**L4**), were synthesized following the published literature method.<sup>15</sup> The palladium complexes [Pd(**L1**)Cl<sub>2</sub>] (**6**), [Pd(**L2**)Cl<sub>2</sub>] (**7**) [Pd(**L3**)Cl<sub>2</sub>] (**8**), [Pd(**L4**)Cl<sub>2</sub>] (**9**), [Pd(**L2**)ClMe] (**10**) and [Pd(**L2**)ClPPh<sub>3</sub>]BAr<sub>4</sub> (**11**), were prepared following our recently published procedure.<sup>14</sup>

### 3.2.2. Density Functional Theory (DFT) studies

DFT calculations were performed in a gas phase to identify the energy-minimized structures based on B3LYP/LANL2DZ (Los Almos National Laboratory 2 double  $\zeta$ ) level theory.<sup>16</sup> A split bases set, LANL2DZ for palladium and 6-311G for all other atoms was used to optimize the geometries and energies of the complexes. The Gaussian09 suite of programs was used for all the computations.

### 3.2.3. General procedure for the hydrogenation reactions of alkenes and alkynes

The catalytic hydrogenation reactions were performed in a stainless-steel autoclave equipped with temperature control unit and a sample valve. In a typical experiment, styrene (0.5 mL, 4.20 mmol) and complex **7** (3.47 mg, 0.007 mmol, S/C 600) were dissolved in toluene (50 mL). The reactor was evacuated, flushed with nitrogen and the catalytic solution was introduced to the reactor *via* a cannula. The reactor was purged three times with hydrogen, and then set at the equipped pressure, heated to the desired temperature and the reaction stirred at 500 rpm. At the end of the reaction time, the reactor was cooled, excess hydrogen vented off. Samples for GC analyses were drawn *via* a syringe, filtered using 0.45  $\mu\text{m}$  micro filters and analyzed by Varian CP-3800 GC (ZB-5HT column 30 m  $\times$  0.25 mm  $\times$  0.10  $\mu\text{m}$ ) GC instrument to determine the percentage conversion of styrene to ethylbenzene. The samples were also analysed by ESI-MS (recorded on a Waters API Quatro Micro spectrometer) to determine the reaction intermediates. The percentage conversions were determined by comparing the peak areas of the alkene/alkyne substrate and respective products, assuming 100% mass balance. For example, comparison of peak areas of styrene and ethylbenzene at regular time intervals allowed the determination of the rate of conversion of styrene to ethylbenzene. Standard authentic samples; ethylbenzene (97%), *trans*-2-hexene (97%), *cis*-2-hexene (98%), *trans*-2-octene (98%) and octane (98%) were purchased from Sigma-Aldrich and used to confirm the presence and composition of hydrogenation products.

### 3.2.4. General procedure for the Hg-poisoning test

A solution of styrene (0.41 g, 4.00 mmol), complex 7 (3.47 mg, 0.007 mmol, S/C 600) in toluene (50 mL) was stirred with 5 drops of Hg(0) for 1 h, so that the Hg(0) has a chance to contact any metal particles present. The solution mixture was introduced into a stainless-steel autoclave fitted with internal stirring system. The solution mixture was purged three times with hydrogen before the autoclave was finally charged with hydrogen and the pressure and temp adjusted to 5 bar and 30 °C, respectively. The stirring speed was set to 500 rpm and the stirring started when the temperature reached equilibrium. The mixture was stirred under constant hydrogen and the sample was withdrawn after 1.5 h, filtered using 0.45 µm micro filters and analysed by Varian CP-3800 GC (ZB-5HT column 30 m × 0.25 mm × 0.10 µm) GC instrument to determine the percentage conversion of styrene to ethylbenzene.

## 3.3. Results and discussion

### 3.3.1. Hydrogenation reactions of alkenes and alkynes using palladium (II) complexes 6-11 as catalysts

Preliminary evaluations of complexes 6-11 (Figure 3.1) in the hydrogenation of styrene were performed at 5 bar of H<sub>2</sub> pressure, 30 °C, 1.5 h and ([styrene]/catalysts) = 600:1. Under these conditions, all the complexes showed catalytic activities to afford 100% ethylbenzene with conversions ranging from 54% to 99% within 1.5 h (Figure 3.2).



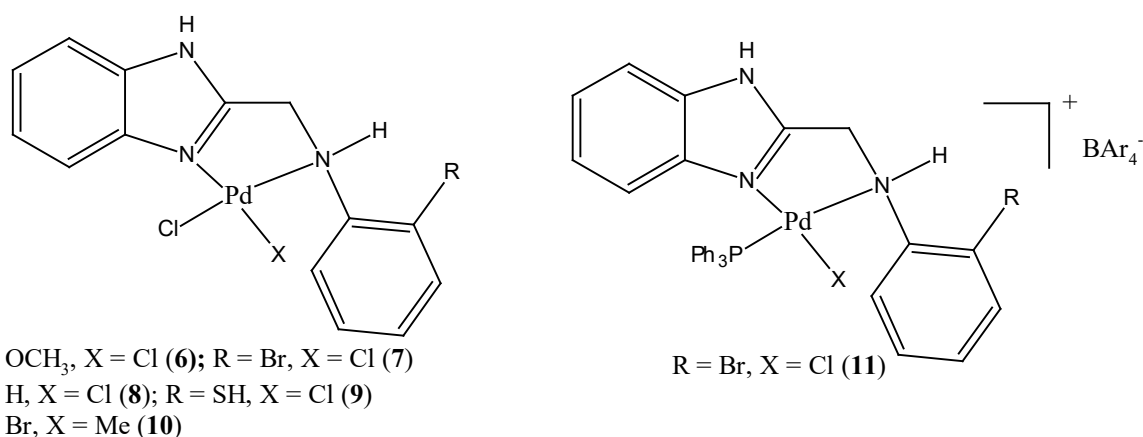


**Figure 3.1:** Neutral and cationic (benzimidazol-2-ylmethyl)amine palladium(II) complexes **6-11** used as catalysts in the hydrogenation reactions.

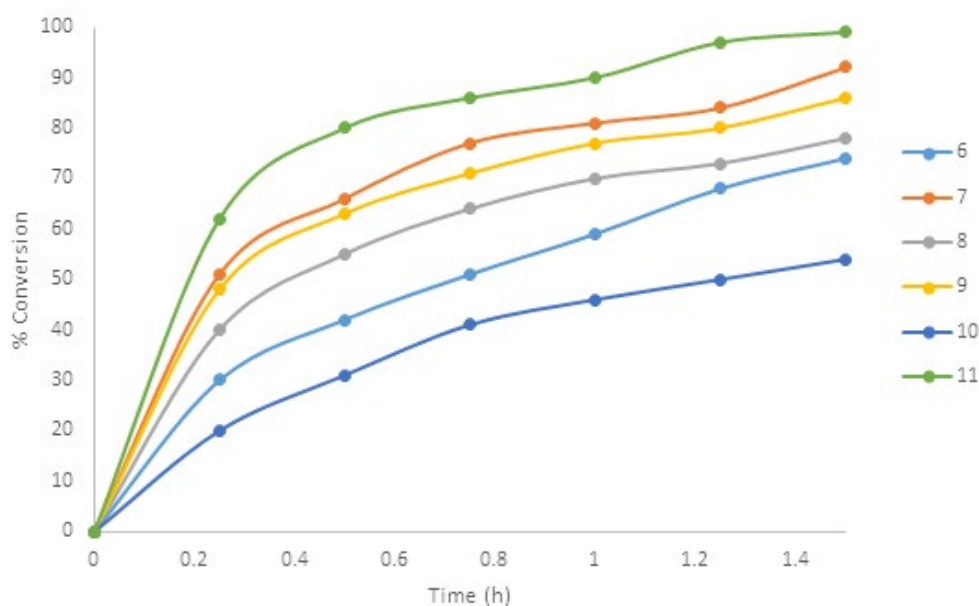


**Figure 3.2:** Plot of % conversion *vs* time for styrene hydrogenation using **6-11**.

In order to fully account for the role of complexes **6-11** in the observed catalytic hydrogenation reactions, control experiments were conducted without the use of the palladium(II) complexes and also in the presence of the ligand **L2** only under similar reaction conditions. The low percentage conversions of 4% and 6% obtained

respectively within 10 h (Table 3.1, entries 7 and 8) confirmed that complexes **6-11** were responsible for the observed catalytic activities. We thus further carried out kinetics, selectivity, theoretical and mechanistic studies of hydrogenation reactions of alkenes and alkynes using complexes **6-11** as catalysts.

**Table 3.1:** Effect of catalyst structure on the hydrogenation of styrene by complexes **6-11**<sup>a</sup>

Entry	Catalyst	Conversion <sup>b</sup> (mol <sup>0</sup> %)	<i>k</i> <sub>obs</sub> (h <sup>-1</sup> )	TOF <sup>c</sup> (h <sup>-1</sup> )
1	<b>6</b>	74	0.91 (±0.03)	296
2	<b>7</b>	92	1.67 (±0.01)	368
3	<b>8</b>	78	0.98 (±0.05)	312
4	<b>9</b>	86	1.38 (±0.07)	344
5	<b>10</b>	54	0.56 (±0.04)	215
6	<b>11</b>	99	2.93 (±0.1)	396
7 <sup>d</sup>	—	4	—	—
8 <sup>e</sup>	—	6	—	—

<sup>a</sup>Conditions: styrene (0.41 g, 4.00 mmol); [styrene]/[catalyst], 600; substrate, catalyst (0.007 mmol); solvent, toluene (50 mL); pressure, 5 bar; temperature, 30 °C; time, 1.5 h. <sup>b</sup>Determined by GC by comparing the peak areas of styrene substrate to ethylbenzene at regular time intervals. <sup>c</sup>TOF in mol<sub>substrate</sub>mol<sub>catalyst</sub><sup>-1</sup> h<sup>-1</sup> (h<sup>-1</sup>). <sup>d</sup>Control experiment, no catalyst used, time, 10 h. <sup>e</sup>Control experiment, in the presence of the ligand **L2**; time, 10 h.

### 3.3.2. Kinetic studies of styrene hydrogenation reactions

#### 3.3.2.1. Effect of complex structure on catalytic hydrogenation of styrene by 6-11

Kinetics of the hydrogenation reactions of styrene were investigated for complexes 6-11 by monitoring the reactions using GC chromatography. Table 3.1 contains the initial rate constants derived from the plots of  $\ln[\text{styrene}]_0/[\text{styrene}]_t$  vs time (Figure 3.3). A linear relationship was established consistent with a *pseudo*-first order kinetics with respect to styrene for all the complexes. The dependence of the rate of the hydrogenation reactions on styrene substrate can therefore be represented as given in equation 3.1.

$$\text{Rate} = k[\text{styrene}]^1 \quad (3.1)$$

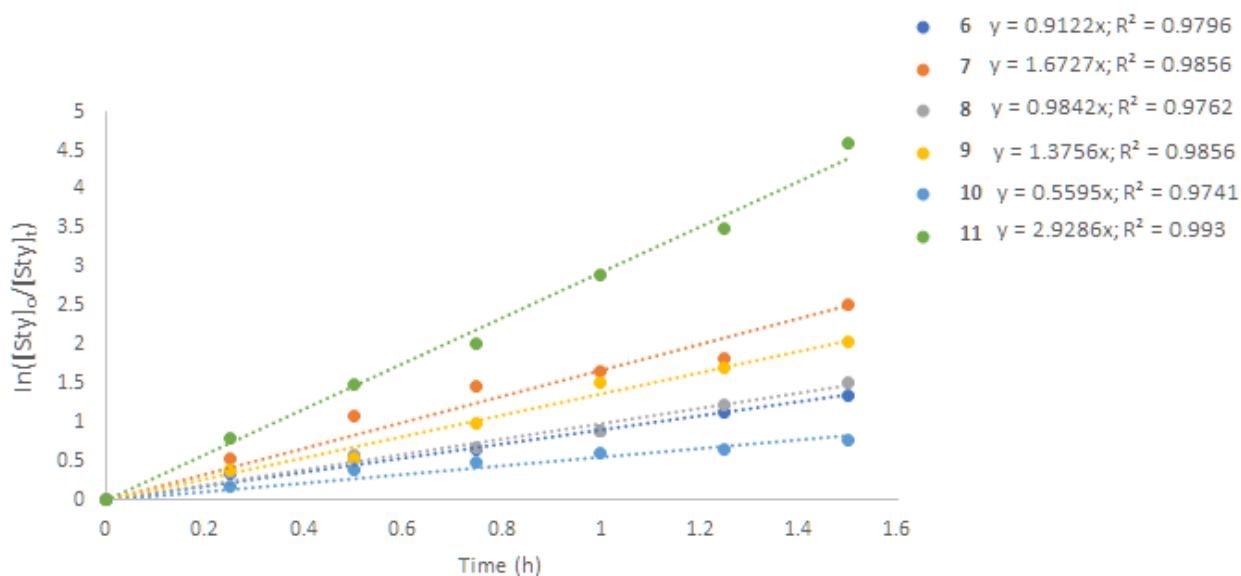


**Figure 3.3:** Plot of  $\ln[\text{Sty}]_0/[\text{Sty}]_t$  vs time for styrene hydrogenation using 6-11.

From the rate constants observed, the cationic complex 11 was the most active compared to 7 (Table 3.1, entries 2 and 6). This trend clearly demonstrates the

importance of complex solubility in controlling their respective catalytic activities.<sup>11</sup> Complex **11** showed the highest solubility in most organic solvents in comparison to **6-10**. Another plausible explanation could be a higher positive charge on the palladium(II) metal atom in the cationic complex **11** relative to the neutral analogues, thus better substrate coordination.<sup>8</sup> A similar trend in the hydrogenation of 1-hexene was reported where higher catalytic activity (TOF = 4000 h<sup>-1</sup>) for the cationic complex ([Rh(PPh<sub>3</sub>)<sub>2</sub>COD]<sup>+</sup>) compared to TOF = 700 h<sup>-1</sup> for the neutral complex [Rh(PPh<sub>3</sub>)<sub>3</sub>Cl] was observed.<sup>17,18</sup> We also observed that the ligand motif had an influence on the catalytic activity. For instance, complex **7**, bearing electron withdrawing Br group on the phenyl ring showed higher catalytic activity, (*k*<sub>obs</sub> of 1.67 h<sup>-1</sup>) than the analogues complex **6** (*k*<sub>obs</sub> of 0.91 h<sup>-1</sup>), containing the electron donating OCH<sub>3</sub> substituent (Table 3.1, entries 1 and 2). This can also be rationalized from electrophilic metal<sup>8</sup> center in **7** compared to **6**, consistent with the argument proposed for the cationic complex **11**.

Another factor that appeared to control the catalytic activity was the Pd-Cl/Me bonds on the complex structure. For example, rate constants of 1.67 h<sup>-1</sup> and 0.56 h<sup>-1</sup> were observed for complexes **7** and **10** bearing Pd-Cl and Pd-Me groups respectively (Table 3.1, entries 2 and 5). This can be attributed to enhanced stability of the dichloride complex **7**, compared to the Pd-Me complex **10**. Generally, metal alkyls are known to readily undergo deactivation due the higher reactivity of metal-alkyl bonds.<sup>19</sup>

3.3.2.2. *Effect of catalyst concentration and hydrogen pressure on the kinetics of hydrogenation reactions of styrene using complexes 7 and 11.*

Kinetic experiments were further conducted to establish the effects of catalyst concentrations on the hydrogenation reactions of styrene using complexes **7** and **11**. The concentrations of catalysts **2** and **6** were thus varied from 200 to 1000 at constant initial concentration of styrene (Table 3.2, entries 1-5). Plots of  $\ln[\text{styrene}]_0/[\text{styrene}]_t$  vs time (Figure 3.4) gave linear relationships from which the observed rate constants ( $k_{obs}$ ) were derived (Table 3.2). It was observed that an increase in catalyst concentration resulted in an increase in catalytic activity. For instance  $k_{obs}$  of  $1.67 \text{ h}^{-1}$  and  $0.91 \text{ h}^{-1}$  were obtained at [styrene]/[**7**] ratios of 600:1 and 1000:1, respectively. However, a closer examination of the TOF values for both **7** and **11** at different catalyst loadings paint a different picture. For example, increased [styrene]/[**11**] ratio (decrease in catalyst concentration) from 600 to 1000 was marked by an increase in TOF from  $396 \text{ h}^{-1}$  and  $513 \text{ h}^{-1}$  respectively (Table 3.2, entries 3-5). It is therefore evident that increasing catalyst concentration did not increase the catalytic activity by a similar magnitude and thus higher [substrate]/[catalyst] ratios (lower catalyst loadings) is not only recommended but would also be industrially beneficial with these systems.

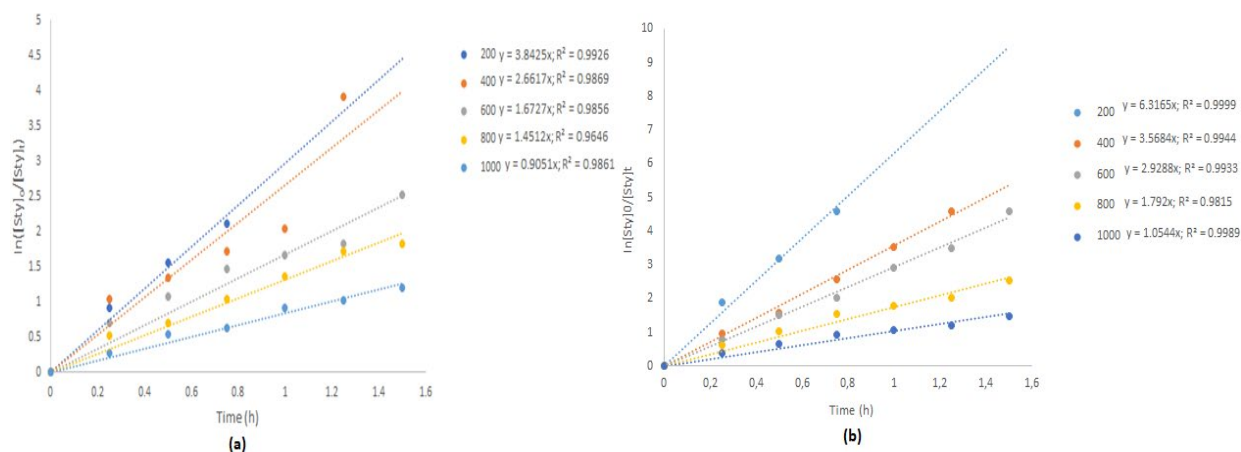


**Figure 3.4:** Plot of  $\ln[\text{styrene}]_0/[\text{styrene}]_t$  vs time for effect of catalyst concentration using complexes **7** (a) and **11** (b). The  $[\text{styrene}]/[\mathbf{7}]$  and  $[\mathbf{11}]$  was varied from 200 to 1000 at fixed concentration of styrene of 0.41 g (4.00 mmol).

The orders of reaction with respect to catalysts **7** and **11** were extracted from the plots of  $-\ln(k_{obs})$  vs  $-\ln[\mathbf{7}]$  and  $-\ln[\mathbf{11}]$  (Figure 3.5) and obtained as  $0.73 \pm 0.08$  and  $1.03 \pm 0.06$  respectively (Eqs. 3.2 and 3.3). Ogweno *et. al.* reported fractional orders with respect to catalyst concentration in hydrogenation reactions of styrene catalyzed by palladium(II) complexes and was associated with possible catalyst aggregation during the hydrogenation reactions and/or formation of palladium(0) nanoparticles as the active species.<sup>20,21</sup> On the other hand, integer order with respect to the cationic complex **11** thus shows minimum aggregation of the active species, in good agreement with the value of  $1.08 \text{ h}^{-1}$  reported by Kluwer *et al.*<sup>22</sup>

$$\text{Rate} = k[\text{styrene}]^1 [\mathbf{7}]^{0.73} \quad (3.2)$$

$$\text{Rate} = k[\text{styrene}]^1 [\mathbf{11}]^{1.03} \quad (3.3)$$

To shed some light on the possible formation of palladium(0) nanoparticles, a mercury poisoning test was conducted for catalysts **7** and **11** by adding few drops of mercury to the reaction solutions.<sup>20</sup> While appreciable drop in catalytic activity from 92% ( $k_{obs} = 1.67 \text{ h}^{-1}$ ) to 67% ( $k_{obs} = 0.69 \text{ h}^{-1}$ ) was observed for catalyst **7**, catalyst **11** exhibited minimal decline in catalytic activity from 99% ( $k_{obs} = 2.92$ ) to 94% ( $k_{obs} = 1.81$ ), (Table 3.2, entries 3 and 9). This showed the possible formation of more nanoparticles in catalyst **7** compared to catalyst **11**<sup>22</sup> in good agreement with kinetic equations 3.2 and 3.3. In general, the absence of induction periods (Figures 3.2 - 3.4) point to a largely homogeneous catalyst systems for both complexes **7** and **11**.

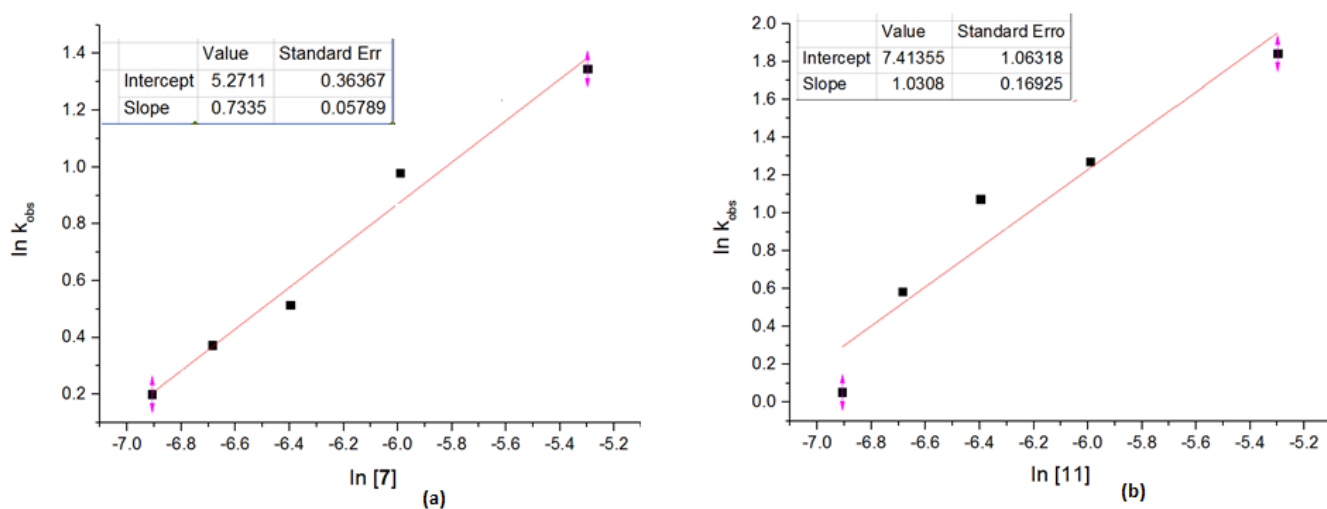


**Figure 3.5:** Plot of  $\ln(k_{obs})$  vs  $\ln[7]$  (a) and  $\ln[11]$  (b) for the determination of the order of reaction with respect to catalyst **7** and **11** in the hydrogenation of styrene.  $R^2=0.98237$ ; slope = 0.73, Intercept = 5.27 (a)  $R^2=0.96186$ ; slope = 1.03, Intercept = 7.41 (b)

The effect of H<sub>2</sub> concentration on the kinetics of styrene hydrogenation reactions was also investigated at different H<sub>2</sub> pressures of 5 bar to 12.5 bar (Table 3.2, entries 3, 6-8). From the data obtained, it was evident that an increase in H<sub>2</sub> pressure resulted in an increase in the observed rate constants ( $k_{obs}$ ). For example,  $k_{obs}$  of 1.67 h<sup>-1</sup> and 2.02 h<sup>-1</sup> were recorded at H<sub>2</sub> pressures of 5 and 7.5 bar (Table 3.2, entries 3 and 6). Linear relationships were observed from the plot of  $\ln[\text{Sty}]_0/[\text{Sty}]_t$  vs time at different H<sub>2</sub> pressures (Figure 3.6) to generate a rate order of  $0.73 \pm 0.1$  with respect to H<sub>2</sub> concentration (Figure 3.7). This fractional and lower order indicates a complex reaction mechanism with respect to [H<sub>2</sub>] and possibly the formation of a Pd-monohydride species as the active species,<sup>23</sup> and possible catalyst aggregation *vide supra*. The rate law for the hydrogenation reactions of styrene using catalyst 7 can therefore be expressed as given in equation 4.4.

$$\text{Rate} = k[\text{styrene}]^1 [\mathbf{7}]^{0.73} [P_{H_2}]^{0.73} \quad (3.4)$$

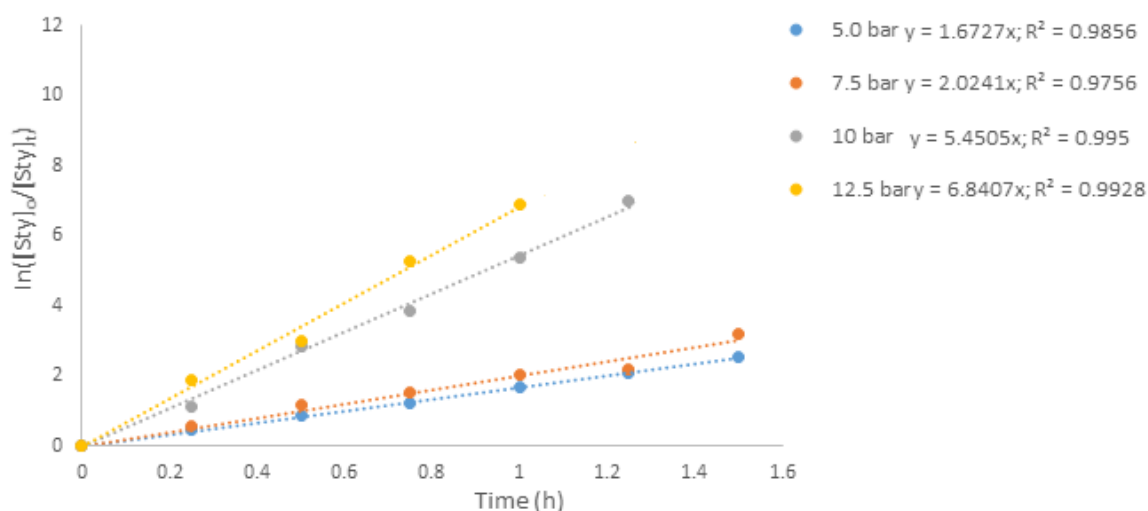


**Figure 3.6:** Plot of  $\ln[\text{styrene}]_0/[\text{styrene}]_t$  vs time for styrene hydrogenation pressures.



**Table 3.2:** Effect of catalyst concentration and pressure on the hydrogenation of styrene using catalysts **7** and **11**<sup>a</sup>

Entry	[sub]/[cat]	$P_{H_2}$ (bar)	$K_{obs}$ (h <sup>-1</sup> )		TOF (h <sup>-1</sup> ) <sup>b</sup>	
			<b>7</b>	<b>11</b>	<b>7</b>	<b>11</b>
1 <sup>c</sup>	200	5	3.84 (±0.02)	6.32 (±0.01)	158	198
2 <sup>d</sup>	400	5	2.66 (±0.02)	3.56 (±0.03)	267	316
3	600	5	1.67 (±0.01)	2.92 (±0.02)	368	396
4	800	5	1.45 (±0.03)	1.79 (±0.04)	448	501
5	1000	5	0.91 (±0.05)	1.05 (±0.05)	466	513
6	600	7.5	2.02 (±0.02)	—	392	—
7 <sup>c</sup>	600	10	5.45 (±0.13)	—	475	—
8 <sup>d</sup>	600	12.5	6.84 (±0.06)	—	594	—
9 <sup>e</sup>	600	5	0.69 (±0.03)	1.81 (±0.03)	268	376

<sup>a</sup>Conditions: styrene, (4.00 mmol); solvent; toluene (50mL); temperature, 30 °C; time, 1.5 h. <sup>b</sup>TOF in mol<sub>substrate</sub>mol<sub>catalyst</sub><sup>-1</sup> h<sup>-1</sup>. <sup>c</sup>Time, 1.0 h, <sup>d</sup>Time, 1.25 h. <sup>e</sup>Mercury drop test (5 drops of mercury were added to the reaction mixture).

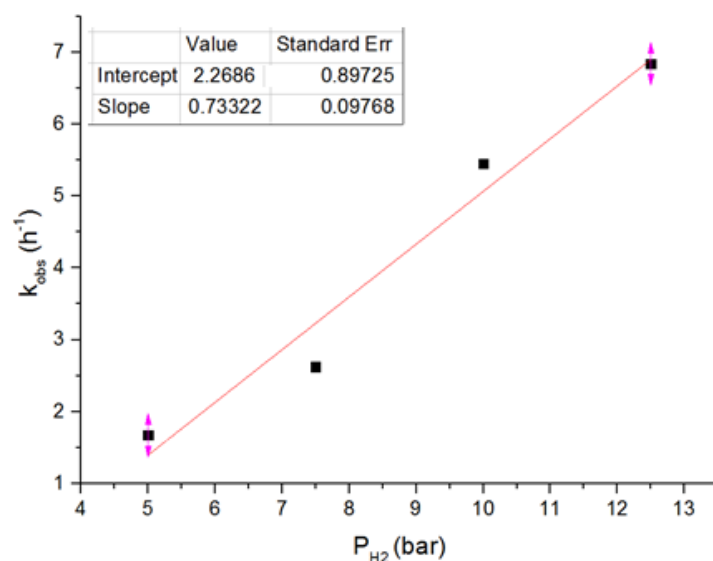


**Figure 3.7:** Plot of  $k_{obs}$  vs  $P_{H_2}$  (bar) for the determination of the order of reaction with respect to  $H_2$  pressure in the hydrogenation of styrene using catalyst **7**.  $R^2 = 0.98271$ ; slope = 0.73, Intercept = 2.26.

### 3.3.2.3. Effect of temperature and solvents on rate of styrene hydrogenation reactions

The effect of temperature on the kinetics of hydrogenation of styrene using catalyst **7** was investigated by comparing the catalytic activities of **7** from 30 °C to 60 °C (Table 3.3, entries 1-4). The observed rate constants at different temperatures in Table 3.3 were extracted from the plot of  $\ln[\text{styrene}]_0/[\text{styrene}]_t$  vs time (Figure 3.8). Expectedly, a significant increase in the rate constant from 1.67 h<sup>-1</sup> to 6.30 h<sup>-1</sup> was recorded with an increase in reaction temperature from 30 °C to 60 °C.

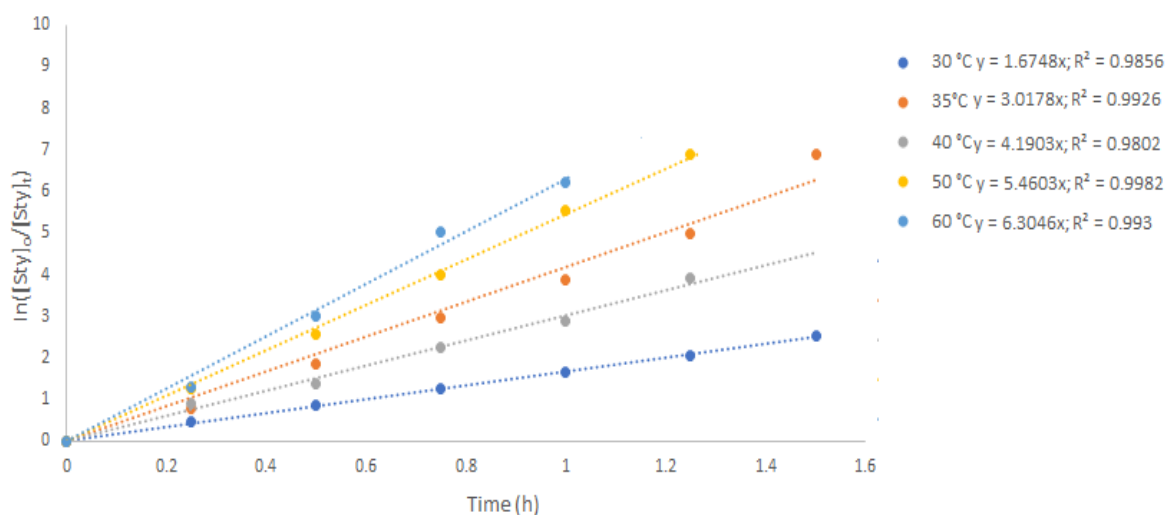


**Figure 3.8:** Plot of  $\ln[\text{styrene}]_0/[\text{styrene}]_t$  vs time for the effect of temperature using **7**.

The overall activation energy ( $E_a$ ) of the hydrogenation of styrene using **7** was calculated from the Arrhenius plot of  $\ln k_{obs}$  vs  $1/T$  (Figure 3.9a) as  $35.61 \pm 1.6$  kJ mol<sup>-1</sup>. This value is comparable to the value of  $42.05 \pm 0.01$  kJ mol<sup>-1</sup> ( $10.05 \pm 0.01$  kcal.mol<sup>-1</sup>) reported by Pelagatti *et. al.*<sup>24</sup> using Pd(PNO)AcO (PNO = tridentate hydrazonic) in the hydrogenation reaction of alkenes at 40 °C. These results are in good agreement with

the similar TOFs of 600 h<sup>-1</sup> and 580 h<sup>-1</sup> obtained for **7** and the Pelagatti catalysts respectively. The Eyring plot in Figure 3.9b was used to obtain the enthalpy of activation ( $\Delta H^\ddagger = 32.98 \pm 1.9$  kJ mol<sup>-1</sup>) and entropy of activation ( $\Delta S^\ddagger = -127.9 \pm 1.9$  KJ mol<sup>-1</sup> K<sup>-1</sup>). The significance of these thermodynamic parameters is that they support largely homogeneous nature of catalyst **7** as has been previously reported by others.<sup>25,26</sup> Typical heterogeneous catalysts in which the hydrogenation reactions are diffusion controlled display lower values of  $E_a$  between 8 kJ mol<sup>-1</sup> to 17 kJ mol<sup>-1</sup>.<sup>28,29</sup>

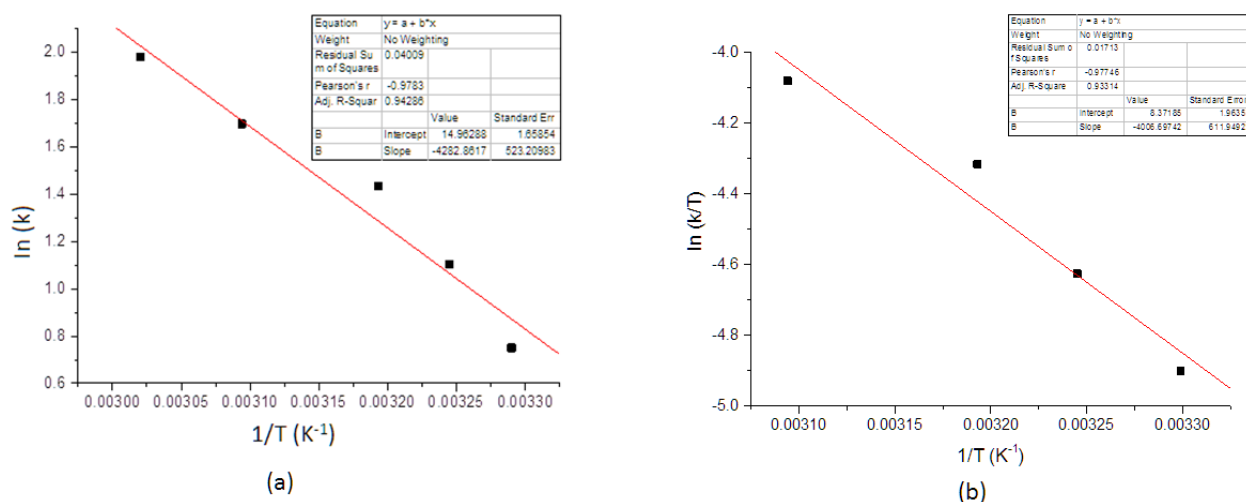


**Figure 3.9:** Arrhenius plot (a) and Eyring plot (b) for the determination of the  $E_a = 35.61 \pm 1.6$  kJ mol<sup>-1</sup>,  $\Delta H^\ddagger = 32.98 \pm 1.9$  kJ mol<sup>-1</sup>, and  $\Delta S^\ddagger = -127.9 \pm 1.9$  J mol<sup>-1</sup> K<sup>-1</sup> for the hydrogenation of styrene using catalyst **7**.

We also studied the effects of solvents using toluene, THF, dichloromethane, methanol and DMSO in the hydrogenation reactions of styrene using complex **7** (Table 3.3, entries 1, 5 - 8). The order of reactivity was established as follows: DMSO < methanol < THF < toluene. For example, higher catalytic activities were obtained in toluene ( $k_{obs}$  of 1.67 h<sup>-1</sup>,

TOF = 368 h<sup>-1</sup>) than DMSO ( $k_{obs}$  of 0.52 h<sup>-1</sup>, TOF = 183 h<sup>-1</sup>). This trend is in line with different coordinating abilities of the solvents; where strongly coordination solvents are known to compete with the alkene substrate, for the active site resulting in diminished activities.<sup>27,28</sup> Consistent with our observations, Unver and Yilmaz recently reported 27% and 63% conversions in DMSO and toluene solvents respectively in the hydrogenation of 1-octene catalyzed by ruthenium complexes.<sup>29</sup>

**Table 3.3:** Effect of temperature and solvent on the hydrogenation of styrene using catalyst **7**<sup>a</sup>

Entry	Solvent	T (°C)	Conv (%) <sup>b</sup>	$k_{obs}$ (h <sup>-1</sup> )	TOF (h <sup>-1</sup> ) <sup>c</sup>
1	Toluene	30	92	1.67 (±0.01)	368
2 <sup>d</sup>	Toluene	40	99	4.19 (±0.03)	475
3 <sup>d</sup>	Toluene	50	>99	5.46 (±0.1)	480
4 <sup>e</sup>	Toluene	60	>99	6.30 (±0.07)	600
5	Methanol	30	49	0.61 (±0.08)	196
6	DCM	30	68	0.90 (±0.04)	272
7	THF	30	86	1.40 (±0.03)	343
8	DMSO	30	35	0.52 (±0.06)	183

<sup>a</sup>Conditions: styrene (0.41 g, 4.00 mmol); solvent; toluene (50mL); [styrene]/[**7**] = 600; time, 1.5 h, pressure, 5 bar. <sup>b</sup>Determined by GC by comparison of peak areas of styrene and ethylbenzene product. <sup>c</sup>TOF in mol<sub>substrate</sub>mol<sub>catalyst</sub><sup>-1</sup> h<sup>-1</sup> (h<sup>-1</sup>). <sup>d</sup>Time, 1.25 h, <sup>e</sup>Time, 1.0 h.

#### 3.3.2.4. *Effect of the nature of the alkene and alkyne substrates on hydrogenation reactions and selectivity*

Complexes **7** and **11** were further used to investigate the hydrogenation reactions of a range of alkene and alkyne substrates: 1-hexene, 1-octene, 1-nonene, 1-decene, phenyl-

acetylene, 1-hexyne and 1-octyne. It was observed that the catalytic performance of complexes **7** and **11** were controlled by the nature of the substrate (Tables 3.4). The initial rate constants ( $k_{obs}$ ) of each substrate were determined from the plot of  $\ln[\text{substrate}]_0/[\text{substrate}]_t$  vs time (Figure 3.10).

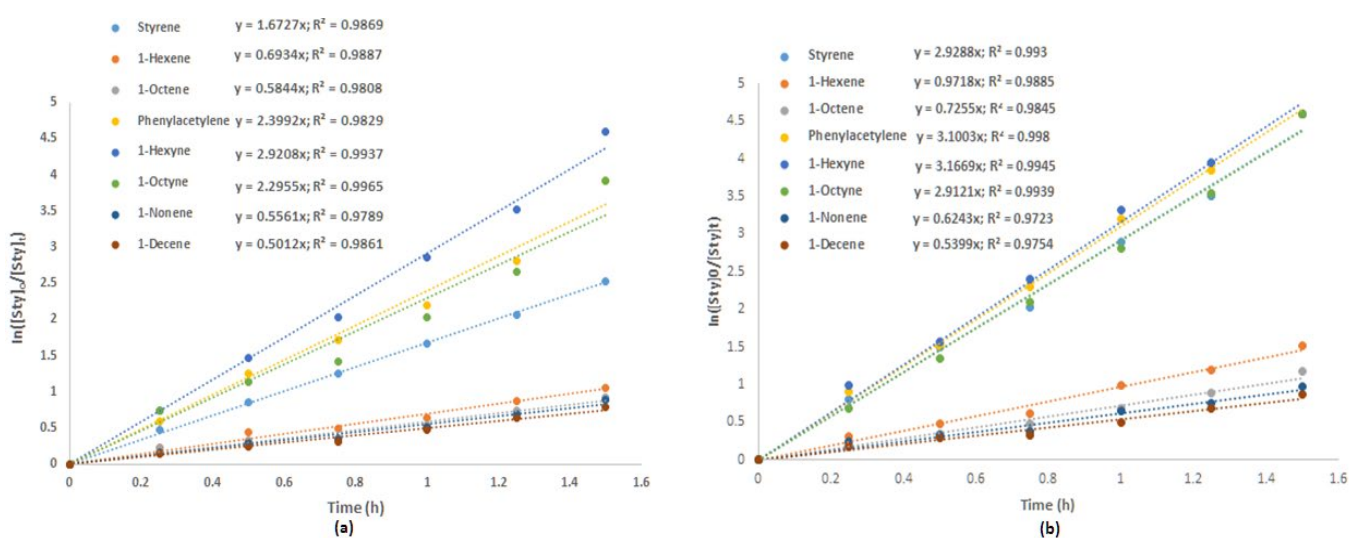


**Figure 3.10:** Plot of  $\ln[\text{substrate}]_0/[\text{substrate}]_t$  vs time for the effect of substrate using catalyst **7** (a) and **11** (b).

The results obtained generally showed that alkynes were more reactive compared to the corresponding alkenes.<sup>30,31</sup> For example,  $k_{obs}$  of  $0.69 \text{ h}^{-1}$  and  $k_{obs}$  of  $2.92 \text{ h}^{-1}$  were obtained for 1-hexene and 1-hexyne respectively (Table 3.4, entries 2 and 7). The alkyl chain length had a profound effect on the reactivity of the substrates, in that shorter chains were more reactive. For instance,  $k_{obs}$  of  $0.97 \text{ h}^{-1}$  and  $0.54 \text{ h}^{-1}$  were observed for 1-hexene and 1-decene respectively (Table 3.4, entries 2 and 5). The decrease in catalytic activity with alkene chain has been attributed to poor coordinating abilities of higher alkenes to the active metal center.<sup>11</sup> With respect to alkenes, the best catalytic activity for both catalysts **7** and **11** was

obtained using an activated alkene, styrene to give  $k_{obs}$  of 1.67 h<sup>-1</sup> and 2.93 h<sup>-1</sup> respectively. This trend has largely been associated with the formation of the more reactive benzylic palladium intermediate, which has a lower energy than analogous alkyl palladium intermediates.<sup>32</sup> The product distribution of terminal alkenes and alkynes was similar to our recent reports;<sup>33,34</sup> where hydrogenation reactions of terminal alkenes were followed by isomerization reactions to give the corresponding internal alkenes, while alkyne hydrogenation reactions occurred in two steps to produce the respective alkenes and alkanes (Figure 3.11). It was clear from Figure 3.11 that catalyst **7** favored isomerization (58% internal isomers) over hydrogenation (42% hexanes), in comparison to catalyst **11** (71% hexanes and 29% internal alkenes). Lower isomerization reactions observed for catalyst **11** can be easily apportioned to the presence of bulkier PPh<sub>3</sub> groups in the metal coordination sphere as has been recently reported by Smarun *et al.*<sup>35</sup> **Figure 2.9:** Nature of the active species in the methoxycarbonylation reactions

**Table 3.4:** Effect of substrate on the catalytic performance of complexes **7** and **11**<sup>a</sup>

Entry	Substrate	$K_{obs}$ ( $h^{-1}$ )		TOF ( $h^{-1}$ ) <sup>b</sup>		%Alkanes <sup>c</sup>	
		<b>7</b>	<b>11</b>	<b>7</b>	<b>11</b>	<b>7</b>	<b>11</b>
1	Styrene	1.67 ( $\pm 0.01$ )	2.93 ( $\pm 0.01$ )	368	396	92	99
2	1-hexene	0.69 ( $\pm 0.06$ )	0.97 ( $\pm 0.03$ )	284	312	42	71
3	1-Octene	0.58 ( $\pm 0.13$ )	0.73 ( $\pm 0.02$ )	268	276	40	67
4	1-Nonene	0.56 ( $\pm 0.05$ )	0.62 ( $\pm 0.11$ )	236	248	37	59
5	1-Decene	0.50 ( $\pm 0.07$ )	0.54 ( $\pm 0.05$ )	220	232	33	55
6	Phenyl- acetylene	2.40 ( $\pm 0.05$ )	3.10 ( $\pm 0.04$ )	400	400	100	100
7	1-Hexyne	2.92 ( $\pm 0.04$ )	3.17 ( $\pm 0.07$ )	260	372	59	65
8	1-Octyne	2.29 ( $\pm 0.02$ )	2.91 ( $\pm 0.06$ )	208	356	52	52

<sup>a</sup>Conditions: substrate, substrate/catalyst = 600; solvent, toluene; pressure, 5 bar; temperature, 30 °C; time, 1.5 h. <sup>b</sup>TOF in  $\text{mol}_{\text{substrate}}\text{mol}_{\text{catalyst}}^{-1} \text{h}^{-1}$ . <sup>c</sup>Selectivity towards alkane hydrogenation products after 1.5 h.

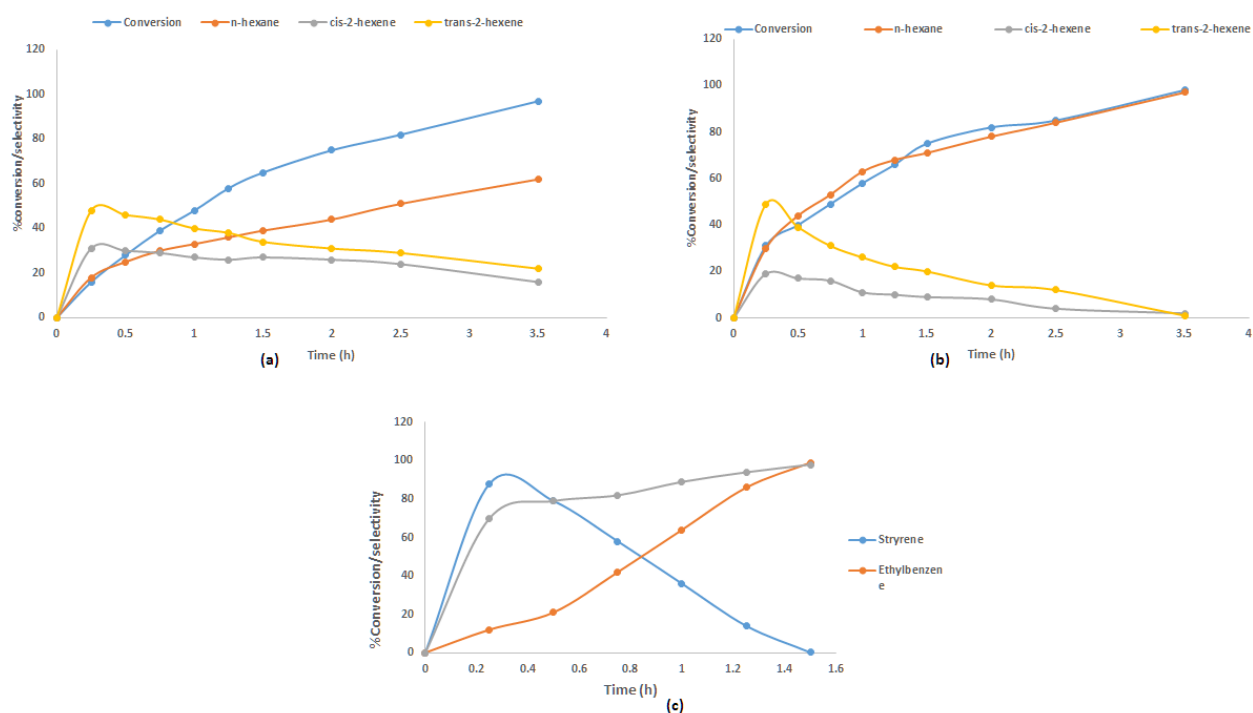


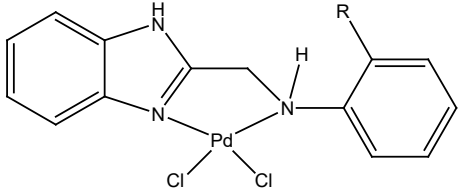
**Figure 3.11.** Product distribution over time in the hydrogenation of (a) 1-hexene using catalyst **7** (b) 1-hexene using catalyst **11** and (c) phenyl-acetylene using catalyst **7**.

### 3.3.3. Theoretical insights of the hydrogenation reactions of alkenes

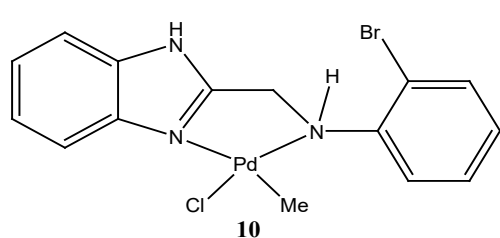
Density Functional Theory (DFT) calculations were conducted in order to have an understanding of the effect of the ligand motif and catalyst structure on the catalytic activities of complexes **6-9**. The geometries-optimized structures and frontier orbital energy (HOMO and LUMO) maps are summarized in Table 3.5 and Table 3.6, respectively. The charge on the metal ion was also observed to influence the catalytic activities of complexes **6-9** (Figure 3.12). For instance, catalyst **7** carrying a positive charge of 0.392 was more active than catalyst **6**, with a charge of 0.326 on the palladium(II) atom. This trend is in agreement with a more facile substrate coordination to an electrophilic palladium atom.<sup>36</sup>



**Table 3.5:** DFT calculated data for palladium (II) complexes using B3LYP/LANL2DZ level of theory.



R = OCH<sub>3</sub> (**6**); Br (**7**); H (**8**); SH (**9**)



**10**

Parameter	<b>6</b>	<b>7</b>	<b>8</b>	<b>9</b>	<b>10</b>
LUMO (eV) 1.88	-1.87	-1.83	-1.77	-1.81	-
HOMO (eV) 7.82	-7.13	-6.38	-6.75	-6.35	-
$\Delta E_{L-H}$	5.26	4.55	4.98	4.54	5.94
$\Delta \epsilon$ [kcal mol <sup>-1</sup> ]	121	104	115	105	137
NBO charges (Pd)	0.326	0.392	0.354	0.358	0.292
TOF (h <sup>-1</sup> ) <sup>a</sup>	296	368	312	344	215
$k_{obs}$ (h <sup>-1</sup> )	0.91	1.67	0.98	1.38	0.56

<sup>a</sup>TOF in mol<sub>substrate</sub> mol<sub>catalyst</sub><sup>-1</sup> h<sup>-1</sup>

**Table 3.6:** DFT-calculated HOMO and LUMO frontier molecular orbitals of palladium(II) complexes **7-10** using LANL2DZ for palladium and 6-311G for all other atoms.

Complex	Structure	HOMO Map	LUMO Map
6			
7			
8			
9			
10			

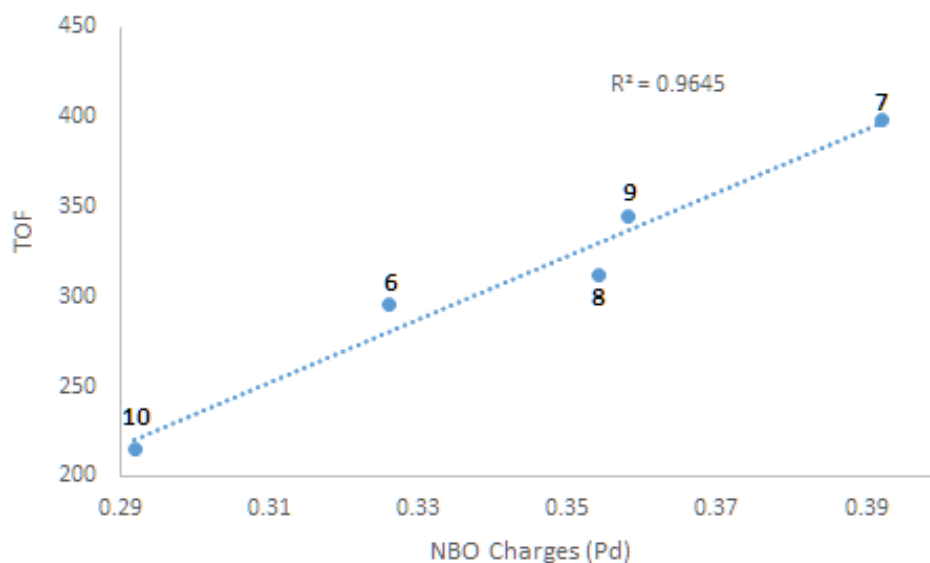
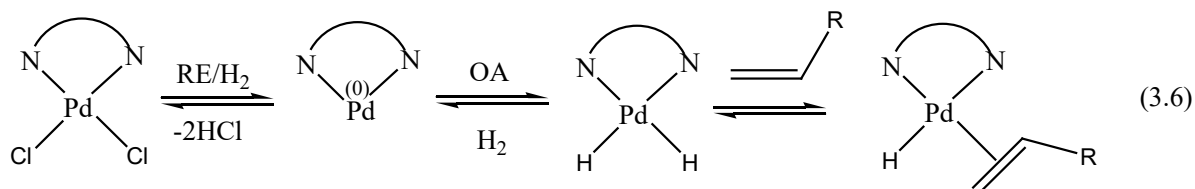
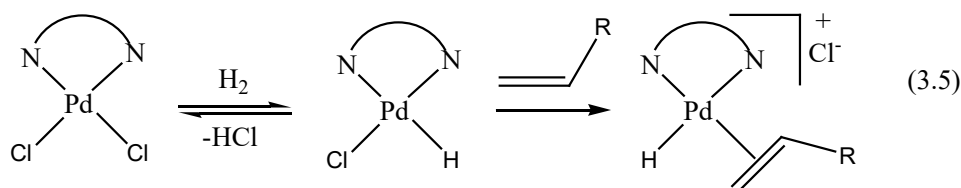


**Figure 3.12:** Plot of TOF *vs* NBO charges for palladium(II) metal atom depicting a linear correlation between catalytic activities of complexes **6-10** and palladium(II) atom NBO charges.

### 3.4. Proposed mechanism of the hydrogenation of styrene

The dependency of the rate of hydrogenation reactions on styrene, catalyst and hydrogen pressure (eq. 3.4) is consistent with either of the following equations 3.5 and 3.6. The partial and lower order of reaction with respect to  $[H_2]$  of  $0.7 \pm 0.1$  support the formation of a monohydride species as the rate determining step. This points to the first mechanism (3.5) as the most probable pathway.<sup>37</sup>



In order to fully establish if the pathway given in eq. 3.5 is indeed the preferred one, we used ESI-MS (Fig. 3.13) to detect the reaction intermediates (Scheme 3.1). This was done by sampling of the reaction mixture of complex **7** at various intervals and analysing the aliquots using ESI-MS. The first intermediate (**7a**) observed from the MS ( $m/z = 445$  amu) believed to have occurred *via* heterolytic cleavage leading to the formation of an HCl by-product<sup>38</sup> pointed to the eq. 3.5 as the operative mechanism. Coordination of the styrene substrate to **7a** affords the Pd-styrene adduct (**7b**) as deduced from the base peak at  $m/z = 514$  amu. A Markovnikov migration of the hydride to the coordinated substrate to form a 14-electron Pd-alkyl species (**7c**) was established from the  $m/z$  signal at 510 amu. Subsequent oxidative addition in the presence of H<sub>2</sub> to give the Pd(IV) dihydride compound (**7d**) was confirmed from the signal at  $m/z = 515$  amu. Hydride migration to give coordinated alkyl ligand in **7d** followed by reductive elimination to produce the monohydride Pd(II) intermediate **7e** ( $m/z = 409$ ) -and elimination of the ethylbenzene product was also confirmed. Finally, it is believed that regeneration of the active hydride species **7a** ( $m/z = 445$ ) completes the catalytic cycle.

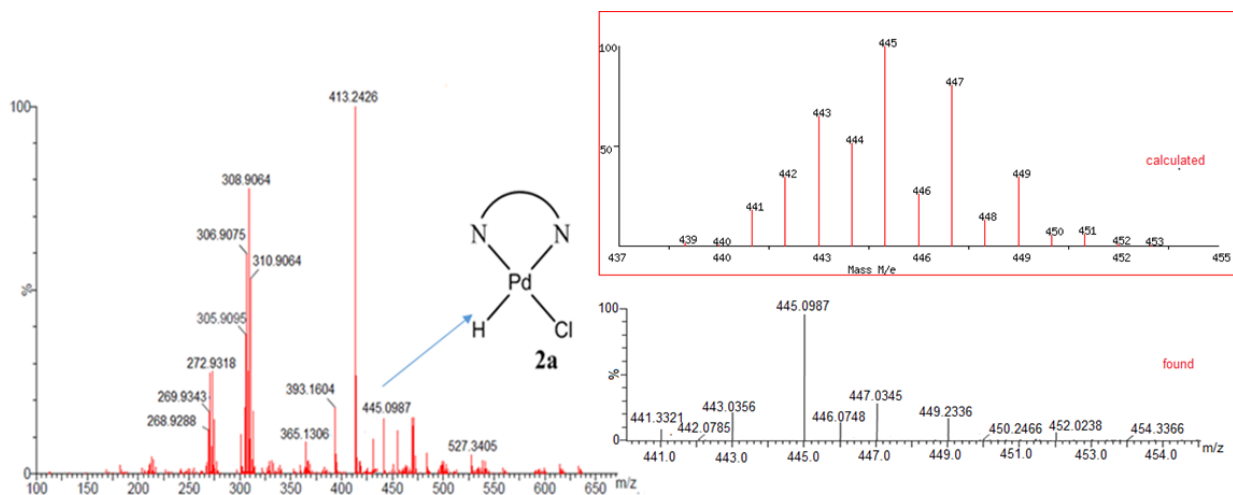
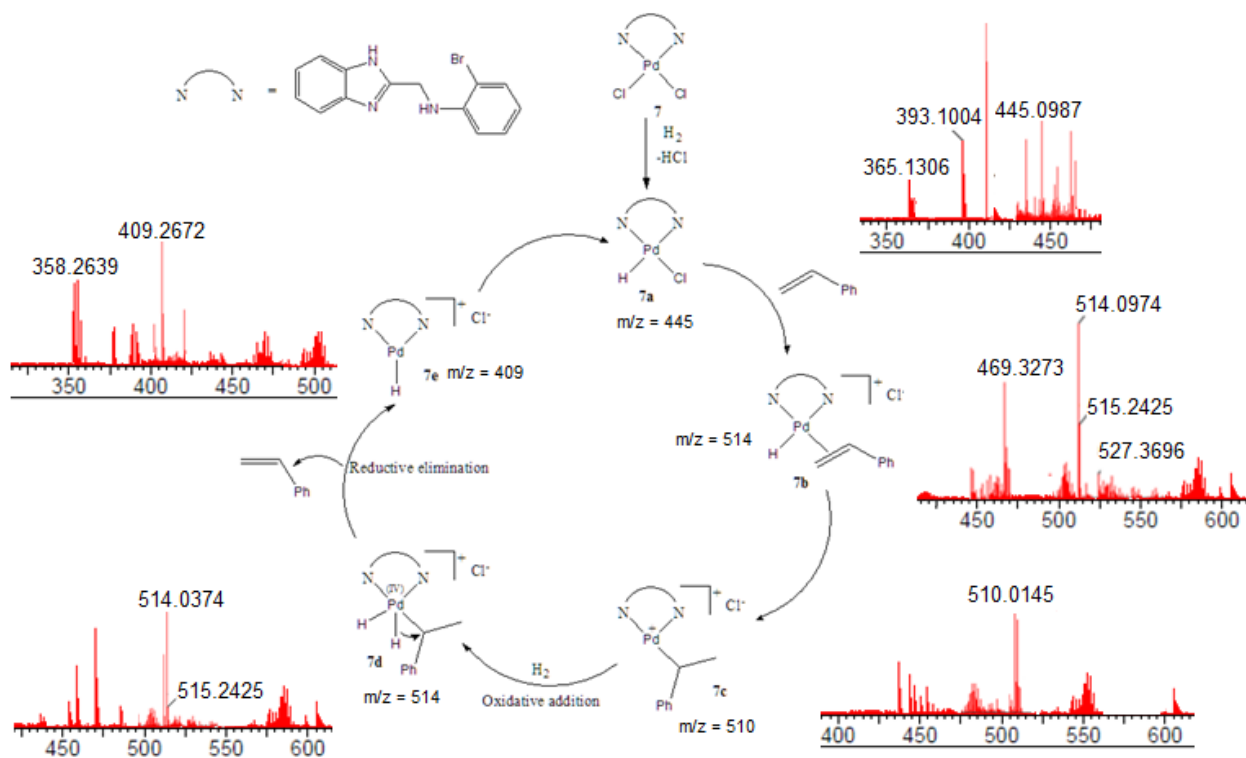


**Figure 3.13:** ESI-MS spectra for intermediates **7a** (insert calculated and found isotopic distribution).



**Scheme 3.1:** Mechanism for the hydrogenation of styrene catalyzed by **7** as established from ESI-MS,  $m/z$  corresponds to the cationic palladium fragments.

Attempts to confirm the formation of the Pd-hydride intermediates using  $^1\text{H}$  NMR spectroscopy was not successful even at elevated temperatures (Figure 3.14). We did not observe any signal associated with the Pd-H (around -5 ppm) and this may be due to low pressures (atmospheric) employed in the NMR studies as opposed to higher pressures of 5-30 bar used in the catalytic experiments.

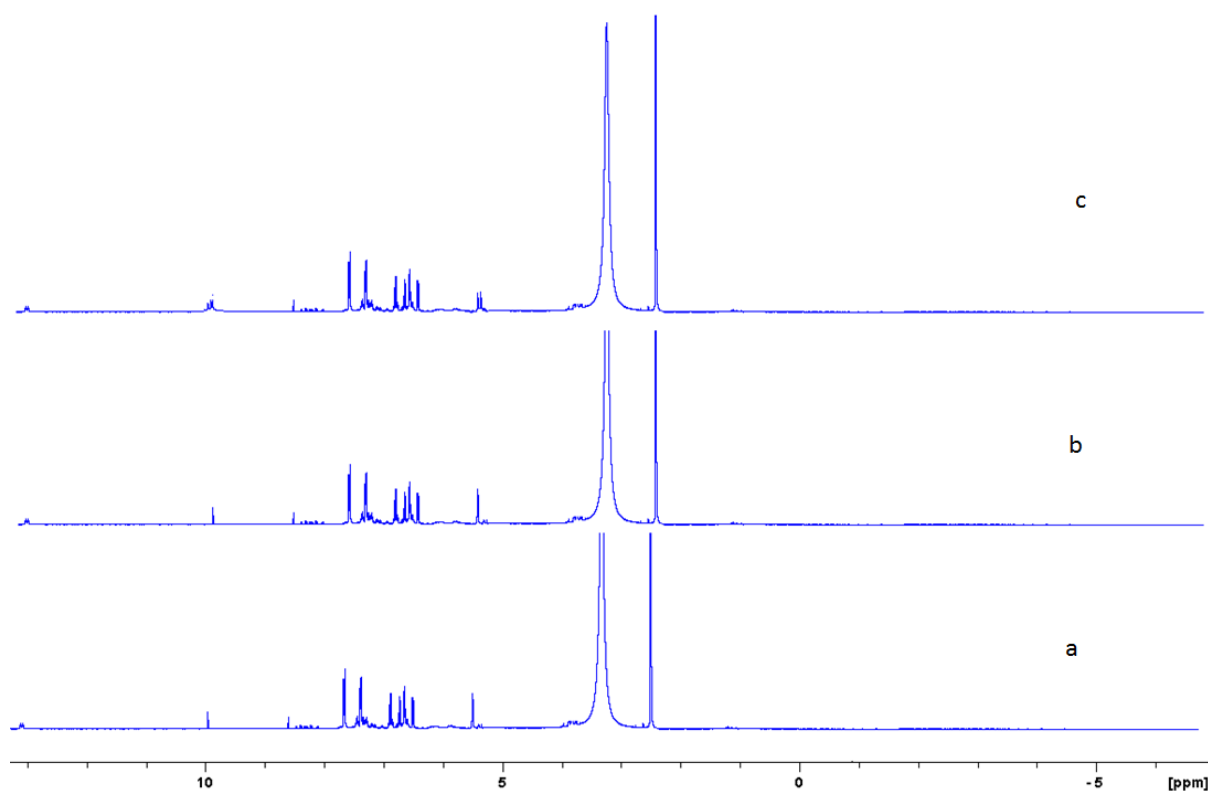


**Figure 3.14:**  $^1\text{H}$  NMR ( $\text{DMSO-d}_6$ ) spectra for complex **7** in the presence of hydrogen at room temperature (a), 20 °C (b) and 60 °C (c)

### 3.5. Conclusions

In summary, we have established that neutral and cationic palladium(II) complexes anchored on (benzoimidazol-2-ylmethyl)amine ligands form active catalysts for the hydrogenation reactions of alkenes and alkynes in which isomerization of terminal

alkenes also occur. The electrophilicity of the metal palladium atom of the complexes atom as supported by DFT calculations, enhanced the reactivity of the respective catalysts. Longer chain alkenes showed diminished reactivity while alkynes were generally more reactive compared to the correspond alkenes. Kinetics, thermodynamics and mercury drop experiments point to largely homogeneous systems. A mechanistic pathway involving the formation of a palladium monohydride intermediate as the active species was established from mass spectrometry.

### 3.6. References

- 1 K. A. Vallianatou, D. J. Frank, G. Antonopoulou, S. Georgakopoulos, E. Siapi, M. Zervou and I. D. Kostas, *Tetrahedron Lett.*, 2013, **54**, 397–401.
- 2 H. E. Hoelscher, W. G. Poynter and E. Weger, *Chem. Rev.*, 1954, **54**, 575–592.
- 3 C. Bianchini, A. Meli, M. Peruzzini, P. Frediani, C. Bohanna, M. A. Esteruelas and L. A. Oro, *Organometallics*, 1992, **11**, 138–145.
- 4 D. Schleyer, H. G. Niessen and J. Bargon, *New J. Chem.*, 2001, 423–426.
- 5 J. Navarro, M. Sagi, E. Sola, F. J. Lahoz, I. T. Dobrinovitch, A. Katho, F. Joo and L. A. Oro, *Adv. Synth. Catal.*, 2003, **345**, 280–288.
- 6 F. Nerozzi, *Platin. Met. Rev.*, 2012, **56**, 236–241.
- 7 M. Irfan, T. N. Glasnov and C. O. Kappe, *ChemSusChem*, 2011, **4**, 300–316.
- 8 E. Negishi, *Handbook of Organopalladium Chemistry for Organic Synthesis*, Wiley & Sons, New York, 2002, **1**, 229–247.
- 9 A. Bacchi, M. Carcelli, M. Costa, A. Leporati, E. Leporati, P. Pelagatti, C. Pelizzi and G. Pelizzi, *J. Organomet. Chem.*, 1997, **535**, 107–120.
- 10 D. Drago and P. S. Pregosin, *Organometallics*, 2002, **21**, 1208–1215.
- 11 P. W. N. M. Leeuwen and J. C. Chadwick, *Homogeneous catalysts: activity-stability-deactivation*, Wiley-VCH Verlag, 2011.

- 12 M. W. van Laren, M. A. Duin, C. Klerk, M. Naglia, D. Rogolino, P. Pelagatti, A. Bacchi, C. Pelizzi and C. J. Elsevier, *Organometallics*, 2002, **21**, 1546-1553.
- 13 M. W. van Laren and C. J. Elsevier, *Angew. Chem. Int. Ed.*, 1999, **38**, 3715-3717.
- 14 T. A. Tshabalala, S. O. Ojwach and M. A. Akerman, *J. Mol. Catal. A Chem.*, 2015, **406**, 178-184.
- 15 N. W. Attandoh, S. O. Ojwach and O. Q. Munro, *Eur. J. Inorg. Chem.*, 2014, **2014**, 3053-3064.
- 16 M. J. T. Frisch, G. W. Trucks, H. B. Schlegel, G. E. Scuseria, M. A. Robb, J. R. Cheeseman, G. Scalmani, V. Barone, B. Mennucci, G. A. Petersson, H. Nakatsuji, M. Caricato, X. Li, H. P. Hratchian, A. F. Izmaylov, J. Bloino, G. Zheng, J. L. Sonnenberg, M. Hada, M. Ehara, K. Toyota, R. Fukuda, J. Hasegawa, M. Ishida, T. Nakajima, Y. Honda, O. Kitao, H. Nakai, T. Vreven, J. A. Montgomery Jr., J. E. Peralta, F. Ogliaro, M. Bearpark, J. J. Heyd, E. Brothers, K. N. Kudin, V. N. Staroverov, R. Kobayashi, J. Normand, K. Raghavachari, A. Rendell, J. C. Burant, S. S. Iyengar, J. Tomasi, M. Cossi, N. Rega, J. M. Millam, M. Klene, J. E. Knox, J. B. Cross, V. Bakken, C. Adamo, J. Jaramillo, R. Gomperts, R. E. Stratmann, O. Yazyev, A. J. Austin, R. Cammi, C. Pomelli, J. W. Ochterski, R. L. Martin, K. Morokuma, V. G. Zakrzewski, G. A. Voth, P. Salvador, J. J. Dannenberg, S. Dapprich, A. D. Daniels, O. Farkas, J. B. Foresman, J. V. Ortiz, J. Cioslowski and D. J. Fox, GAUSSIAN 09 (Revision A.1), Gaussian, Inc., Wallingford, CT, 2009.
- 17 R. R. Schrock and J. A. Osborn, *J. Am. Chem. Soc.*, 1976, **98**, 2134-2143.
- 18 J. A. Osborn, F. H. Jardine, J. F. Young and G. Wilkinson, *J. Chem. Soc. A Inorganic, Phys. Theor.*, 1966, **0**, 1711.
- 19 V. Goudy, A. Jaoul, M. Cordier, C. Clavaguéra and G. Nocton, *J. Am. Chem. Soc.*, 2017, **139**, 10633-10636.
- 20 S. O. Ojwach, A. O. Ogwenno and M. P. Akerman, *Catal. Sci. Technol.*, 2016, **6**, 5069-5078.
- 21 S. O. Ojwach and A. O. Ogwenno, *Transit. Met. Chem.*, 2016, **41**, 539-546.
- 22 J. A. Widegren and R. G. Finke, *J. Mol. Catal. A Chem.*, 2003, **198**, 317-341.
- 23 V. P. Ananikov and I. P. Beletskaya, *Organometallics*, 2012, **31**, 1595-1604.



- 24 P. Pelagatti, A. Bacchi, M. Carcelli, M. Costa, A. Fochi, P. Ghidini, E. Leporati, M. Masi, C. Pelizzi and G. Pelizzi, *J. Organomet. Chem.*, 1999, **583**, 94–105.
- 25 P. J. Rheinlander, J. Herranz, J. Durst and H. A. Gasteiger, *J. Electrochem. Soc.*, 2014, **161**, F1448–F1457.
- 26 A. M. Kluwer, T. S. Koblenz, T. T. Jonischkeit, K. Woelk and C. J. Elsevier, *J. Am. Chem. Soc.*, 2005, **127**, 15470–15480.
- 27 F. Joó, L. Nádasdi, A. C. Bényei and D. J. Darensbourg, *J. Organomet. Chem.*, 1996, **512**, 45–50.
- 28 E. Gonzo and M. Boudart, *J. Catal.*, 1978, **52**, 462–471.
- 29 P. J. Dyson and P. G. Jessop, *Catal. Sci. Technol.*, 2016, **6**, 3302–3316.
- 30 F. Yilmaz, A. Mutlu, H. Ünver, M. Kurta and I. Kani, *J. Supercrit. Fluids.*, 2010, **54**, 202–209.
- 31 H. Ünver and F. Yilmaz, *Catalysts*, 2016, **6**, 147.
- 32 D. Teschner, J. Borsodi, A. Wootsch, Z. Revay, M. Havecker, A. Knop-Gericke, S. D. Jackson and R. Schlogl, *Science (80-. )*, 2008, **320**, 86–89.
- 33 H. Yoshida, T. Zama, S. Fujita, J. Panpranot and M. Arai, *RSC Adv.*, 2014, **4**, 24922.
- 34 P. K. Santra and P. Sagar, *J. Mol. Catal. A Chem.*, 2003, **197**, 37–50.
- 35 A. V. Smarun, W. Shahreel, S. Pramono, S. Y. Koo, L. Y. Tan, R. Ganguly and D. Vidović, *J. Organomet. Chem.*, 2017, **834**, 1–9.
- 36 T. Sperger, I. A. Sanhueza, I. Kalvet and F. Schoenebeck, *Chem. Rev.*, 2015, **115**, 9532–9586.
- 37 K. C. Dewhurst, W. Keim and C. A. Reilly, *Inorg. Chem.*, 1968, **7**, 546–551.
- 38 S. P. Smidt, N. Zimmermann, M. Studer and A. Pfaltz, *Chem. - A Eur. J.*, 2004, **10**, 4685–4693.

## CHAPTER 4

### Hydrogenation of alkenes and alkynes catalysed by N<sup>^</sup>O (imino)phenol palladium(II) complexes: structural, kinetics and chemoselectivity studies

This chapter is adapted from the paper published in *J. Organomet. Chem.* 873 (2018) 35-42 and is based on the experimental work of the first author, Thandeka A Tshabalala. Copyright © 2018 Elsevier B.V. The contributions of the first author include: synthesis, characterization of the compounds, carrying out the catalytic reactions and drafting of the manuscript.

#### 4.1. Introduction

Transition metal catalysed hydrogenation reactions are among the most valuable organic, widely used in the conversion of unsaturated systems to a range of useful domestic and industrial feedstock's.<sup>1,2</sup> Catalysts in these reactions have been derived mainly from platinum<sup>3</sup>, ruthenium<sup>4</sup>, chromium<sup>5</sup>, rhodium<sup>6</sup> and iron<sup>7</sup> complexes. Among these systems, palladium catalysts are currently receiving much attention due to their superior catalytic activities and selectivity.<sup>8</sup> To date, a number of palladium catalysts containing varied ligand architectures have been reported to show variable catalytic activities and selectivity in homogenous hydrogenation of alkenes and alkynes. Established examples include palladium(II) complexes derived from bidentate phosphine<sup>9</sup> and nitrogen-donor<sup>10</sup> catalysts. Even though palladium(II) catalysts of N<sup>^</sup>N and P<sup>^</sup>P-donor ligands show appreciable catalytic activities, improved catalyst robustness have been witnessed with complexes containing hybrid ligands such as P<sup>^</sup>N<sup>11</sup>, N<sup>^</sup>S<sup>12</sup> and N<sup>^</sup>O donors.<sup>13</sup>

Another approach that is currently gaining momentum in the design of active and stable catalyst systems are the hemilabile ligands, first introduced by Jeffrey and Rauchfuss.<sup>14</sup> The hemi-labile nature of the ligands in these catalysts have been demonstrated in a number of reports of palladium(II) catalysts bearing P<sup>^</sup>N<sup>^</sup>O<sup>^</sup><sup>15</sup>, P<sup>^</sup>N<sup>^</sup>S<sup>16</sup>, N<sup>^</sup>N<sup>^</sup>S<sup>17</sup>; S<sup>^</sup>O<sup>^</sup>S donor sites.<sup>18</sup> In one such study by Bacchi *et al.*,<sup>16</sup> palladium(II) complexes of hemilabile potential P<sup>^</sup>N<sup>^</sup>S ligands were found to be inactive due to the strong coordination ability of the pendant S-donor atom, thus limiting substrate coordination, i.e ligand adopts tridentate coordination upon activation. On the other hand, Yilmas *et al.*<sup>18</sup> employed palladium(II) complexes of S<sup>^</sup>O<sup>^</sup>S and S<sup>^</sup>O<sup>^</sup>O donor ligands, which display improved catalytic activities. The higher catalytic activities of S<sup>^</sup>O<sup>^</sup>S and S<sup>^</sup>O<sup>^</sup>O systems has been assigned to the weakly coordinating ability of the O donor atom compared to the S atom.<sup>18</sup>

We recently reported the use of palladium(II) complexes supported by (pyridyl)benzoazole<sup>19</sup> and (pyrazolylmethyl)pyridine<sup>20</sup> ligands to give active catalysts in the molecular hydrogenation of alkenes and alkynes. However, these systems suffered from catalyst decomposition to form palladium nanoparticles, and partly behave like heterogeneous systems. In attempt to design relatively stable and more active palladium(II) catalysts, we have designed potential hemilabile ligand systems based on hybrid N<sup>^</sup>O<sup>^</sup>O, N<sup>^</sup>N<sup>^</sup>O donor ligands. Indeed, the complexes showed significant improvement in terms of stability and activity in molecular hydrogenation of alkenes and alkynes. In this contribution, we report the synthesis of palladium(II) complexes of (imino)phenol ligands containing pendant arms and their applications

as catalysts in molecular hydrogenation of alkenes and alkynes. Detailed kinetics, chemo-selectivity and theoretical studies have been performed and are herein discussed.

## 4.2. Experimental section

### 4.2.1. Material, instrumentation and methods

All moisture and air sensitive reactions were performed using standard Schlenk line techniques. Methanol (ACS reagent,  $\geq 99.8\%$ ), toluene (ACS reagent,  $\geq 99.5\%$ ), diethyl ether (ACS reagent,  $\geq 98\%$ ), dichloromethane (ACS reagent,  $\geq 99.8\%$ ), absolute ethanol (ACS reagent,  $\geq 98\%$ ), DMSO- $d_6$  (99.8%), were purchased from Merck. Chloroform- $CDCl_3$  (98%), *p*-TsOH (ACS reagent,  $\geq 98.5\%$ ), and  $PPh_3$  (Reagent Plus®, 99%) were obtained from Sigma–Aldrich. Solvents were dried and distilled under nitrogen atmosphere in the presence of suitable drying agents: diethyl ether, toluene and acetone were dried over sodium wire/benzophenone, methanol and absolute ethanol over calcium oxide, and dichloromethane over phosphorus pentoxide. The chemicals, 1-(2-hydroxyphenyl)ethanone (99%), 2-methoxyethanamine (98%), 2-aminoethanol ( $\geq 98\%$ ), ethane-1,2-diamine (Reagent Plus®,  $\geq 99\%$ ), 2-hydroxybenzaldehyde (reagent grade, 98%) were purchased from Sigma–Aldrich and were used without further purification. The starting material  $[PdCl_2(COD)]$  was synthesized following a literature method.<sup>21</sup> Nuclear magnetic resonance spectra were acquired at 400 MHz for  $^1H$ , 100 MHz for  $^{13}C$  and 162 MHz for  $^{31}P$  on a Bruker Avance spectrometer equipped with Bruker magnet (9.395 T). All coupling constants (*J*) are measured in Hertz, Hz. The mass spectra (ESI-MS) were recorded on a Waters API Quatro Micro

spectrometer, using 50% MeOH/DMSO, 16-36 V cone voltage, source (720 V) and desolvation temperature of 450 °C. The elemental analyses were performed on a Thermal Scientific Flash 2000. The infrared spectra were recorded on a Perkin-Elmer spectrum 100 in the 4000-650 cm<sup>-1</sup> range. X-ray data were recorded on a Bruker Apex Duo diffractometer equipped with an Oxford Instruments.

#### 4.2.2. Synthesis of (ethylimino)ethylphenol amine ligands and palladium(II) complexes

##### 4.2.2.1. 2-(2-methoxyethylimino)ethylphenol (L5)

To a solution of 1-(2-hydroxyphenyl)ethanone (1.50 g, 11.00 mmol) in ethanol (50 mL) was added 2-methoxyethanamine (0.83 g, 11.00 mmol), and catalytic amount of *p*-TsOH (85 mg). The reaction mixture was refluxed for 24 h at 60 °C and ethanol was removed after the reaction period under reduced pressure to give L5 as a brown oil. Yield = 1.93 g (91%). <sup>1</sup>H NMR (400 MHz, CDCl<sub>3</sub>): δ<sub>H</sub> (ppm): 2.41 (s, 3H, CH<sub>3</sub>); 3.45 (s, 3H, OCH<sub>3</sub>); 3.78 (t, <sup>3</sup>J<sub>HH</sub> = 4.0 Hz, 2H, CH<sub>2</sub>-N); 3.82 (t, <sup>3</sup>J<sub>HH</sub> = 4.0 Hz, 2H, CH<sub>2</sub>-O); 6.81 (t, <sup>3</sup>J<sub>HH</sub> = 8.0 Hz, 1H, H-Ph); 6.99 (d, <sup>3</sup>J<sub>HH</sub> = 8.0 Hz, 1H, H-Ph); 7.34 (t, <sup>3</sup>J<sub>HH</sub> = 12.0 Hz, 1H, H-Ph); 7.55 (d, <sup>3</sup>J<sub>HH</sub> = 8.0 Hz, 1H, H-Ph). <sup>13</sup>C NMR (CDCl<sub>3</sub>): δ<sub>C</sub>(ppm): 14.74 (CH<sub>3</sub>); 26.62 (OCH<sub>3</sub>); 51.42 (CH<sub>2</sub>-N); 62.23 (CH<sub>2</sub>-O); 116.98 (Ph); 119.03 (Ph); 128.17 (Ph); 130.71 (Ph); 132.82 (Ph); 161.24 (Ph-OH); 164.47 (C=N). MS (ESI) m/z (%) 194 (M<sup>+</sup>, 100). HRMS-ESI ([M<sup>+</sup>+H<sup>+</sup>]): m/z calc: 193.1236; found: 194.0478. FT-IR (cm<sup>-1</sup>): ν<sub>(OH)</sub> = 3157; ν<sub>(C=N)</sub> = 1613.

Compounds **L6** - **L8** were prepared following the same procedure described for compound **L5**.

#### 4.2.2.2. *2-(2-hydroxyethylimino)ethylphenol (L6)*

Compound **L6** was synthesized from 1-(2-hydroxyphenyl)ethanone (1.50 g, 11.00 mmol) and 2-aminoethanol (0.67 g, 11.00 mmol). Brown solid. Yield = 1.80 g (92%). <sup>1</sup>H NMR (400 MHz, CDCl<sub>3</sub>): δ<sub>H</sub> (ppm): 2.39 (s, 3H, CH<sub>3</sub>); 3.76 (t, <sup>3</sup>J<sub>HH</sub> = 5.4 Hz, 2H, CH<sub>2</sub>-N); 4.02 (t, <sup>3</sup>J<sub>HH</sub> = 5.3 Hz, 2H, CH<sub>2</sub>-OH); 6.80 (t, <sup>3</sup>J<sub>HH</sub> = 16.0 Hz, 1H, H-Ph); 6.94 (d, <sup>3</sup>J<sub>HH</sub> = 8.2 Hz, 1H, H-Ph); 7.32 (t, <sup>3</sup>J<sub>HH</sub> = 15.5 Hz, 1H, H-Ph); 7.54 (d, <sup>3</sup>J<sub>HH</sub> = 8.0 Hz, 1H, H-Ph). <sup>13</sup>C NMR (CDCl<sub>3</sub>): δ<sub>C</sub> (ppm): 18.04 (CH<sub>3</sub>); 40.99 (CH<sub>2</sub>-N); 62.59 (CH<sub>2</sub>-N); 75.37 (Ph); 93.25 (Ph); 128.06 (Ph); 149.60 (Ph); 151.02 (Ph); 162.35 (Ph-OH); 164.45 (C=N). MS (ESI) m/z (%) 180 (M<sup>+</sup>, 100). HRMS-ESI ([M<sup>+</sup>+H<sup>+</sup>]): m/z calc: 179.1102; found: 180.0145. FT-IR (cm<sup>-1</sup>): ν<sub>(OH<sub>ph</sub>)</sub> = 3158; ν<sub>(C=N)</sub> = 1603.

#### 4.2.2.3. *2-(2-aminoethylimino)ethylphenol (L7)*

Ethane-1,2-diamine (0.66 g, 11.00 mmol) and 1-(2-hydroxyphenyl)ethanone (1.50 g, 11.00 mmol). Yellow solid. Yield = 1.77 g (90%). <sup>1</sup>H NMR (400 MHz, CDCl<sub>3</sub>): δ<sub>H</sub> (ppm): 2.41 (s, 3H, CH<sub>3</sub>); 4.02 (dd, <sup>3</sup>J<sub>HH</sub> = 5.9 Hz, 4H, CH<sub>2</sub>-CH<sub>2</sub>); 6.82 (t, <sup>3</sup>J<sub>HH</sub> = 16.3 Hz, 1H, H-Ph); 6.93 (d, <sup>3</sup>J<sub>HH</sub> = 8.3 Hz, 1H, H-Ph); 7.32 (t, <sup>3</sup>J<sub>HH</sub> = 17.0 Hz, 1H, H-Ph); 7.55 (d, <sup>3</sup>J<sub>HH</sub> = 9.4 Hz, 1H, H<sub>g</sub>). <sup>13</sup>C NMR (CDCl<sub>3</sub>): δ<sub>C</sub> (ppm): 16.70 (CH<sub>3</sub>); 43.61 (CH<sub>2</sub>-N); 51.05 (CH<sub>2</sub>-O); 116.04 (Ph); 121.54 (Ph); 124.91 (Ph); 130.69 (Ph); 132.57 (Ph); 161.14 (Ph-OH); 164.68 (C=N). MS (ESI) m/z (%) 179 (M<sup>+</sup>, 100). HRMS-ESI ([M<sup>+</sup>+H<sup>+</sup>]): m/z calc: 178.10427; found: 179.0047. FT-IR (cm<sup>-1</sup>): ν<sub>(OH<sub>ph</sub>)</sub> = 3055; ν<sub>(C=N)</sub> = 1607.

#### 4.2.2.4. 2-(2-hydroxyethylimino)methylphenol (**L8**)

Ligand **L8** was prepared using 2-hydroxybenzaldehyde (1.50 g, 12.30 mmol) and 2-aminoethanol (0.75 g, 12.30 mmol). Brown oil. Yield = 1.81 g (88%).  $^1\text{H}$  NMR (400 MHz,  $\text{CDCl}_3$ ):  $\delta_{\text{H}}$  (ppm): 3.73 (t,  $^3J_{\text{HH}} = 4.0$  Hz, 2H,  $\text{CH}_2\text{-N}$ ); 3.89 (t,  $^3J_{\text{HH}} = 4.0$  Hz, 2H,  $\text{CH}_2\text{-OH}$ ); 6.84 (t,  $^3J_{\text{HH}} = 12.0$  Hz, 1H, H-Ph); 6.95 (d,  $^3J_{\text{HH}} = 8.0$  Hz, 1H, H-Ph); 7.25 (d,  $^3J_{\text{HH}} = 8.0$  Hz, 1H, H-Ph); 7.32 (t,  $^3J_{\text{HH}} = 12.0$  Hz, 1H, H-Ph); 8.36 (s, 1H, H-C=N).  $^{13}\text{C}$  NMR ( $\text{CDCl}_3$ ):  $\delta_{\text{C}}$  (ppm): 43.55 ( $\text{CH}_2\text{-N}$ ); 61.90 ( $\text{CH}_2\text{-O}$ ); 117.15 (Ph); 118.60 (Ph); 121.25 (Ph); 131.49 (Ph); 132.52 (Ph); 161.47 (Ph-OH); 166.83 (C=N). MS (ESI)  $m/z$  (%) 166 ( $\text{M}^+$ , 100). HRMS-ESI ( $[\text{M}^++\text{H}^+]$ ):  $m/z$  calc: 165.2013; found: 166.0102. FT-IR ( $\text{cm}^{-1}$ ):  $\nu_{(\text{OH}_{\text{Ph}})}$  = 3321;  $\nu_{(\text{C}=\text{N})}$  = 1631.

#### 4.2.2.5. [2-(2-methoxyethylimino)ethyl]phenol $\text{PdCl}_2$ (**12**)

To a solution of **L5** (0.06 g, 0.31 mmol) in  $\text{CH}_2\text{Cl}_2$  (10 mL) was added a solution of  $\text{Pd}(\text{COD})\text{Cl}_2$  (0.10 g, 0.31 mmol) in  $\text{CH}_2\text{Cl}_2$  (10 mL) and the mixture was stirred for 24 h to give a yellow precipitate. The crude product was filtered and recrystallized from  $\text{CH}_2\text{Cl}_2$ -hexane mixture to afford complex **12** as an analytically pure light yellow solid. Yield = 0.12 g (68%).  $^1\text{H}$  NMR (400 MHz,  $\text{DMSO-d}_6$ ):  $\delta_{\text{H}}$  (ppm): 2.63 (s, 3H,  $\text{CH}_3$ ); 3.31 (s, 3H,  $\text{OCH}_3$ ); 5.46 (d,  $^3J_{\text{HH}} = 6.2$  Hz, 2H,  $\text{CH}_2\text{-N}$ ); 5.51 (d,  $^3J_{\text{HH}} = 5.3$  Hz, 2H,  $\text{CH}_2\text{-OCH}_3$ ); 6.94 (t,  $^3J_{\text{HH}} = 7.9$  Hz, 1H, H-Ph); 7.38 (t,  $^3J_{\text{HH}} = 7.8$  Hz, 1H, H-Ph); 7.47 (t,  $^3J_{\text{HH}} = 8.1$  Hz, 1H, H-Ph); 7.71 (d,  $^3J_{\text{HH}} = 8.1$  Hz, 1H, H-Ph).  $^{13}\text{C}$  NMR ( $\text{DMSO-d}_6$ ):  $\delta_{\text{C}}$  (ppm): 12.01 ( $\text{CH}_3$ ); 16.75 ( $\text{CH}_2\text{-N}$ ); 59.03 ( $\text{CH}_2\text{-O}$ ); 73.34 (Ph); 116.00 (Ph); 121.55 (Ph); 124.92 (Ph); 130.66 (Ph); 132.64 (Ph); 161.11 (Ph-OH); 164.04 (C=N). MS (ESI)  $m/z$  (%) 299 ( $\text{M}^+ - \text{Cl}_2$ , 55%). FT-IR ( $\text{cm}^{-1}$ ):  $\nu_{(\text{OH})}$  = 3398;  $\nu_{(\text{C}=\text{N})}$  = 1628. Anal. Calc. for

$C_{11}H_{15}Cl_2NO_2Pd:0.25CH_2Cl_2$ : C, 34.49; H, 3.99; N, 3.57. Found: C, 34.41; H, 3.90; N, 3.39.

#### 4.2.2.6. [2-(2-hydroxyethylimino)ethyl)phenol)PdCl<sub>2</sub>] (**13**)

Complex **13** was synthesized following the procedure described for complex **12** using **L6** (0.06 g, 0.31 mmol) and Pd(COD)Cl<sub>2</sub> (0.10 g, 0.31 mmol) in CH<sub>2</sub>Cl<sub>2</sub> (10 mL). Yield = 0.09 g (78%). <sup>1</sup>H NMR (400 MHz, DMSO-d<sub>6</sub>): δ<sub>H</sub> (ppm): 3.73 (s, 3H, CH<sub>3</sub>); 5.52 (dd, <sup>3</sup>J<sub>HH</sub> = 11.4 Hz, 4H, CH<sub>2</sub>-CH<sub>2</sub>); 6.87 (t, <sup>3</sup>J<sub>HH</sub> = 8.4 Hz, 2H, H-Ph); 7.38 (t, <sup>3</sup>J<sub>HH</sub> = 8.4 Hz, 1H, H-Ph); 7.68 (d, <sup>3</sup>J<sub>HH</sub> = 7.8 Hz, 1H, H-Ph). <sup>13</sup>C NMR (DMSO-d<sub>6</sub>): δ<sub>C</sub> (ppm): 17.70 (CH<sub>3</sub>); 31.01 (CH<sub>2</sub>-N); 58.25(CH<sub>2</sub>-O); 116.04 (Ph); 121.54 (Ph); 124.96 (Ph); 130.65 (Ph); 132.53 (Ph); 157.88 (Ph-OH); 164.61 (C=N). MS (ESI) m/z (%) 322 (M<sup>+</sup>- Cl, 71%). FT-IR (cm<sup>-1</sup>): ν<sub>(OH)</sub> = 3381; ν<sub>(C=N)</sub> = 1625. Anal. Calc. for C<sub>10</sub>H<sub>13</sub>Cl<sub>2</sub>NO<sub>2</sub>Pd: C, 33.69; H, 3.68; N, 3.93. Found: C, 33.65; H, 3.62; N, 3.63.

#### 4.2.2.7. [2-(2-aminoethylimino)ethyl)phenol )PdCl<sub>2</sub>] (**14**)

Complex **14** was synthesized following the procedure described for complex **12** using **L7** (0.06 g, 0.31 mmol) and Pd(COD)Cl<sub>2</sub> (0.10 g, 0.31 mmol) in CH<sub>2</sub>Cl<sub>2</sub> (20 mL). Yield = 0.10 g (91%). <sup>1</sup>H NMR (400 MHz, DMSO-d<sub>6</sub>): δ<sub>H</sub> (ppm): 2.29 (s, 3H, CH<sub>3</sub>); 4.68 (dd, <sup>3</sup>J<sub>HH</sub> = 10.8 Hz, 4H, CH<sub>2</sub>-CH<sub>2</sub>); 6.58 (t, <sup>3</sup>J<sub>HH</sub> = 14.0 Hz, 1H, H-Ph); 6.86 (d, <sup>3</sup>J<sub>HH</sub> = 8.4 Hz, 1H, H-Ph); 7.24 (t, <sup>3</sup>J<sub>HH</sub> = 14.0 Hz, 1H, H-Ph); 7.66 (d, <sup>3</sup>J<sub>HH</sub> = 9.7 Hz, 1H, H-Ph). <sup>13</sup>C NMR (DMSO-d<sub>6</sub>): δ<sub>C</sub> (ppm): 17.72 (CH<sub>3</sub>); 32.01 (CH<sub>2</sub>-N); 43.03 (CH<sub>2</sub>-O); 116.08 (Ph); 121.55 (Ph); 124.98 (Ph); 130.64 (Ph); 132.53 (Ph); 157.60 (Ph-OH); 164.61 (C=N). MS (ESI) m/z (%) 283 (M<sup>+</sup>- Cl<sub>2</sub>, 40%). FT-IR (cm<sup>-1</sup>): ν<sub>(OH)</sub> = 3014; ν<sub>(C=N)</sub> = 1639. Anal. Calc. for C<sub>10</sub>H<sub>14</sub>Cl<sub>2</sub>N<sub>2</sub>OPd: C, 31.68; H, 3.80; N, 7.04. Found: C, 31.66; H, 3.79; N, 6.98.



#### 4.2.2.8. [2-(2-hydroxyethylimino)methyl)phenol)PdCl<sub>2</sub>] (**15**)

Complex **15** was synthesized following the procedure described for complex **12** using **L8** (0.05 g, 0.31 mmol) and Pd(COD)Cl<sub>2</sub> (0.10 g, 0.31 mmol) in CH<sub>2</sub>Cl<sub>2</sub> (20 mL). Yield = 0.10 g (91%). <sup>1</sup>H NMR (400 MHz, DMSO-d<sub>6</sub>): δ<sub>H</sub> (ppm): 5.15 (t, <sup>3</sup>J<sub>HH</sub> = 5.5 Hz, 2H, CH<sub>2</sub>-N); 5.51 (t, <sup>3</sup>J<sub>HH</sub> = 5.6 Hz, 2H, CH<sub>2</sub>-OH); 6.59 (t, <sup>3</sup>J<sub>HH</sub> = 8.3 Hz, 1H, H-Ph); 6.77 (d, <sup>3</sup>J<sub>HH</sub> = 7.8 Hz, 1H, H<sub>d</sub>); 7.27 (t, <sup>3</sup>J<sub>HH</sub> = 8.6 Hz, 1H, H-Ph); 7.86 (d, <sup>3</sup>J<sub>HH</sub> = 7.8 Hz, 1H, H-Ph); 8.36 (s, 1H, H-C=N). <sup>13</sup>C NMR (DMSO-d<sub>6</sub>): δ<sub>C</sub> (ppm): 61.24 (CH<sub>2</sub>-N); 65.34 (CH<sub>2</sub>-O); 115.22 (Ph); 120.25 (Ph); 120.51 (Ph); 128.98 (Ph); 139.32 (Ph); 163.82 (Ph-OH); 164.01 (C=N). MS (ESI) m/z (%) 307 (M<sup>+</sup> - Cl, 15%). FT-IR (cm<sup>-1</sup>): ν<sub>(OH)</sub> = 3399; ν<sub>(C=N)</sub> = 1626. Anal. Calc. for C<sub>9</sub>H<sub>11</sub>Cl<sub>2</sub>NO<sub>2</sub>Pd: C, 31.56; H, 3.24; N, 4.09 Found: C, 31.29; H, 3.18; N, 3.73. Recrystallization of a solution of complex **15** in CH<sub>2</sub>Cl<sub>2</sub> solution at room temperature afforded single crystals of the homoleptic derivative (**15a**) containing two anionic/deprotonated ligands (**L8**) suitable for X-ray analyses.

#### 4.2.2.9. [2-(2-methoxyethylimino)ethyl)phenol PdClPPh<sub>3</sub>] (**16**)

To a suspension of complex **12** (0.05 g, 0.11 mmol) in CH<sub>2</sub>Cl<sub>2</sub> (10 mL), PPh<sub>3</sub> (0.13 g, 0.11 mmol) was added and stirred for 24 h. The mixture was filtered and the filtrate concentrated to approximately 3 mL and recrystallized from hexane/CH<sub>2</sub>Cl<sub>2</sub> solvent mixture to obtain complex **16** as a yellow crystalline solid. Yield = 0.06 g (74%). <sup>1</sup>H NMR (CDCl<sub>3</sub>): δ<sub>H</sub> (ppm): 2.51 (s, 3H, CH<sub>3</sub>); 3.35 (s, 3H, OCH<sub>3</sub>); 5.77 (dd, J<sub>HH</sub> = 3.60 Hz, 4H, CH<sub>2</sub>-CH<sub>2</sub>); 7.30 (m, 1H, Ph-Phenol); 7.43 (m, 1H, Ph-Phenol); 7.55 (m, 7H, PPh<sub>3</sub>); 7.61 (m, 2H, Ph-Phenol); 7.64 (m, 8H, PPh<sub>3</sub>). <sup>13</sup>C NMR (CDCl<sub>3</sub>): δ<sub>C</sub> (ppm): 18.56; 39.00; 59.01; 74.15; 116.03; 121.53; 124.91; 128.81; 128.96; 130.66; 132.52; 137.33; 137.47; 157.88; 164.62. <sup>31</sup>P NMR (CDCl<sub>3</sub>): δ (ppm): 32.96; 23.78. MS (ESI) m/z (%) 561 (M<sup>+</sup> - Cl, 19%).

Anal. Calc. for  $C_{29}H_{30}C_{12}NO_2PPd:0.5CH_2Cl_2$ : C, 52.48; H, 4.63; N, 2.07. Found: C, 52.41; H, 4.59; N, 2.00.

#### 4.2.2.10. $[{2-(2-methoxyethylimino)ethyl}phenol]Pd(OTs)(PPh_3)$ (**17**)

To a solution of **L5** (0.08 g, 0.44 mmol) in chloroform (5 mL), was added drop-wise a solution of  $Pd(OAc)_2$  (0.10 g, 0.44 mmol) in chloroform (10 mL) followed by a solution of  $PPh_3$  (0.23 g, 0.89 mmol) and *p*-TsOH (0.15 g, 0.89 mmol) in chloroform (10 mL) and stirred at room temperature for 24 h. The organic volatiles were removed *in vacuo*, and recrystallization from  $CH_2Cl_2$ -hexane gave complex **6** as a light yellow solid. Yield = 0.29 g (91%).  $^1H$  NMR ( $CDCl_3$ ):  $\delta_H$  (ppm): 2.33 (s, 3H,  $CH_3-N$ ). 2.50 (s, 3H,  $CH_3-OTs$ ); 3.34 (s, 3H,  $OCH_3$ ); 4.28 (dd,  $^3J_{HH} = 12.0$  Hz, 4H,  $CH_2-CH_2$ ); 7.28 (m, 2H, Ph-ethanone); 7.36 (m, 2H, Ph-ethanone); 7.48 (m, 2H, Ph-OTs); 7.51 (m, 9H,  $PPh_3$ ); 7.52 (m, 6H,  $PPh_3$ ); 7.67 (m, 2H, Ph-OTs).  $^{31}P$  NMR ( $CDCl_3$ ):  $\delta$  (ppm): 29.55; 22.22.  $^{13}C$  NMR ( $CDCl_3$ ):  $\delta_C$  (ppm): 19.30; 24.30; 32.00; 57.81; 59.10; 74.92; 116.02; 121.55; 124.93; 128.00; 128.81; 128.93; 130.44; 130.65; 132.54; 137.36; 137.48; 142.22; 146.89; 164.63. MS (ESI)  $m/z$  (%) 732 ( $M^+$ , 22%). Anal. Calc. for  $C_{36}H_{36}NO_5PPdS$ : C, 59.06; H, 4.96; N, 1.91; O, 10.93. Found: C, 59.36; H, 4.98; N, 2.02; O, 10.95.

### 4.2.3. General procedure for the hydrogenation reactions of alkenes and alkynes

The catalytic hydrogenation reactions were performed in a stainless steel autoclave equipped with temperature control unit and a sample valve. In a typical experiment, styrene (0.5 mL, 4.36 mmol) and complex **12** (16 mg, 0.004 mmol, S/C 1000) were dissolved in toluene (50 mL). The reactor was evacuated and the catalytic solution was

introduced to the reactor via a cannula. The reactor was purged three times with hydrogen, and then set at the equipped pressure, heated to the desired temperature and the reaction stirred at 500 rpm. At the end of the reaction time, the reaction was cooled, excess hydrogen was vented off and the samples drawn, filtered using 0.45  $\mu\text{m}$  micro filters and analysed by Gas Chromatography to determine the percentage conversion of styrene to ethylbenzene. Standard authentic samples were used to confirm the presence and composition of the hydrogenation products.

#### 4.2.4. General procedure of kinetic experiments

Kinetics of the hydrogenation reactions were investigated for complexes **12-17** by monitoring the reactions using Gas Chromatography. Sampling was done by cooling the reaction mixture, venting off the excess hydrogen and withdrawing aliquots of the reaction mixture at regular time intervals (15 min – 1.5 h). The samples were analysed by Gas Chromatography to determine the percentage conversions of styrene to ethylbenzene. The observed rate constants,  $k_{obs}$ , were extracted from the slopes of the lines of best-fit of the plots of  $\ln[\text{Sty}]_0/[\text{Sty}]_t$  vs time.

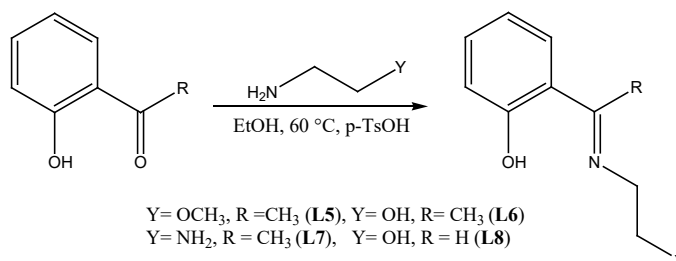
#### 4.2.5. Density Functional Theoretical (DFT) studies

DFT calculations were performed in a gas phase to identify the energy-minimized structures based on B3LYP/LANL2DZ (Los Almos National Laboratory 2 double  $\zeta$ ) level theory.<sup>22</sup> Split bases set, LANL2DZ for palladium and 6-311G for all other atoms was used to optimize the geometries and energies of the complexes. The Gaussian09 suite of programs was used for all the computations.

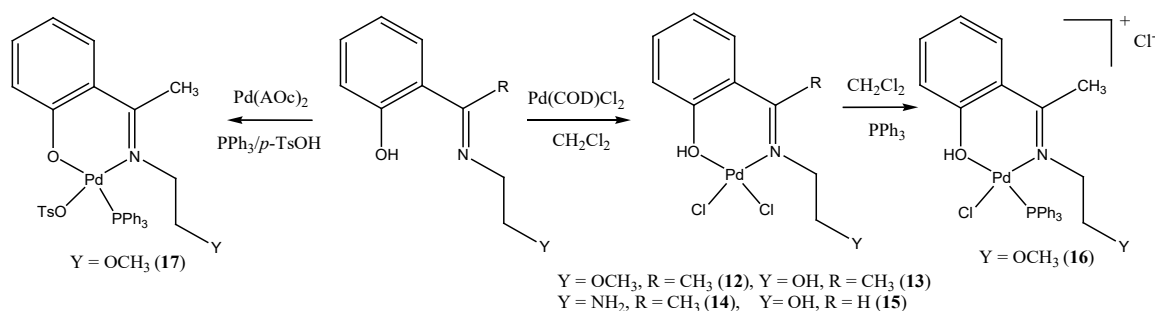
### 4.3. Results and discussion

#### 4.3.1. Synthesis and characterization of (ethylimino)ethylphenol ligands and their palladium complexes 12-17

The (ethylimino)ethylphenol ligands **L5** – **L8** were obtained in good yields (75-92%) from condensation reactions between appropriate aldehydes or ketones and the corresponding amines (Scheme 4.1). Reactions of **L5** – **L8** with  $[\text{PdCl}_2(\text{COD})]$  afforded the corresponding palladium(II) complexes **12** – **15** (Scheme 4.2) in good yields. Treatment of the neutral complex **12** with  $\text{PPh}_3$  resulted in the formation of the corresponding cationic complex, while reactions of **L5** with  $\text{Pd}(\text{OAc})_2$  and equivalence of *p*-TsOH in the presence of  $\text{PPh}_3$  afforded the neutral complex **17** in moderate yields (Scheme 4.2).



**Scheme 4.1:** Synthesis of (ethylimino)ethylphenol ligands **L5** – **L8** bearing pendant arms.



**Scheme 4.2:** Synthesis of neutral and cationic palladium(II) complexes **12** - **17**

All the new compounds were characterized by <sup>1</sup>H, <sup>13</sup>C, <sup>31</sup>P NMR and IR spectroscopy, mass spectrometry, elemental analysis to establish their identity and purity. For example, the <sup>1</sup>H NMR spectra of **L5** and the corresponding complex **12** (Fig. 4.1) showed a downfield shift of the ethylene linker protons from 3.78 ppm and 3.82 ppm to 5.46 ppm and 5.51 ppm respectively.

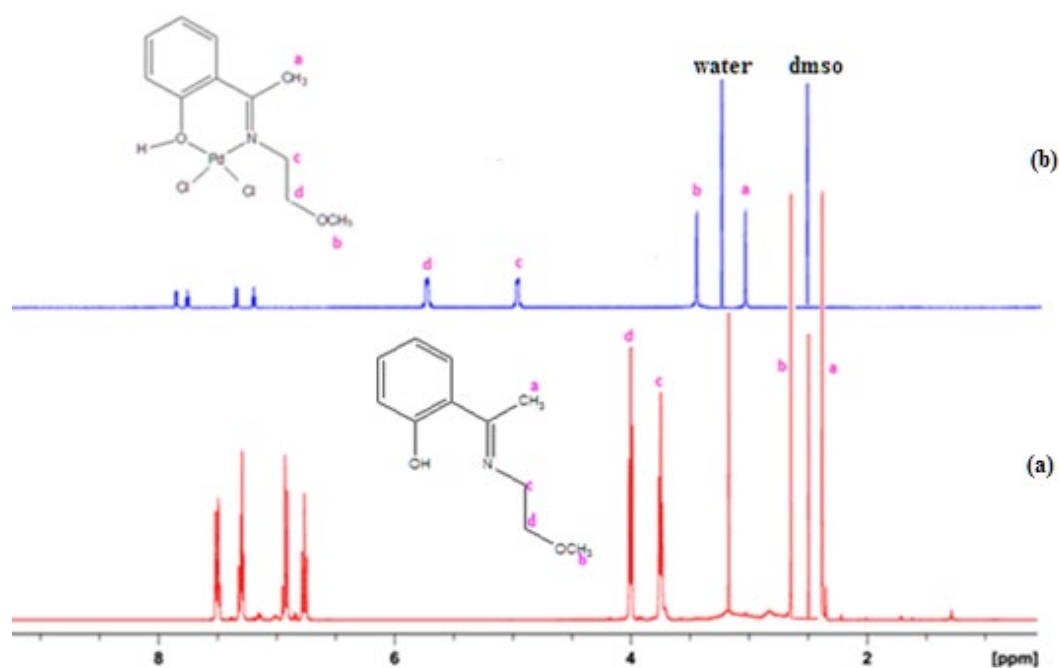


**Figure 4.1:** <sup>1</sup>H NMR spectra of **L5** in DMSO-d<sub>6</sub> (a) and the respective complex **12** (b) showing a shift in the ethylene protons.

The  $^{13}\text{C}$  NMR spectral data was consistent with the  $^1\text{H}$  NMR spectra (Fig. 4.2). Complexes **16** and **17** were also analysed using  $^{31}\text{P}$  NMR spectroscopy. In both cases, two peaks between 22.78 ppm and 29.55 ppm were recorded (Fig. 4.3), in good agreement with coordinated  $\text{PPh}_3$  ligand as observed in related palladium(II) complexes.<sup>23,24</sup>

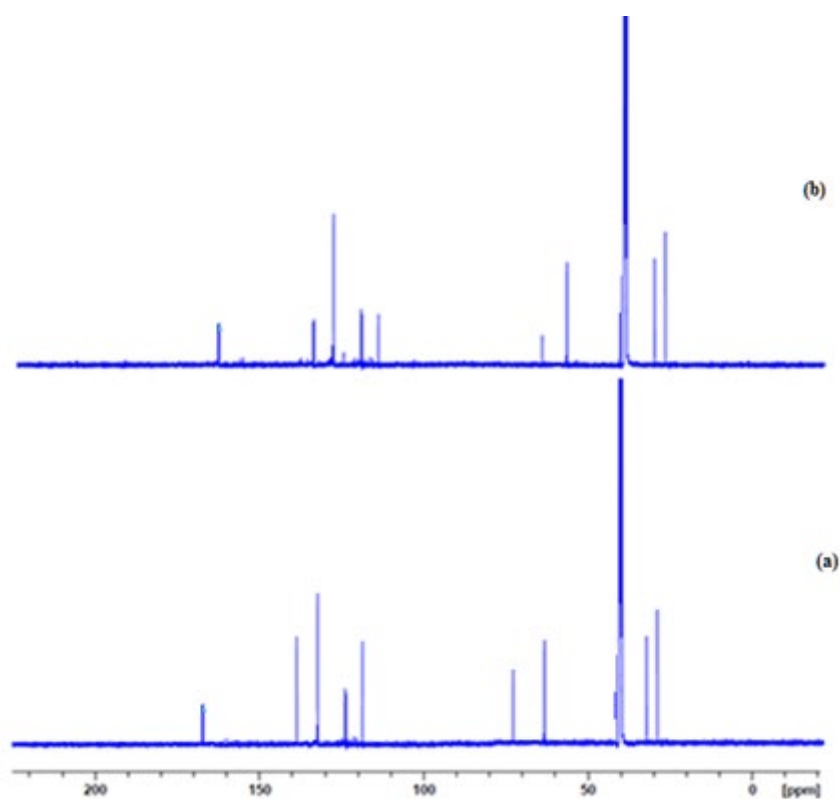


**Figure 4.2:**  $^{13}\text{C}$  NMR spectra of **L8** in  $\text{DMSO-d}_6$  (a) and its corresponding complex **15** (b) showing upfield shift in the imine carbon from 166.83 ppm to 164.01 ppm respectively.

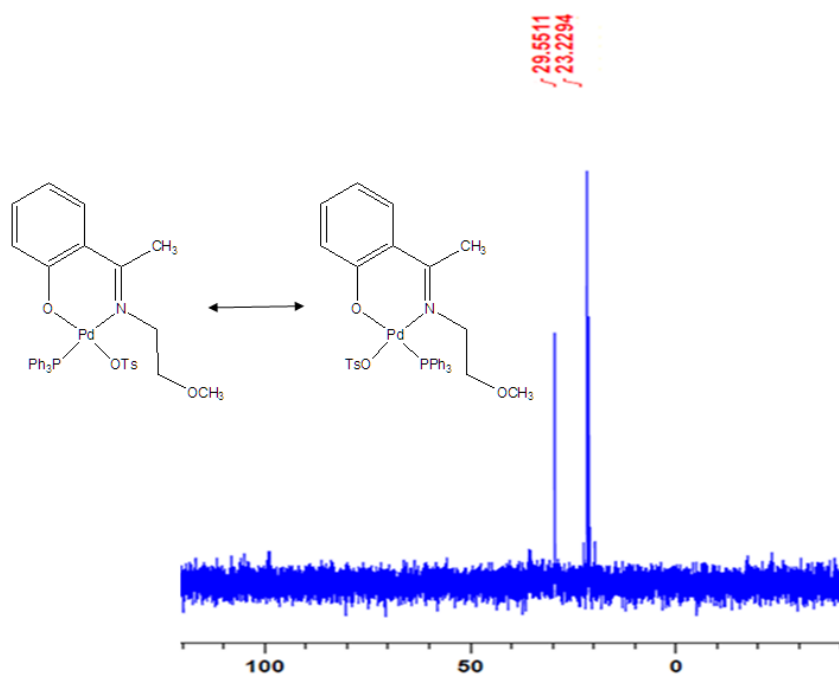


**Figure 4.3:**  $^{31}\text{P}$  NMR spectrum of complex **17** in  $\text{CDCl}_3$  displaying two signals consistent with the the *cis* and *trans* arrangements.

FT-IR spectrum of complex **15** in relation to its ligand **L8** also established the successful formation of the complexes. For instance, the phenolic OH IR frequencies were observed as broad and sharp peaks at  $3321\text{ cm}^{-1}$  and  $3399\text{ cm}^{-1}$  in **L8** and complex **15** respectively, indicating coordination of the OH group to palladium(II) atom. Similarly, an up field shift of the imine signal from  $1631\text{ cm}^{-1}$  in **L8** to  $1626\text{ cm}^{-1}$  in complex **15** was consistent with the proposed structures in Scheme 4.2.

Mass spectra of all the complexes showed typical fragmentation patterns consistent with a loss of a halide group. For instance, complex **14**, showed an  $m/z$  peak at 318.9

amu corresponding to the  $[\text{Pd}(\text{L7})\text{Cl}]^+$  fragment (Fig. 4.4). Elemental analyses data of all the complexes were in tandem with the proposed structures in Scheme 5.2 and also confirmed the purity of the bulk materials.

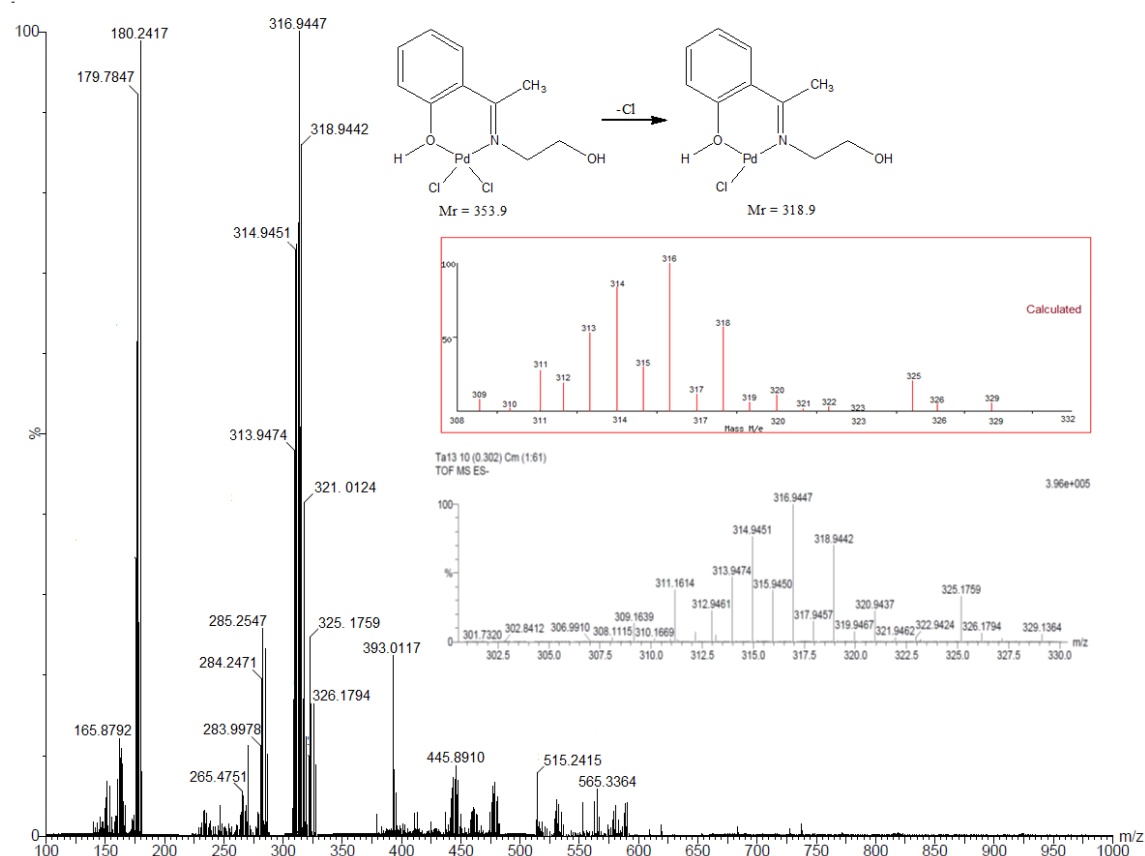


**Figure 4.4:** ESI-MS of complex **14** showing  $m/z$  signal at 318.9 (80%) corresponding to the fragmentation pattern,  $M^+-\text{Cl}$  (insert showing mass spectrum of the calculated and found isotopic distribution).

In order to confirm the proposed binding modes of **L5** – **L8** and coordination chemistry of the formed palladium complexes, attempts were made to grow single crystals suitable for X-ray analysis of the complexes. In one such instance, single



crystals of compound **15** suitable for X-ray analysis were isolated. Crystal data collection and structural refinement parameters of complex **15a** are given in Table 4.1.

**Table 4.1:** Crystal data and structure refinement details for complex **15a**

Crystal data	<b>15a</b>	
Identification code	shelx	
Chemical formula	C <sub>18</sub> H <sub>20</sub> N <sub>2</sub> O <sub>4</sub> Pd	
Molar mass (g mol <sup>-1</sup> )	434.76	
Temperature	100(2) K	
Wavelength	0.71073 Å	
Crystal system, space group	Monoclinic, P 21/c	
Unit cell dimensions	a = 18.1551(12) Å	α = 90°.
	b = 4.9654(3) Å	β = 97.057(3)°.
	c = 19.0901(12) Å	γ = 90°.
Volume	1707.88(19) Å <sup>3</sup>	
Z	4	
Density (calculated)	1.691 Mg/m <sup>3</sup>	
Absorption coefficient	1.112 mm <sup>-1</sup>	
F(000)	880	
Crystal size	0.220 × 0.060 × 0.040 mm <sup>3</sup>	
Theta range for data collection	2.150 to 28.490°.	
Index ranges	-24 ≤ h ≤ 24, -6 ≤ k ≤ 5, -25 ≤ l ≤ 25	
Reflections collected	15930	
Independent reflections	4268 [R(int) = 0.0192]	
Completeness to theta = 25.242°	98.5 %	
Absorption correction	Semi-empirical from equivalents	
Max. and min. transmission	0.968 and 0.781	
Refinement method	Full-matrix least-squares on F <sup>2</sup>	
Data / restraints / parameters	4268 / 0 / 229	
Goodness-of-fit on F <sup>2</sup>	1.052	
Final R indices [I > 2σ(I)]	R1 = 0.0236, wR2 = 0.0558	
R indices (all data)	R1 = 0.0306, wR2 = 0.0624	
Extinction coefficient	n/a	
Largest diff. peak and hole	0.907 and -0.505 e.Å <sup>-3</sup>	

However, the structure obtained (**15a**) contained two anionic bidentate **L8** units (Fig. 4.5), indicating *in situ* deprotonation of **L8** during crystallisation as shown in equation 4.1. We recently observed a similar transformation for nickel(II) complexes of **L8**.<sup>25</sup> Separately, Boltina *et. al.* previously reported the *in-situ* deprotonation of O<sup>-</sup>N<sup>-</sup>O (pyrazolyl/imadazolyl)imine ligands to form pincer-type palladium(II) complexes.<sup>26</sup>

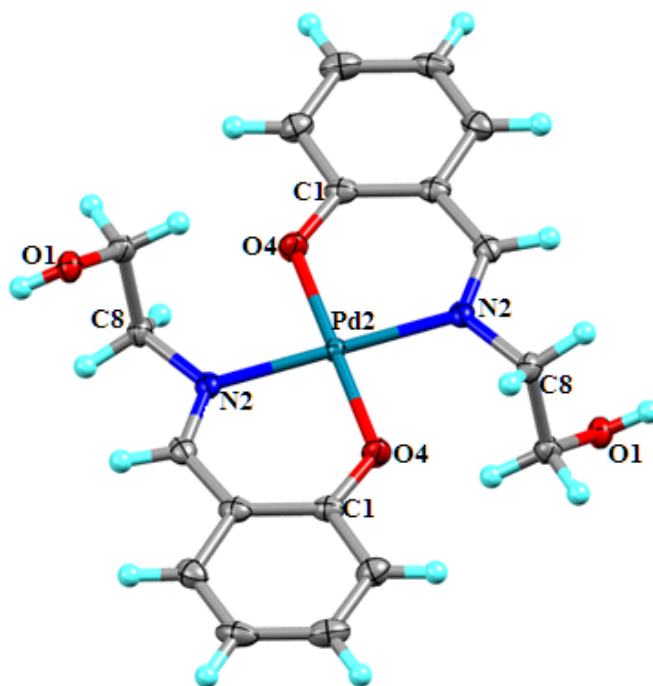


**Figure 4.5:** Thermal ellipsoid plot (50% probability) of **15a** illustrating the square planar coordination geometry of the Pd(II) ion. Hydrogen atoms and the atoms of the minor conformer have been rendered as spheres of arbitrary radius. Selected bond lengths [Å] and angles [°]: Pd(2)-N(2), 2.019(15); Pd(2)-O(4), 1.982(13); Pd(2)-O(4), 1.982(13); O(4)-Pd(2)-O(4), 180.00; O(4)-Pd(2)-N(2), 92.00(6); N(2)-Pd(2)-N(2), 180.00.

The bond angles around the palladium(II) atom for O(4)-Pd(2)-O(4) of 180.00° and O(4)-Pd(2)-N(2) of 92.00°(6) show little deviation from the expected 180° and 90°, an indication of minimal distortion from a square planar geometry. This is not surprising due to the limited steric encumbrance around the metal center. The bond length for Pd(2)-N(2) of 2.019(15) Å is comparable to the average for Pd-N<sub>imine</sub> bond distances of 2.017 Å reported for 105 similar palladium(II) complexes.<sup>27</sup> Similarly, the bond distance for Pd-O(4) of 1.982(13) Å compares favourably to the average for Pd-O bond lengths of 1.988 Å observed in 302 related palladium complexes.<sup>27</sup> There exists intermolecular hydrogen bonding between the OH groups.

#### **4.3.2. Hydrogenation reactions of alkenes and alkynes catalysed by complexes 12-17**

##### *4.3.2.1. Preliminary screening of palladium complexes 12-17 in molecular hydrogenation of styrene*

Preliminary evaluation of complexes **12-17** in the molecular hydrogenation reactions of styrene were performed at 5 bar, 30 °C and [styrene]:[Pd] ratio of 1000:1. Under these conditions, all the complexes (**12-17**) formed active catalysts giving conversions ranging from 50% - 97% within 1.5 h (Table 4.2). The identities and compositions of the products were determined by GC-MS and GC (Fig. 4.6). Control experiments conducted without the use of a palladium(II) complex gave only 2% conversions (Table 4.2, entry 8), clearly demonstrating that higher catalytic activities observed were due to the complexes **12-17**. Upon establishing that complexes **12-17** form active hydrogenation catalysts, we further performed detailed kinetics, selectivity and

theoretical studies of the hydrogenation reactions of a range substrates including higher alkenes and alkynes.

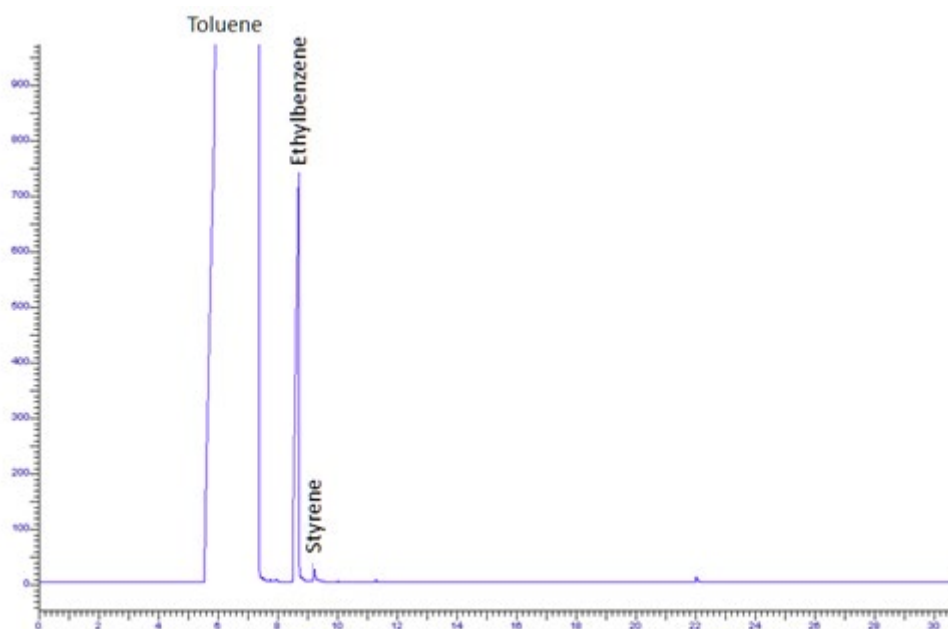


**Figure 4.6:** GC chromatogram of the product obtained from the hydrogenation of styrene using catalyst **12**. Reaction conditions: [styrene]/[**12**] = 1000; substrate, 4.00 mmol; catalyst; 0.004 mmol; solvent, toluene (50 ml); pressure, 5 bar; temperature, 30 °C; time, 1.5 h.

#### 4.3.2.2. *Influence of complex structure on the kinetics of hydrogenation reactions of styrene*

The influence of complex structure on the molecular hydrogenation of styrene was investigated by determining the rate constants for complexes **12-17** (Table 4.2). A linear plot of  $\ln[\text{Sty}]_0/[\text{Sty}]_t$  vs time (Fig. 4.7) established that the hydrogenations reactions were *pseudo*-first order with respect to styrene according to equation 4.2.

$$\text{Rate} = k[\text{styrene}]^1 \quad (4.2)$$

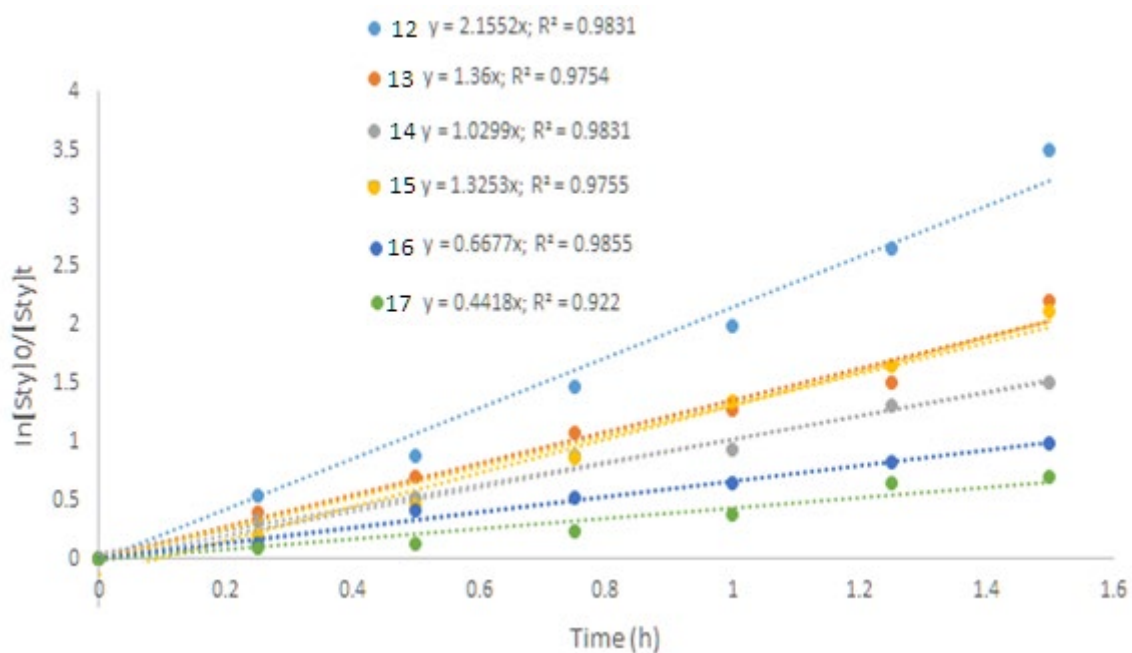


**Figure 4.7:** Plot of  $\ln[\text{Sty}]_0/[\text{Sty}]_t$  vs time for styrene hydrogenation using complexes 12-17. Reaction conditions: substrate, styrene;  $[\text{styrene}]/[\text{catalyst}] = 1000$ ; styrene, (0.41 g, 4.00 mmol); catalyst; 0.004 mmol; solvent, toluene (50 ml); pressure, 5 bar; temperature, 30 °C; time, 1.5 h.

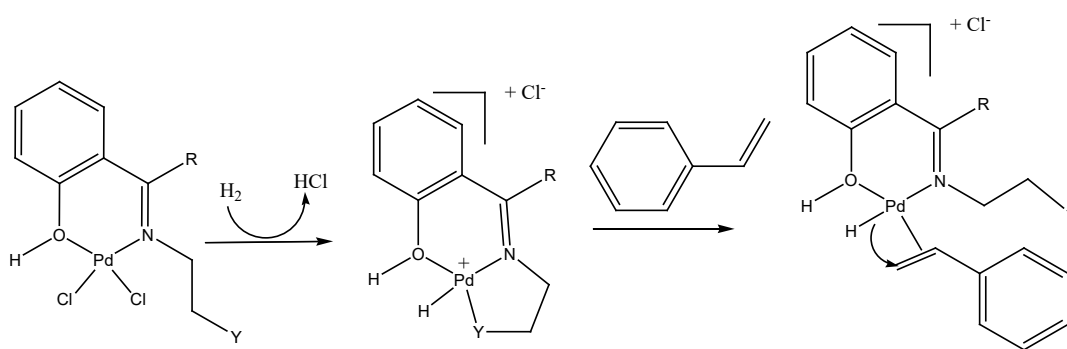
**Table 4.2:** Effect of catalyst structure on the hydrogenation of styrene by complexes **1-6<sup>a</sup>**

Entry	Catalysts	Conversion <sup>b</sup> (mol%)	$k_{obs}$ (h <sup>-1</sup> )	TOF <sup>c</sup> (h <sup>-1</sup> )
1	<b>12</b>	97	2.15 (±0.07)	646
2	<b>13</b>	89	1.36 (±0.13)	592
3	<b>14</b>	78	1.03 (±0.07)	519
4	<b>15</b>	88	1.32 (±0.05)	586
5	<b>16</b>	63	0.67 (± 0.05)	420
6	<b>17</b>	51	0.55 (± 0.06)	339
<b>7<sup>d</sup></b>	<b>12</b>	86	nd	526
<b>8<sup>e</sup></b>	—	2	nd	—

<sup>a</sup>Conditions: styrene, substrate/catalyst = 1000; substrate, 4.36 mmol; catalyst, 0.01 mmol; solvent, toluene; pressure, 5 bar; temperature, 30 °C; time, 1.5 h. <sup>b</sup>Determined by GC. <sup>c</sup>TOF in mol<sub>substrate</sub>mol<sub>catalyst</sub><sup>-1</sup> h<sup>-1</sup> (h<sup>-1</sup>). <sup>d</sup>Mercury drop test (5 drops of mercury were added to the reaction mixture). <sup>e</sup>Control experiment, no catalyst used, time 8 h.

It is clear that the catalytic activity of the complexes was influenced by the pendant arm of the ligands. For example, replacing the pendant OCH<sub>3</sub> group in **12** by an ammine group (**14**) was followed by a drop in  $k_{obs}$  from 2.15 h<sup>-1</sup> (TOF = 646 h<sup>-1</sup>) to 1.03 h<sup>-1</sup> (TOF = 519 h<sup>-1</sup>). This is likely to result from a stronger coordination of the nitrogen atom to palladium(II)<sup>28</sup> resulting in competition with the styrene substrate for the active site (Scheme 4.3). The observed catalytic activities of complexes **12-17**, in

comparison to the inactive palladium(II) complexes of P<sup>^</sup>N<sup>^</sup>S ligands<sup>16</sup> point to the hemi-lability of ligands **L5** – **L8**. On the other hand, there was no discernible effect of the imine carbon substituent on the catalytic activities of the complexes as shown by comparable catalytic activities of complexes **13** and **15** (Table 4.2, entries 2 and 4). This behaviour shows that the methyl substituent is remotely located away from the metal atom to confer any significant influence on the eventual catalytic activities of the catalysts.



**Scheme 4.3:** Hemi-labile nature of the ligands (Y = OH, NH<sub>2</sub>, OCH<sub>3</sub>); a strongly coordinating Y group is likely to reduce the catalytic activity by limiting substrate coordination to the metal centre.

Consistent with our previous reports, a comparison of the catalytic activities of the neutral and cationic systems, revealed that the neutral complexes were more active.<sup>19,20</sup> For example, rate constants of  $k_{\text{obs}} = 2.15 \text{ h}^{-1}$  and  $k_{\text{obs}} = 0.67 \text{ h}^{-1}$  were reported for catalysts **12** and **16** respectively (Table 4.2, entries 1, 5). This behaviour may be assigned to the poor lability of the PPh<sub>3</sub> and *p*-TsOH groups, in addition to increased steric bulk in catalyst **16**.<sup>29</sup>

#### 4.3.2.3. *Influence of catalyst concentration on the kinetics of hydrogenation reactions of styrene*

The effect of catalyst concentration and order of reaction with respect to complex **12** was investigated by varying the substrate/catalyst ratios from 400 to 1800 at fixed substrate concentration. A plot of  $\ln[\text{Sty}]_0/[\text{Sty}]_t$  vs time (Fig. 4.8) gave a straight line from which the  $k_{\text{obs}}$  at each ratio was determined (Table 4.3). It is significant to note that, while a decrease in catalyst loading resulted in increased TOFs, there was an appreciable decrease in  $k_{\text{obs}}$ . For example,  $k_{\text{obs}}$  of  $2.15 \text{ h}^{-1}$  and  $0.96 \text{ h}^{-1}$  were observed at substrate/catalyst ratios of 1000 and 1400 corresponding to TOFs of  $646 \text{ h}^{-1}$  and  $718 \text{ h}^{-1}$  respectively (Table 4.3, entries 3 and 5). This behaviour showed that increasing catalyst loading did not increase the catalytic activity by a similar magnitude and may be consistent with some degree of catalyst degradation/ aggregation with increased catalyst loading, hence loss of efficiency. However, it would be beneficial (economically viable) to use lower catalyst loading due to higher turn-over frequencies reported.



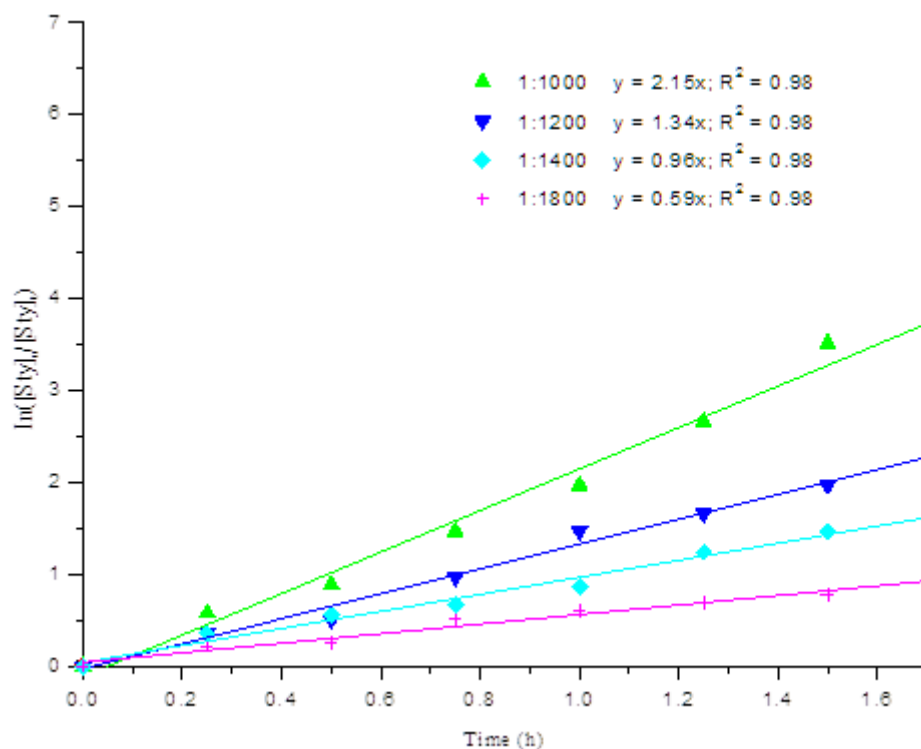


**Figure 4.8:** Plot of  $\ln([\text{Sty}]_0/[\text{Sty}]_t)$  vs time to establish the dependency of the rates of the reactions on the catalyst concentrations using catalyst **12**. The  $[\text{styrene}]/[\mathbf{12}]$  was varied from 1000 to 1800 at fixed concentration of styrene of 0.41 g (4.00 mmol).

A plot of  $-\ln(k_{\text{obs}})$  vs  $-\ln[\mathbf{12}]$  allowed us to determine the order of the reaction with respect to catalyst **12** as  $2.6 \pm 0.2 \text{ h}^{-1}$  (Fig. 4.9). The higher reaction order with respect to catalyst **12**, is indicative that the reaction is highly sensitive to a change in catalyst concentration. Fractional orders of reaction with respect to catalyst concentrations is known to arise from the possible existence of different active sites or catalyst aggregation.<sup>30,31</sup> In order to understand the nature of the active species and possible formation of palladium nanoparticles, we carried out a mercury drop test by adding a few drops of mercury to the reaction mixture of styrene and catalyst **12**. The minimal reduction in catalytic activity from 97% (TOF = 646  $\text{h}^{-1}$ ) to 86% (TOF = 526  $\text{h}^{-1}$ ) pointed

to lack of formation of palladium(0) nanoparticles as active species, hence homogenous nature of the reactions.<sup>32</sup> This contrasts our previous reports using (pyridyl)benzoazole palladium(II)<sup>13</sup> complexes which recorded significant reduction in catalytic activity from 98% to 55%; a feature we can allude to enhanced stabilization of the active species by the pendant arms of the ligand L5 in this this current study.

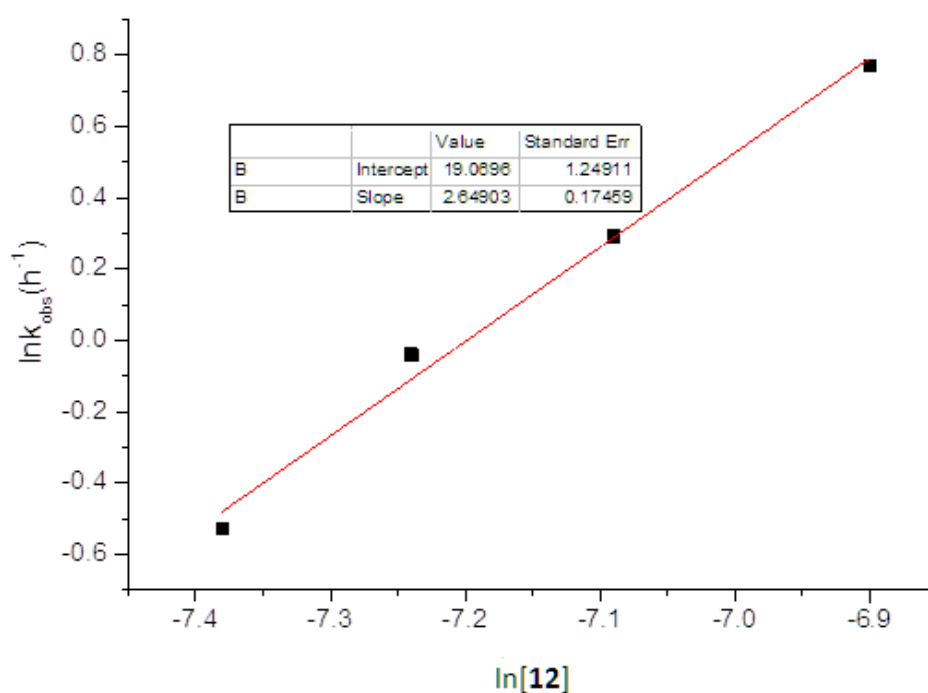


**Figure 4.9:** Plot of  $\ln(k_{\text{obs}})$  vs  $\ln[12]$  for the determination of the order of reaction with respect to catalyst **12**.

The effect of  $\text{H}_2$  concentration was also investigated by varying the pressure from 2.5 to 12.5 bar at S/C of 1000. From the plot of  $\ln[\text{Sty}]_0/[\text{Sty}]_t$  vs time the rate of hydrogenation reaction is seen to linearly dependent on the  $\text{H}_2$  pressure (Fig. 4.10).

From the plot of  $k_{\text{obs}}$  vs  $\text{H}_2$  pressure, the order of reaction with respect to  $[\text{H}_2]$  was derived as  $0.39 \pm 0.04$  (Fig. 4.11). This partial and low reaction orders with respect to  $\text{H}_2$  concentration has been associated with disfavoured activation of the  $\text{H}_2$  molecule to form the dihydride species.<sup>33</sup> The observed dependency of the rate of hydrogenation reactions on styrene and hydrogen pressure is consistent with either of the following reactions:

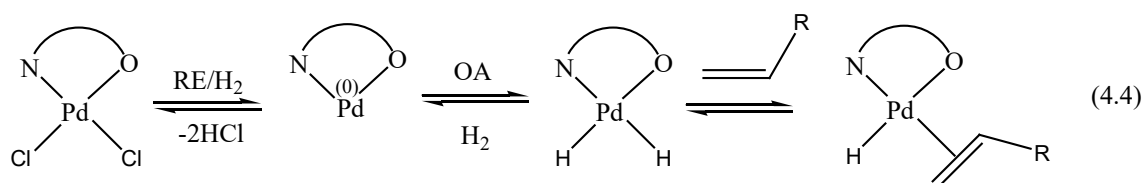
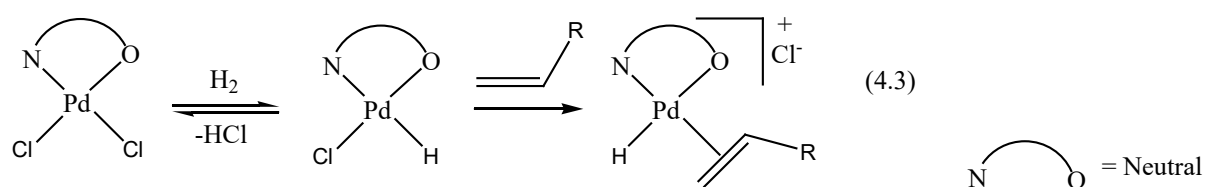


**Table 4.3:** Effect of reaction conditions on the hydrogenation of styrene using **12**<sup>a</sup>

Entry	Sub/Cat	$P_{\text{H}_2}$ (bar)	T (°C)	Conversion <sup>b</sup>	$k_{\text{obs}}$ (h <sup>-1</sup> )	TOF <sup>c</sup> (h <sup>-1</sup> )
1 <sup>d</sup>	400	5	30	>99	—	800
2 <sup>d</sup>	800	5	30	>99	—	1066
3	1000	5	30	97	2.15	646
4	1200	5	30	86	1.34	688
5	1400	5	30	77	0.96	718
6	1800	5	30	54	0.59	648
7	1000	2.5	30	62	0.63	412
8	1000	7.5	30	>99	2.99	666
9 <sup>e</sup>	1000	10	30	>99	4.36	799
10 <sup>d</sup>	1000	12.5	30	>99	—	1998
11	1000	5	20	77	1.01	542
12	1000	5	40	>99	3.15	659
13 <sup>f</sup>	1000	5	50	>99	4.93	999
14 <sup>d</sup>	1000	5	60	>99	—	1998

<sup>a</sup>Conditions: styrene, 4.36 mmol; solvent, toluene; pressure, 5 bar; temperature, 30 °C; time, 1.5 h. <sup>b</sup>Determined by GC. <sup>c</sup>TOF in mol<sub>substrate</sub>mol<sub>catalyst</sub><sup>-1</sup> h<sup>-1</sup>. <sup>d</sup>Time, 0.5 h, time too short to get enough data. <sup>e</sup>Time, 1.25 h. <sup>f</sup> time, 1.0 h.

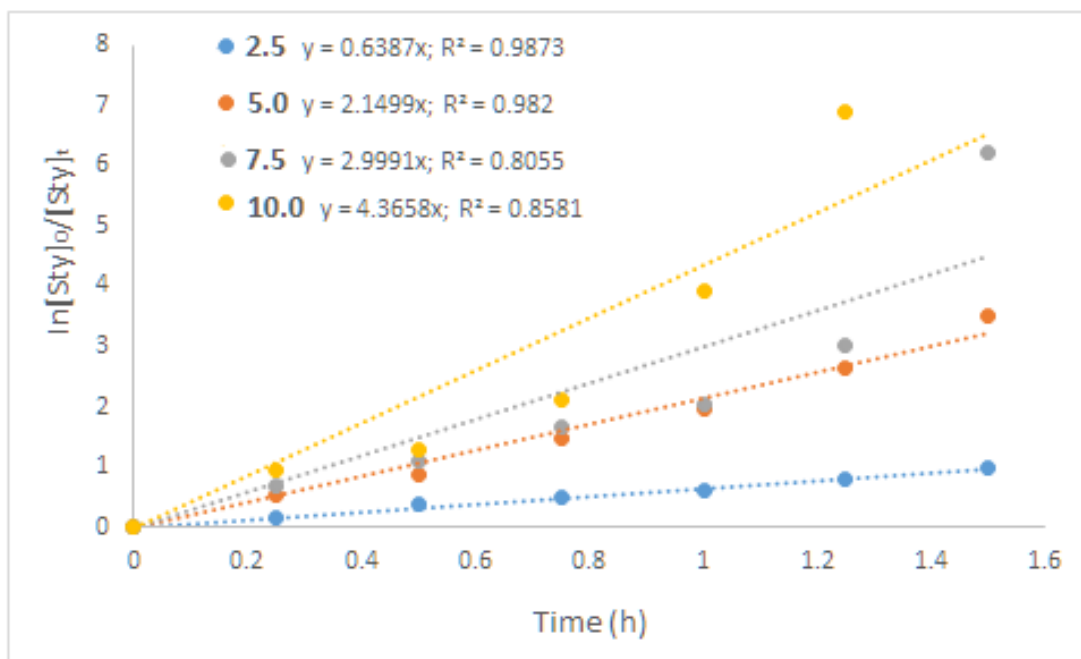


**Figure 4.10:** Plot of  $\ln[\text{Sty}]_0/[\text{Sty}]_t$  vs time to establish the dependency of the rates of the reactions on the dihydrogen pressure using catalyst **12**. Reaction conditions: substrate, styrene;  $[\text{styrene}]/[\text{catalyst}] = 1000$ ; styrene 0.41 g, 4.00 mmol; catalyst; 0.004 mmol; solvent, toluene (50 ml); temperature, 30 °C; time, 1.5 (5 bar), h, 0.5 h (12,5 bar), 1.25 h (10 bar).

The lower order of reaction with respect to  $[\text{H}_2]$  of  $0.39 \pm 0.04$  in addition to the absence of colour change during hydrogenation reactions support the formation of monohydride species. This points to the first mechanism (4.3) as the most probable pathway,<sup>34</sup> consistent with Scheme 4.3. From these kinetics result, the overall experimental rate law for the hydrogenation of styrene catalysed by catalyst **12** can thus be formulated as given in equation 4.5. The major importance of this equation is that the formation of the hydride species appears to be rate limiting step.<sup>35</sup>

$$\text{Rate} = k[\text{styrene}]^1[\mathbf{12}]^{2.6}[P_{\text{H}_2}]^{0.39} \quad (4.5)$$

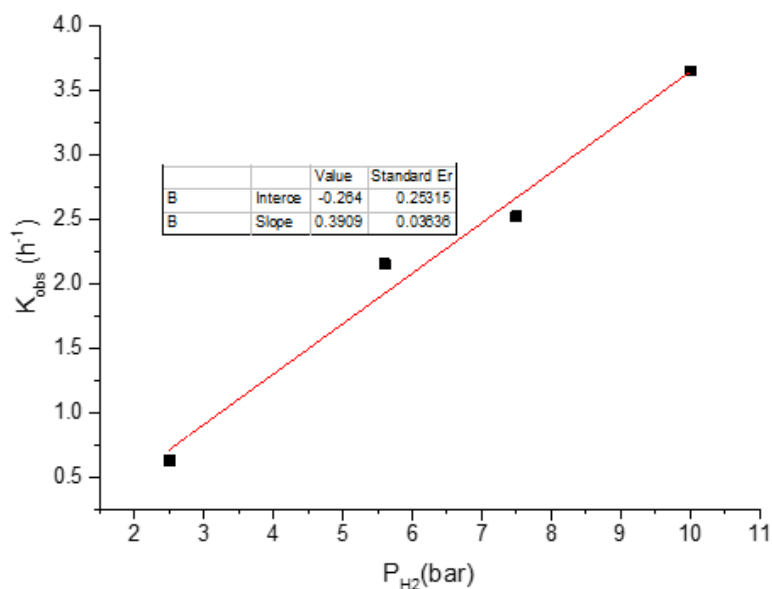


**Figure 4.11:** Plot of observed rate constant ( $k_{\text{obs}}$ ) vs hydrogen pressure to determine the order of reaction with respect to  $\text{H}_2$  concentration for catalyst **12**.

To determine the activation parameters of the hydrogenation reactions, we varied the temperature from 20 °C to 60 °C using catalyst **12** at [sty]/[**12**] ratio of 100 and  $\text{H}_2$  pressure of 5 bar. Expectedly, an increase in temperature from 20 °C to 40 °C, was followed by a significant increase in  $k_{\text{obs}}$  from 1.01  $\text{h}^{-1}$  (TOF = 542  $\text{h}^{-1}$ ) to 3.15  $\text{h}^{-1}$  (TOF = 659  $\text{h}^{-1}$ ) respectively (Table 4.3, entries 11 and 12).<sup>36,37</sup> It is important to note that, we did not witness the formation of palladium(0) black deposits even at elevated temperatures, confirming the thermal stability of catalyst **12**. The activation energy, standard enthalpy ( $\Delta H^\ddagger$ ) and entropy ( $\Delta S^\ddagger$ ) of activation were obtained from the

Arrhenius and Eyring plots (Figure 4.12). The large negative entropy value for  $\Delta S^\ddagger$  of  $-118.91 \pm 1.6$  J/mol K indicates a highly ordered transition state consistent with the formation of a Pd-hydride intermediate as the active species.<sup>35</sup> In addition, the parameters:  $E_a = 40.17 \pm 1.6$  kJ/mol and  $\Delta H^\ddagger = 37.60 \pm 1.6$  kJ/mol are comparable to those reported in literature for related homogeneous catalysts.<sup>38</sup>

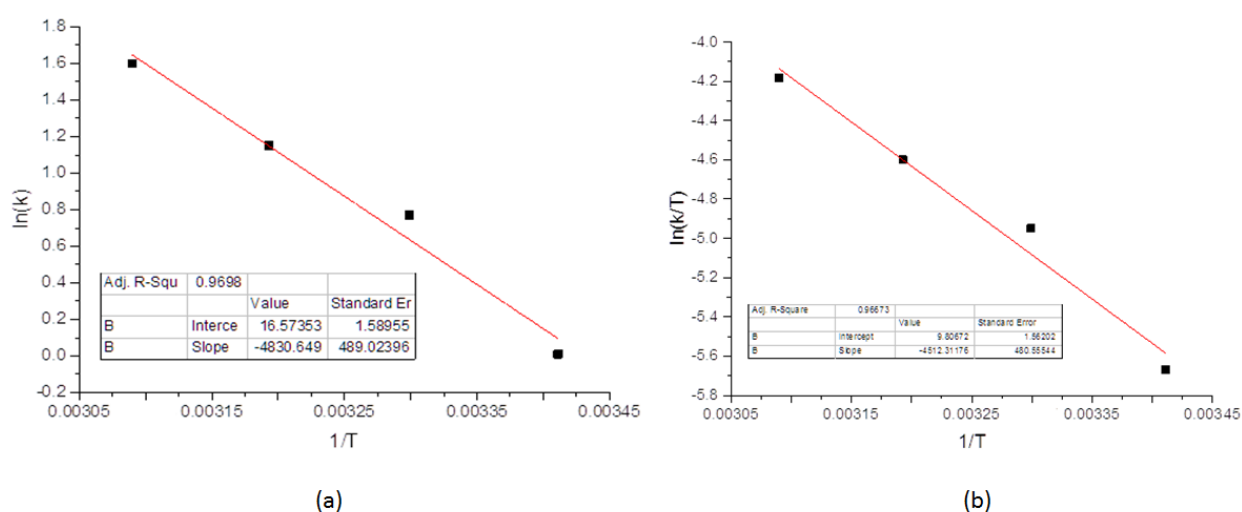


**Figure 4.12:** Arrhenius plot (a) and Eyring plot (b) for the determination of the  $E_a = 40.17 \pm 1.6$  kJ/mol,  $\Delta H^\ddagger = 37.60 \pm 1.6$  kJ/mol,  $\Delta S^\ddagger = -118.91 \pm 1.6$  J/mol K and  $\Delta G^\ddagger = 420.8 \pm 1.6$  kJ/mol.

### 4.3.3. Substrate scope and chemo-selectivity studies using complex

Complex **12** was further used to expand the scope of the alkene and alkyne substrates which included; 1-hexene, 1-octene, 1-hexyne, 1-octyne and phenyl acetylene (Table 4.4, Fig. 4.13). The trends in both the reactivity and product distribution obtained (Table 4.4 and Fig. 4.14) were similar to our recent reports,<sup>19,20</sup> hence does not require further elaborations. As illustration, alkynes were more reactive than the

corresponding alkenes while the reactivities of the substrates diminished with increase in chain length. In terms of production distribution, hydrogenation of alkenes were accompanied by isomerization reactions, while alkyne hydrogenation reactions occurred in two steps to sequentially produce the respective alkenes and alkanes (Fig. 4.14).

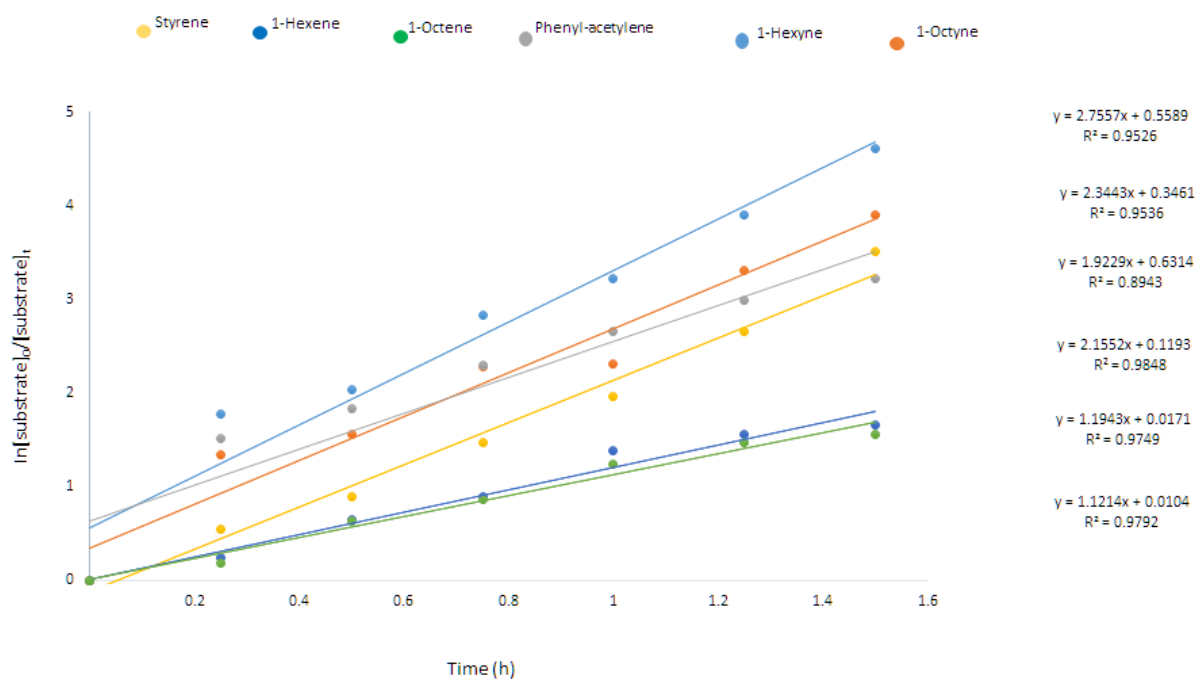


**Figure 4.13:** Effect of substrate on the kinetics of hydrogenation of alkenes and alkynes using catalyst **12**. Reaction conditions: [substrate]/[**12**] of 1000; substrate, solvent, toluene (50 mL); pressure, 5 bar; solvent, toluene; temperature, 30 °C; time, 1.5 h.



**Table 4.4:** Effect of substrates on the catalytic activity of catalyst **12**<sup>a</sup>

Entry	Substrate	( $k_{\text{obs}}$ )( $\text{h}^{-1}$ )	TOF <sup>b</sup> ( $\text{h}^{-1}$ )	%Alkane <sup>c</sup>
1	Styrene	2.15	646	97
2	1-Hexene	1.19( $\pm 0.07$ )	540	78
3	1-Octene	1.12 ( $\pm 0.09$ )	527	72
4	Phenyl-acetylene	1.92 ( $\pm 0.03$ )	640	100
5	1-Hexyne	2.75 ( $\pm 0.07$ )	440	66
6	1-Octyne	2.34 ( $\pm 0.11$ )	367	55
7	<i>trans</i> -2-hexene	0.68 ( $\pm 0.05$ )	488	53
8	<i>trans</i> -2-octene	0.62 ( $\pm 0.06$ )	460	44

<sup>a</sup>Conditions: substrate, substrate/catalyst = 1000; substrate, 4.36 mmol; catalyst; 0.01 mmol; solvent, toluene; pressure, 5 bar; solvent, toluene; temperature, 30 °C; time, 1.5 h. <sup>b</sup>TOF in  $\text{mol}_{\text{substrate}}\text{mol}_{\text{catalyst}}^{-1} \text{h}^{-1}$ . <sup>c</sup>selectivity towards alkane hydrogenation products after 1.5 h.

To gain more insight in the isomerization reactions and incomplete conversions of internal alkenes to alkanes, we used internal alkenes *trans*-2-hexene and *trans*-2-octene substrates (Table 4.4, entries 7 and 8). A significant drop in catalytic activity observed from 72% to 44% observed for 1-octene and *trans*-2-octene respectively, may thus explain the incomplete hydrogenations of the internal alkenes to their corresponding alkanes (Fig. 4.14a). Additionally, it was observed that like in terminal alkenes, there

occurred tandem hydrogenation and isomerization reactions for internal alkenes. For example, final compositions of 66% for n-octane and 34% for internal octenes (*trans*-3-octene = 27%, 2/4-octene = 7%) was observed for hydrogenation of *trans*-2-octene (Fig. 4.14b).

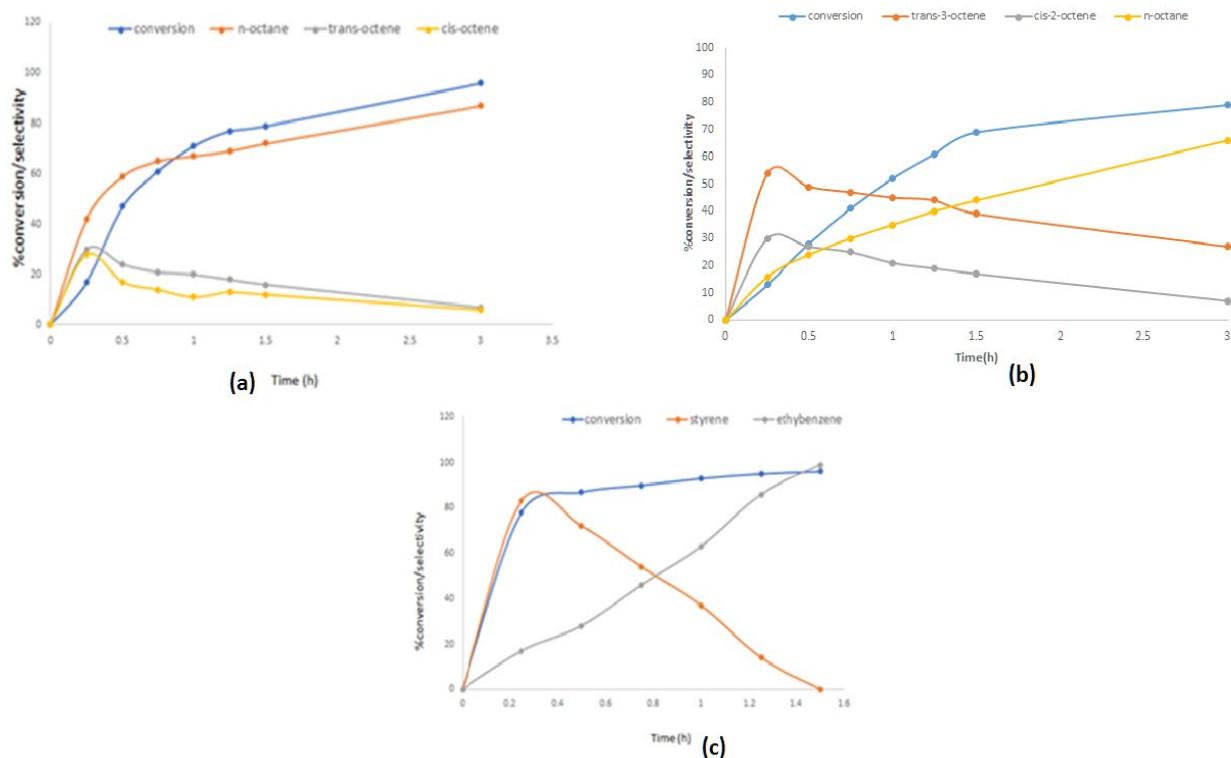


**Figure 4.14:** Product distribution over time in the hydrogenation of (a) 1-octene; (b) *trans*-2-octene and (c) phenyl-acetylene using complex **12** as a catalyst. Reaction conditions: [substrate]/[**12**] ratio of 1000; substrate (6.00 mmol) catalyst **12**; 0.006 mmol; solvent, toluene (50 ml); pressure, 5 bar; temperature, 30 °C; time, 15 min.

#### 4.3.4. Evidence of hemi-lability from DFT studies

The structure/property-activity relationships and trends observed in the hydrogenation reactions using complexes **12-17** pointed to potential hemi-lability of ligands **L5-L8**. We therefore ventured to establish this phenomenon using Density Functional Theory (DFT) calculations. The geometry-optimized structures for the palladium(II) complexes are shown in Table 4.5. The relationship between the Pd-Y bond length (Y = pendant arm) and the catalytic activity showed significant correlation (Fig. 4.15). For example, while complex **12b** (derived from **12**) with a Pd-OCH<sub>3</sub> bond length of 2.08 Å displayed  $k_{obs}$  of 2.15 h<sup>-1</sup>, complex **14b**, with Pd-NH<sub>2</sub> bond length of 1.95 Å had a  $k_{obs}$  of 1.03 h<sup>-1</sup> (Table 4.6). From these results, it is evident that coordination of styrene substrate to the vacant palladium atom is preceded by breaking of the Pd-Y bond, thus essential in controlling the overall reactivity (Scheme 4.3).<sup>39</sup> Another parameter that appeared to control the catalytic activities of the complexes was the charge density on the metal atom. For instance, catalyst **12b** carrying a positive charge of 0.420 was more active than catalyst **14b**, with a charge of 0.314 on the palladium(II) atom, in agreement with enhanced substrate coordination to an electrophilic metal centre.<sup>40</sup>

**Table 4.5:** DFT-calculated HOMO and LUMO frontier molecular orbitals of palladium(II) complexes **12b-15b**.

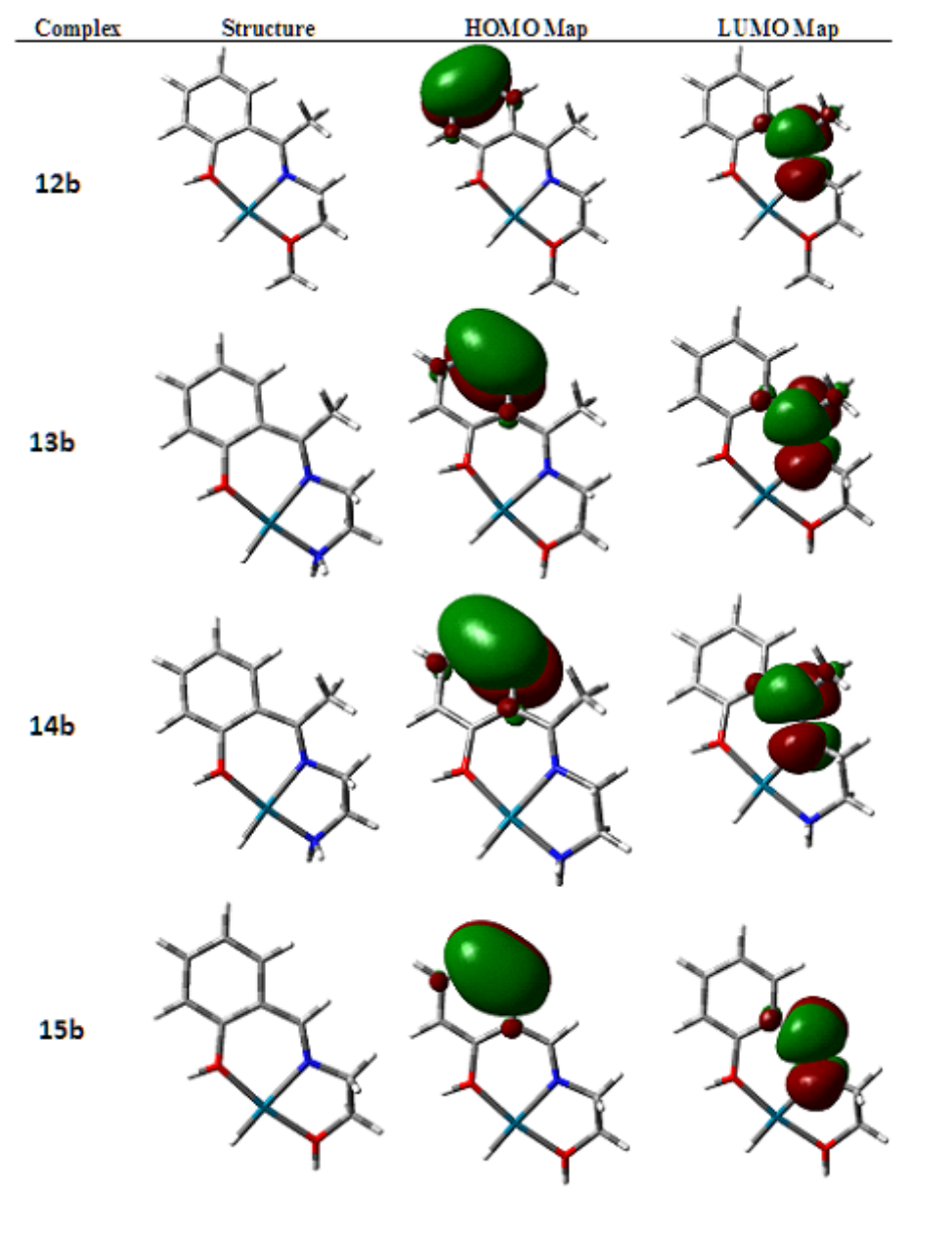
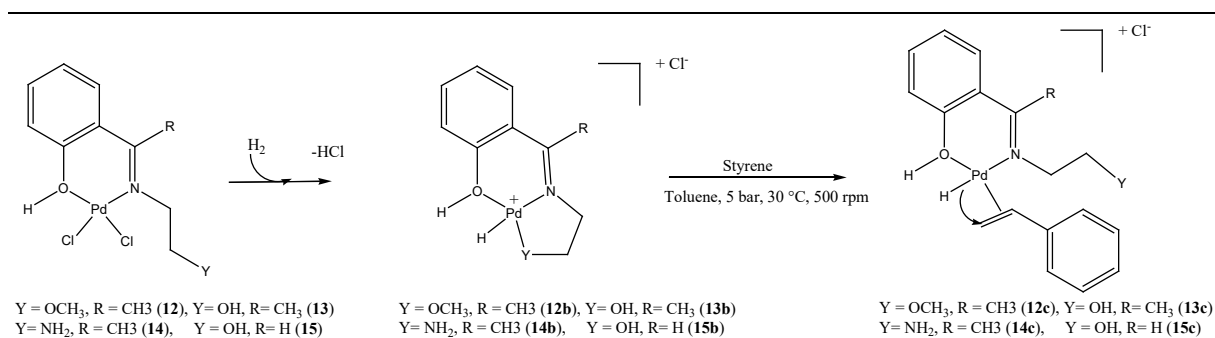


**Table 4.6:** DFT-calculated data for the bifunctional palladium (II) complexes.



LUMO (eV)	-4.28	-3.82	-3.76	-3.90
HOMO (eV)	-10.47	-10.12	-10.24	-10.35
$\Delta E_{\text{L-H}}$ (eV)	6.18	6.30	6.48	6.45
$\Delta \epsilon$ [kcal mol <sup>-1</sup> ]	142.61	145.26	149.47	148.66
NBO charges (Pd)	0.420	0.408	0.314	0.407
Pd-Y (Å)	2.08	2.02	1.95	2.00
TOF (h <sup>-1</sup> ) <sup>a</sup>	646	592	519	586
$k_{\text{obs}}$ (h <sup>-1</sup> )	2.15	1.36	1.03	1.32

<sup>a</sup>TOF in mol<sub>substrate</sub>mol<sub>catalyst</sub><sup>-1</sup> h<sup>-1</sup> (h<sup>-1</sup>).

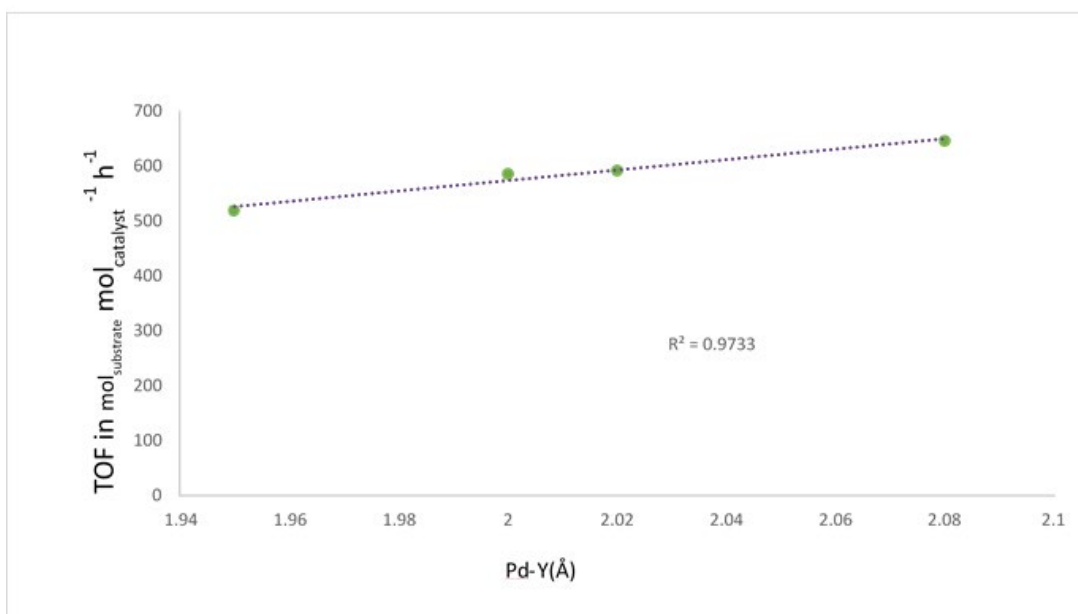


**Figure 4.15:** Plot of TOF in  $\text{mol}_{\text{substrate}} \text{mol}_{\text{catalyst}}^{-1} \text{h}^{-1}$  against Pd-Y(Å) showing a correlation between catalytic activity and Pd-Y(Å) bond lengths of complexes **12b-15b**.

#### 4.4. Conclusions

In summary, palladium(II) complexes based on (imino)phenol ligands with pendant donor groups have been synthesized and structurally characterized. Single crystal X-ray diffraction studies of complex **15a** showed that the complex contained two bidentate anionic ligands. The complexes formed active catalysts in the hydrogenation of alkenes and alkynes under mild conditions. Hydrogenation reactions of terminal alkenes were accompanied by isomerization reactions, while hydrogenation of alkynes occurred in two steps *via* alkenes. Kinetic studies on the hydrogenation reactions were established to be *pseudo*-first order with respect to alkene substrate, but partial orders with respect to H<sub>2</sub> and catalyst concentrations. The activation

parameters indicate a highly ordered transition state and homogenous nature of the active species. DFT studies point to the hemi-labile nature of the ligands, in which breaking the Pd-pendant donor atom bonds prior to substrate coordination controls the reactivity of the complexes.

## 5.6. References

- 1 H. E. Hoelscher, W. G. Poynter and E. Weger, *Chem. Rev.*, 1954, **54**, 575–592.
- 2 A. M. Kluwer and C. J. Elsevier, *Homogeneous Hydrogenation of Alkynes and Dienes*, Wiley & Sons, New York, 2008.
- 3 N. Toshima and T. Takahashi, *Bull. Chem. Soc. Jpn.*, 1992, **65**, 400–409.
- 4 T. Suarez and B. Fontal, *J. Mol. Catal.*, 1988, **45**, 335–344.
- 5 M. Chen, Z. Yang, H. Wu, X. Pan, X. Xie and C. Wu, *Int. J. Nanomedicine.*, 2011, **6**, 2873–2877.
- 6 E. Drinkel, A. Briceño, R. Dorta and R. Dorta, *Organometallics*, 2010, **29**, 2503–2514.
- 7 C. Bianchini, A. Meli, M. Peruzzini, P. Frediani, C. Bohanna, M. A. Esteruelas and L. A. Oro, *Organometallics*, 1992, **11**, 138–145.
- 8 E. Negishi, *Handbook of Organopalladium Chemistry for Organic Synthesis*, Wiley & Sons, New York, 2002, **1**, 229–247.
- 9 D. Drago and P. S. Pregosin, *Organometallics*, 2002, **21**, 1208–1215.10
- 10 M. W. van Laren, M. A. Duin, C. Klerk, M. Naglia, D. Rogolino, P. Pelagatti, A. Bacchi, C. Pelizzi and C. J. Elsevier, *Organometallics*, 2002, **21**, 1546–1553.
- 11 C. A. Ghilardi, S. Midollini, S. Moneti and A. Orlandini, *J. Chem. Soc. Dalt. Trans.*, 1992, 3371–3376.

- 12 J. V. Allen, J. F. Bower and J. M. J. Williams, *Tetrahedron: Asymmetry.*, 1994, **5**, 1895–1898.
- 13 K. E. Frankcombe, K. J. Cavell, B. F. Yates and R. B. Knott, *Organometallics*, 1997, **16**, 3199–3206.
- 14 J. C. Jeffrey and T. B. Rauchfuss, *Inorg. Chem.*, 1979, **18**, 2658–2666.
- 15 P. Pelagatti, A. Bacchi, M. Carcelli, M. Costa, A. Fochi, P. Ghidini, E. Leporati, M. Masi, C. Pelizzi and G. Pelizzi, *J. Organomet. Chem.*, 1999, **583**, 94–105.
- 16 A. Bacchi, M. Carcelli, M. Costa, A. Leporati, E. Leporati, P. Pelagatti, C. Pelizzi and G. Pelizzi, *J. Organomet. Chem.*, 1997, **535**, 107–120.
- 17 D. E. Barber, Z. Lu, T. Richardson, R. H. Crabtree and P. Street, *Inorg. Chem.*, 1992, **31**, 4709–4711.
- 18 F. Yilmaz, A. Mutlu, H. Ünver, M. Kurta and I. Kani, *J. Supercrit. Fluids.*, 2010, **54**, 202–209.
- 19 S. O. Ojwach, A. O. Ogwenio and M. P. Akerman, *Catal. Sci. Technol.*, 2016, **6**, 5069–5078.
- 20 S. O. Ojwach and A. O. Ogwenio, *Transit. Met. Chem.*, 2016, **41**, 539–546.
- 21 K. Bittler, N. V. Kutepow, D. Neubauer and H. Reis, *Angew. Chem. Int. Ed. English.*, 1968, **7**, 329–335.
- 22 M. J. T. Frisch, G. W. Trucks, H. B. Schlegel, G. E. Scuseria, M. A. Robb, J. R. Cheeseman, G. Scalmani, V. Barone, B. Mennucci, G. A. Petersson, H. Nakatsuji, M. Caricato, X. Li, H. P. Hratchian, A. F. Izmaylov, J. Bloino, G. Zheng, J. L. Sonnenberg, M. Hada, M. Ehara, K. Toyota, R. Fukuda, J. Hasegawa, M. Ishida, T. Nakajima, Y. Honda, O. Kitao, H. Nakai, T. Vreven, J. A. Montgomery Jr., J. E. Peralta, F. Ogliaro, M. Bearpark, J. J. Heyd, E. Brothers, K. N. Kudin, V. N. Staroverov, R. Kobayashi, J. Normand, K. Raghavachari, A. Rendell, J. C. Burant, S. S. Iyengar, J. Tomasi, M. Cossi, N. Rega, J. M. Millam, M. Klene, J. E. Knox, J. B. Cross, V. Bakken, C. Adamo, J. Jaramillo, R. Gomperts, R. E.



- Stratmann, O. Yazyev, A. J. Austin, R. Cammi, C. Pomelli, J. W. Ochterski, R. L. Martin, K. Morokuma, V. G. Zakrzewski, G. A. Voth, P. Salvador, J. J. Dannenberg, S. Dapprich, A. D. Daniels, O. Farkas, J. B. Foresman, J. V. Ortiz, J. Cioslowski and D. J. Fox, GAUSSIAN 09 (Revision A.1), Gaussian, Inc., Wallingford, CT, 2009.
- 23 E. Sindhuja, R. Ramesh and Y. Liu, *Dalton Trans*, 2012, **41**, 5351.
- 24 V. S. Tkach, D. S. Suslov, N. V. Kurat'eva, M. V. Bykov, M. V. Belova and N. V. Kurat'Eva, *Russ. J. Coord. Chem.*, 2011, **37**, 752–756.
- 25 M. Ngcobo and S. O. Ojwach, *J. Organomet. Chem.*, 2017, **846**, 33–39.
- 26 S. Boltina, M. Yankey, I. Guzei, L. Spencer, S. Ojwach and J. Darkwa, *S. Afr. J. Chem.*, 2012, **65**, 75-83.
- 27 I. J. Bruno, J. C. Cole, M. Kessler, J. Luo, W. D. S. Momerwell, L. H. Purkis, B. R. Smith, R. Taylor, R. I. Cooper, S. E. Harris and A. G. Orpen, *J. Chem. Inf. Comput. Sci.*, 2004, **44**, 2133–2144.
- 28 R. G. Pearson, *Surv.Progr.Chem.*, 1969, **5**, 1–52.
- 29 R. E. Harmon, S. K. Gupta and D. J. Brown, *Chem. Rev.*, 1973, **73**, 21–52.
- 30 V. P. Ananikov and I. P. Beletskaya, *Organometallics*, 2012, **31**, 1595–1604.
- 31 J. A. Widegren and R. G. Finke, *J. Mol. Catal. A Chem.*, 2003, **198**, 317–341.
- 32 G. Süß-Fink, M. Faure and T. R. Ward, *Angew. Chemie. Int. Ed.*, 2002, **41**, 99–101.
- 33 D. E. Budd, D. G. Holah, A. N. Hughes and B. C. Hui, *Can. J. Chem.*, 1974, **52**, 775–781.
- 34 K. C. Dewhirst, W. Keim and C. A. Reilly, *Inorg. Chem.*, 1968, **7**, 546–551.
- 35 A. M. Kluwer, T. S. Koblenz, T. T. Jonischkeit, K. Woelk and C. J. Elsevier, *J. Am. Chem. Soc.*, 2005, **127**, 15470–15480.
- 36 H. Yoshida, T. Zama, S. Fujita, J. Panpranot and M. Arai, *RSC Adv*, 2014, **4**, 24922.

- 37 M. Costa, P. Pelagatti, C. Pelizzi and D. Rogolino, *J. Mol. Cat. A.*, 2002, **178**, 21–26.
- 38 J. Lin and C. U. Pittman, *J. Organomet. Chem.*, 1996, **512**, 69–78.
- 39 T. Sperger, I. A. Sanhueza, I. Kalvet and F. Schoenebeck, *Chem. Rev.*, 2015, **115**, 9532–9586.
- 40 G. S. Nyamato, S. O. Ojwach and M. P. Akerman, *Dalton Trans*, 2016, **45**, 3407–3416.

## CHAPTER 5

### Synthesis, kinetic and mechanistic studies of hydrogenation reactions of alkenes and alkynes catalysed by P<sup>N</sup> (imino-diphenylphosphino) palladium(II) complexes

#### 5.1 Introduction

A number of palladium(II) complexes have been successfully applied in the homogeneous hydrogenation of alkenes and alkynes. The ligand architecture has been the major focus in the homogeneous hydrogenation reactions as the catalytic activities and selectivities lies in the coordination around the metal atom. Established examples include palladium(II) complexes derived from bidentate phosphines<sup>1</sup> of the type P<sup>N</sup><sup>2</sup> and nitrogen-donor<sup>3</sup> catalysts of the type N<sup>S</sup><sup>4</sup> and N<sup>O</sup>.<sup>5</sup> Even though the bidentate nitrogen (N<sup>S</sup>, N<sup>O</sup>) and phosphine-donor (P<sup>N</sup>) palladium(II) catalysts have been successfully used in the homogeneous hydrogenation reactions of alkenes and alkynes, these systems suffer from lack of stability.<sup>6</sup> For example Ogweno *et. al.*<sup>7,8</sup> reported the catalytic active palladium(II) complexes of the type (pyridyl)benzoazole and (pyrazolylmethyl)pyridine ligand which were catalytically active but suffered from catalyst decomposition to form palladium nanoparticles and partly behaved like heterogeneous systems.

To overcome the issue of catalyst decomposition, hemilabile palladium(II) complexes of the type N<sup>O</sup> were used in Chapter 4. These hemilabile systems in Chapter 4 showed improved stability and activity in molecular hydrogenation of alkenes and alkynes. While Chapter 4 addressed hemilability, this Chapter addresses mixed donor

ligand from N<sup>^</sup>O to N<sup>^</sup>P. The shift from hard-hard donor atoms (N<sup>^</sup>O) to hard-soft donor atoms (N<sup>^</sup>P) is because it has been reported in literature that good results in terms of activity, selectivity, robustness and efficiency of the catalyst can be obtained with complexes containing both a 'soft' P and 'hard' N donor atoms.<sup>9</sup> For example, excellent turnover frequency up to 120 000 h<sup>-1</sup> in transfer hydrogenation of acetophenone were reported by the groups of Baratta and Hermann, applying ruthenium(II) complexes anchored on N<sup>^</sup>P ligands.<sup>10</sup> However, lower turnover frequency (333 h<sup>-1</sup>) were reported for N<sup>^</sup>O ruthenium(II) complexes.<sup>10</sup>

Therefore, in this chapter, the synthesis and characterization of palladium(II) complexes of hybrid N<sup>^</sup>P donor ligands and their applications in the catalytic hydrogenation of alkenes and alkynes are reported.

## 5.2 Experimental section

### 5.2.1. *Material, instrumentation and methods*

All moisture and air sensitive reactions were performed using standard Schlenk line techniques. Methanol (ACS reagent, ≥99.8%), toluene (ACS reagent, ≥99.5%), dichloromethane (ACS reagent, ≥99.8%), absolute ethanol (ACS reagent, ≥98%), DMSO-d<sub>6</sub> (99.8%), were purchased from Merck. Chloroform-CDCl<sub>3</sub> (98%), *p*-TsOH (ACS reagent, ≥98.5%), PPh<sub>3</sub> (Reagent Plus®, 99%), 2-(diphenylphosphino)benzaldehyde (97%), 2-methoxyethanamine (98%), NaBAR<sub>4</sub> (Ar<sub>4</sub> = 3,5-(CF<sub>3</sub>)<sub>2</sub>C<sub>6</sub>H<sub>3</sub>) (99%) were obtained from Sigma-Aldrich and were used without further purification. Solvents were dried and distilled under nitrogen atmosphere in

the presence of suitable drying agents: Toluene and acetone were dried over sodium wire/benzophenone, methanol and absolute ethanol over calcium oxide, and dichloromethane over phosphorus pentoxide.<sup>11</sup> Nuclear magnetic resonance spectra were acquired at 400 MHz for <sup>1</sup>H, 100 MHz for <sup>13</sup>C and 162 MHz for <sup>31</sup>P on a Bruker Avance spectrometer equipped with Bruker magnet (9.395 T). All coupling constants (*J*) are measured in Hertz, Hz. The mass spectra (ESI-MS) were recorded on a Waters API Quattro Micro spectrometer, using 50% MeOH/DMSO, 16-36 V cone voltage, source (720 V) and desolvation temperature of 450 °C. The elemental analyses were performed on a Thermal Scientific Flash 2000. The infrared spectra were recorded on a Perkin-Elmer spectrum 100 in the 4000-650 cm<sup>-1</sup> range.

## 5.2.2. Synthesis of P<sup>AN</sup> (diphenylphosphino)benzalidene ethanamine ligands and their palladium(II) complexes

### 5.2.2.1. [2-(2-(diphenylphosphino)benzylidene)methoxyethanamine] (L9)

To a dichloromethane solution (10mL) of 2-(diphenylphosphino)benzaldehyde (0.20 g, 0.69 mmol) was added drop-wise a solution of 2-methoxyethanamine (0.05 g, 0.69 mmol) in dichloromethane (volume), followed by magnesium sulphate (800 mg). The reaction was left to stir at ambient temperature for 72 h, resulting in a light yellow-orange mixture. The magnesium sulphate was filtered off, followed by evaporation of the solvent in *vacuo* to obtain L9 as a yellow-orange oil. Yield = 0.19 g (80%). <sup>1</sup>H NMR (400 MHz, CDCl<sub>3</sub>) : δ<sub>H</sub> (ppm): 3.23 (s, 3H, OCH<sub>3</sub>); 3.51 (t, 2H, CH<sub>2</sub>-N); 3.61 (t, 2H, CH<sub>2</sub>-O); 6.93 (t, 1H, H-Ph); 7.31 (m, 4H, H-PPh<sub>2</sub>); 7.34 (m, 6H, H-PPh<sub>2</sub>); 7.37 (dd, 2H, H-Ph); 8.04 (d, 1H, H-Ph); 8.94 (s, 1H, H-C=N). <sup>13</sup>C NMR (CDCl<sub>3</sub>): δ<sub>C</sub>(ppm): 58.02 (OCH<sub>3</sub>); 67.21 (CH<sub>2</sub>-N); 73.66 (CH<sub>2</sub>-O); 128.04 (Ph); 128.77 (Ph); 128.80 (Ph-PPh<sub>2</sub>); 128.83 (Ph-

PPh<sub>2</sub>); 128.86 (Ph-PPh<sub>2</sub>); 128.92 (Ph-PPh<sub>2</sub>); 128.98 (Ph-PPh<sub>2</sub>); 129.30 (Ph-PPh<sub>2</sub>); 129.50 (Ph); 132.25 (Ph-P); 132.70 (Ph); 133.69 (Ph-PPh<sub>2</sub>); 133.73 (Ph-PPh<sub>2</sub>); 133.84 (Ph-PPh<sub>2</sub>); 133.99 (Ph-PPh<sub>2</sub>); 137.13 (Ph-PPh<sub>2</sub>); 137.36 (Ph-PPh<sub>2</sub>); 142.53 (Ph); 160.99 (C=N). <sup>31</sup>P NMR (CDCl<sub>3</sub>): δ<sub>p</sub>(ppm): -13.70. MS (ESI) m/z (%) 370 (M<sup>+</sup> + Na, 100). HRMS-ESI ([M<sup>+</sup>+H<sup>+</sup>]): 347.7847; found: 348.1849. FT-IR (cm<sup>-1</sup>): ν<sub>(C=N)imine</sub> = 1633.

Compounds **L9–L12** were prepared following the same procedure described for compound **L9**.

#### 5.2.2.2. [2-(2-(diphenylphosphino)benzylideneamino)ethanol] (**L10**)

Compound **L10** was synthesized from 2-(diphenylphosphino)benzaldehyde (0.20 g, 0.69 mmol) and 1-(2-hydroxyphenyl)ethanone (0.08 g, 0.69 mmol). Brown oil. Yield = 0.21 g (92%). <sup>1</sup>H NMR (400 MHz, CDCl<sub>3</sub>) : δ<sub>H</sub> (ppm): 3.67 (dd, 4H, CH<sub>2</sub>-CH<sub>2</sub>); 6.93 (t, 1H, H-Ph); 7.32 (m, 4H, H-PPh<sub>2</sub>); 7.37 (m, 6H, H-PPh<sub>2</sub>); 7.39 (dd, 2H, H-Ph); 8.02 (d, 1H, H-Ph); 8.83 (s, 1H, H-C=N). <sup>13</sup>C NMR (CDCl<sub>3</sub>): δ<sub>C</sub>(ppm): 58.51 (CH<sub>2</sub>-OH); 69.91 (CH<sub>2</sub>-N); 127.98 (Ph); 128.51 (Ph); 128.74 (Ph-PPh<sub>2</sub>); 128.81 (Ph-PPh<sub>2</sub>); 128.85 (Ph-PPh<sub>2</sub>); 128.89 (Ph-PPh<sub>2</sub>); 128.96 (Ph-PPh<sub>2</sub>); 129.12 (Ph-PPh<sub>2</sub>); 129.46 (Ph); 132.19 (Ph-P); 132.67 (Ph); 133.64 (Ph-PPh<sub>2</sub>); 133.69 (Ph-PPh<sub>2</sub>); 133.80 (Ph-PPh<sub>2</sub>); 133.96 (Ph-PPh<sub>2</sub>); 137.09 (Ph-PPh<sub>2</sub>); 137.29 (Ph-PPh<sub>2</sub>); 142.50 (Ph); 160.82 (C=N). <sup>31</sup>P NMR (CDCl<sub>3</sub>): δ<sub>p</sub>(ppm): -13.62. MS (ESI) m/z (%) 356 (M<sup>+</sup> + Na, 100). HRMS-ESI ([M<sup>+</sup>+H<sup>+</sup>]): 333.1345; found: 334.1987. FT-IR (cm<sup>-1</sup>): ν<sub>(C=N)imine</sub> = 1634; ν<sub>(OH)</sub> = 3391

#### 5.2.2.3. (2-(diphenylphosphino)benzylidene)ethane-1,2-diamine (**L11**)

2-(diphenylphosphino)benzaldehyde (0.20 g, 0.69 mmol) and ethane-1,2-diamine (0.04 g, 0.69 mmol). Yellow-orange oil. Yield = 0.23 g (83%). <sup>1</sup>H NMR (400 MHz, CDCl<sub>3</sub>) : δ<sub>H</sub> (ppm): 3.55 (t, 2H, CH<sub>2</sub>-N); 3.65 (t, 2H, CH<sub>2</sub>-NH<sub>2</sub>); 6.95 (t, 1H, H-Ph); 7.33

(m, 4H, H-PPh<sub>2</sub>); 7.36 (m, 6H, H-PPh<sub>2</sub>); 7.41 (dd, 2H, H-Ph); 8.05 (d, 1H, H-Ph); 8.98 (s, 1H, H-C=N). <sup>13</sup>C NMR (CDCl<sub>3</sub>): δ<sub>c</sub>(ppm): 43.30 (CH<sub>2</sub>-NH<sub>2</sub>); 57.52 (CH<sub>2</sub>-N); 127.81 (Ph); 128.61 (Ph); 128.74 (Ph-PPh<sub>2</sub>); 128.80 (Ph-PPh<sub>2</sub>); 128.81 (Ph-PPh<sub>2</sub>); 128.90 (Ph-PPh<sub>2</sub>); 128.96 (Ph-PPh<sub>2</sub>); 129.22 (Ph-PPh<sub>2</sub>); 129.35 (Ph); 132.08 (Ph-P); 132.63 (Ph); 133.58 (Ph-PPh<sub>2</sub>); 133.70 (Ph-PPh<sub>2</sub>); 133.78 (Ph-PPh<sub>2</sub>); 133.85 (Ph-PPh<sub>2</sub>); 137.06 (Ph-PPh<sub>2</sub>); 137.25 (Ph-PPh<sub>2</sub>); 142.41 (Ph); 160.79 (C=N). <sup>31</sup>P NMR (CDCl<sub>3</sub>): δ<sub>p</sub>(ppm): -13.56. MS (ESI) m/z (%) 355 (M<sup>+</sup> + Na, 100). HRMS-ESI ([M<sup>+</sup>+H<sup>+</sup>]): 332.1728; found: 333.8425. FT-IR (cm<sup>-1</sup>): ν<sub>(C=N)imine</sub> =1626.

#### 5.2.2.4. (2-(diphenylphosphino)benzylidene)diethylethane-1,2-diamine (L12)

2-(diphenylphosphino)benzaldehyde (0.20 g, 0.69 mmol) and N,N-diethylenediamine (0.08 g, 0.69 mmol). Yellow. Yield = 0.21 g (78%). <sup>1</sup>H NMR (400 MHz, CDCl<sub>3</sub>): δ<sub>H</sub> (ppm): 1.02 (m, 6H, CH<sub>3</sub>-NEt<sub>2</sub>); 2.56 (m, 4H, CH<sub>3</sub>-NEt<sub>2</sub>); 3.63 (dd, 4H, CH<sub>2</sub>-CH<sub>2</sub>); 6.89 (t, 1H, H-Ph); 7.31 (m, 4H, H-PPh<sub>2</sub>); 7.37 (m, 6H, H-PPh<sub>2</sub>); 7.43 (dd, 2H, H-Ph); 7.98 (d, 1H, H-Ph); 8.91 (s, 1H, H-C=N). <sup>13</sup>C NMR (CDCl<sub>3</sub>): δ<sub>c</sub>(ppm): 13.31 (CH<sub>3</sub>-NEt<sub>2</sub>); 13.32 (CH<sub>3</sub>-NEt<sub>2</sub>); 49.61 (CH<sub>2</sub>-NEt<sub>2</sub>); 49.59 (CH<sub>2</sub>-NEt<sub>2</sub>); 53.11 (CH<sub>2</sub>-N); 62.12 (CH<sub>2</sub>-NEt<sub>2</sub>); 125.71 (Ph-PPh<sub>2</sub>); 128.63 (Ph-PPh<sub>2</sub>); 128.64 (Ph-PPh<sub>2</sub>); 128.69 (Ph-PPh<sub>2</sub>); 128.70 (Ph-PPh<sub>2</sub>); 127.73 (Ph-PPh<sub>2</sub>); 128.82 (Ph); 129.01 (Ph-PPh<sub>2</sub>); 129.03 (Ph-PPh<sub>2</sub>); 129.22 (Ph); 131.00 (Ph); 131.11 (Ph); 131.72 (Ph-P); 133.12 (Ph-PPh<sub>2</sub>); 133.13 (Ph-PPh<sub>2</sub>); 134.03 (Ph-PPh<sub>2</sub>); 136.43 (Ph); 160.83 (C=N). <sup>31</sup>P NMR (CDCl<sub>3</sub>): δ<sub>p</sub>(ppm): -13.71. MS (ESI) m/z (%) 388 (M<sup>+</sup>, 100). HRMS-ESI ([M<sup>+</sup>+H<sup>+</sup>]): 388.9251; found: 389.0312. FT-IR (cm<sup>-1</sup>): ν<sub>(C=N)imine</sub> =1632.

#### 5.2.2.5. [2-(2-(diphenylphosphino)benzylidene)methoxyethanamine) PdCl<sub>2</sub>] (**18**)

To a solution of **L9** (0.05 g, 0.15 mmol) in CH<sub>2</sub>Cl<sub>2</sub> (7 mL) was added drop-wise a solution of Pd(COD)Cl<sub>2</sub> (0.05 g, 0.15 mmol) in CH<sub>2</sub>Cl<sub>2</sub> (15 mL). A yellow precipitate formed immediately. The reaction mixture was allowed to stir at ambient temperature for 36 h and the yellow product filtered. The product was then washed three times with 15 mL CH<sub>2</sub>Cl<sub>2</sub> and dried in vacuum to give complex **18** as a yellow powder. Yield = 0.07 g (85%). <sup>1</sup>H NMR (400 MHz, DMSO-d<sub>6</sub>): δ<sub>H</sub> (ppm): 2.77 (s, 3H, OCH<sub>3</sub>); 3.55 (t, 2H, CH<sub>2</sub>-N); 4.47 (t, 2H, CH<sub>2</sub>-O); 7.02 (t, 1H, H-Ph); 7.42 (m, 4H, H-PPh<sub>2</sub>); 7.60 (m, 6H, H-PPh<sub>2</sub>); 7.68 (dd, 2H, H-Ph), 7.80 (d, 1H, H-Ph); 8.55 (s, 1H, H-C=N). <sup>13</sup>C NMR (DMSO-d<sub>6</sub>): δ<sub>C</sub>(ppm): 59.01 (OCH<sub>3</sub>); 68.32 (CH<sub>2</sub>-N); 73.01 (CH<sub>2</sub>-O); 128.85; 128.89; 128.93; 129.01; 131.14; 137.35; 137.42; 137.58; 138.88; 137.97; 142.51; 163.75 (C=N). <sup>31</sup>P NMR (DMSO-d<sub>6</sub>): δ<sub>P</sub>(ppm): 31.63. MS (ESI) m/z (%) 490 (M<sup>+</sup> - Cl, 100). FT-IR (cm<sup>-1</sup>): ν(C=N)<sub>imine</sub> = 1641. Anal. Calc. for C<sub>22</sub>H<sub>22</sub>Cl<sub>2</sub>NOPPd: C, 50.36; H, 4.23; N, 2.67. Found: C, 50.01; H, 4.11; N, 2.24.

Compounds **19–21** were prepared following the same procedure described for compound **18**.

#### 5.2.2.6. [2-(2-(diphenylphosphino)benzylideneamino)ethanol PdCl<sub>2</sub>] (**19**)

Pd(COD)Cl<sub>2</sub> (0.05 g, 0.16 mmol) and **L10** (0.05, 0.16 mmol) in CH<sub>2</sub>Cl<sub>2</sub> (20 mL). Yield = 0.06g (74%). <sup>1</sup>H NMR (400 MHz, DMSO-d<sub>6</sub>): δ<sub>H</sub> (ppm): 3.93 (dd, 4H, CH<sub>2</sub>); 7.01 (t, 1H, H-Ph); 7.54 (m, 4H, H-PPh<sub>2</sub>); 7.61 (m, 6H, H-PPh<sub>2</sub>); 7.39 (dd, 2H, H-Ph), 7.76 (d, 1H, H-Ph), 8.63 (s, 1H, H-C=N). <sup>13</sup>C NMR (DMSO-d<sub>6</sub>): δ<sub>C</sub>(ppm): 57.96 (CH<sub>2</sub>-N); 61.28 (CH<sub>2</sub>-O); 128.81; 128.87; 128.91; 129.05; 129.22; 131.14; 137.35; 137.48; 137.49; 137.52; 137.96; 142.56; 163.71 (C=N). <sup>31</sup>P NMR (DMSO-d<sub>6</sub>): δ<sub>P</sub>(ppm): 31.53. MS (ESI) m/z (%) 475 (M<sup>+</sup>



- Cl, 100). FT-IR ( $\text{cm}^{-1}$ ):  $\nu_{(\text{C}=\text{N})\text{imine}} = 1640$ ;  $\nu_{(\text{OH})} = 3396$ . Anal. Calc. for  $\text{C}_{21}\text{H}_{20}\text{Cl}_2\text{NOPPd}$ : C, 49.39; H, 3.95; N, 2.74. Found: C, 49.26; H, 3.83; N, 2.00.

#### 5.2.2.7. [(2-(diphenylphosphino)benzylidene)ethane-1,2-diamine $\text{PdCl}_2$ ] (**20**)

$\text{Pd}(\text{COD})\text{Cl}_2$  (0.05 g, 0.16 mmol) and **L11** (0.04, 0.16 mmol) in  $\text{CH}_2\text{Cl}_2$  (20 mL). Yield = 0.07g (93%).  $^1\text{H}$  NMR (400 MHz,  $\text{DMSO-d}_6$ ):  $\delta_{\text{H}}$  (ppm): 3.57 (t, 2H,  $\text{CH}_2\text{-N}$ ); 4.49 (t, 2H,  $\text{CH}_2\text{-NH}_2$ ); 7.03 (t, 1H, H-Ph); 7.45 (m, 4H, H- $\text{PPh}_2$ ); 7.63 (m, 6H, H- $\text{PPh}_2$ ); 7.71 (dd, 2H, H-Ph); 8.02 (d, 1H, H-Ph); 8.78 (s, 1H, H- $\text{C}=\text{N}$ ).  $^{13}\text{C}$  NMR ( $\text{DMSO-d}_6$ ):  $\delta_{\text{C}}$ (ppm): 43.24 ( $\text{CH}_2\text{-N}$ ); 44.78 ( $\text{CH}_2\text{-NH}_2$ ); 128.74; 128.81; 128.89; 129.00; 129.21; 131.14; 137.28; 137.46; 137.48; 137.51; 137.93; 142.49; 163.70 ( $\text{C}=\text{N}$ ).  $^{31}\text{P}$  NMR ( $\text{DMSO-d}_6$ ):  $\delta_{\text{P}}$ (ppm): 31.70. MS (ESI)  $m/z$  (%) 474 ( $\text{M}^+ - \text{Cl}$ , 82). FT-IR ( $\text{cm}^{-1}$ ):  $\nu_{(\text{C}=\text{N})\text{imine}} = 1643$ . Anal. Calc. for  $\text{C}_{21}\text{H}_{21}\text{Cl}_2\text{N}_2\text{PPd}$ : C, 49.48; H, 4.15; N, 5.50. Found: C, 49.36; H, 4.01; N, 4.98.

#### 5.2.2.8. [(2-(diphenylphosphino)benzylidene)diethylethane-1,2-diamine $\text{PdCl}_2$ ] (**21**)

$\text{Pd}(\text{COD})\text{Cl}_2$  (0.04 g, 0.14 mmol) and **L12** (0.05, 0.14 mmol) in  $\text{CH}_2\text{Cl}_2$  (20 mL). Yield = 0.06g (81%).  $^1\text{H}$  NMR (400 MHz,  $\text{DMSO-d}_6$ ):  $\delta_{\text{H}}$  (ppm): 1.38 (m, 6H,  $\text{CH}_3\text{-NEt}_2$ ); 3.03 (m, 4H,  $\text{CH}_3\text{-NEt}_2$ ), 4.29 (dd, 4H,  $\text{CH}_2\text{-CH}_2$ ); 7.38 (t, 1H, H-Ph); 7.56 (m, 4H, H- $\text{PPh}_2$ ); 7.59 (m, 6H, H- $\text{PPh}_2$ ); 7.69 (dd, 2H, H-Ph); 7.97 (d, 1H, H-Ph); 8.14 (s, 1H, H- $\text{C}=\text{N}$ ).  $^{13}\text{C}$  NMR ( $\text{DMSO-d}_6$ ):  $\delta_{\text{C}}$ (ppm): 13.42 ( $\text{CH}_3\text{-NEt}_2$ ); 13.49 ( $\text{CH}_3\text{-NEt}_2$ ); 49.27 ( $\text{CH}_2\text{-NEt}_2$ ); 49.31 ( $\text{CH}_2\text{-NEt}_2$ ); 58.91 ( $\text{CH}_2\text{-N}$ ); 60.50 ( $\text{CH}_2\text{-NEt}_2$ ); 128.77; 128.81; 128.92; 128.99; 129.08; 129.18; 131.14; 137.33; 137.36; 137.39; 137.41; 137.44; 137.56; 137.61; 142.52; 163.72 ( $\text{C}=\text{N}$ ).  $^{31}\text{P}$  NMR ( $\text{DMSO-d}_6$ ):  $\delta_{\text{P}}$ (ppm): 31.54. MS (ESI)  $m/z$  (%) 530 ( $\text{M}^+ - \text{Cl}$ , 100). FT-IR ( $\text{cm}^{-1}$ ):  $\nu_{(\text{C}=\text{N})\text{imine}} = 1642$ . Anal. Calc. for  $\text{C}_{25}\text{H}_{29}\text{Cl}_2\text{N}_2\text{PPd}$ : C, 53.07; H, 5.17; N, 4.95. Found: C, 53.16; H, 5.04; N, 4.45.

5.2.2.9.  $[\{2-(2-(\text{diphenylphosphino})\text{benzylidene})\text{methoxyethanamine}\}\text{Pd}(\text{OTs})(\text{PPh}_3)]^+\text{TsO}^-$  (**22**)

To a solution of **L9** (0.05 g, 0.15 mmol) in chloroform (5 mL), was added drop-wise a solution of  $\text{Pd}(\text{AOc})_2$  (0.03 g, 0.15 mmol) in chloroform (10 mL) followed by a solution of  $\text{PPh}_3$  (0.08 g, 0.3 mmol) and *p*-TsOH (0.05 g, 0.3 mmol) in chloroform (10 mL) and stirred at room temperature for 24 h. The organic volatiles were removed *in vacuo*, and recrystallization from  $\text{CH}_2\text{Cl}_2$ -hexane and gave complex **5** as a light-yellow solid. Yield = 0.09 g (67%).  $^1\text{H}$  NMR (400 MHz,  $\text{CDCl}_3$ ):  $\delta_{\text{H}}$  (ppm): 2.52 (s, 6H,  $\text{CH}_3\text{-OTs}$ ); 3.36 (s, 3H,  $\text{OCH}_3$ ); 3.81 (dd, 4H,  $\text{CH}_2\text{-CH}_2$ ); 7.04 (t, 1H, H-Ph); 7.40 (m, 4H, H- $\text{PPh}_2$ ); 7.46 (m, 6H, H- $\text{PPh}_2$ ); 7.48 (m, 6H, H- $\text{PPh}_2$ ); 7.51 (m, 4H, Ph-OTs); 7.55 (m, 9H,  $\text{PPh}_3$ ); 7.59 (m, 6H,  $\text{PPh}_3$ ); 7.69 (m, 4H, Ph-OTs); 8.02 (d, 1H, H-Ph); 9.28 (s, 1H, H-C=N).  $^{13}\text{C}$  NMR ( $\text{CDCl}_3$ ):  $\delta_{\text{C}}$ (ppm): 21.35 ( $\text{CH}_3\text{-OTs}$ ); 46.10 ( $\text{CH}_2\text{-N}$ ); 59.01 ( $\text{OCH}_3$ ); 74.62 ( $\text{CH}_2\text{-O}$ ); 126.72; 126.77; 128.71; 128.75; 128.78; 128.81; 128.83; 128.88; 128.96; 128.99; 129.21; 130.31; 130.46; 131.00; 136.25; 136.31; 136.33; 136.37'; 136.39; 136.41; 136.42; 136.48; 137.42; 137.93; 138.22; 142.53; 146.81; 163.71 (C=N).  $^{31}\text{P}$  NMR ( $\text{CDCl}_3$ ):  $\delta_{\text{P}}$ (ppm): 25.61 ( $\text{PPh}_3$ ); 29.14 ( $\text{PPh}_3$ ); 31.56 ( $\text{PPh}_2$ ). MS (ESI)  $m/z$  (%) 887 ( $\text{M}^+$ , 81%). FT-IR ( $\text{cm}^{-1}$ ):  $\nu_{(\text{C}=\text{N})\text{imine}} = 1644$ . Anal. Calc. for  $\text{C}_{54}\text{H}_{51}\text{NO}_7\text{P}_2\text{PdS}_2$ .Hexane: C, 62.96; H, 5.01; N, 1.22. Found: C, 63.71; H, 4.15; N, 1.09.

5.2.2.10.  $[\{2-(2-(\text{diphenylphosphino})\text{benzylidene})\text{methoxyethanamine}\}\text{PdCl}(\text{PPh}_3)]\text{BAr}_4$  (**23**)

To a suspension of **18** (0.03 g, 0.06 mmol), in  $\text{CH}_2\text{Cl}_2$  (10 mL),  $\text{PPh}_3$  (0.02 g, 0.06 mmol) and  $\text{NaBAr}_4$  ( $\text{Ar}_4 = 3,5\text{-(CF}_3)_2\text{C}_6\text{H}_3$ ) (0.02 g, 0.06 mmol) were added and stirred for 24 h. The solution mixture was filtered and the filtrate concentrated to approximately 3 mL and recrystallized from hexane/ $\text{CH}_2\text{Cl}_2$  solvent mixture to obtain compound **6** as a yellow crystalline solid. Yield = 0.05 g (97%).  $^1\text{H}$  NMR (400 MHz,  $\text{CDCl}_3$ ):  $\delta_{\text{H}}$  (ppm):

$^{13}\text{C}$  NMR ( $\text{CDCl}_3$ ):  $\delta_{\text{C}}$ (ppm): 2.76 (s, 3H,  $\text{OCH}_3$ ); 3.52 (t, 2H,  $\text{CH}_2\text{-N}$ ); 4.43 (t, 2H,  $\text{CH}_2\text{-O}$ ); 7.00 (t, 1H, H-Ph); 7.21 (m, 6H, H- $\text{PPh}_3$ ); 7.35 (m, 8H, H- $\text{BAr}_4$ ); 7.40 (m, 4H, H- $\text{PPh}_2$ ); 7.51 (m, 9H, H- $\text{PPh}_3$ ); 7.62 (m, 6H, H- $\text{PPh}_2$ ); 7.69 (dd, 2H, H-Ph), 7.71 (m, 4H, H- $\text{BAr}_4$ ); 7.83 (d, 1H, H-Ph); 8.54 (s, 1H, H-C=N).  $^{13}\text{C}$  NMR (DMSO):  $\delta_{\text{C}}$ (ppm): 59.01 ( $\text{OCH}_3$ ); 68.32 ( $\text{CH}_2\text{-N}$ ); 73.01 ( $\text{CH}_2\text{-O}$ ); 128.85; 128.89; 128.93; 129.01; 131.14; 137.35; 137.42; 137.58; 138.88; 137.97; 142.51; 163.75 (C=N).  $^{31}\text{P}$  NMR ( $\text{CDCl}_3$ ):  $\delta_{\text{P}}$ (ppm): 25.69 ( $\text{PPh}_3$ ); 29.01 ( $\text{PPh}_3$ ); 31.60 ( $\text{PPh}_2$ ). FT-IR ( $\text{cm}^{-1}$ ):  $\nu_{(\text{C}=\text{N})\text{imine}} = 1645$ . Anal. Calc. for  $\text{C}_{73}\text{H}_{52}\text{BCl}_2\text{F}_{24}\text{NOP}_2\text{Pd}$ : C, 53.80; H, 3.22; N, 0.86. Found: C, 53.92; H, 3.31; N, 1.01.

### 5.2.3. General procedure for the hydrogenation reactions of alkenes and alkynes

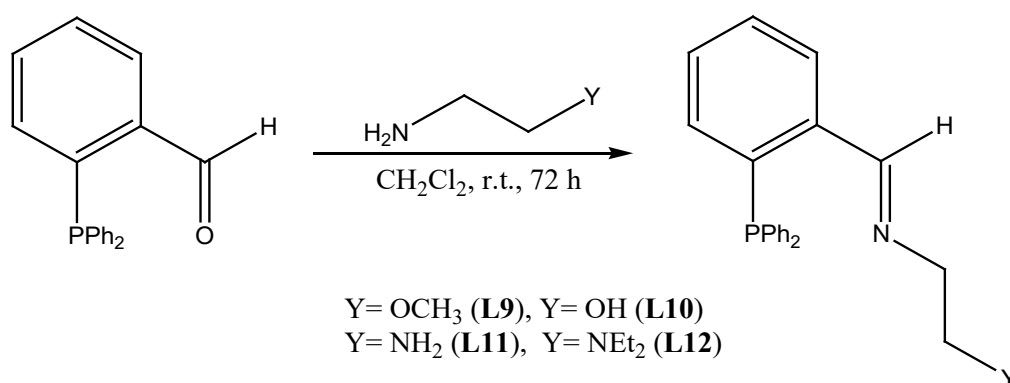
The catalytic hydrogenation reactions were performed in a stainless-steel autoclave equipped with temperature control unit and a sample valve. In a typical experiment, styrene (0.50 mL, 4.44 mmol) and complex **18** (0.46 mg,  $8.7 \times 10^{-4}$  mmol, S/C 600) were dissolved in toluene (50 mL). The reactor was evacuated, flushed with nitrogen and the catalytic solution was introduced to the reactor via a cannula. The reactor was purged three times with hydrogen, and then set at the required pressure, heated to the desired temperature and the reaction mixture stirred at 500 rpm. At the end of the reaction time, the reactor was cooled, excess hydrogen vented off. Samples for GC analyses were drawn via a syringe, filtered using 0.45  $\mu\text{m}$  micro filters and analysed by Varian CP-3800 GC (ZB-5HT column 30 m  $\times$  0.25 mm  $\times$  0.10  $\mu\text{m}$ ) GC instrument to determine the percentage conversion of styrene to ethylbenzene. The percentage conversions were determined by comparing the peak areas of the alkene/alkyne substrate and respective products, assuming 100% mass balance. For example,

comparison of peak areas of styrene and ethylbenzene at regular time intervals allowed the determination of the rate of conversion of styrene to ethylbenzene.

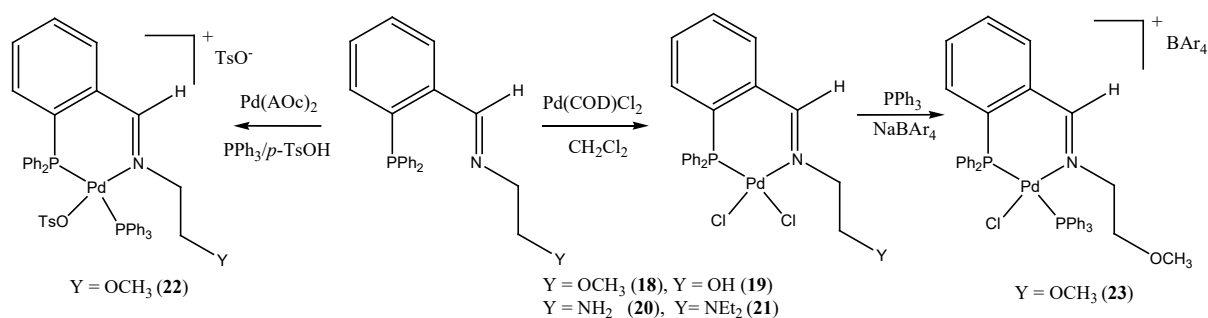
### 5.3. Results and discussion

#### 5.3.1. Synthesis and characterization of ligands L9-L12 and their palladium complexes 18-23

The Schiff-base condensation reactions between 2-(diphenylphosphino)benzaldehyde and the corresponding amines in  $\text{CH}_2\text{Cl}_2$  at ambient temperature resulted in the formation of compounds **L9-L12** in good yields (78-92%, Scheme 5.1).<sup>12,13</sup> The corresponding palladium(II) complexes **18-21** were prepared from the reactions of **L9-L12** with  $\text{Pd}(\text{COD})\text{Cl}_2$  in  $\text{CH}_2\text{Cl}_2$  (Scheme 5.2), and were isolated as yellow powders in good yields (74 - 93%). On the other hand, reactions of **L9** with  $\text{Pd}(\text{AOC})_2$  in the presence of equivalent amounts of *p*-TsOH and  $\text{PPh}_3$  afforded complex **22** (Scheme 6.2), while subsequent treatment of complex **18** with one equivalent of  $\text{NaBAr}_4$  ( $\text{Ar}_4 = 3,5\text{-(CF}_3)_2\text{C}_6\text{H}_3$ ) in the presence of  $\text{PPh}_3$  afforded the cationic complex **23** in high yields (Scheme 5.2).



**Scheme 5.1:** Synthesis of imino-diphenylphosphino ligands **L9-L12**



**Scheme 5.2:** Synthesis of neutral and cationic imino-diphenylphosphino palladium(II) complexes **18-23**

The ligands and complexes were characterized by NMR spectroscopy, mass spectrometry, FT-IR spectroscopy and elemental analysis. In the <sup>1</sup>H NMR spectra of the ligands, the Schiff-base condensation of the aldehydes and the amines was confirmed from the disappearance of the aldehyde signal at 10.54 ppm and appearance of a doublet in the region 8.82 - 9.06 ppm. The appearance of the doublet is believed to be due to the amine proton coupling to phosphine ligands.<sup>14</sup> The coordination of the ligands to the palladium centre was confirmed from their respective <sup>1</sup>H NMR spectra of the complexes. For example, <sup>1</sup>H NMR spectra of complex **18** showed an up-field shift in the ethylene linker protons from 3.55 ppm and 4.47 ppm to 3.51 ppm and 3.69 ppm for **L9** respectively (Fig. 5.1).

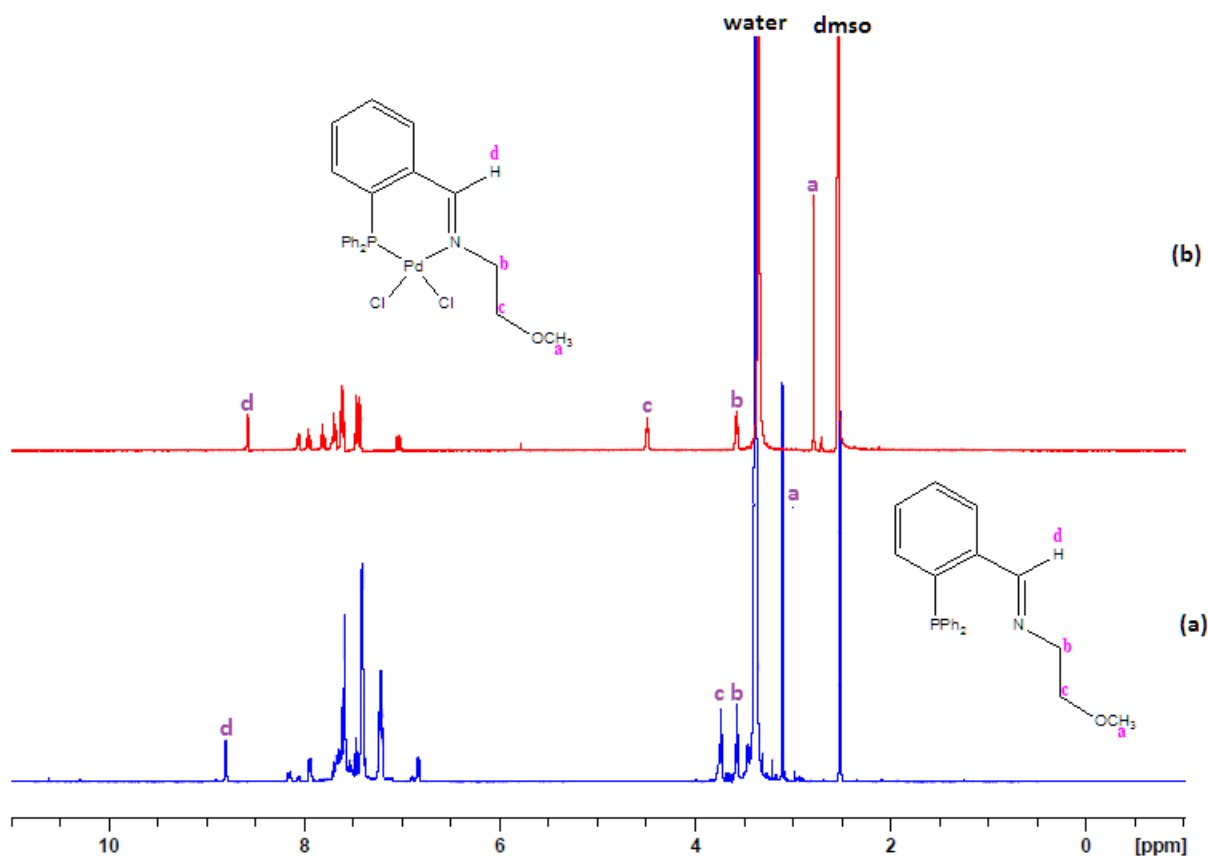


**Figure 5.1:**  $^1\text{H}$  NMR spectra of **L9** in  $\text{DMSO-d}_6$  (a) and complex **18** (b) showing a shift of the ethylene protons from 3.61 to 4.47 ppm.

In the  $^{31}\text{P}$  NMR spectra of the ligands, up-field singlets in the region -13.56 to -13.71 ppm were observed, characteristic of the  $\text{PPh}_2$  group.<sup>15,16</sup> The coordination of the  $\text{PPh}_2$  moiety in ligands **L9-L12** to the palladium atom in complexes **18-23** was confirmed from the  $^{31}\text{P}$  NMR spectra by the downfield shift of the signals from -13.56 to -13.71 ppm in the ligands to about 31.53 – 31.70 in complexes **18-23**. For instance, the  $\text{PPh}_2$  signals were observed at -13.56 ppm and 31.53 ppm in **L11** and its corresponding complex **20** respectively (Fig. 5.2). These values are in good agreement with those reported for  $\text{PPh}_2$  coordinated palladium centres.<sup>17,18</sup>

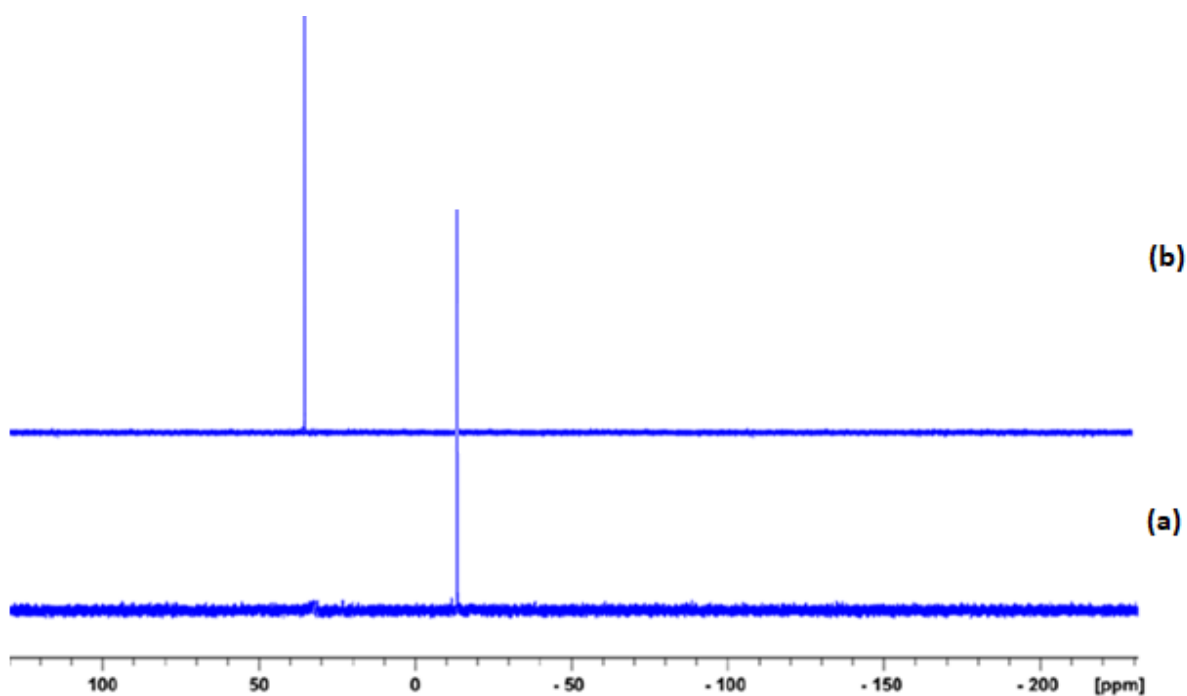


**Figure: 5.2:**  $^{31}\text{P}$  NMR (DMSO- $d_6$ ) spectra of ligand **L11** (a) and its corresponding complex **20** (b) showing shift from -13.56 ppm in **L11** to 31.70 ppm in complex **20** thus establishing coordination of the  $\text{PPh}_2$  to the palladium centre.

$^{31}\text{P}$  NMR spectroscopy was also useful in determination of the presence and nature of coordination of the auxiliary  $\text{PPh}_3$  ligands in cationic complexes **22** and **23**. For example, the  $^{31}\text{P}$  NMR spectra of complex **23** (Fig 5.3) displayed three peaks at 25.69 ppm, 29.01 ppm and 31.60 ppm assignable to  $\text{PPh}_2$  (31.60 ppm) and  $\text{PPh}_3$  (25.69 ppm and 29.01 ppm), respectively. The two peaks for the coordinated  $\text{PPh}_3$  groups may arise from possible existence of *cis* and *trans* isomers in good agreement with those observed in related palladium(II) complexes.<sup>19,20</sup>

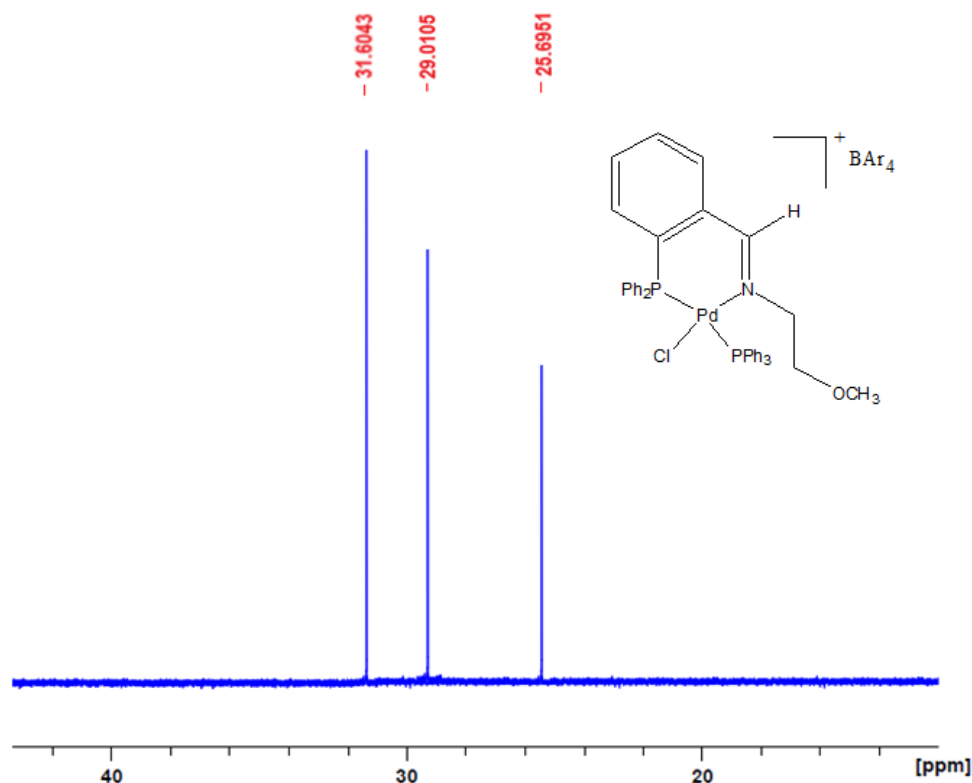


**Figure 5.3:**  $^{31}\text{P}$  NMR ( $\text{CDCl}_3$ ) spectrum of complex **23**.

The successful formation of the imine functionality in **L9-L12** and their corresponding palladium complexes was also established from their FT-IR spectra. In general strong absorption bands in the region  $1628\text{-}1636\text{ cm}^{-1}$  were observed in the IR spectra of all the ligands **L9-L12** assignable to the  $\text{C}=\text{N}$  functionality.<sup>14,21,22</sup> Bathochromic shifts of about  $6\text{-}18\text{ cm}^{-1}$  with respect to the free ligands were observed in the IR spectra of the corresponding complexes **18-27** ( $\nu_{\text{C}=\text{N}} = 1638\text{ - }1651\text{ cm}^{-1}$ ) and alluded to coordination of the imine nitrogen to the palladium metal centre.<sup>15,16</sup> For example, **L10** showed an absorption band at  $1634\text{ cm}^{-1}$  in comparison to complex **19** which exhibited a signal at  $1640\text{ cm}^{-1}$  for the imine group (Fig. 5.4).



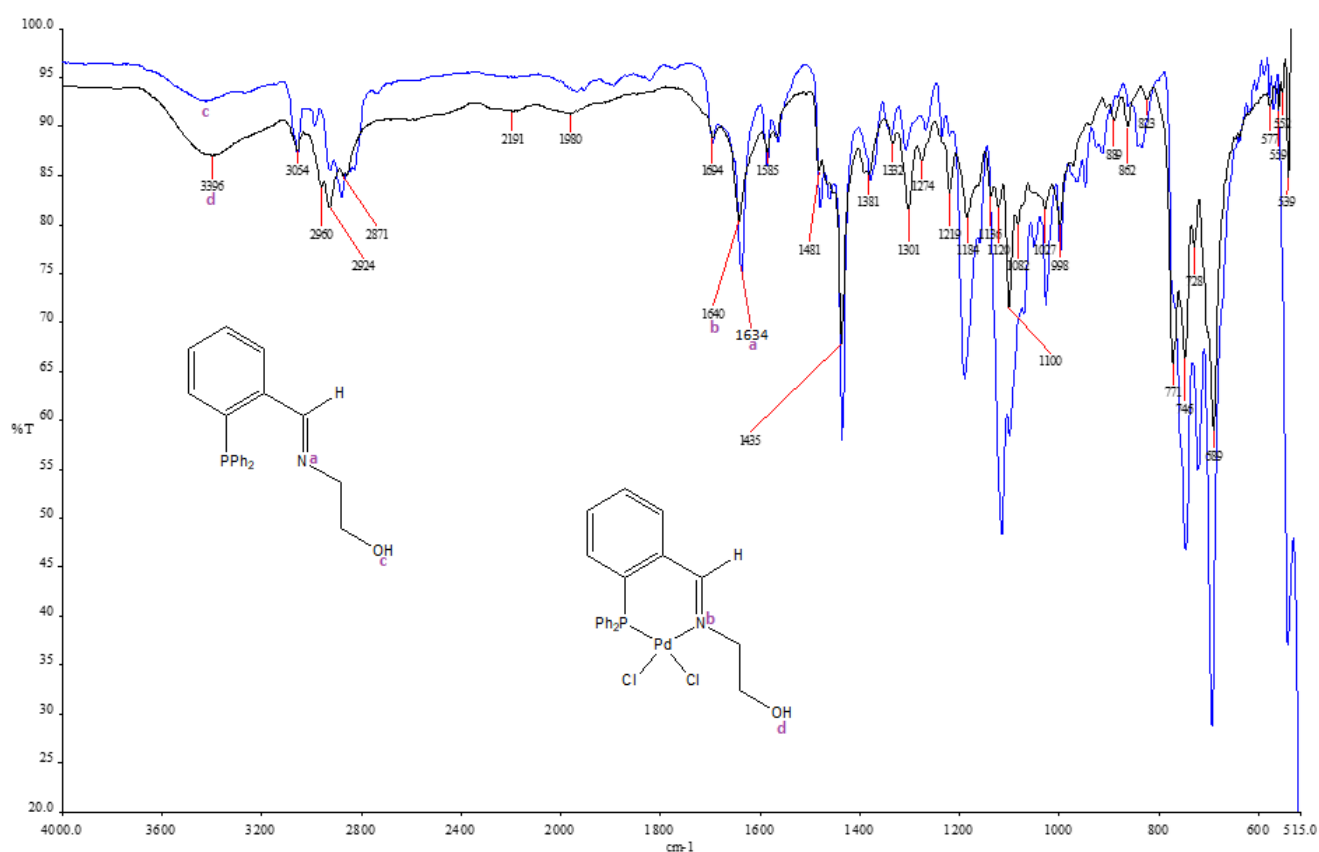


**Figure 5.4:** FT-IR spectrum of ligand **L10** and complex **19** showing a bathochromic shift in **L10** in comparison to complex **19**.

Mass spectrometry also proved useful in establishing the formation and identity of the complexes. In general, mass spectra of all the complexes exhibited loss of a Cl<sup>-</sup> group to give the [Pd(L)Cl]<sup>+</sup> fragments as the base peak. For example, **18** was found to lose a Cl<sup>-</sup> group to form a species with  $m/z = 490$ , corresponding to [Pd(L9)Cl]<sup>+</sup>. Figure 5.5 shows the stimulated and found isotopic distributions for [Pd(L9)Cl]<sup>+</sup>. Elemental analysis data of all the complexes were in agreement with the proposed mononuclear palladium complexes and also established the purity of the bulk materials.

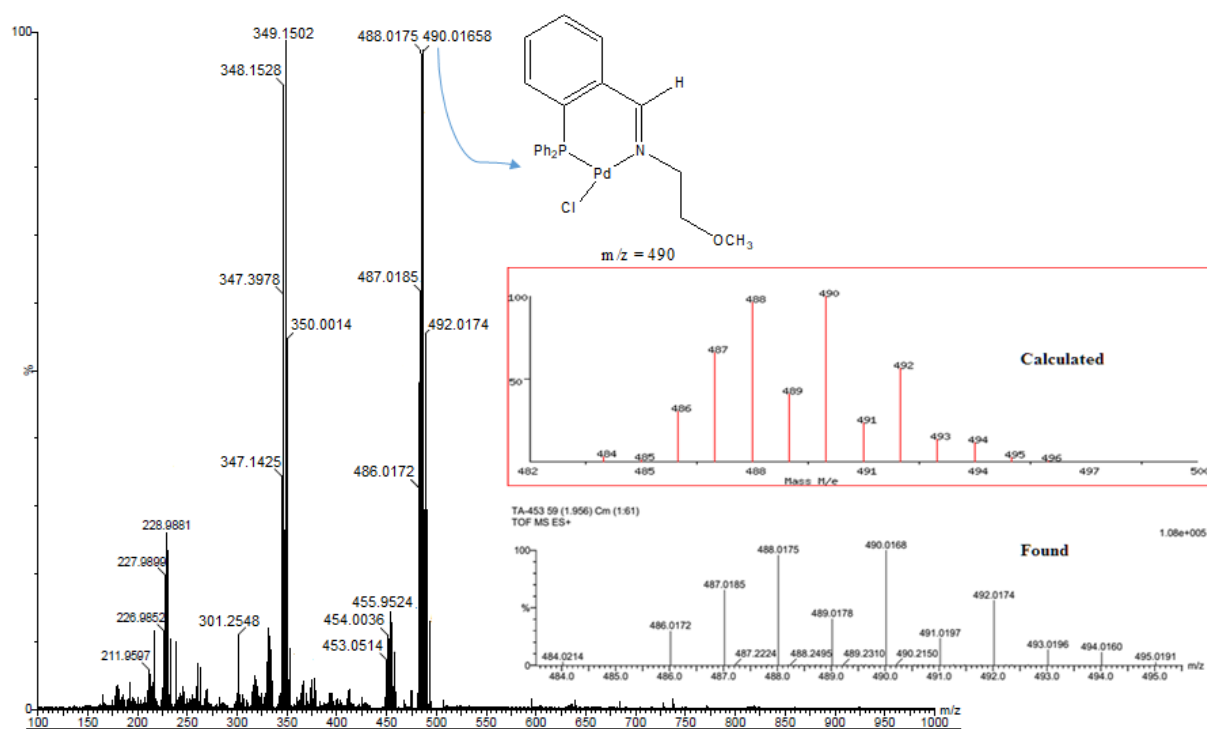


**Figure 5.5:** ESI-MS showing  $m/z$  signal at 490.0 (100%) corresponding to  $[\text{Pd}(\text{L}9)\text{Cl}]^+$  fragment of **18** (insert showing mass spectrum of the calculated and found isotopic distribution).

### 5.3.2. Hydrogenation reactions using complexes 18-23

Preliminary tests in which complexes **18-23** were used in the hydrogenation reactions were carried out using styrene as a model substrate in order to determine the optimal experimental conditions. The reactions were performed at 5 bar, 25 °C, 50 min and [styrene]:[Pd] ratio 5000:1. Complexes **18-23** formed efficient pre-catalysts for the styrene hydrogenation to give ethylbenzene in conversion of 57% – 99% (Table 5.1.). A control experiment performed without the use of palladium complex resulted in no conversion of styrene to ethylbenzene. In the next sections, detailed kinetics,

selectivity, stability studies to establish the structure-activity relationship are presented

**Table 5.1:** Effect of catalyst structure on the hydrogenation of styrene by complexes **18-23**.<sup>a</sup>

Entry	Catalyst	Conv. <sup>b</sup>	$k_{obs}$ (h <sup>-1</sup> )	TOF <sup>c</sup> (h <sup>-1</sup> )
1	<b>18</b>	96	4.75 (±0.05)	5783
2	<b>19</b>	93	3.87 (±0.08)	5602
3	<b>20</b>	81	2.37 (±0.03)	4880
4	<b>21</b>	73	1.89 (±0.12)	4398
5	<b>22</b>	57	1.35 (±0.14)	3434
6	<b>23</b>	99	6.09 (±0.07)	5964

<sup>a</sup>Conditions: styrene, substrate/catalyst = 5000; substrate, 4.36 mmol; catalyst; 8.0x10<sup>4</sup> mmol; solvent, toluene; pressure, 5 bar; temperature, 25 °C; time, 50 min. <sup>b</sup>percentage of styrene converted to ethylbenzene; Determined by GC. <sup>c</sup>TOF in mol<sub>substrate</sub>mol<sub>catalyst</sub><sup>-1</sup> h<sup>-1</sup> (h<sup>-1</sup>).

#### 5.3.2.1. Effect of complex structure on the hydrogenation reactions of styrene

Kinetics and the influence of the complex structure on the molecular hydrogenation of styrene were investigated for complexes **18-23** by monitoring the reactions GC chromatography. A plot of  $\ln[\text{Sty}]_0/[\text{Sty}]_t$  vs time gave a linear relationship consistent with *pseudo*-first order kinetics with respect to styrene for all the complexes (Fig. 5.6). Therefore, the kinetics of styrene hydrogenation reactions proceed according to the simple *pseudo*-first order kinetics with respect to styrene as shown in equation 5.1.

$$\text{Rate} = k[\text{styrene}]^1 \quad (5.1)$$

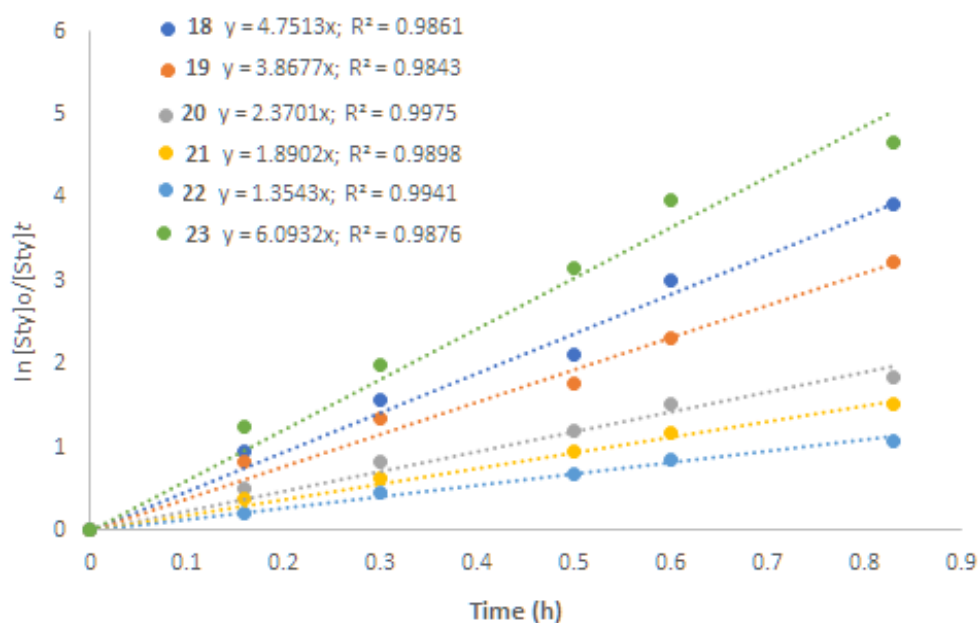


**Figure 5.6:** Plot of  $\ln[\text{Sty}]_0/[\text{Sty}]_t$  vs time for styrene hydrogenation using complexes **18-23**.

The cationic complex **23** was the most active in comparison to its analogous neutral complex **18** (Table 5.1, entries 1 and 6). The observed higher catalytic activity may be due to higher solubility of complex **23**<sup>23</sup> and/or higher positive charge on the palladium(II) metal atom compared to the neutral complexes **18-21**.<sup>24</sup> Similar results were also observed by Schrock and Osborn in the hydrogenation of 1-hexene.<sup>25,26</sup> Interestingly, the cationic complex **22**, bearing the tolyl group, was the least active. This behaviour may be due to the poor lability of the *p*-TsOH groups and the bulkiness of tolyl group hinders substrate coordination.<sup>27</sup> In addition, the presence of Cl in **18-21, 23** allows the formation of Pd-hydride which is believed to be the active species.<sup>28</sup>

Furthermore, the catalytic activity trends obtained (Table 5.1, Fig. 5.6) with regards to the nature of the pendant arm were similar to those reported in Chapter 4, hence does not require further elaborations. As an illustration, replacement of the OCH<sub>3</sub> pendant group in complex **18** with an ammine group in **20**, resulted in a drastic drop in  $k_{obs}$  from 4.75 h<sup>-1</sup> (TOF = 5783 h<sup>-1</sup>) to 2.37 h<sup>-1</sup> (TOF = 4880 h<sup>-1</sup>). This has been attributed to stronger coordination of the nitrogen atom to the palladium(II) metal resulting in competition with the styrene substrate for the active site.<sup>29</sup>

### 5.3.2.2. *The dependency of the reaction rate on catalyst concentration*

The dependency of the rate of styrene hydrogenation on catalyst concentration was studied by the varying the concentration of complex **8** from 4000 - 8000 substrate/catalyst ratios at constant pressure and temperature. A plot of  $\ln[\text{Sty}]_0/[\text{Sty}]_t$  as a function of time (Fig. 5.7), showed a linear dependency of the reaction rate with respect to [**18**]. For example, an increase in substrate/catalyst ratio from 5000 - 7000 was marked by a simultaneous increase in TOF from 5783 h<sup>-1</sup> to 6578 h<sup>-1</sup> (Table 6.2, entries 2-5). However, a further increase of the substrate/catalyst ratio to 8000 led to a decrease in TOF to 5590 h<sup>-1</sup> (Table 6.2, entry 6). On the other hand, increase in substrate/catalyst ratio had an opposite effect on the  $k_{obs}$ . For instance, an increase in substrate/catalyst ratio from 4000 - 8000 resulted in a decrease in  $k_{obs}$  from 5.94 h<sup>-1</sup> - 1.28 h<sup>-1</sup>. This therefore shows that an increase in catalyst loading does not increase the catalytic activity by the same magnitude and this is very beneficial in industry.

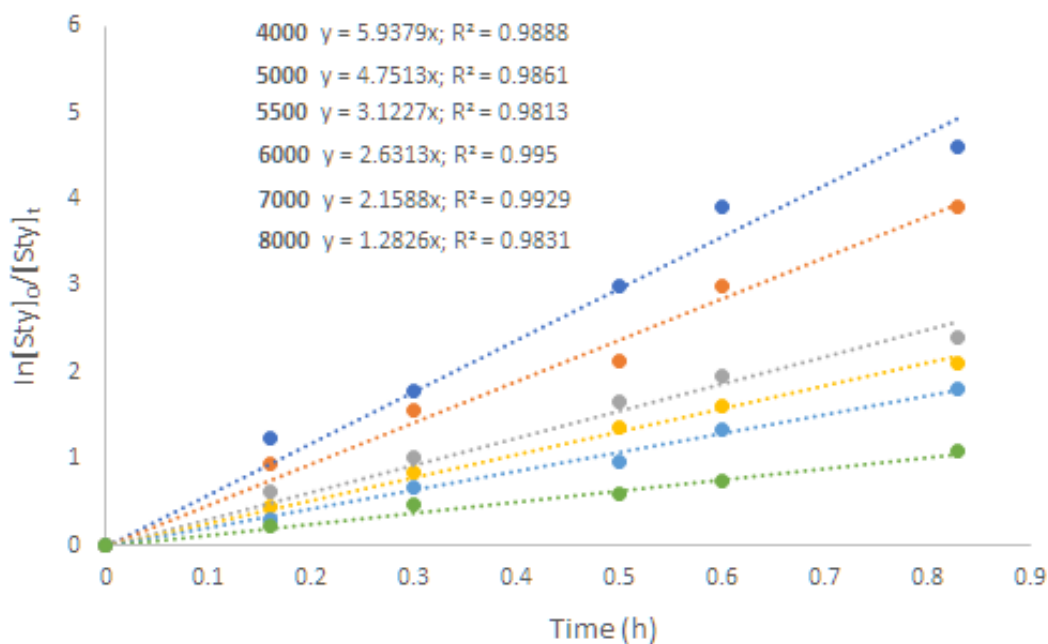


**Figure 5.7:** Plot of  $\ln[\text{Sty}]_0/[\text{Sty}]_t$  vs time for the effect of catalyst concentration using complex **18**. The  $[\text{styrene}]/[\mathbf{18}]$  was varied from 4000-8000 at fixed concentration of styrene of 0.5 mL (4.44 mmol).

From the plot of  $-\ln(k_{\text{obs}})$  vs  $-\ln[\mathbf{18}]$  (Fig. 5.8), an order of reaction of  $2.20 \pm 0.25 \text{ h}^{-1}$  (Eqs 5.2) with respect to catalyst **18** was observed, which is an indicative that the reaction is highly sensitive to change in catalyst concentration. This order is similar to the one obtained in Chapter 4 ( $2.6 \pm 0.2 \text{ h}^{-1}$ ). These fractional orders of reaction with respect to catalyst concentration are known to rise from the possible presence of difference active sites or catalyst aggregation.<sup>8,30,31</sup>

$$\text{Rate} = k[\text{styrene}]^1[\mathbf{18}]^{2.2} \quad 5.2$$

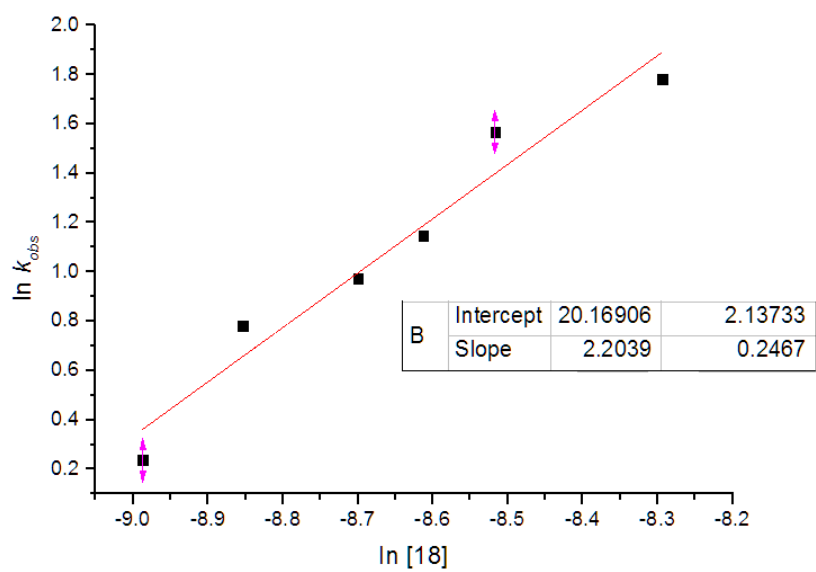


**Figure 5.8:** Plot of  $\ln(k_{\text{obs}})$  vs  $\ln[18]$  for the determination of the order of reaction with respect to catalyst **18** in the hydrogenation of styrene.

**Table 5.2:** Kinetic data for the hydrogenation of styrene catalysed by **18**<sup>a</sup>

Entry	[sub]/[cat]	$P_{\text{H}_2}$ (bar)	Conversion <sup>b</sup>	$k_{\text{obs}}$ (h <sup>-1</sup> )	TOF <sup>c</sup> (h <sup>-1</sup> )
1	4000	5	>99	5.94 ( $\pm 0.03$ )	4771
2	5000	5	96	4.75 ( $\pm 0.12$ )	5783
3	5500	5	90	3.12 ( $\pm 0.02$ )	5964
4	6000	5	86	2.63 ( $\pm 0.01$ )	6217
5	7000	5	78	2.16 ( $\pm 0.05$ )	6578
6	8000	5	58	1.28 ( $\pm 0.07$ )	5590
7	5000	2.5	91	3.05 ( $\pm 0.04$ )	5482
8	5000	7.5	>99	5.22 ( $\pm 0.04$ )	5964
9	5000	10.0	>99	6.01 ( $\pm 0.03$ )	5964
10	5000	12.5	>99	6.78 ( $\pm 0.05$ )	5964

<sup>a</sup>Conditions: styrene, 4.36 mmol; solvent, toluene; pressure, 5 bar; temperature, 25 °C; time, 50 min. <sup>b</sup>Determined by GC. <sup>c</sup>TOF in  $\text{mol}_{\text{substrate}}\text{mol}_{\text{catalyst}}^{-1} \text{h}^{-1}$ .

### 5.3.2.3. The dependency of the reaction rate on hydrogen pressure with respect to **18**

To determine the dependence of the hydrogenation rate on the hydrogen concentration, a series of experiments were carried out where hydrogen pressure was varied over the range from 2.5 bar to 12.5 bar at constant initial substrate concentration, catalyst concentration and reaction temperature. The rate of hydrogenation depended linearly on H<sub>2</sub> pressure as derived from the plot of  $\ln[\text{Sty}]_0/[\text{Sty}]_t$  vs time (Fig. 5.9).



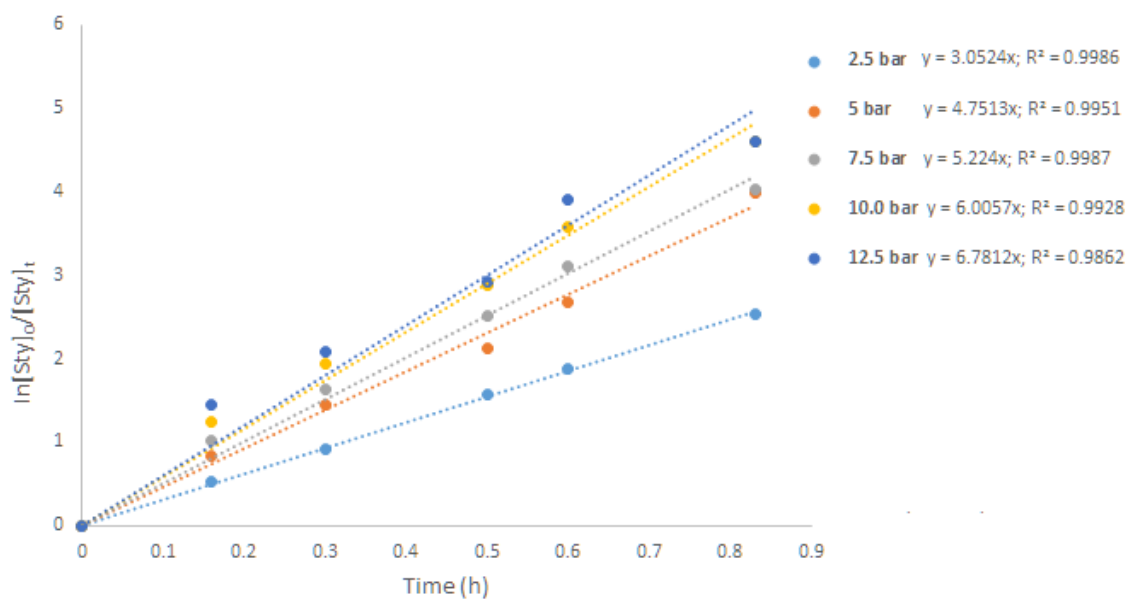


**Figure 5.9:** Plot of  $\ln[\text{Sty}]_0/[\text{Sty}]_t$  vs time for the effect of hydrogen pressure using **18**.

A plot of  $k_{\text{obs}}$  vs  $\text{H}_2$  (Fig. 5.10) shows that the rate of hydrogenation reaction is linearly depended on the  $\text{H}_2$  pressure, yielding the order of reaction with respect to  $[\text{H}_2]$  as  $0.35 \pm 0.04$ . This partial and low order of reaction is indicative of the possible formation of the palladium-monohydride species as a result of disfavoured activation of the  $\text{H}_2$  molecule.<sup>32</sup> From this data the rate law can be represented by equation 5.3, which indicates that the hydride species formation is the rate-determining step.<sup>33</sup>

$$\text{Rate} = k[\text{styrene}]^1[\mathbf{18}]^{2.2}[\text{P}_{\text{H}_2}]^{0.35} \quad 5.3$$

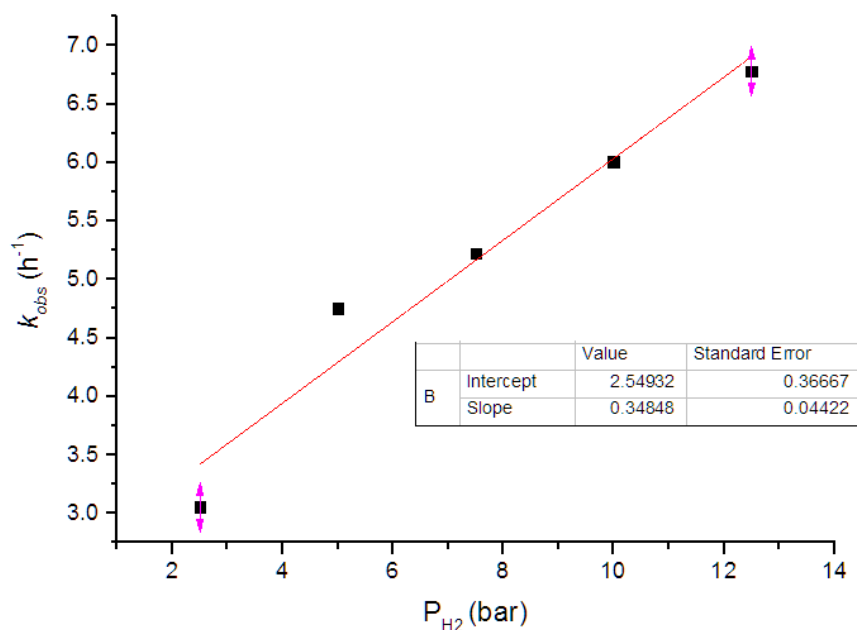


**Figure 5.10:** Plot of  $k_{obs}$  vs  $P_{H_2}$  (bar) for the determination of the order of reaction with respect to  $H_2$  pressure in the hydrogenation of styrene using catalyst **18**.

#### 5.3.2.4. *The dependency of the reaction rate on temperature and nature of solvents using complex 18*

A series of experiments were carried out over the temperature range of 0 – 50 °C, at constant catalyst concentration, substrate concentration, and dihydrogen pressure (Table 5.3). From the plot of  $\ln[Sty]_0/[Sty]_t$  vs time (Fig. 5.11) the observed rate constants were obtained. As expected there was an increase in the rate constants from 0.87  $h^{-1}$  to 5.95  $h^{-1}$  with an increase in reaction temperature from 0 – 50 °C.<sup>34,35</sup> It is also very significant to note that, we did not observe the formation of palladium(0) black deposits even at higher temperatures, showing the thermal stability of catalyst **18**.

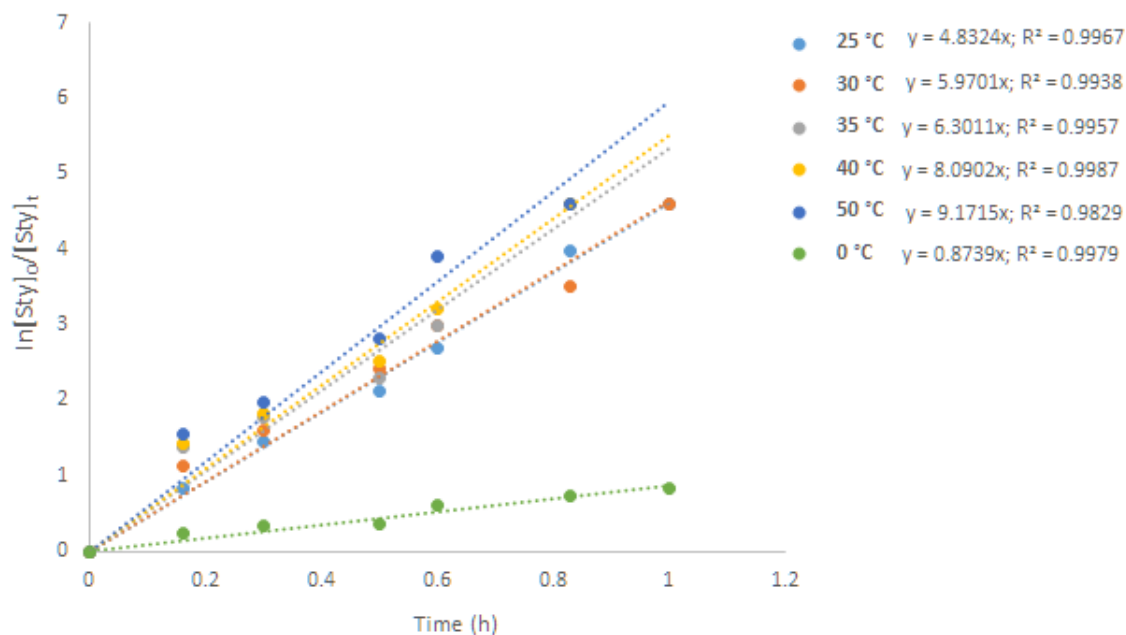


**Figure 5.11:** Plot of  $\ln[\text{Sty}]_0/[\text{Sty}]_t$  vs time for the effect of temperature using 18.

Figure 5.12a shows an Arrhenius plot from which an activation energy,  $E_a = 20.50 \pm 0.70 \text{ kJ mol}^{-1}$  was obtained. Based on the Eyring plot (Fig 5.12b), the apparent activation enthalpy and entropy obtained are  $\Delta H^\ddagger = 17.91 \pm 0.98 \text{ kJ mol}^{-1}$  and  $\Delta S^\ddagger = -224 \pm 0.98 \text{ J mol}^{-1} \text{ K}^{-1}$ . The lower values of  $E_a$  and enthalpy ( $\Delta H^\ddagger$ ) show that the reactions are less sensitive to temperature change and as a result higher reactions rates were obtained for these systems compared to the ones reported in chapter 4 and 5 which showed higher energies ( $E_a$  and enthalpy). The large negative entropy value for  $\Delta S^\ddagger$  indicates a highly ordered transition state consistent with the formation of Pd-hydride intermediate as the active species.<sup>33</sup>

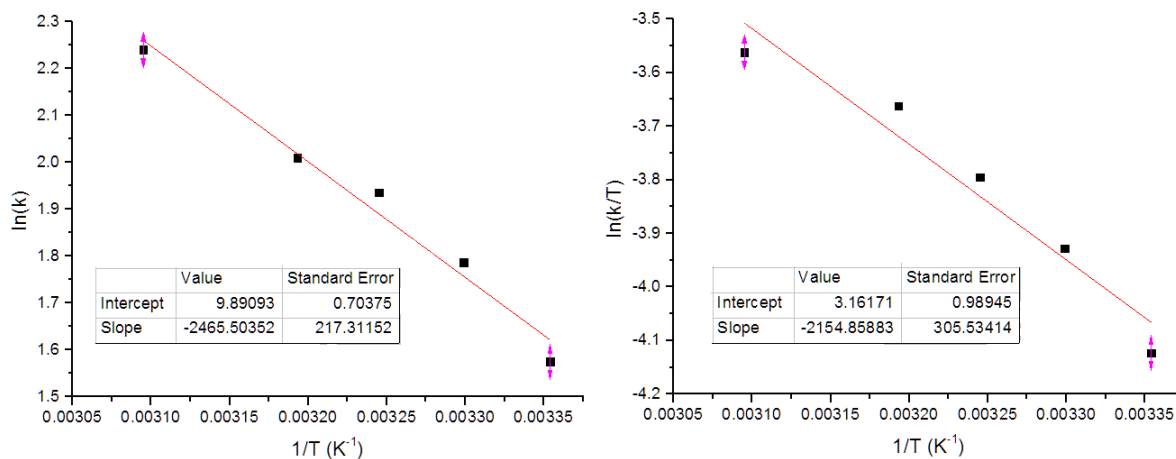


**Figure 5.12:** Arrhenius plot (a) and Eyring plot (b) for the determination of the  $E_a = 20.50 \pm 0.70 \text{ kJ mol}^{-1}$ ,  $\Delta H^\ddagger = 17.91 \pm 0.98 \text{ kJ mol}^{-1}$ , and  $\Delta S^\ddagger = -224 \pm 0.98 \text{ J mol}^{-1} \text{ K}^{-1}$  for the hydrogenation of styrene using catalyst **18**.

In order to better understand the role of a solvent in the hydrogenation reactions a range of solvents such as toluene, hexane, methanol and DMSO were investigated (Table 5.3, entries 2, 7-9). The order of reactivity was established as follows: toluene > hexane > MeOH > DMSO. This trend shows that the use of non-polar solvents, toluene and hexane produces higher catalytic activities ( $k_{obs} = 4.83 \text{ h}^{-1}$  and  $3.52 \text{ h}^{-1}$ ). Similar results were obtained by Yilmaz and co-workers in the hydrogenation of styrene with methanol giving lower conversions of 67.5% (TOF =  $34 \text{ h}^{-1}$ ) compared to hexane (97.5%, TOF =  $65 \text{ h}^{-1}$ ).<sup>36</sup> Another observation was that the strongly coordinating solvents (DMSO and methanol) gave lower catalytic activities and they are known in literature to compete with the substrate, for the active site resulting in lower activities.<sup>36,37</sup>

**Table 5.3:** Effect of temperature and solvent on the hydrogenation of styrene using **18**<sup>a</sup>.

Entry	Solvent	T (°C)	Conv (%) <sup>b</sup>	$k_{obs}$ (h <sup>-1</sup> )	TOF (h <sup>-1</sup> ) <sup>c</sup>
1	Toluene	0	56	0.87 (±0.01)	2800
2	Toluene	25	99	4.83 (±0.03)	4950
3	Toluene	30	>99	5.97 (±0.02)	4950
4	Toluene	35	>99	6.93 (±0.04)	4950
5 <sup>d</sup>	Toluene	40	>99	8.09 (±0.05)	5964
6 <sup>d</sup>	Toluene	50	>99	9.17 (±0.01)	5964
7	Hexane	25	96	3.52 (±0.14)	4800
8	Methanol	25	65	1.31 (±0.05)	3250
9	DMSO	25	43	0.62 (±0.07)	2150

<sup>a</sup>Conditions: styrene, 4.36 mmol; catalyst **18**, 8.7×10<sup>-4</sup> mmol, solvent, toluene; pressure, 5 bar; time, 1.0 h. <sup>b</sup>Determined by GC. <sup>c</sup>TOF in mol<sub>substrate</sub>mol<sub>catalyst</sub><sup>-1</sup> h<sup>-1</sup>. <sup>d</sup>Time, 50 min.

#### 5.3.2.5. *Effect of alkene and alkyne substrates on styrene hydrogenation kinetics and selectivity*

Complex **18** was further used to investigate the hydrogenation reactions of alkenes and alkynes such as 1-hexene, 1-octene, 1-hexyne, 1-octyne and phenyl acetylene (Table 6.4, Fig. 5.13). It was observed that the catalytic activities of **18** depended on the nature of the substrate. For instance, from Figure 5.13 and Table 6.4, alkynes were more active than alkenes while shorter chains were more reactive than longer chains.

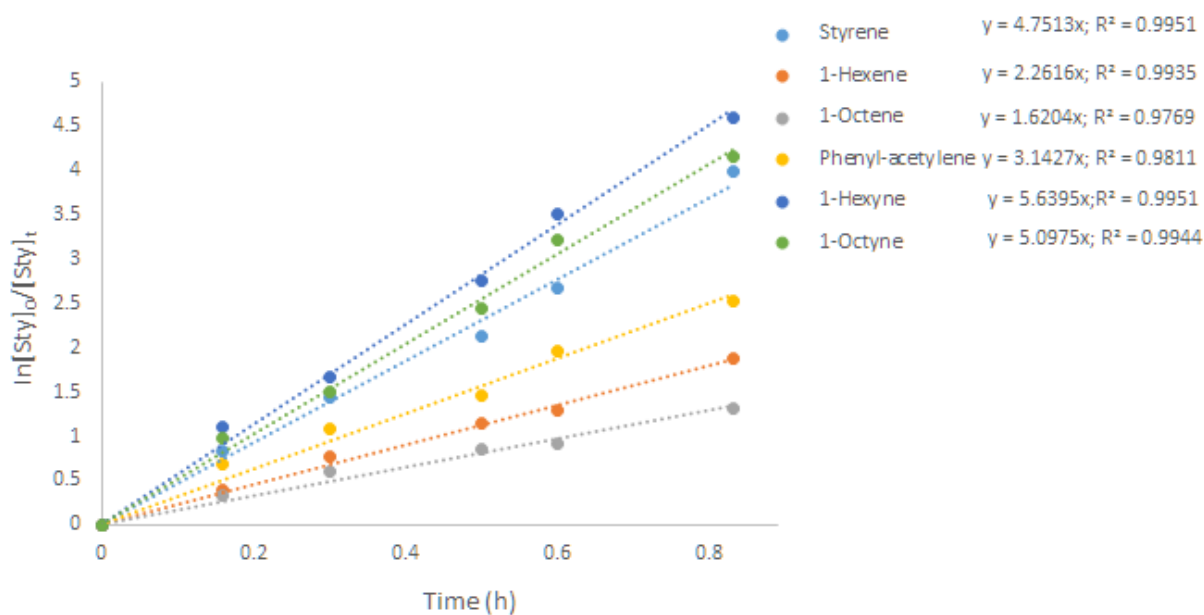


**Figure 5.13:** Plot of  $\ln[\text{Sty}]_0/[\text{Sty}]_t$  vs time for the effect of substrate using catalyst **18**.

**Table 5.4:** Effect of substrates on the catalytic activity of catalyst **18**<sup>a</sup>

Entry	Substrate	( $k_{\text{obs}}$ )(h <sup>-1</sup> )	TOF <sup>b</sup> (h <sup>-1</sup> )	%Alkane <sup>c</sup>
1	Styrene	4.75 ( $\pm 0.06$ )	5783	96
2	1-Hexene	2.26 ( $\pm 0.03$ )	4699	76
3	1-Octene	1.62 ( $\pm 0.04$ )	5398	71
4	Phenyl-acetylene	3.14 ( $\pm 0.07$ )	5542	100
5	1-Hexyne	5.64 ( $\pm 0.08$ )	5964	68
6	1-Octyne	5.10 ( $\pm 0.02$ )	5843	57

<sup>a</sup>Conditions: substrate, substrate/catalyst = 5000; substrate, 4.36 mmol; catalyst;  $8.7 \times 10^{-4}$  mmol; solvent, toluene; pressure, 5 bar; solvent, toluene; temperature, 25 °C; time, 50 min. <sup>b</sup>TOF in  $\text{mol}_{\text{substrate}}\text{mol}_{\text{catalyst}}^{-1} \text{h}^{-1}$ . <sup>c</sup>selectivity towards alkane hydrogenation products after 50 min.

### 5.3.3. Determination of the true active species: Homogeneous *vs* heterogeneous

#### 5.3.3.1. *Sub-stoichiometric poisoning tests*

Solubility has conservatively been used as a norm to distinguish between homogeneous and heterogeneous catalyst<sup>38-40</sup>, until recently when Schmidt<sup>41</sup> was able to give a distinctive definition of homogeneous and heterogeneous catalysts on numerous active sites of a catalyst. A number of experiments such as catalyst poisoning, identification and characterization of nanoparticles formation are employed in distinguishing between homogeneous and heterogeneous catalysts.<sup>42-45</sup> The mostly used experiment in sub-stoichiometric amounts of poisonous ligands such as amines, thiols, phosphines and alcohols.<sup>39</sup> Homogeneous catalysts need an equivalent or slight excess amounts of the poisoning/deactivating ligands to inhibit their catalytic activities, whereas sub-stoichiometric amounts (approx. 10%) are sufficient to deactivate heterogeneous catalysts due to minimal availability of active sites.<sup>46,47</sup>

We thus investigated the true nature of the active species by using sub-stoichiometric amounts (20%) of poisoning ligands such as CS<sub>2</sub>, PPh<sub>3</sub> and PCy<sub>3</sub> (Fig. 5.14). From the plot of  $\ln[\text{Sty}]_0/[\text{Sty}]_t$  *vs* time (Fig. 5.14), the rate constants upon introduction of poisoning ligands are obtained. For example, when PPh<sub>3</sub> was used a reduction in catalytic activity from 4.75 h<sup>-1</sup> to 3.07 h<sup>-1</sup> **18** was observed. This therefore provided evidence for irreversible binding of the poisoning ligands to the metal centre thereby preventing the substrate to access the active sites of the catalysts.<sup>48</sup> Although the use

of PPh<sub>3</sub>, CS<sub>2</sub> and PCy<sub>3</sub> poisoning test on their own is insufficient to confirm the true nature of the active species, a clue is provided about the heterogeneity of our catalyst system i.e. the system is not 100% homogeneous.

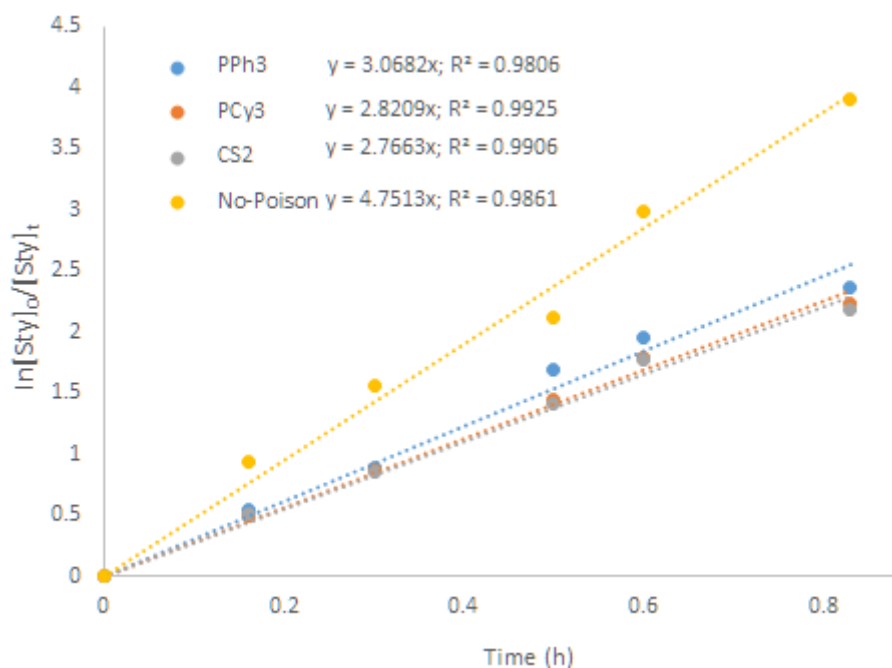


**Figure 5.14:** Plot of  $\ln[\text{Sty}]_0/[\text{Sty}]_t$  vs time for the effect of ligand poisoning using catalyst **18** and 20% PPh<sub>3</sub>, PCy<sub>3</sub> or CS<sub>2</sub>.

### 5.3.3.2. Mercury poisoning test

A mercury poisoning test is another well-established method that is widely used for distinguishing between homogeneous and heterogeneous catalysts.<sup>39</sup> Soft metals such as Fe(II), Ni(II) and Pd(II) form amalgams with Hg(0), this suppresses their catalytic activity in low oxidation state.<sup>39,40</sup> In this study, five drops of mercury were added into the reaction mixture at the beginning of the reaction. Minimal reduction in catalytic



activity from 96% ( $k_{obs} = 4.75 \text{ h}^{-1}$ ) to 84% ( $k_{obs} = 3.11 \text{ h}^{-1}$ ) was observed (Fig. 5.15). This minimal reduction in catalytic activity provided evidence for possible formation of metal nanoparticles, which shows that this catalytic systems are not 100% homogeneous but largely homogeneous.<sup>31,32</sup>

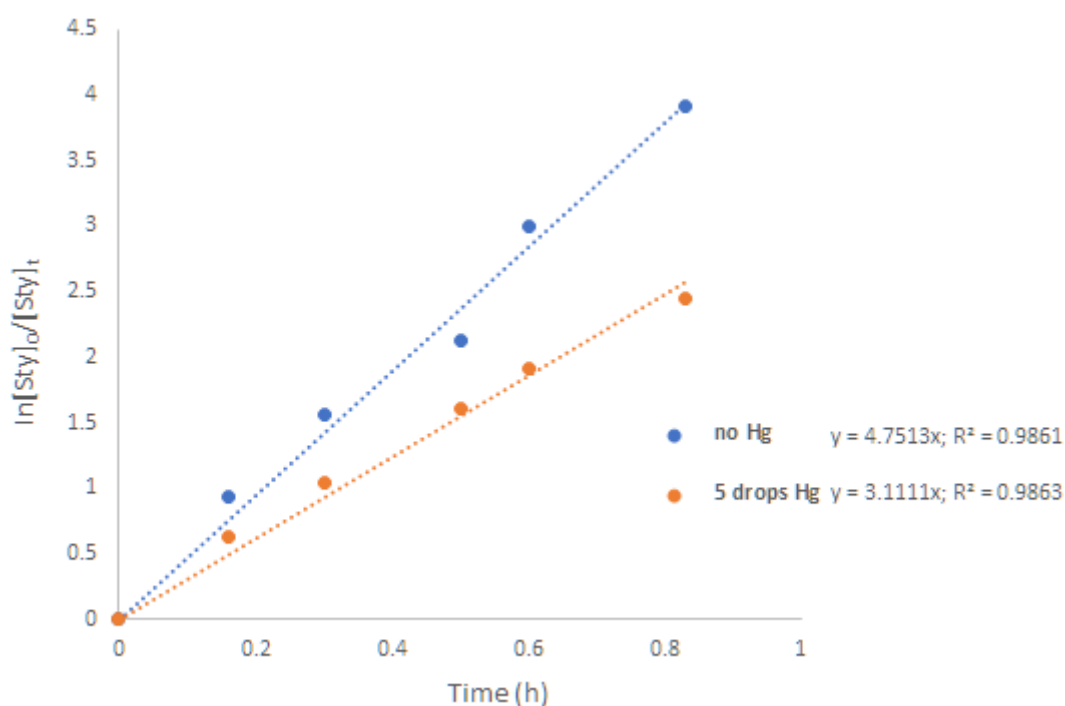


**Figure 5.15:** Plot of  $\ln[\text{Sty}]_0/[\text{Sty}]_t$  vs time for the effect of mercury (Hg) using catalyst 18 and 5 drops of Hg

### 5.3.3.3. Kinetic reproducibility

Furthermore, we used kinetic reproducibility to try and investigate whether our catalysts behaved as homogeneous and heterogeneous. From the plot of  $\ln[\text{Sty}]_0/[\text{Sty}]_t$  vs time (Fig. 5.16), rate constants for runs 1-4 at substrate/catalyst ratio of 5000 were obtained.

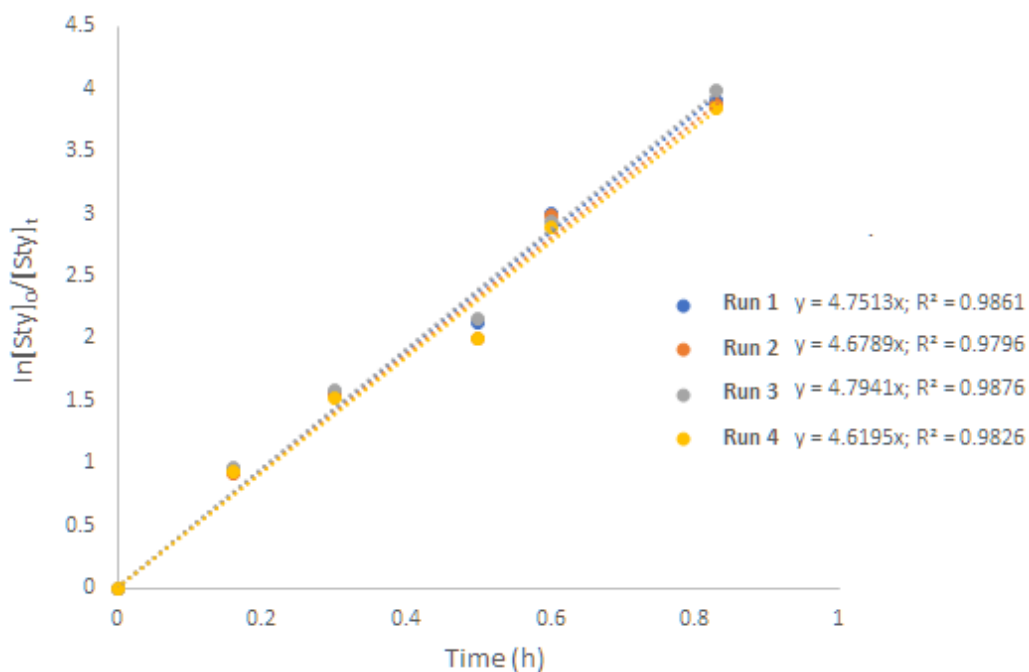


**Figure 5.16:** Plot of  $\ln[\text{Sty}]_0/[\text{Sty}]_t$  vs time for runs 1-4 at  $[\text{styrene}]/[\mathbf{18}]$  of 5000 with fixed concentration of styrene of 0.5 mL (4.44 mmol).

Reproducible kinetics (Fig. 5.17) were observed with orders of 2.20, 2.19, 2.22 and 2.17 (Table 5.5), thus allowing us to deduce that the active catalysts derived from complex **18** is homogeneous in nature. From fundamental studies and literature accounts, heterogeneous catalysts exhibit irreproducible kinetics data due to the non-uniformity and varied compositions of the active species.<sup>49</sup>

**Table 5.5:** Reproducible kinetic data from the effects of catalyst loading

Rate = $k[\text{styrene}]^1[\mathbf{18}]^x$				
Run	1	2	3	4
X	2.20	2.19	2.22	2.17
Error	$\pm 0.02$	$\pm 0.05$	$\pm 0.03$	$\pm 0.06$

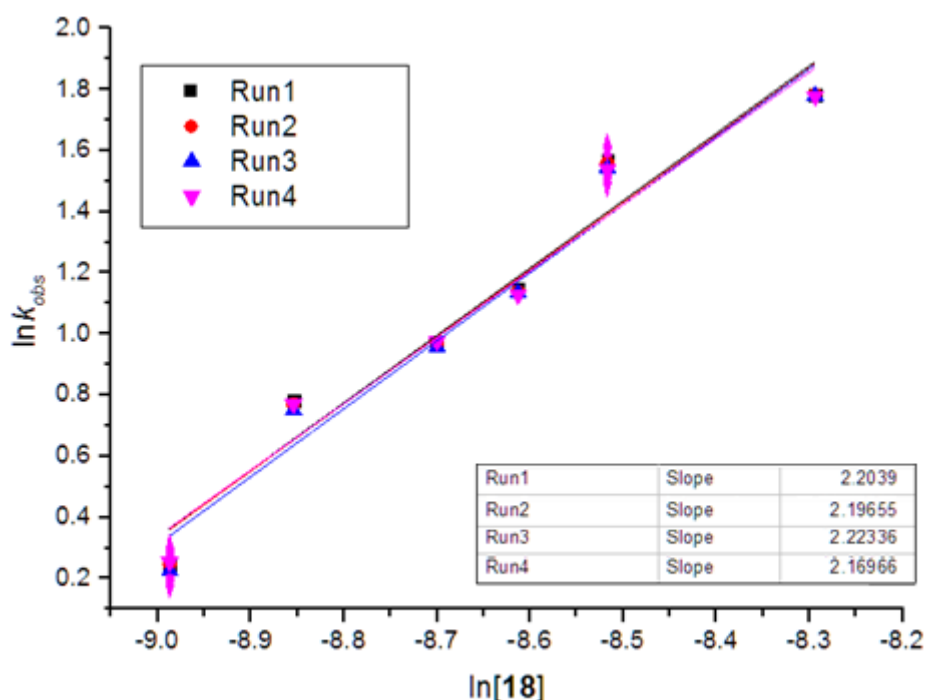


**Figure 5.17:** Kinetic results for catalyst **18** in the hydrogenation of styrene.

#### 5.4. Proposed mechanism of the hydrogenation of styrene using catalyst **18**

To establish the possible pathway for the mechanism of styrene hydrogenation using catalyst **18**, mass spectrometry (Fig. 5.18) was used to detect the intermediates and possible active species (Scheme 5.3). This was performed by sampling the reaction mixture at regular time intervals during the course of the reaction and analysing the

samples using ESI-MS. From a typical mass spectrum obtained (Fig 5.18), the first stage of the pathway involves the dissociation of Cl and is believed to occur *via* heterolytic cleavage of H<sub>2</sub><sup>48</sup> to form intermediate **18a** observed from the ESI-MS ( $m/z$  = 454 amu) with HCl as a by-product (Scheme 5.3). Coordination of styrene substrate to the metal center in **18a** through the displacement of the OMe group affords the palladium alkene intermediate **18b** as deduced from the base peak at  $m/z$  = 558 amu. A palladium alkyl intermediate **18c** was detected as a fragment at  $m/z$  = 558 amu which is formed by the Markovnikov migration of the hydride to the coordinated styrene substrate. Oxidative addition of H<sub>2</sub> transforms the palladium(II) to palladium(IV) (dihydride **18d**) which was confirmed from the signal at  $m/z$  = 560 amu. The monohydride palladium(II) intermediate **18e** ( $m/z$  = 454 amu) is formed by the hydride migration to the coordinated alkyl ligand in **18d**. Product elimination results in regeneration of the active species **18a**.

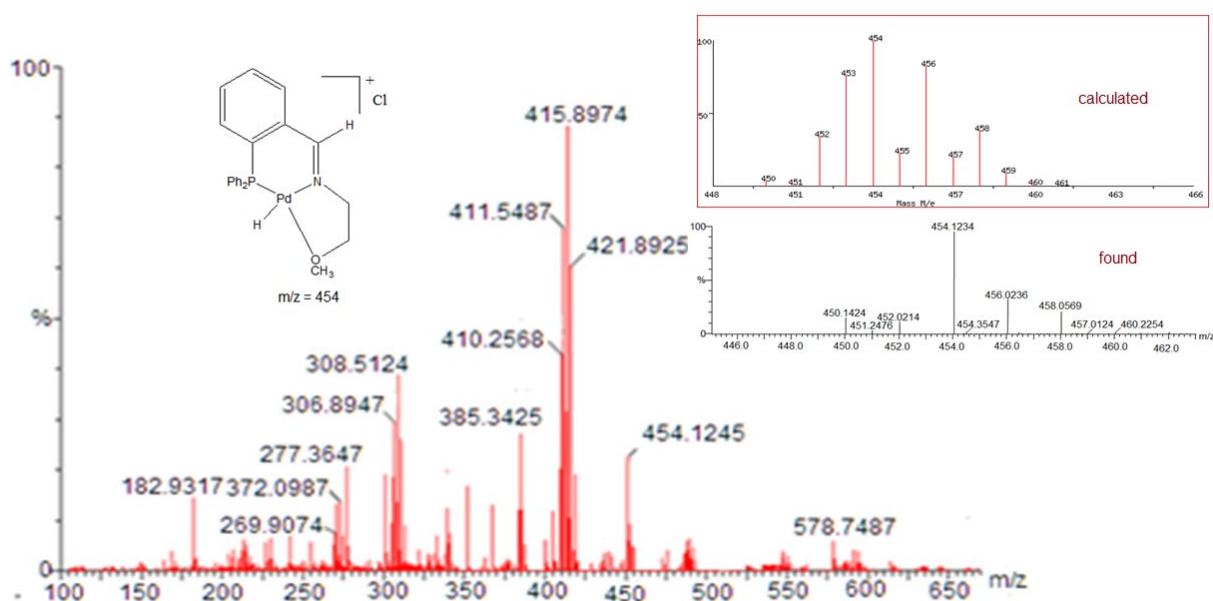
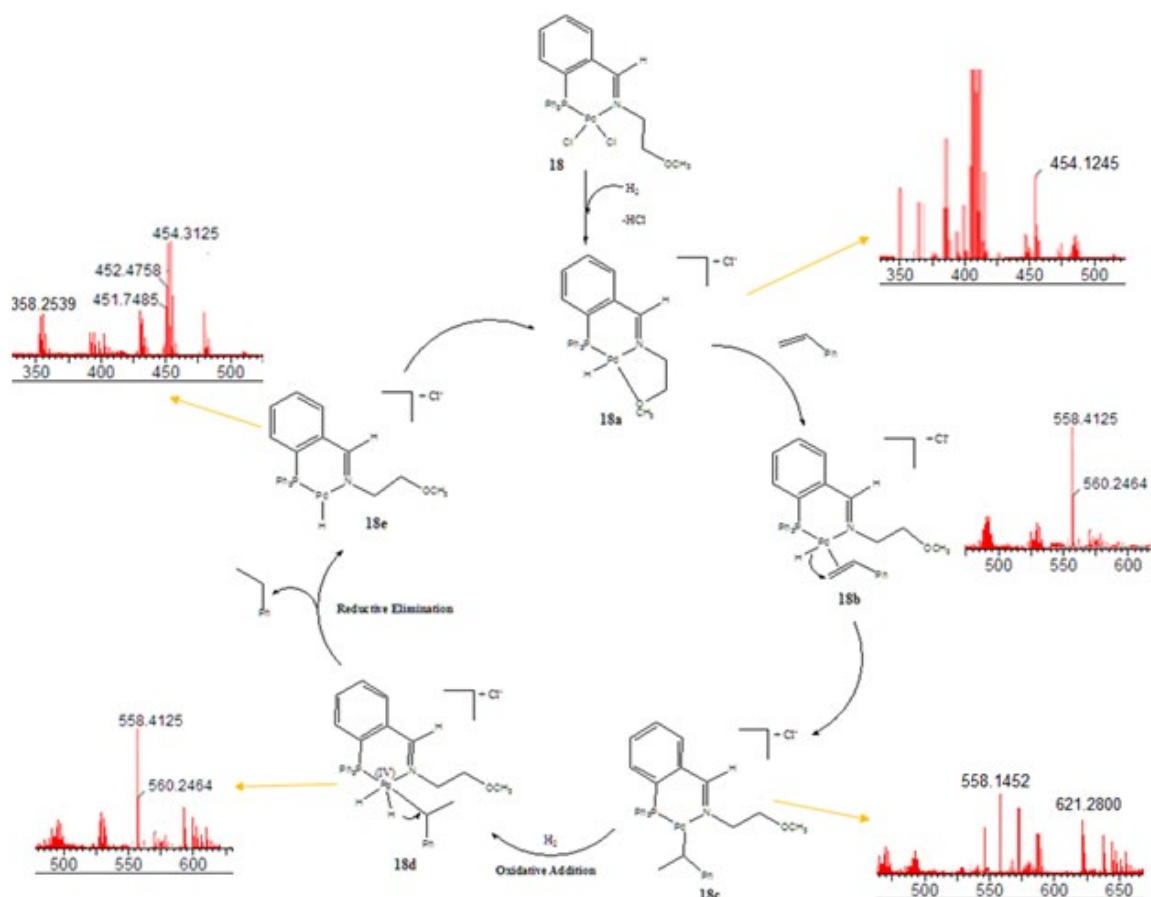


**Figure 5.18:** ESI-MS showing molecular mass corresponding to a fragment of reactive intermediate (**18a**) present in a reaction mixture sampled after 15 min (insert showing mass spectrum of the calculated and found isotopic distribution).



**Scheme 5.3:** Proposed mechanism for the hydrogenation of styrene catalysed by **18** as deduced from mass spectral data of the reaction samples.

## 5.5. Conclusions

In summary, palladium(II) complexes anchored on (diphenylphosphino)benzalidene with pendant donor groups have been successfully isolated and structurally

characterized. Complexes **18-23** formed active catalysts in the hydrogenation of alkenes and alkynes while isomerization of terminal alkenes also occurred. Kinetic experiments, sub-stoichiometry poisoning tests, mercury poisoning and kinetic reproducible data indicate a largely homogeneous nature of the active species.

## 5.6. References

- 1 D. Drago and P. S. Pregosin, *Organometallics*, 2002, **21**, 1208-1215.10.
- 2 C. A. Ghilardi, S. Midollini, S. Moneti and A. Orlandini, *J. Chem. Soc. Dalt. Trans.*, 1992, 3371-3376.
- 3 M. W. Van Laren, M. A. Duin, C. Klerk, M. Naglia, D. Rogolino, P. Pelagatti, A. Bacchi, C. Pelizzi and C. J. Elsevier, *Organometallics*, 2002, **21**, 1546-1553.
- 4 J. V. Allen, J. F. Bower and J. M. J. Williams, *Tetrahedron: Asymmetry*, 1994, **5**, 1895-1898.
- 5 K. E. Frankcombe, K. J. Cavell, B. F. Yates and R. B. Knott, *Organometallics*, 1997, **16**, 3199-3206.
- 6 P. W. N. M. van (Piet W. N. M. . Leeuwen, J. C. Chadwick and Wiley InterScience (Online service), *Homogeneous catalysts: activity-stability-deactivation*, Wiley-VCH Verlag, 2011.
- 7 S. O. Ojwach, A. O. Ogwenno and M. P. Akerman, *Catal. Sci. Technol.*, 2016, **6**, 5069-5078.
- 8 S. O. Ojwach and A. O. Ogwenno, *Transit. Met. Chem.*, 2016, **41**, 539-546.
- 9 P. Pelagatti, A. Bacchi, M. Carcelli, M. Costa, A. Fochi, P. Ghidini, E. Leporati, M. Masi, C. Pelizzi and G. Pelizzi, *J. Organomet. Chem.*, 1999, **583**, 94-105.
- 10 W. Baratta and J. Schu, *J. Organomet. Chem.*, 2005, **690**, 5570-5575.
- 11 T. Suárez, B. Fontal, M. Reyes, F. Bellandi, R. R. Contreras, A. Bahsas, G. León, P. Cancines and B. Castillo, *React.Kinet.Catal.Lett.*, 2004, **82**, 317-324.

- 12 S. Antonaroli and B. Crociani, *J. Organomet. Chem.*, 1998, **560**, 137–146.
- 13 E. Shirakawa, Y. Nakao, Y. Murota and T. Hiyama, *J. Organomet. Chem.*, 2003, **670**, 132–136.
- 14 R. E. Ru, V. E. Kaasjager, P. Wehman, C. J. Elsevier, P. W. N. M. Van Leeuwen, K. Vrieze and A. L. Spek, *Organometallics*, 1996, **15**, 3022–3031.
- 15 M. M. Mogorosi, T. Mahamo, J. R. Moss, S. F. Mapolie, J. C. Sloomweg, K. Lammertsma and G. S. Smith, *J. Organomet. Chem.*, 2011, **696**, 3585–3592.
- 16 W. M. Motswainyana, M. O. Onani, R. A. Lalancette and P. K. Tarus, *Chemical Papers.*, 2014, **68**, 932–939.
- 17 S. Doherty, J. G. Knight, T. H. Scanlan, M. R. J. Elsegood and W. Clegg, *J. Organomet. Chem.*, 2002, **650**, 231–248.
- 18 K. R. Reddy, K. Surekha, G. Lee and S. Peng, *Organometallics*, 2000, 2637–2639.
- 19 E. Sindhuja, R. Ramesh and Y. Liu, *Dalton Trans.*, 2012, **41**, 5351.
- 20 V. S. Tkach, D. S. Suslov, N. V. Kurat'eva, M. V. Bykov, M. V. Belova and N. V. Kurat'Eva, *Russ. J. Coord. Chem.*, 2011, **37**, 752–756.
- 21 J. C. Jeffrey and T. B. Rauchfuss, *Inorg. Chem.*, 1979, **18**, 2658–2666.
- 22 S. Garci and P. Crochet, *New J. Chem.*, 2003, **2**, 0–6.
- 23 M. W. van Laren and C. J. Elsevier, *Angew. Chem. Int. Ed.*, 1999, **38**, 3715–3717.
- 24 E. Negishi, *Handbook of Organopalladium Chemistry for Organic Synthesis*, Wiley & Sons, New York, 2002, **1**, 229–247.
- 25 R. R. Schrock and J. A. Osborn, *J. Am. Chem. Soc.*, 1976, **98**, 2134–2143.
- 26 J. A. Osborn, F. H. Jardine, J. F. Young and G. Wilkinson, *J. Chem. Soc.*, 1966, 1711–1732.
- 27 R. E. Harmon, S. K. Gupta and D. J. Brown, *Chem. Rev.*, 1973, **73**, 21–52.
- 28 L. S. Hegedus, *Transition metals in the synthesis of complex organic molecules*,

- University science books, Sausalito, CA, 1999, 15-21.*
- 29 R. G. Pearson, *Surv.Progr.Chem.*, 1969, **5**, 1-52.
- 30 V. P. Ananikov and I. P. Beletskaya, *Organometallics*, 2012, **31**, 1595-1604.
- 31 J. A. Widegren and R. G. Finke, *J. Mol. Catal. A Chem.*, 2003, **198**, 317-341.
- 32 G. Süß-Fink, M. Faure and T. R. Ward, *Angew. Chem. Int. Ed.*, 2002, **41**, 99-101.
- 33 A. M. Kluwer, T. S. Koblenz, T. T. Jonischkeit, K. Woelk and C. J. Elsevier, *J. Am. Chem. Soc.*, 2005, **127**, 15470-15480.
- 34 H. Yoshida, T. Zama, S. Fujita, J. Panpranot and M. Arai, *RSC Adv.*, 2014, **4**, 24922.
- 35 M. Costa, P. Pelagatti, C. Pelizzi and D. Rogolino, *J. Mol. Cat. A*, 2002, **178**, 21-26.
- 36 F. Yilmaz, A. Mutlu, H. Ünver, M. Kurta and I. Kani, *J. Supercrit. Fluids*, 2010, **54**, 202-209.
- 37 P. J. Dyson and P. G. Jessop, *Catal. Sci. Technol.*, 2016, **6**, 3302-3316.
- 38 R. H Crabtree, *Chem. Rev.*, 2011, **112**, 1536-1554.
- 39 J. A. Widegren and R. G. Finke, *J. Mol. Catal. A Chem.*, 2003, **198**, 317-341.
- 40 C. M. Hagen, J. A. Widegren, P. M. Maitlis, R. G. Finke, *J. Am. Chem. Soc.* 2005, **127**, 4423-4432.
- 41 A. Schmidt, A. Kurokhtina, *Kinet. Catal.*, 2012, **53**, 714-730.
- 42 Y. Lin and R. G. Finke, *Inorg. Chem.*, 1994, 4891-4910.
- 43 J. F. Sonnenberg and R. H. Morris, *Catal. Sci. Technol.*, 2014, **4**, 3426-3438.
- 44 J. F. Sonnenberg, R. H. Morris, *ACS Catalysis.*, 2013, **3**, 1092-1102.
- 45 E. Bayram, J. C. Linehan, J. L. Fulton, J. A. S. Roberts, N. K. Szymczak, T. D. Smurthwaite, S. Ozkar, M. Balasubramanian and R. G. Finke, *J. Am. Chem. Soc.*, 2011, **133**, 18889-18902.



- 46 B. J. Hornstein, J. D. A. Iii and R. G. Finke, *Inorg. Chem.*, 2002, **41**, 1625–1638.
- 47 M. A. Watzky, R. G. Finke and F. Collins, *J. Am. Chem. Soc.*, 1997, **119**, 10382–10400.
- 48 S. P. Smidt, N. Zimmermann, M. Studer and A. Pfaltz, *Chem. - A Eur. J.*, 2004, **10**, 4685–4693.
- 49 J. D. Aiken III, R. G. Finke, *J. Mol. Catal. A: Chem.* 1999, **145**, 1–44.

## CHAPTER 6

### Syntheses of P<sup>N</sup> (imino-diphenylphosphino) palladium(II) complexes and their applications as recyclable catalysts in biphasic hydrogenation of alkenes

#### 6.1. Introduction

Catalysis either homogeneous or heterogeneous is used in the manufacturing and processing industries to produce about 85% of fine and bulk chemicals.<sup>1,2</sup> Homogeneous catalysis is preferred over heterogeneous systems mainly because of high catalytic activity and selectivity in addition to understanding of the mechanisms involved.<sup>3-5</sup> Despite these positive attributes of homogeneous catalysis, it suffers from some drawbacks. For example catalyst recovery is a problem, it also requires the use of toxic organic solvents and suffers from the possible contamination of the products.<sup>6-8</sup> Whereas, heterogeneous catalysis offers catalyst recovery and recycling, and greater purity of products.<sup>9,10</sup> However, heterogeneous systems have low catalytic activities, poor selectivity and the probing of their reaction mechanisms is not possible.<sup>11</sup>

The best way to overcome these challenges in both heterogeneous and homogeneous systems, is to heterogenize homogeneous systems which is an approach that is currently gaining momentum.<sup>12,13</sup> One of the methods used in heterogenization homogeneous systems is the use of water-soluble complexes in biphasic reactions.<sup>14,15</sup> These biphasic systems allows the catalyst to be recycled without losing its catalytic activity and selectivity, as well as allowing for facile catalyst separation.<sup>16-19</sup> Besides easy catalyst recovery, this method is advantageous as it makes use of water (a green solvent), which is non-toxic, odourless, non-flammable and readily accessible in vast

quantities at low cost.<sup>20-23</sup> For example, water-soluble rhodium catalysts supported on TPPTS (Trisodium 3,3',3-phosphinetriyltribenzenesulfonate)<sup>24</sup> and rhodium complexes containing carbene ligands<sup>25</sup> have been successfully used in the biphasic hydrogenation of benzene and acetophenone. These systems were found to be highly efficient and recyclable. In this chapter, the synthesis and characterization of potential hemilabile Water-soluble P<sup>N</sup>O and P<sup>N</sup>N palladium(II) complexes and their applications in the biphasic hydrogenation catalysis is reported.

## 6.2. Experimental section

### 6.2.1. Material, instrumentation and methods

All moisture and air sensitive reactions were performed using standard Schlenk line techniques. Toluene (ACS reagent, ≥99.5%), dichloromethane (ACS reagent, ≥99.8%), absolute ethanol (ACS reagent, ≥98%), DMSO-d<sub>6</sub> (99.8%), were purchased from Merck. *p*-TsOH (ACS reagent, ≥98.5%), PPh<sub>3</sub> (Reagent Plus®, 99%), were obtained from Sigma-Aldrich and were used without further purification. Solvents were dried and distilled under nitrogen atmosphere in the presence of suitable drying agents: Toluene and acetone were dried over sodium wire/benzophenone, absolute ethanol over calcium oxide, and dichloromethane over phosphorus pentoxide. The sodium salt starting material of TPPMS (triphenylphosphine monosulfonate) was synthesized following literature methods.<sup>26</sup> Nuclear magnetic resonance spectra were acquired at 400 MHz for <sup>1</sup>H, 100 MHz for <sup>13</sup>C and 162 MHz for <sup>31</sup>P on a Bruker Avance spectrometer equipped with Bruker magnet (9.395 T). All coupling constants (*J*) are measured in Hertz, Hz. The mass spectra (ESI-MS) were recorded on a Waters API

Quatro Micro spectrometer, using 50% MeOH/DMSO, 16-36 V cone voltage, source (720 V) and desolvation temperature of 450°C. The elemental analyses were performed on a Thermal Scientific Flash 2000. The infrared spectra were recorded on a Perkin-Elmer spectrum 100 in the 4000-650 cm<sup>-1</sup> range.

## 6.2.2. Synthesis of biphasic P<sup>AN</sup> (diphenylphosphino)benzalidene ethanamine palladium(II) complexes

### 6.2.2.1. $\{[2-(2-(\text{diphenylphosphino})\text{benzylidene})\text{methoxyethanamine}]\text{Pd}(\text{OTs})(\text{TPPMS})\}^+ \text{TsO}^-$ (**24**)

To a suspension of **L9** (0.05 g, 0.15 mmol) in chloroform (5 mL), was added drop-wise a solution of Pd(AOc)<sub>2</sub> (0.03 g, 0.15 mmol) in chloroform (10 mL), followed by a solution of PPh<sub>3</sub> (0.08 g, 0.3 mmol) and *p*-TsOH (0.05 g, 0.3 mmol) in chloroform (10 mL) and stirred at room temperature for 24 h. After the reaction period, the organic volatiles were removed *in vacuo*, and recrystallization from CH<sub>2</sub>Cl<sub>2</sub>-hexane gave the crude product as a light-yellow solid. The yellow solid was then redissolved in butanone (10 mL) and shaken vigorously with 2 equiv. of TPPMS (0.11 g, 0.33 mmol) in water (6 mL). The yellow solution was filtered under nitrogen, washed with ethanol followed by diethyl ether and dried under vacuum to give complex **24** as a yellow powder. Yield = 0.08 g (78%). <sup>1</sup>H NMR (400 MHz, DMSO-d<sub>6</sub>): δ<sub>H</sub> (ppm): 2.37 (s, 6H, CH<sub>3</sub>-OTs); 3.24 (s, 3H, OCH<sub>3</sub>); 3.78 (t, 2H, CH<sub>2</sub>-N); 4.49 (t, 2H, CH<sub>2</sub>-O); 6.98 (m, 2H, Ph-OTs); 7.12 (m, 2H, Ph-OTs); 7.24 (m, 4H, H-PPh<sub>2</sub>); 7.28 (t, 1H, H-Ph); 7.30 (m, 2H, TPPMS-Ph-SO<sub>3</sub>Na); 7.54 (m, 11H, TPPMS); 7.59 (m, 6H, H-PPh<sub>2</sub>); 7.60 (m, 3H, H-Ph); 7.93 (m, 2H, TPPMS-Ph-SO<sub>3</sub>Na); 8.45 (s, 1H, H-C=N). <sup>13</sup>C NMR (DMSO-d<sub>6</sub>): δ<sub>C</sub>(ppm): 24.30 (CH<sub>3</sub>-OTs); 59.01 (OCH<sub>3</sub>); 69.08 (CH<sub>2</sub>-N); 74.61 (CH<sub>2</sub>-OCH<sub>3</sub>); 128.10; 128.18; 128.85; 128.96;

128.99; 128.01; 129.24; 129.37; 129.48; 130.15; 130.57; 131.14; 132.17; 132.24; 135.27; 137.37; 137.39; 137.42; 137.56; 137.91; 142.52; 149.86; 163.75 (C=N).  $^{31}\text{P}$  NMR (DMSO- $d_6$ ):  $\delta_{\text{p}}$ (ppm): 31.55 (PPh $_2$ ); 38.40 (TTPMS); 38.60 (TPPMS). MS (ESI)  $m/z$  (%) 988 ( $\text{M}^+$ , 100). FT-IR ( $\text{cm}^{-1}$ ):  $\nu_{(\text{C}=\text{N})}$  = 1651. Anal. Calc. for  $\text{C}_{55}\text{H}_{54}\text{NNaO}_8\text{P}_2\text{PdS}_3\cdot\text{CHCl}_3$ : C, 53.28; H, 4.39; N, 1.11. Found: C; 54.11, H; 4.35, N; 2.24.

Compounds **25–27** were prepared following the same procedure described for compound **24**.

6.2.2.2.  $[\{2-(2-(\text{diphenylphosphino})\text{benzylideneamino})\text{ethanol}\}\text{Pd}(\text{OTs})(\text{TPPMS})]^+\text{TsO}^-$  (**25**)

**L10** (0.05 g, 0.17 mmol), Pd(AOc) $_2$  (0.06 g, 0.17 mmol), *p*-TsOH (0.06 g, 0.34 mmol), PPh $_3$  (0.09 g, 0.3 mmol), *p*-TsOH (0.06 g, 0.34 mmol) and TPPMS (0.13 g, 0.34 mmol). Yield = 0.09 g (88%).  $^1\text{H}$  NMR (400 MHz, DMSO- $d_6$ ):  $\delta_{\text{H}}$  (ppm): 2.30 (s, 6H, CH $_3$ -OTs); 3.74 (t, 2H, CH $_2$ -N); 3.89 (t, 2H, CH $_2$ -OH); 6.95 (m, 4H, Ph-OTs); 7.01 (m, 4H, Ph-OTs); 7.21 (m, 4H, H-PPh $_2$ ); 7.26 (t, 1H, H-Ph); 7.29 (m, 2H, TPPMS-Ph-SO $_3$ Na); 7.51 (m, 11H, TPPMS); 7.56 (m, 6H, H-PPh $_2$ ); 7.60 (m, 2H, H-Ph); 7.91 (d, 1H, H-Ph); 7.90 (m, 2H, TPPMS-Ph-SO $_3$ Na); 8.41 (s, 1H, H-C=N).  $^{13}\text{C}$  NMR (DMSO- $d_6$ ):  $\delta_{\text{C}}$ (ppm): 24.35 (CH $_3$ -OTs); 59.51 (CH $_2$ -OH); 69.99 (CH $_2$ -N); 128.14; 128.16; 128.24; 128.75; 128.92; 128.96; 128.00; 128.07; 129.15; 129.31; 129.44; 130.08; 130.17; 130.87; 131.13; 132.16; 132.21; 135.24; 137.34; 137.36; 137.42; 137.55; 137.90; 142.54; 149.85; 163.73 (C=N).  $^{31}\text{P}$  NMR (DMSO- $d_6$ ):  $\delta_{\text{p}}$ (ppm): 31.74 (PPh $_2$ ); 38.43 (TPPMS); 38.54 (TPPMS). MS (ESI)  $m/z$  (%) 974 ( $\text{M}^+$ , 100). FT-IR ( $\text{cm}^{-1}$ ):  $\nu_{(\text{C}=\text{N})}$  = 1649;  $\nu_{(\text{OH})}$  = 3393. Anal. Calc. for  $\text{C}_{54}\text{H}_{52}\text{NNaO}_8\text{P}_2\text{PdS}_3\cdot\text{CHCl}_3$ : C, 52.85; H, 4.27; N, 1.12. Found: C; 53.28, H; 3.91, N; 1.15.

6.2.2.3.  $[[2-(\text{diphenylphosphino})\text{benzylidene})\text{ethane-1,2-diamine}]\text{Pd}(\text{OTs})(\text{TPPMS})]^+\text{TsO}^-$   
(26)

**L11** (0.05 g, 0.17 mmol), Pd(AOc)<sub>2</sub> (0.06 g, 0.17 mmol), PPh<sub>3</sub> (0.09 g, 0.3 mmol), *p*-TsOH (0.06 g, 0.34 mmol) and TPPMS (0.13 g, 0.34 mmol). Yield = 0.06 g (76%). <sup>1</sup>H NMR (400 MHz, DMSO-d<sub>6</sub>): δ<sub>H</sub> (ppm): 2.33 (s, 6H, CH<sub>3</sub>-OTs); 3.01 (t, 2H, CH<sub>2</sub>-N); 3.81 (t, 2H, CH<sub>2</sub>-NH<sub>2</sub>); 6.99 (m, 4H, Ph-OTs); 7.06 (m, 4H, Ph-OTs); 7.25 (m, 4H, H-PPh<sub>2</sub>); 7.29 (t, 1H, H-Ph); 7.33 (m, 2H, TPPMS-Ph-SO<sub>3</sub>Na); 7.54 (m, 11H, TPPMS); 7.58 (m, 6H, H-PPh<sub>2</sub>); 7.63 (m, 2H, H-Ph); 7.94 (d, 1H, H-Ph); 7.97 (m, 2H, TPPMS-Ph-SO<sub>3</sub>Na); 8.47 (s, 1H, H-C=N). <sup>13</sup>C NMR (DMSO-d<sub>6</sub>): δ<sub>C</sub>(ppm): 24.36 (CH<sub>3</sub>-OTs); 44.04 (CH<sub>2</sub>-N); 47.38 (CH<sub>2</sub>-NH<sub>2</sub>); 128.14; 128.24; 128.68; 128.88; 128.01; 129.11; 129.32; 129.41; 130.07; 130.14; 130.86; 131.11; 132.17; 135.15; 137.24; 137.37; 137.42; 137.53; 137.89; 142.47; 149.74; 163.72 (C=N). <sup>31</sup>P NMR (DMSO-d<sub>6</sub>): δ<sub>P</sub>(ppm): 31.65 (PPh<sub>2</sub>); 38.32 (TPPMS); 38.51 (TPPMS). MS (ESI) m/z (%) 973 (M<sup>+</sup>, 100). FT-IR (cm<sup>-1</sup>): ν<sub>(C=N)</sub> = 1646. Anal. Calc. for C<sub>54</sub>H<sub>53</sub>N<sub>2</sub>NaO<sub>7</sub>P<sub>2</sub>PdS<sub>3</sub>: C, 57.42; H, 4.73; N, 2.48. Found: C; 58.46, H; 4.35, N; 2.86.

6.2.2.4.  $[[2-(\text{diphenylphosphino})\text{benzylidene})\text{diethylethane-1,2-diamine}]\text{Pd}(\text{OTs})(\text{TPPMS})]^+\text{TsO}^-$   
(27)

**L12** (0.05 g, 0.13 mmol), Pd(AOc)<sub>2</sub> (0.04 g, 0.13 mmol), PPh<sub>3</sub> (0.03 g, 0.3 mmol), *p*-TsOH (0.04 g, 0.26 mmol) and TPPMS (0.09 g, 0.26 mmol) and *p*-TsOH (0.04 g, 0.26 mmol). Yield = 0.09 g (91%). <sup>1</sup>H NMR (400 MHz, DMSO-d<sub>6</sub>): δ<sub>H</sub> (ppm): 1.01 (m, 6H, CH<sub>3</sub>-NEt<sub>2</sub>); 2.98 (m, 4H, CH<sub>3</sub>-NEt<sub>2</sub>); 2.35 (s, 6H, CH<sub>3</sub>-OTs); 3.45 (t, 2H, CH<sub>2</sub>-NEt<sub>2</sub>); 3.78 (t, 2H, CH<sub>2</sub>-N); 6.93 (m, 4H, Ph-OTs); 7.03 (m, 4H, Ph-OTs); 7.21 (m, 4H, H-PPh<sub>2</sub>); 7.28 (t, 1H, H-Ph); 7.30 (m, 2H, TPPMS-Ph-SO<sub>3</sub>Na); 7.51 (m, 11H, TPPMS); 7.56 (m, 6H, H-PPh<sub>2</sub>); 7.60 (m, 2H, H-Ph); 7.91 (d, 1H, H-Ph); 7.94 (m, 2H, TPPMS-Ph-SO<sub>3</sub>Na); 8.43 (s, 1H, H-C=N). <sup>13</sup>C NMR

(DMSO- $d_6$ ):  $\delta_C$ (ppm): 13.42 ( $\text{CH}_3\text{-NEt}_2$ ); 13.44 ( $\text{CH}_3\text{-NEt}_2$ ); 49.24 ( $\text{CH}_2\text{-NEt}_2$ ); 49.28 ( $\text{CH}_2\text{-NEt}_2$ ); 56.73 ( $\text{CH}_2\text{-N}$ ); 60.51 ( $\text{CH}_2\text{-NEt}_2$ ); 128.01; 128.16; 128.24; 128.60; 128.81; 128.00; 129.15; 129.40; 129.52; 130.05; 130.08; 130.45; 131.11; 132.17; 135.05; 137.21; 137.41; 137.42; 137.51; 137.76; 142.35; 149.71; 163.69 ( $\text{C=N}$ ).  $^{31}\text{P}$  NMR (DMSO- $d_6$ ):  $\delta_P$ (ppm): 31.60 ( $\text{PPh}_2$ ); 38.25 (TPPMS); 38.61 (TPPMS). MS (ESI)  $m/z$  (%) 1029 ( $\text{M}^+$ , 100). FT-IR ( $\text{cm}^{-1}$ ):  $\nu_{(\text{C=N})}$  =1643. Anal. Calc. for  $\text{C}_{58}\text{H}_{61}\text{N}_2\text{NaO}_7\text{P}_2\text{PdS}_3\cdot\text{CHCl}_3$ : C, 54.30; H, 4.79; N, 2.15. Found: C; 54.61, H; 4.61, N; 1.98.

### 6.2.3. Hydrogenation reactions

#### 6.2.3.1. Homogeneous hydrogenation experiments

A typical procedure for the catalytic hydrogenation of alkenes was as follows. The reactor was charged with styrene (0.50 mL, 4.36 mmol), catalyst **24** (0.85 mg,  $8.7 \times 10^{-4}$  mmol) and toluene (50 mL) and sealed. It was then evacuated, flushed with  $\text{H}_2$  three times and the pressure adjusted to 10 bar. The mixture was stirred at 5 bar hydrogen pressure for the duration of the reaction period. After the reaction time, the autoclave was vented off and samples drawn for GC analyses. The samples were filtered using 0.45  $\mu\text{m}$  micro filters and the solutions analysed by Varian CP3800 GC (ZB-5HT column 30 m  $\times$  0.25 mm  $\times$  0.10  $\mu\text{m}$ ). Commercial ethylbenzene (99%) was used as an authentic standard to determine the percentage hydrogenation of styrene to ethylbenzene.

### 6.2.3.2. Biphasic hydrogenation experiments

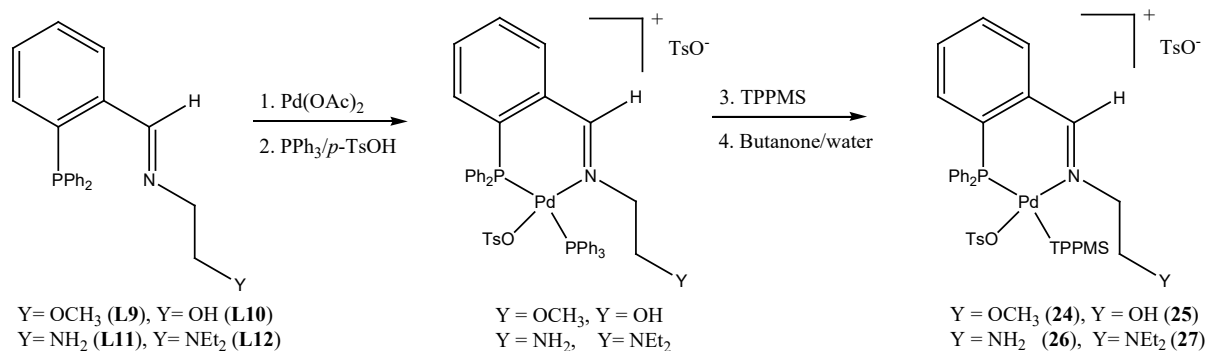
These reactions were carried-out in a biphasic system containing a mixture of water and toluene. In a typical experiment, complex **24** (0.85 mg,  $8.7 \times 10^{-4}$  mmol, equivalent to a substrate/catalyst ratio of 5000) was weighed and dissolved in water (25 mL). A solution of styrene 0.50 mL (4.36 mmol) in toluene (25 mL) was added and the mixture transferred to the reactor via cannula and then sealed. The autoclave was evacuated and flushed with H<sub>2</sub> three times, filled with H<sub>2</sub> to the desired pressure and temperature and the reaction was stirred at 500 rpm. After the reaction period, the autoclave was depressurized and the mixture allowed to settle for approximately 10 min. The aqueous layer was then separated from the organic layer using a separatory funnel. The organic layer was filtered and analysed by GC to determine the percentage conversion of the substrate to the products. In the recycling experiments, a fresh solution of styrene (0.50 mL, 4.36 mmol) in toluene (25 mL) was added without addition of the catalyst in the aqueous phase. This experiment was repeated for six consecutive cycles.

## 6.3. Results and discussion

### 6.3.1. *Synthesis and characterization of palladium(II) complexes 24-27*

The water-soluble palladium(II) complexes **24-27** were synthesized from the reactions of **L9-L12** with Pd(AOc)<sub>2</sub> and equivalent amount of *p*-TsOH, PPh<sub>3</sub> and TPPMS in butanone (Scheme 6.1) in good yields (76-91%). The complexes, **24-27**, were soluble in methanol, ethanol, toluene and water but were insoluble in chlorinated solvents.





**Scheme 6.1:** Synthesis of water-soluble imino-diphenylphosphino palladium(II) complexes **24-27**

Compounds **24-27** were characterized by NMR spectroscopy, mass spectrometry and FT-IR spectroscopy. The coordination of the ligands to the palladium centre was established from their respective  $^1\text{H}$  NMR spectra. For example,  $^1\text{H}$  NMR spectra of complex **24** showed an up-field shift in the ethylene linker protons from 3.78 ppm and 4.49 ppm to 3.51 ppm and 3.69 ppm in **L9** (Fig. 6.1). Furthermore, the appearance of a singlet peak in the  $^1\text{H}$  NMR spectrum of complex **24** at 2.37 ppm confirmed the presence of  $\text{CH}_3$  protons of the coordinated and uncoordinated OTs group (Fig. 6.1).

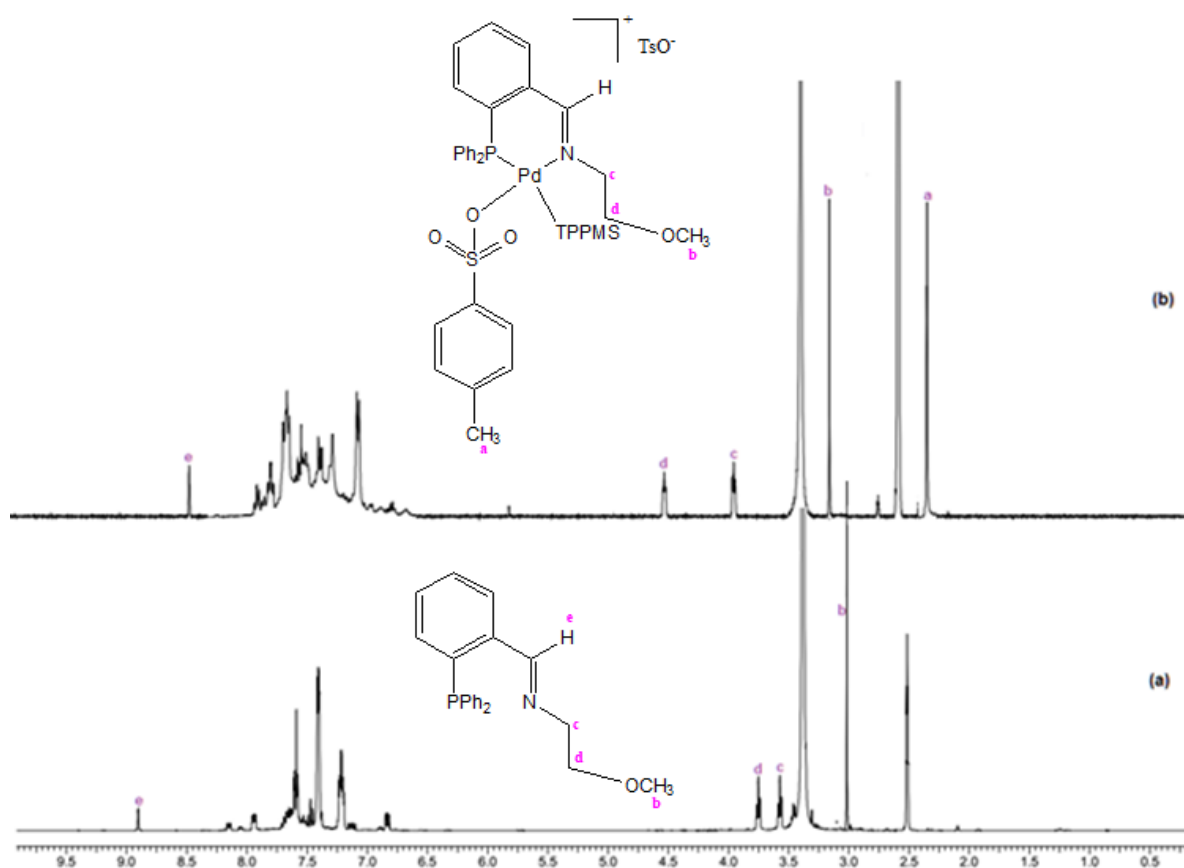


**Figure 6.1:**  $^1\text{H}$  NMR spectrum in  $\text{DMSO-d}_6$  of **L9** (a) and complex **24** (b) showing a shift in the ethylene protons and the appearance of  $\text{CH}_3$  protons of OTs in **24**.

The coordination of the  $\text{PPh}_2$  moiety in ligands **L9-L12** to the palladium centre in complexes **24-27** was confirmed from the  $^{31}\text{P}$  NMR spectra by the downfield shift of the signals in the free ligands relative to the metal complexes. For example, the  $\text{PPh}_2$  signal in **L9** shifted from  $-13.70$  ppm to  $31.55$  ppm in the respective complex **24** (Fig 6.2). The  $^{31}\text{P}$  NMR spectroscopy was also useful in the determination of the TPPMS signals in complexes **24-27**. For instance, the  $^{31}\text{P}$  NMR spectrum of complex **25** (Fig 6.2) showed three peaks at  $31.66$  ppm,  $38.43$  ppm and  $38.54$  ppm which are a result of

the coordinated  $\text{PPh}_2$  (31.74 ppm) and TPPMS (38.43 ppm and 38.54 ppm) in good agreement with those reported in literature.<sup>26-27</sup>

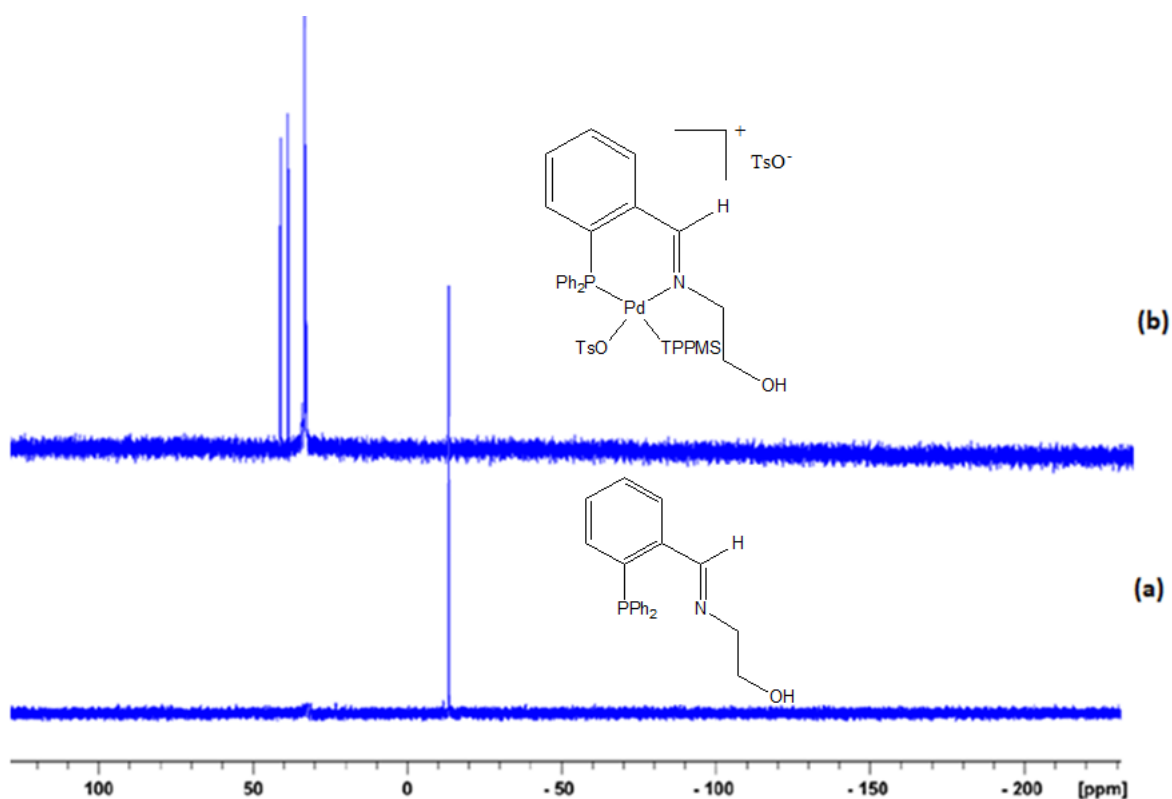


**Figure 6.2:**  $^{31}\text{P}$  NMR ( $\text{DMSO-d}_6$ ) spectrum of L9 (a) and complex 25 (b).

Mass spectrometry was also employed in the elucidation of the identity of the complexes. Figure 6.3 shows found ESI-MS and simulated isotopic distribution of complex 26 with base peak at 973 amu corresponding to the molecular mass of the compound for 26.

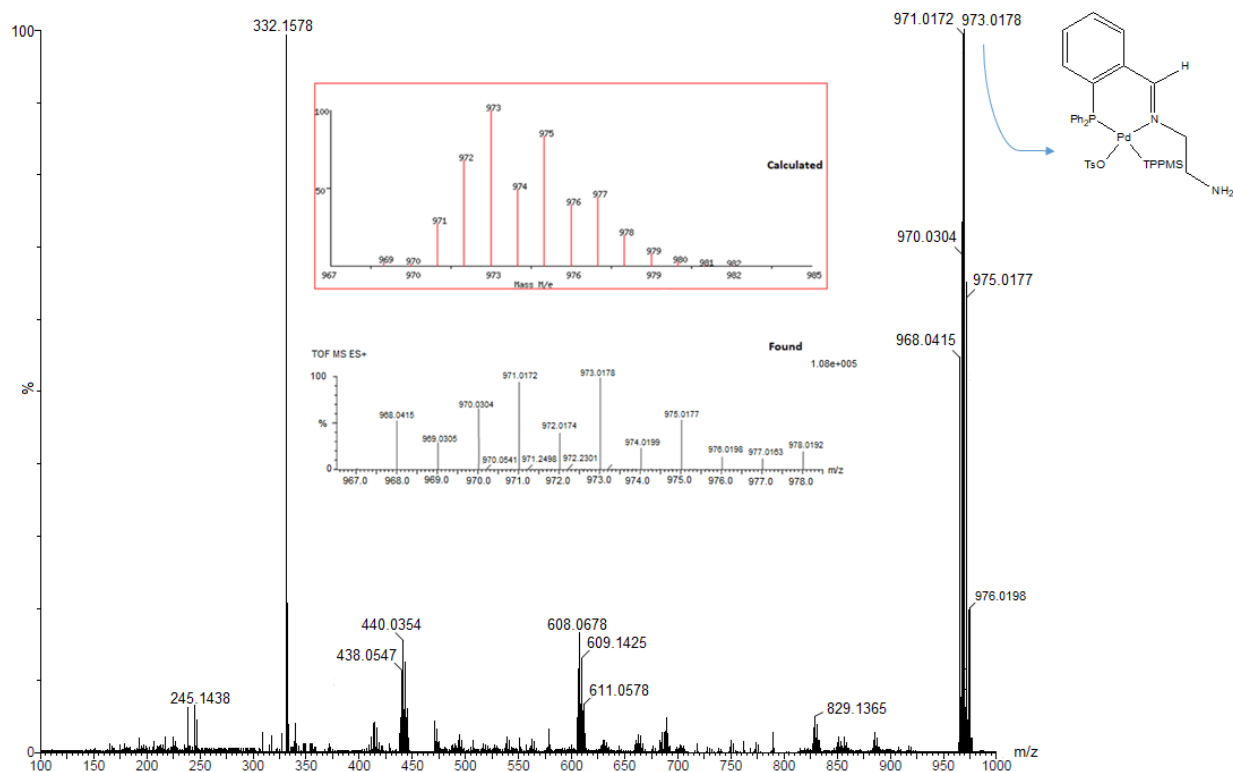


**Figure 6.3:** ESI-MS of complex **26** showing  $m/z$  signal at 973.0 (100%) corresponding to the molecular ion,  $M^+$  (insert showing mass spectrum of the calculated and found isotopic distribution).

### 6.3.2. High pressure catalytic hydrogenation of olefins

Preliminary investigations of complexes **24-27** in high pressure catalytic hydrogenation of alkenes were performed using styrene as a model substrate. The reactions were performed at 10 bar, 25 °C, 1.5 h and [styrene]:[Pd] ratio 5000:1. All the complexes showed significant catalytic activities in the hydrogenation of styrene to ethylbenzene giving conversions between 80%-99% within 1.5 h (Table 6.1). Plots of  $\ln[\text{Sty}]_0/[\text{Sty}]_t$  vs time (Fig. 6.4) was used to compare the rates of hydrogenation reactions using complexes **24-27**. No further elaborations in the effect of catalyst

structure on catalytic activity is necessary as the catalytic activity trend was similar to those obtained in Chapters 4 and 5, in which the nature of the pendant arm had an effect on catalytic activity of the complexes. Thus, this Chapter mainly discusses the biphasic hydrogenation reactions using the water-soluble catalysts **24-27**.

**Table 6.1:** Effect of catalyst structure on the hydrogenation of styrene by complexes **24-27**.<sup>a</sup>

Entry	Catalyst	Conv. <sup>b</sup>	$k_{obs}$ (h <sup>-1</sup> )	TOF <sup>c</sup> (h <sup>-1</sup> )
1	<b>24</b>	99	2.81 (± 0.01)	3300
2	<b>25</b>	94	2.20 (± 0.04)	3133
3	<b>26</b>	87	1.29 (± 0.02)	2900
4	<b>27</b>	80	1.01 (± 0.02)	2666

<sup>a</sup>Conditions: styrene, substrate/catalyst = 5000; substrate, 4.36 mmol; catalyst, 8.0x10<sup>-4</sup> mmol; solvent, toluene; pressure, 10 bar; temperature, 25 °C; time, 1.5. <sup>b</sup>percentage of styrene converted to ethylbenzene; Determined by GC. <sup>c</sup>TOF in mol<sub>substrate</sub>mol<sub>catalyst</sub><sup>-1</sup> h<sup>-1</sup> (h<sup>-1</sup>).

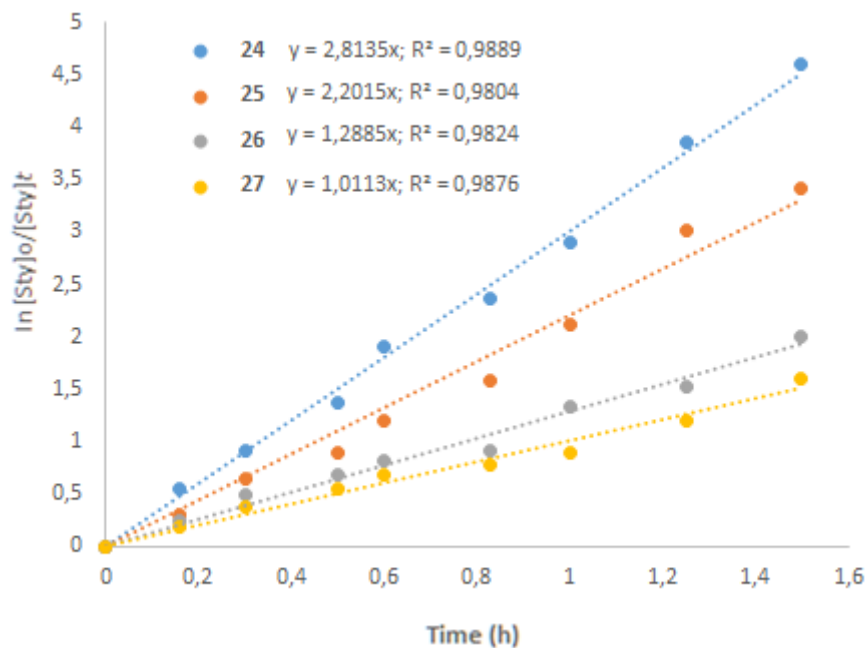


**Figure 6.4:** Plot of  $\ln[\text{Sty}]_0/[\text{Sty}]_t$  vs time for styrene hydrogenation using **24-27**.

### 6.3.3. Biphasic catalysis and catalyst recycling in the hydrogenation of styrene using **24-27**

Homogeneous catalysts offer a number of significant advantages over their heterogeneous catalysts.<sup>28</sup> However, the major challenge of homogeneous catalysts is the difficulty in separation of the catalyst from the reaction mixture and lack of catalyst recycling.<sup>5,29</sup> Various technologies have been employed to improve catalyst recovery and product separation.<sup>6</sup> The water soluble properties of **24-27** were exploited to investigate their catalytic activities and recovery in biphasic medium. In a typical experiment, substrate/catalyst ratio = 5000 of the complex was dissolved in water (25 mL) to form the aqueous phase and the alkene substrate (4.36 mmol) dissolved in toluene (25 mL) to give the organic phase.

The catalytic activities for several consecutive recycling of the aqueous phase was studied and is represented in Figure 6.5. The aqueous phase, which contained the palladium complex was decanted after each catalytic run. Fresh styrene in toluene was added to the aqueous phase without further catalysts addition for six runs. The catalytic behaviour for six consecutive reruns indicated that the catalytic activities were maintained for 9 h total reaction time. The catalytic activities of complexes **24-27** were comparable to the monophasic reactions performed in toluene to give complete conversions within 1.5 h. There was retention of appreciable activities even in run 6 giving conversions of 65, 67, 75 and 71 for complexes **24, 25, 26** and **27** respectively compared to 99, 96, 85 and 78 in run 1 for the same catalysts (Fig. 6.5).

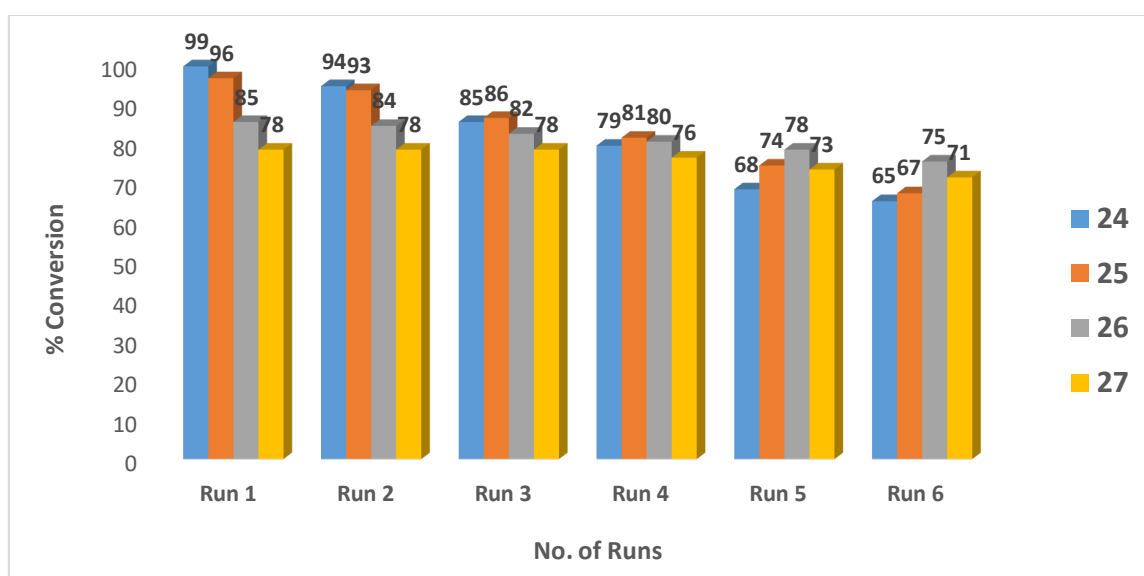


**Figure 6.5:** Conversion of styrene as a function of cycles by complexes **24-27**. Reaction conditions: styrene, 4.36 mmol; catalyst;  $8.7 \times 10^{-4}$  mmol; 10 bar; H<sub>2</sub>O:Toluene (1:1, total volume, 50 mL), temperature, 25 °C, time, 1.5 h.

Table 6.2 displays the comparative TOF and  $k_{obs}$  values obtained for complexes **24-27** in the 1<sup>st</sup> and 6<sup>th</sup> runs and their corresponding percentage drops (obtained from difference in %conversion in the 1<sup>st</sup> and 6<sup>th</sup> runs) in their catalytic activities. Drastic drops in catalytic activities of 34% ( $k_{obs} = 0.82 \text{ h}^{-1}$ ) and 29% ( $k_{obs} = 0.79 \text{ h}^{-1}$ ) for complexes **24** and **25** was observed significantly in the 6<sup>th</sup> run compared to depletions of 10% ( $k_{obs} = 0.92 \text{ h}^{-1}$ ) and 7% ( $k_{obs} = 0.82 \text{ h}^{-1}$ ) for complexes **26** and **27** (Table 6.2, entries 2-4). This drastic reduction in activity for complex **24** and **25** may be due to the weaker coordination of OCH<sub>3</sub> and OH pendant group to palladium(II), leading to a very active but unstable active species.<sup>30</sup> These results are consistent with the observed higher catalytic activity (99% and 94%,  $k_{obs} = 2.81 \text{ h}^{-1}$  and  $2.20 \text{ h}^{-1}$ ) in homogeneous experiments (Table 6.1, entry 1-2). This observation demonstrates one of the major challenges in catalyst design on balancing activity and stability.<sup>31</sup> Figure 6.6 shows the TOF values to characterize the level of activity for complexes **24-27** from the 1<sup>st</sup> to the 6<sup>th</sup> run. Higher TOF's in the 6<sup>th</sup> run were observed which showed that the catalysts were efficient and stable in the recycling experiments.



**Table 6.2:** Comparison of catalytic activities of complexes **24-27** in the 1<sup>st</sup> and 6<sup>th</sup> cycle experiments<sup>a</sup>

Entry	Catalyst	H <sub>2</sub> O/toluene	TOF <sup>b</sup> (h <sup>-1</sup> )		<i>k</i> <sub>obs</sub> (h <sup>-1</sup> )		%Drop <sup>c</sup>
			Run 1	Run 6	Run 1	Run 6	
1	<b>24</b>	1:1	3300	13000	2.23	0.82	34
2	<b>25</b>	1:1	3200	13400	1.73	0.79	29
3	<b>26</b>	1:1	2833	15000	1.18	0.92	10
4	<b>27</b>	1:1	2600	14200	0.95	0.82	7
5	<b>27</b>	2:1	2330	11800	0.80	0.63	11
6	<b>27</b>	1:2	2200	11400	0.78	0.61	9
<b>7<sup>c</sup></b>	<b>27</b>	1:1	2733	13800	1.13	0.81	13

<sup>a</sup>Conditions: styrene, 4.36 mmol; catalyst; 8.7x10<sup>-4</sup> mmol ; 10 bar; temperature 25 °C, Determined by GC. <sup>b</sup>TOF in mol<sub>substrate</sub> mol<sup>-1</sup> catalyst h<sup>-1</sup>. <sup>c</sup>Temperature 50 °C. time, 1.5 h. <sup>c</sup>Difference in %conversion in the 1<sup>st</sup> and 6<sup>th</sup> runs.

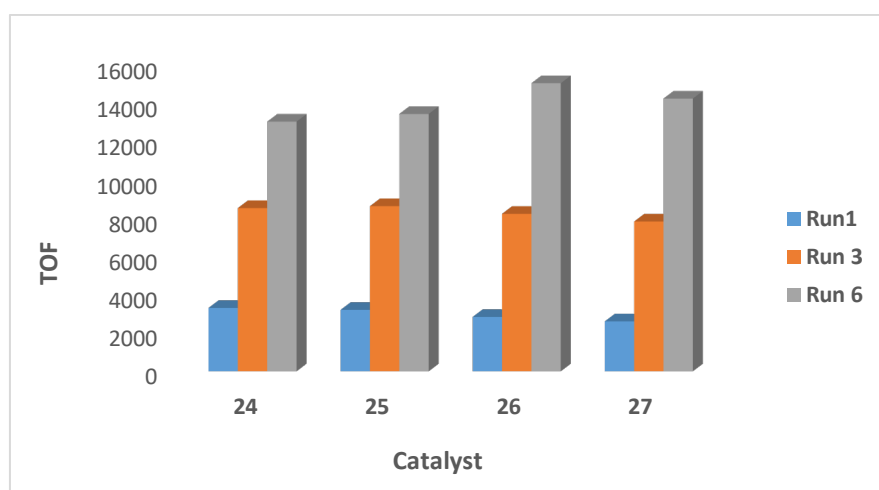


**Figure 6.6:** Plot of TOF *vs* catalysts **24-27** for runs 1, 3 and 6. Reaction conditions: styrene, 4.36 mmol; catalyst; 8.7x10<sup>-4</sup> mmol; 10 bar; H<sub>2</sub>O:Toluene (1:1, total volume, 50 mL), temperature, 25 °C, time, 1.5 h.

### 6.3.3.1. Effect of aqueous/organic volume ratios and thermal stability on the biphasic hydrogenation of styrene using complex **27**

We also studied the effect of aqueous/organic volume ratios on biphasic hydrogenation of styrene using catalyst **27**. This is because in biphasic reactions, the distribution co-efficient of the substrate and catalyst between the solvent systems employed greatly affects catalysts performance.<sup>32-33</sup> From Table 6.2 (entries 4 and 5) and Figure 6.7, a slight drop in catalytic activity from 78% to 70% ( $k_{obs} = 0.95 \text{ h}^{-1}$  to  $0.80 \text{ h}^{-1}$ ) was observed when the aqueous/organic ratio was increased from 1:1 to 2:1. Furthermore, increasing the organic phase (aqueous/organic ratio of 1:2) resulted in a drastic reduction in catalytic activity to 66% ( $k_{obs} = 0.78 \text{ h}^{-1}$ ). Ogwen *et. al.*<sup>34</sup> reported a decrease in catalytic activity when aqueous/organic ratios of 2:1 (96% to 86%) and 1:2 (96% to 70%) were used in the biphasic hydrogenation of styrene and was associated with greater volumes of aqueous/organic phase limiting diffusion of the catalyst interphase.

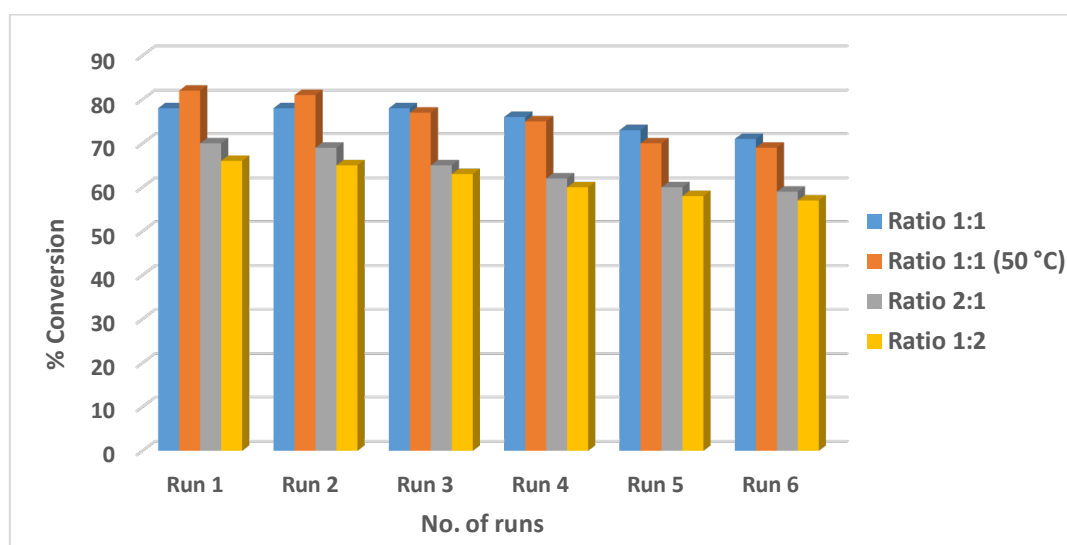


**Figure 6.7:** Effect of aqueous/organic solvent volume ratio and temperature on catalyst recycling using complex **27**

Another important feature in catalyst recycling and biphasic hydrogenation reactions is thermal stability of the catalysts, which leads to catalyst deactivation and loss of activity in subsequent experiments.<sup>32,33,35</sup> We therefore studied the thermal stability of catalyst **27** by comparing the recycling experiments at 25 °C and 50 °C (Table 6.2, Fig. 6.7). Increasing the temperature to 50 °C resulted in an increase in catalytic activity (78%,  $k_{obs} = 0.95 \text{ h}^{-1}$  to 82%,  $k_{obs} = 1.13 \text{ h}^{-1}$ ) in the 1<sup>st</sup> run and a slight drop in the 6<sup>th</sup> run from 78% ( $k_{obs} = 0.95 \text{ h}^{-1}$ ) to 65% ( $k_{obs} = 0.81 \text{ h}^{-1}$ ) was observed (Table 6.2, entries 4 and 7), respectively. This therefore indicated that the catalyst was thermally stable.

#### 6.4. Conclusions

In summary, water-soluble palladium(II) complexes anchored on (diphenylphosphino)benzalidene have been successfully isolated and structurally characterized and studied in the homogeneous and biphasic hydrogenation of styrene. All the complexes formed active catalysts for hydrogenation of styrene under mild reaction conditions. These complexes, **24-27**, were found to be stable and recyclable in biphasic hydrogenation reactions retaining significant catalytic activities in six consecutive runs. The temperature and aqueous/organic volume ratio influenced the catalytic activities and recovery of these complexes from biphasic medium. This study has demonstrated a very simple synthetic protocol to the design of effective and recoverable water-soluble catalysts in biphasic hydrogenation.

## 6.5. References

- 1 B. Cornils W. A. Herrman, *J. Catal.*, 2003, **216**, 23-31.
- 2 J. Hagen, *Industrial Catalysis: A Practical Approach*, Wiley-VCH: Weinheim, Germany, 2006, 1-14.
- 3 E. L. V Goetheer, A. W. Verkerk, L. J. P. Van Den Broeke, E. De Wolf, B. Deelman, G. Van Koten and J. T. F. Keurentjes, *J. Catal.* 2003, **219**, 126–133.
- 4 P.G. Jessop, T. Ikariya, R. Noyori, *Chem. Rev.*, 1999, **99**, 475-493.
- 5 K. De Smet, S. Aerts, E. Ceulemans, I. F. J. Vankelecom and P. A. Jacobs, *Chem. Comm.*, 2001, 597–598.
- 6 I. W. Davies, L. Matty, D. L. Hughes and P. J. Reider, *J. Am. Chem. Soc.*, 2001, **123**, 10139–10140.
- 7 N. Ren, Y. Yang, Y. Zhang, Q. Wang and Y. Tang, *J. Catal.*, 2007, **246**, 215–222.
- 8 C. De Bellefon, N. Tanchoux and S. Caravieilhés, *J. Organomet. Chem.*, 1998, **567**, 143–150.
- 9 S. Alexander, V. Udayakumar and V. Gayathri, *J. Mol. Catal., A. Chem.*, 2009, **314**, 21–27.
- 10 V. Caballero, F. M. Bautista, J. Manuel, D. Luna, R. Luque, J. Maria, A. Angel, I. Romero, I. Serrano, J. Miguel and A. Llobet, *J. Mol. Catal., A. Chem.*, 2009, **308**, 41–45.
- 11 I. Del Río, N. Ruiz, C. Claver, L. A. Van Der Veen and P. W. N. M. Van Leeuwen, *J. Mol. Catal. A Chem.*, 2000, **161**, 39–48.
- 12 J. Dupont, G. S. Fonseca, A. P. Umpierre, P. F. P. Fichtner, S. R. Teixeira, P. Alegre and R. S. Brazil, *J. Am. Chem. Soc.*, 2002, **124**, 4228–4229.
- 13 Y. Ma, H. Liu, L. Chen, X. Cui, J. Zhu and J. Deng, *Org. Lett.*, 2003, **5**, 10–13.
- 14 F. Joó, L. Nádasdi, A. C. Bényei and D. J. Darensbourg, *J. Organomet. Chem.*, 1996, **512**, 45–50.
- 15 D. C. Mudalige and G. L. Rempel, *J. Mol. Catal. A Chem.*, 1997, **116**, 309-316.
- 16 E.A. Karakhanov, A.L. Maksimov, *Russ. J. Gen. Chem.*, 2009, **79**, 1370-1380.
- 17 C. De, R. Saha, S.K. Ghosh, A. Ghosh, K. Mukherjee, S.S. Bhattacharyya, B. Saha, *Res. Chem. Intermed.*, 2013, **39**, 3463-3471.
- 18 R. Franke, D. Selent, A. Börner, *Chem. Rev.*, 2012, **112**, 5675-5683.
- 19 D.F. Foster, D. Gudmunsen, D.J. Adams, A.M. Stuart, E.G. Hope, D.J. Cole-Hamilton, G.P. Schwarz, P. Pogorzelec, *Tetrahedron*, 2002, **58**, 3901-3909.
- 20 E. G. Kuntz, *Chem. Tech.*, 1987, **17**, 570-578.

- 21 E. B. Hager, B. C. E. Makhubela and G. S. Smith, *Dalton Trans.*, 2012, **41**, 13927-13935.
- 22 K. H. Shaughnessy, *Chem. Rev.*, 2009, **109**, 643-651.
- 23 P. T. Anastas and J. C. Warner, *Green Chemistry Theory and Practice*, Oxford University Press, New York, 1998, 30-41.
- 24 F. A. Harraz, S. E. El-Hout, H. M. Killa and I. A. Ibrahim, *J. Catal.*, 2012, **286**, 184-192.
- 25 H. Syska, W. A. Herrmann and F. E. Kühn, *J. Organomet. Chem.*, 2012, **703**, 56-62.
- 26 T. Suárez, B. Fontal, M. Reyes, F. Bellandi, R. R. Contreras, A. Bahsas, G. León, P. Cancines and B. Castillo, *React.Kinet.Catal.Lett.*, 2004, **82**, 317-324.
- 27 E. Paetzold and G. Oehme, *J. Mol. Catal. A Chem.*, 2000, **152**, 69-76.
- 28 D. J. Cole-hamilton and D. J. Cole-hamilton., *Science*, 2003, **299**, 1702-1706.
- 29 M. Heitbaum, F. Glorius, I. Escher, *Angew. Chem. Int. Ed.* **45** (2006) 4732-4762.
- 30 F. Yilmaz, A. Mutlu, H. Ünver, M. Kurta and I. Kani, *J. Supercrit. Fluids.*, 2010, **54**, 202-209.
- 31 X. Yang, A. Wang, B. Qiao and J. U. N. Li, *Acc. Chem. Research.*, 2013, **46**, 1740-1748.
- 32 P. J. Dyson, D. J. Ellis, T. Welton, *Platin. Met. Rev.*, 1998, **42**, 135-140.
- 33 B. Cornils, W. A. Herrmann, *Aqueous-Phase Organometallic Catalysis: Concepts and Applications*, 2<sup>nd</sup> Ed. Wiley-Vch Verlag GmbH and Co. KGaA., Weinheim, Germany, 2004, 130-141.
- 34 A. O.Ogweno, S. O. Ojwach and M. P.Akerman, *J. Mol.Catalysis A: Chem.*, 2000, **152**, 69-76.
- 35 F. Joó, *Aqueous Organometallic Catalysis*, Kluwer Academic Publishers, Dordrecht, Netherlands, 2002, 156-180.

## CHAPTER 7

### General concluding remarks and future prospects

#### 7.1. General conclusions

In summary, this thesis deals with a systematic investigation of some (benzoimidazol-2-ylmethyl)amine, N<sup>^</sup>O (imino)phenol, P<sup>^</sup>N (diphenylphosphino)benzalidine palladium(II) complexes and water soluble P<sup>^</sup>N (diphenylphosphino)benzalidine palladium(II) complexes as potential olefin methoxycarbonylation and hydrogenation catalysts. The ligands (**L1-L10**) coordinate to palladium metal center in a bidentate manner.

(Benzoimidazol-2-ylmethyl)amine palladium(II) complexes, **1-5**, form active catalysts in the methoxycarbonylation of terminal and internal olefins to produce branched and linear esters. The high catalytic activity and regioselectivity towards linear olefins for the (benzoimidazol-2-ylmethyl)amine palladium(II) complexes, **1-3**, is attributed to the presence of PPh<sub>3</sub> and tolyl groups, which enhance stability of the complexes and hinder isomerization of the coordinated substrates. The catalytic activities and regioselectivity of the (benzoimidazol-2-ylmethyl)amine palladium(II) complexes in methoxycarbonylation reactions were also affected by the nature of the phosphine derivative, acid promoter and olefin substrate.

The catalytic activities of (Benzoimidazol-2-ylmethyl)amine palladium(II) complexes (**6-11**), N<sup>^</sup>O (imino)phenol palladium(II) complexes (**12-17**) and P<sup>^</sup>N (diphenylphosphino)benzalidine palladium(II) complexes (**18-23**) in high pressure

hydrogenation were found to be influenced by electronic contributions of the ligands and the nature of the pendant arm. The presence of the labile co-ordinating bond in N<sup>O</sup> (imino)phenol, P<sup>N</sup> (diphenylphosphino)benzalidine palladium(II) complexes, **12-23**, which provides the coordinative flexibility to respond to changes on the palladium metal during catalytic cycles resulted in **12-23** being more stable and active than (benzoimidazol-2-ylmethyl)amine palladium(II) complexes (**6-11**). Furthermore, P<sup>N</sup> (diphenylphosphino)benzalidine palladium(II) complexes were more active and stable than N<sup>O</sup> (imino)phenol palladium(II) complexes, due to the phosphine donor stabilizing the complex and providing electrophilicity to the metal centre. Hydrogenation of aliphatic alkynes and alkenes is followed by isomerization of the terminal alkenes and alkynes to internal alkenes.

Kinetic studies of the hydrogenation reactions indicate *pseudo* first order with respect to the substrate and catalyst (**6-23**). Partial and low reaction orders with respect to H<sub>2</sub> concentration were observed, which were associated with disfavoured activation of the H<sub>2</sub> molecule to form the dihydride species. The activation parameters indicated a highly ordered transition state and homogenous nature of the active species.

A mechanistic pathway involving the formation of a palladium monohydride intermediate as the active species was established from mass spectrometry. Kinetic experiments, stoichiometry poisoning, mercury poisoning and kinetic reproducible data using P<sup>N</sup> (diphenylphosphino)benzalidine palladium(II) complexes (**18-23**) indicate a homogenous nature of the active species.

Water soluble palladium(II) complexes (**24-27**) are discussed along with their application in biphasic high pressure hydrogenation. The complexes are active catalysts for the high pressure hydrogenation of alkenes under mild reaction conditions. The complexes (**24-27**) were found to be stable and recyclable in biphasic hydrogenation reactions without significant loss of activity in six consecutive runs. The activity of the complexes was influenced by catalyst loading, temperature, hydrogen pressure and reaction time. These complexes (**24-27**) also provide an effective method for bridging the gap between homogeneous and heterogeneous catalysis.

## 7.2. Future prospects

The results and findings of this study have significantly contributed towards the design and synthesis of active hydrogenation catalysts. For example, the P<sup>N</sup> (diphenylphosphino)benzalidine palladium(II) complexes (**18-23**) studied in Chapter 6 were active and stable due to the Pd-P bond which prevents decompositions under hydrogen atmosphere, as well as a labile coordinating bond which is prone to dissociation site. These complexes of P<sup>N</sup> (diphenylphosphino)benzalidine palladium(II) complexes were used in Chapter 7 (**24-27**) to demonstrate the significant of water soluble complexes in developing biphasic systems which are recyclable and allows ease of product-catalyst separation in biphasic media. To further enhance the separation of the product from the catalyst product mixture, anchored water-soluble complexes are proposed. (Fig. 7.1).



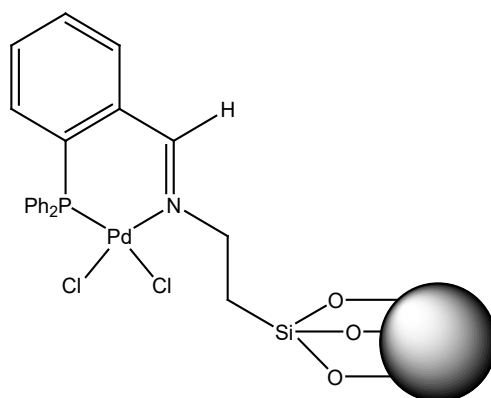


**Figure 7.1:** Heterogeneous palladium(II) complexes based on P<sup>N</sup> chelating agent.

Furthermore, we proposed the development of new chiral palladium(II) complexes of P<sup>N</sup> donor atoms (Fig. 7.2) for asymmetric catalytic hydrogenation reactions of prochiral alkenes (Fig. 7.3). Asymmetric hydrogenation is significant as there is an increase in demand for chiral organic products which are used in pharmaceutical industry.

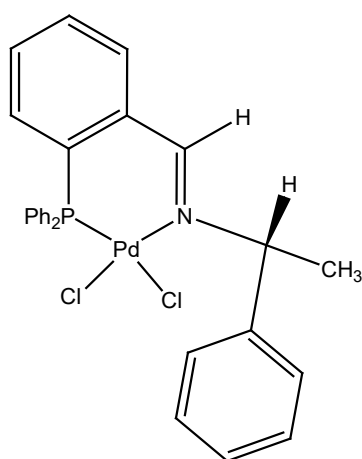
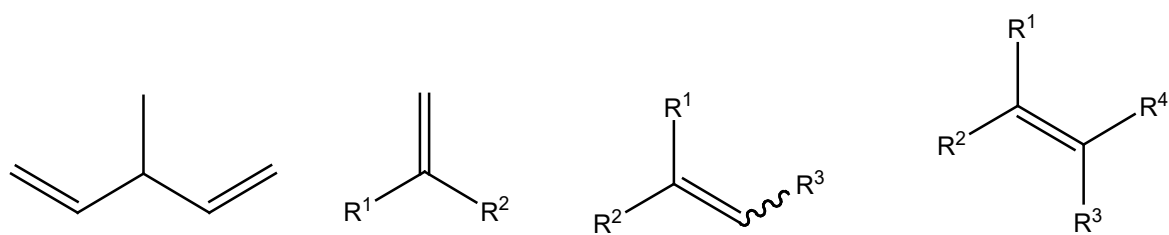


**Figure 7.2:** proposed structure of asymmetric palladium(II) complexes based on P<sup>N</sup> chelating agent.



R<sup>1-3</sup> = alkyl; R<sup>4</sup> = alkyl with "distal functionality"

**Figure 7.3:** Prochiral alkenes, 1, 1-di-, tri-, and tetra substituted alkenes.

In the homogeneous hydrogenation reactions applied in this thesis we have used alkenes and alkynes. For future work, we will employ other substrate such as 1-(4-nitrophenyl)ethanone, 1-methyl-4-nitrobenzene, 1-nitrobenzene, 4-nitrobenzaldehyde and 1,4-dinitrobenzene (Fig. 7.4) in the catalytic hydrogenation reactions.

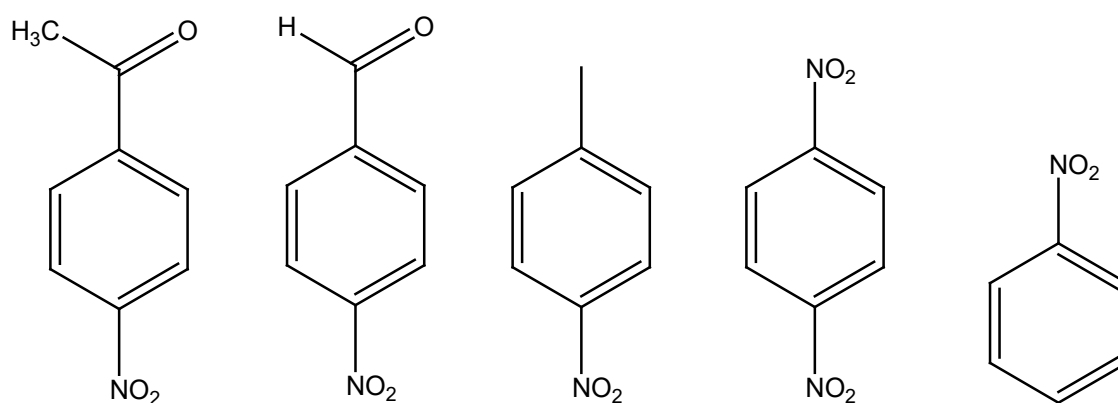


**Figure 7.4:** Potential substrate for catalytic hydrogenation reactions.